

# Dopaminergic Modulation of Executive Control Signals in Primate Prefrontal Cortex Neurons

Dissertation

zur Erlangung des Grades eines  
Doktors der Naturwissenschaften

der Mathematisch-Naturwissenschaftlichen Fakultät  
und  
der Medizinischen Fakultät  
der Eberhard-Karls-Universität Tübingen

vorgelegt von

Ott, Torben

aus Bietigheim-Bissingen, Deutschland

Januar – 2016

Tag der mündlichen Prüfung: 19. April 2016

Dekan der Math.-Nat. Fakultät: Prof. Dr. W. Rosenstiel

Dekan der Medizinischen Fakultät: Prof. Dr. I. B. Autenrieth

1. Berichterstatter: Prof. Dr. A. Nieder

2. Berichterstatter: Prof. Dr. U. Ilg

3. Berichterstatter: Prof. Dr. G. Rainer

Prüfungskommission: Prof. Dr. A. Nieder

Prof. Dr. U. Ilg

Prof. Dr. C. Schwarz

Dr. Z. Hafed

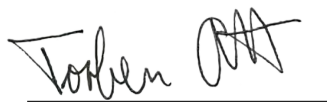
## **Erklärung**

Ich erkläre, dass ich die zur Promotion eingereichte Arbeit mit dem Titel:

„Dopaminergic Modulation of Executive Control Signals in Primate Prefrontal Cortex Neurons“

selbständig verfasst, nur die angegebenen Quellen und Hilfsmittel benutzt und wörtlich oder inhaltlich übernommene Stellen als solche gekennzeichnet habe. Ich versichere an Eides statt, dass diese Angaben wahr sind und dass ich nichts verschwiegen habe. Mir ist bekannt, dass die falsche Abgabe einer Versicherung an Eides statt mit Freiheitsstrafe bis zu drei Jahren oder mit Geldstrafe bestraft wird.

Tübingen, den 25.04.2016

A handwritten signature in black ink, appearing to read 'Torben Ott', written over a horizontal line.

Torben Ott



## **Acknowledgments**

I want to thank my thesis supervisor Andreas Nieder for his guidance during my work in his laboratory. Andreas' door is always open and he continuously provides ideas, gives feedback on my work and is a constant source of motivation and advice during the PhD and beyond.

Thanks to all members of the animal physiology lab for providing a great open environment to work in. In particular, I want to thank Simon Jacob, Lena Veit and Pooja Viswanathan for a lot of discussions inside and outside science. Special thanks to Simon Jacob, who fueled my interest for dopamine and profoundly facilitated this work. Thanks to Anna Marlina Stein for her substantial help in realizing one of the projects in this thesis.

I want to thank my family and friends for their love and support.

Finally, I want to appreciate the contribution of all monkeys I worked with. Thanks to Melvin, Harvey, Emil, Oskar, Louie and Torkel.



**Contents**

<b>Summary</b>	<b>9</b>
<b>I. Synopsis</b>	<b>11</b>
<b>1. Introduction</b>	<b>11</b>
1.1. Goal-directed behavior . . . . .	11
1.1.1. Perception-action cycle . . . . .	11
1.1.2. Executive control functions . . . . .	11
1.2. Neural substrates of executive control . . . . .	14
1.2.1. Prefrontal cortex: ideal candidate region for executive control . . . . .	14
1.2.2. Executive functions involving prefrontal cortex . . . . .	16
1.2.3. Models of prefrontal cortex functions . . . . .	18
1.3. Dopamine modulation of executive control . . . . .	20
1.3.1. Dopamine systems in the brain . . . . .	20
1.3.2. The mesocortical dopamine system . . . . .	21
1.3.3. Dopamine physiology . . . . .	22
1.3.4. Dopamine modulation of prefrontal cortex functions . . . . .	24
1.3.5. Models of dopamine modulation of prefrontal cortex . . . . .	27
1.4. Open questions . . . . .	29
<b>2. Main results</b>	<b>31</b>
2.1. Statement of contributions . . . . .	31
2.2. Dopamine modulation of visual signals . . . . .	32
2.3. D1R and D2R modulation of behavioral rules . . . . .	32
2.4. D2R modulation of working memory . . . . .	34
2.5. D1R and D2R modulation of reward signals . . . . .	35
2.6. Impact of prolonged training on behavioral well-being of rhesus monkeys	36
<b>3. Discussion</b>	<b>37</b>
3.1. Dopamine modulates a variety of signals relevant for executive control . . . . .	37
3.1.1. Visual signals . . . . .	37
3.1.2. Rule signals . . . . .	39
3.1.3. Working memory signals . . . . .	41
3.1.4. Reward signals . . . . .	43
3.2. Dopamine receptors show differential modulation of executive control . . . . .	44
3.2.1. Complementary mechanisms for D1R and D2R . . . . .	44
3.2.2. Opposite mechanisms for D1R and D2R . . . . .	45

3.3. Models of dopamine modulation suggest specific mechanism of action . . .	47
3.3.1. Differential modulation of interneurons and pyramidal cells . . . .	47
3.3.2. Modulation of population dynamics . . . . .	49
3.4. Future directions . . . . .	49
3.5. Conclusion . . . . .	50
<b>Abbreviations</b>	<b>52</b>
<b>References</b>	<b>53</b>
<b>II. Individual studies</b>	<b>67</b>
<b>Study 1: Dopamine modulation of visual signals</b>	<b>69</b>
<b>Study 2: Dopamine receptor modulation of rule signals</b>	<b>83</b>
<b>Study 3: Dopamine D2 receptor modulation of working memory signals</b>	<b>103</b>
<b>Study 4: Dopamine receptor modulation of reward signals</b>	<b>161</b>
<b>Study 5: Effects on prolonged training on behavioral well-being of rhesus monkeys</b>	<b>193</b>



---

## Summary

Executive control refers to the ability of animals and humans to select appropriate actions for achieving goals under varying environmental conditions. Working memory, for example, enables us to manipulate and integrate information about the sensory environment without needing constant sensory input. This information can then be integrated with internal representations about rules, plans, or goal values to guide behavior. Executive functions rely on the integrity of prefrontal cortex (PFC), where single neurons signal information relevant for guiding behavior. PFC networks are strongly innervated by midbrain dopamine neurons, which regulate a variety of executive control functions. However, the neuronal basis for dopaminergic control of executive functions is largely unknown.

In this thesis, we performed several studies addressing dopamine modulation of neuronal signals relevant for executive control. We trained macaque monkeys to perform several tasks requiring a range of executive control functions and recorded single neurons in PFC while stimulating or blocking specific dopamine receptors at the vicinity of the recorded neurons using micro-iontophoresis. We investigated how dopamine influences neuronal signals carrying behavioral relevant information at single neuron and population levels and addressed possible mechanisms of action using computational models of prefrontal networks.

We show that dopamine and dopamine receptors modulate a variety of signals relevant for executive control. First, dopamine enhanced visual signals in PFC relevant for perceptual decisions. Next, working memory activity during subsequent delay periods was strongly improved by activating D2 family receptors, which also controlled dynamic properties of PFC networks. Stimulating either D1 or D2 family receptors enhanced signals about behavioral rules by distinct physiological mechanisms. On the other hand, D1 and D2 family receptors oppositely modulated representation of goal values. Computational modeling proposed a specific mechanism by which dopamine receptors change synaptic properties, suggesting that dopamine acts primarily by changing interneuron-to-pyramidal signaling.

These results show that dopamine receptors assume complementary as well as opposite roles in modulating executive control. Dopamine receptors cooperatively regulate working memory and behavioral flexibility while oppositely influencing reward signals. Thus, dopamine functions might dissociate between different executive control functions. Together, our results suggest that dopamine gates sensory input to PFC and subsequently stabilizes prefrontal representations relevant for executive control. Thus, dopamine modulates the flow of information through PFC, controlling the selection of appropriate actions during goal-directed behavior.



---

# Part I.

## Synopsis

### 1. Introduction

#### 1.1. Goal-directed behavior

##### 1.1.1. Perception-action cycle

During the organization of animal behavior, sensory signals from the environment trigger percepts that lead to specific actions. The actions themselves induce changes in the external environment, which are again fed into sensory systems forming a perception-action cycle (Fuster 2008). To achieve goals that are not a direct consequence of an external stimulus, however, organisms control stimulus-response associations through cognition (Shettleworth 2010). At the cognitive level, internal information about goals influence the behavioral action following a percept (**Figure 1A**). Consider the simple behavior to drink triggered by the percept of a full glass. This behavior is not mediated by a stimulus-response association alone, but influenced by a number of variables that are represented internally. These include motivational states (am I thirsty?), memories (do I like the drink?), attention (do I interrupt my conversation?), social knowledge (does the drink belong to me?) and so on. The set of abilities to organize behavior towards a goal are referred to as executive control functions (Miller and Cohen 2001).

##### 1.1.2. Executive control functions

Executive control functions enable organisms to orchestrate perception, thought and action along the perception-action cycle in accordance with internal goals (Miller and Cohen 2001). They mediate flexible behavior by de-coupling automatic stimulus-response associations thus providing the ability to respond with a variety of behaviors to a stimulus depending on contexts or goals (Miller and Wallis 2009). Executive functions comprise a set of abilities such as working memory, representation of task rules, information about goal values, perceptual decisions and many more (Miller and Cohen 2001, Miller and Wallis 2009, Tanji and Hoshi 2008, Baddeley 2012). However, all executive functions have a common conceptual foundation (Miller and Wallis 2009, Miller and Cohen 2001), which is the control of information flow between stimuli and motor actions (**Figure 1B**). In this framework, automatic processing transforms sensory signals into actions through established associative connections. However, executive control functions control the flow of information between sensory signals and motor actions, thereby flexibly adjusting the behavior following a stimulus to obtain a goal. Thus, executive functions integrate sensory information, internal representations, and motor actions. This inte-

gration is state-dependent on the level of arousal, stress, motivation, or fatigue (Robbins and Arnsten 2009). State-dependent modulation controls executive functioning to adjust the selection of action based on current goals. Here, I want to briefly introduce concepts of different executive functions relevant for my thesis.

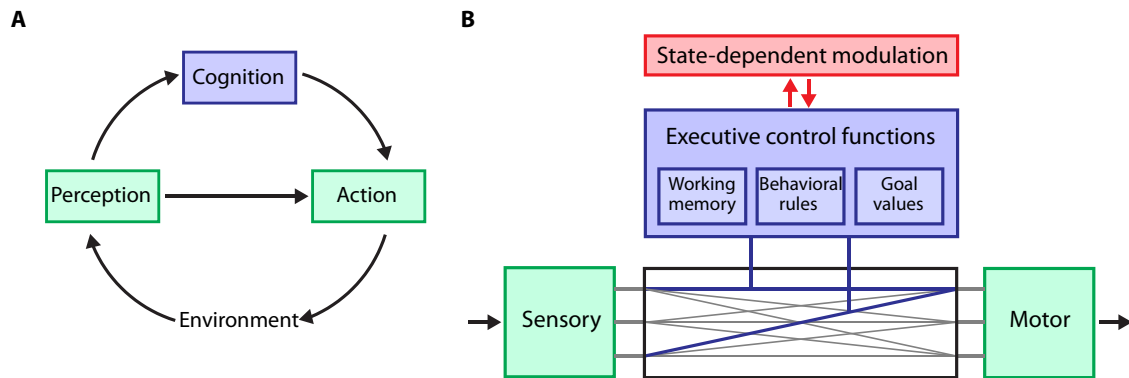


**Figure 1: Conceptual framework for executive control.** **A:** Behavior is organized along a perception-action cycle, in which perception of sensory signals from the environment triggers actions, which themselves lead to changes in the environment following another percept, and so on. After Fuster (2008). **B:** Conceptual model for executive control functions. Sensory signals are associated with motor actions (grey lines between green boxes). Executive control functions (blue box) can modulate existing sensory-motor associations to bias the selection of an action towards a goal. Executive functions are modulated by state-dependent variables (red box). After Miller and Wallis (2009).

**Perceptual decision-making** Decision-making refers to the process of selecting a particular action from a set of alternatives, thus constituting a part of executive control (Gold and Shadlen 2007). Decisions are characterized first by the presence of choice alternatives with expected outcomes (Wang 2008). Second, a decision is based on the accumulation of evidence from external or internal signals. Finally, decisions are inherently risky since they involve evaluation of noisy evidence. The most basic decision is the perceptual decision about presence or absence of a faint external stimulus (Gold and Shadlen 2007, de Lafuente and Romo 2005, 2006, Merten and Nieder 2012). For example when swimming, the perceptual decision if I heard a remote thunder might determine subsequent behavior to leave the water. A perceptual decision involves the accumulation of evidence from a noisy stimulus in the environment into a categorical decision about the presence or absence of the stimulus to select from a set of actions (Deco and Romo 2008). Remarkably, a noisy or ambiguous stimulus may or may not produce a percept. Thus, the integration of sensory information and internal representations to achieve goals underlies perceptual decisions (Deco and Romo 2008).

**Working memory and categories** Working memory is the ability to briefly maintain and manipulate information in mind (Baddeley 2012). It involves transforming sensory

signals into sustained representations and integrating these representations with other goal-relevant information to guide behavior. For example, solving simple arithmetic problems involves not only memorizing numbers for a short amount of time, but also manipulating number information to add or subtract numbers to solve the problem. Working memory comprises short-term memory of sensory signals from different sensory modalities, categories, or long-term memories. Dealing with categories requires working memory representations independent from the precise appearance of sensory signals. For example, animals and humans are able to discriminate numbers, i.e. the number of items in a set, independently from their precise appearance (Nieder 2005). The representation of number categories follows basic principles similar to sensory representations: It is harder to discriminate two numbers the more distant the two numbers are (numerical distance effect). For larger numbers, the minimal distance between two numbers that can be discriminated is larger, too (numerical magnitude effect). Thus, number representations show characteristics of compressed scaling in accordance with Weber's law arguing for an analogue magnitude system (Nieder and Miller 2003, Nieder and Merten 2007, Cantlon and Brannon 2006, 2007).

**Behavioral rules** Using behavioral rules refers to the ability to select an appropriate action in a novel environment according to an internal model, or set of rules, which guides behavior (Miller and Cohen 2001). This enables behavioral flexibility and rapid learning in novel situations without the need to newly learn each stimulus-response association (Miller and Wallis 2009). For example, when using the metro for the first time in Tokyo without speaking the language, we readily apply rules that we learned previously in this novel situation: We are purchasing a ticket, looking for a schedule and checking the map. This allows for navigating successfully in a novel environment without the necessity to learn every aspect of using the metro newly. When training animals, rules can be studied by using conditional learning tasks, in which animals learn conditional associations between a stimulus and a response (Miller and Wallis 2009). For example, animals can remember a visual stimulus and subsequently report if they saw the same stimulus or a different stimulus before, depending on a rule that instructs the animal (Wallis et al. 2001, Miller et al. 2002). Animals are able to handle numerical information, too. Monkeys can perform basic arithmetic tasks by comparing two numerosities and reporting which numerosity is larger or smaller, depending on a cue that instructs the rule currently in effect (Cantlon and Brannon 2006, Bongard and Nieder 2010, Vallentin et al. 2012, Eiselt and Nieder 2013).

**Goal values** Actions are selected according to their value functions, which describe how much future reward is expected from each action (Lee et al. 2012). Value functions can be updated using the reward prediction error describing the mismatch between

expected reward and actual outcome following an action. In this framework, a reward is a stimulus reinforcing an action (Schultz 2006). To enable goal-directed behavior, value functions have to be integrated with other information relevant for executive control, such as sensory information, working memory, and rules (Lee et al. 2012, Kennerley et al. 2009). For example, when planning and deciding where to go to for dinner, we incorporate information about the expected quality of food and other factors, such as distance and price. In animal studies, the expected reward of an action modulates working memory performance. Larger rewards increase working memory accuracy, decrease reaction times, and increase the motivation to complete a task (Amemori and Sawaguchi 2006, Kennerley et al. 2009, Roesch and Olson 2003).

### 1.2. Neural substrates of executive control

#### 1.2.1. Prefrontal cortex: ideal candidate region for executive control

**Structural requirements for implementing executive control** A brain structure implementing executive control functions requires a specific range of characteristics, because it needs to integrate a wide range of information (Miller and Cohen 2001, Tanji and Hoshi 2008). First, it needs cortical inputs from all sensory areas providing information about sensory signals as well as cortical inputs providing memory signals. Second, it needs subcortical inputs providing information about the motivational state of the organism modulating executive control. Thirdly, it requires direct output to motor systems to coordinate action. The prefrontal cortex (PFC) has been shown to meet these and other criteria (Miller et al. 2002, Fuster 2008, Tanji and Hoshi 2008). Accordingly, the PFC is strongly involved in executive functions.

**Prefrontal cortex subdivision** The PFC lies at the anterior pole of the neocortex in mammals and can be anatomically defined by receiving inputs from the mediodorsal nucleus of the thalamus (MDNT) (Fuster 2008). In primates, the PFC comprises different sub-areas with an extensive amount of local connections within PFC (Tanji and Hoshi 2008, Petrides and Pandya 1999). By refining cytoarchitectonic maps from the human frontal lobe and the macaque monkey (Walker 1940), Petrides (2005) and Petrides et al. (2012) describe sub-areas belonging to the primate PFC that can be grouped in three main divisions (Miller and Cohen 2001). These include orbital and medial areas (areas 10, 11, 13, 14), mid-dorsal areas (area 9) and areas constituting the lateral PFC (LPFC) comprising dorsal area 9/46 and ventral areas 12/47 and 45 (**Figure 2A**). Note that the frontal eye field (FEF, mainly area 8A) is here not considered as part of PFC (Miller and Cohen 2001). In primates these areas show a characteristic, i. e. granular layer IV, further distinguishing prefrontal from other cortical areas (Petrides 2005, Fuster 2008).

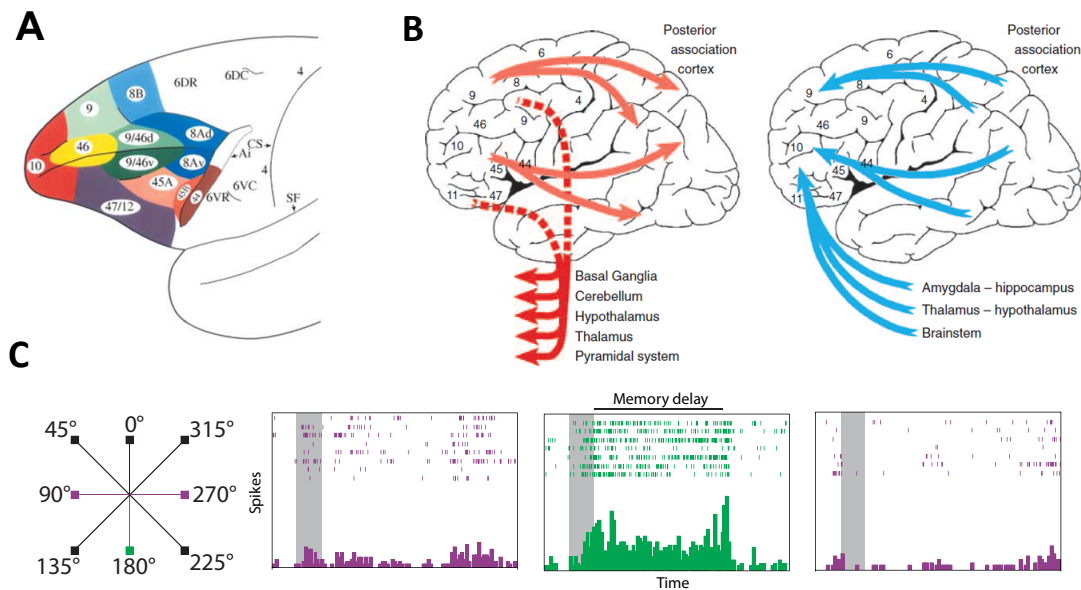


**Figure 2: PFC anatomy and physiology.** **A:** PFC subdivisions after Petrides (2005). Note that some authors do not include FEF (area 8A) to PFC (Miller and Cohen 2001). Copied from Petrides (2005). **B:** PFC is heavily connected to cortical and subcortical areas. Copied from Fuster (2008). **C:** ODR task (left), in which monkeys have to memorize the location of a spatial cue, which can be one of eight locations, during a memory delay to make a saccade towards the remembered location in the subsequent test phase. Neurons in LPFC show characteristic sustained responses during the delay period only for their preferred spatial locations, i. e. are spatially tuned (180° for the example neuron shown here, only an example subset of directions shown). Modified from Arnsten (2009).

**Prefrontal cortex connections** PFC is reciprocally connected to cortical associative sensory areas of all sensory modalities, including connections with somatic, visual, auditory, gustatory and olfactory areas (**Figure 2B**) (Miller and Cohen 2001, Fuster 2008, Tanji and Hoshi 2008). Thus, PFC receives sensory information from all modalities that are previously largely separated. In addition, PFC receives strong inputs from the MDNT, probably relaying information from other subcortical areas such as movement information, since MDNT receives input from parts of the basal ganglia and the cerebellum (Fuster 2008). In addition, PFC receives direct input from basal ganglia, the limbic system including the amygdala, and the hypothalamus (Fuster 2008). Of special interest for my thesis, and because of their regulatory role over broad cortical areas, are PFC afferents from neuromodulatory systems including the cholinergic system of the basal forebrain, the noradrenergic system of the locus coeruleus, the serotonergic system of the raphe nuclei, and the dopaminergic system of the ventral tegmental area and substantia nigra (Fuster 2008, Arnsten and Li 2004). These systems likely provide information about internal states of the organisms, including arousal, attention, motivation, and reward expectation. PFC projects also back to many of these subcortical areas, establishing feedback loops on several levels (Fuster 2008). Finally, PFC is reciprocally

connected to cortical motor areas, in particular pre-motor areas (Tanji and Hoshi 2008).

**Functional heterogeneity** Connections to PFC are not uniformly distributed. Medial and orbital areas in PFC are more strongly connected to limbic areas and, accordingly, are more strongly involved in motivation and emotional processing (Bechara et al. 2000). Within LPFC, which is the focus of my thesis, a functional segregation of dorsal (area 9/46) and ventral areas (area 12/47 and 45) has been proposed. Based on connection patterns and lesion studies, ventral LPFC has been argued to be involved mainly in retrieving and maintaining representations, whereas dorsal LPFC has been proposed to support the manipulation of working memory to select an action (Petrides 2000, Curtis and D'Esposito 2003). In addition, it has been argued that ventral LPFC represents mainly visual information, whereas dorsal PFC represents mainly spatial information based by lesion and electrophysiological studies (Goldman-Rakic 1988, Wilson et al. 1993). However, visuo-spatial integration during working memory has been characterized in both ventral and dorsal LPFC (Rao et al. 1997).

**Conclusion** Together, evidence from functional anatomy suggests that the PFC operates at the top of the cortical hierarchy during sensorimotor processing (Miller and Cohen 2001, Badre and D'Esposito 2009). PFC is strongly interconnected with multi-modal association areas in parietal cortex, which has repeatedly been shown to be involved in executive functions, too, suggesting that PFC does not act in isolation but through a fronto-parietal network (Nieder and Miller 2004, Salazar et al. 2012, Siegel et al. 2015).

### 1.2.2. Executive functions involving prefrontal cortex

**Visual signals and perceptual decision-making** The PFC represents sensory signals similarly to sensory cortices. For example, neurons in LPFC are tuned to motion direction, motion speed, and luminance of visual stimuli (Hussar and Pasternak 2009, 2013, Constantinidis et al. 2001). Strikingly, sensory properties of these stimuli modulate representation of working memory (Constantinidis et al. 2001) and are dependent on the behavioral context: Tuning of neurons in LPFC was stronger when monkeys were required to use that information to guide behavior (Hussar and Pasternak 2009), although it has been repeatedly reported that neurons in PFC represent sensory signals even if they are not behaviorally relevant (Mante et al. 2013, Viswanathan and Nieder 2013). During the detection of faint visual stimuli, the activity of a portion of LPFC neurons correlates with stimulus intensity (Merten and Nieder 2012). However, a larger amount of neurons encoded the subjective percept of the animals. They showed categorical responses in action potential rates, which correlated with the animal's choice about presence and absence of the stimulus independently of motor preparation (Merten and Nieder 2012). Similarly, visual signals during decision making propagate from primary sensory cor-



tics to PFC, where choice signals emerge for the first time, and then to pre-motor areas (Siegel et al. 2015). The same principle was found for somatosensory detection tasks, in which choice signals about the presence or absence of tactile stimuli were stronger for frontal as compared to sensory cortical areas (de Lafuente and Romo 2006). Together, PFC is likely involved in transforming parametric sensory signals into categorical choice signals to support goal-directed behavior.

**Working memory and categories** Single neurons in LPFC show a characteristic sustained response selective for items held in working memory. The most widely used paradigm to investigate neuronal correlates of working memory is the oculo-motor delayed response (ODR) task, in which monkeys are required to remember the location of a target during a memory delay period to make a saccade towards remembered target location in the subsequent choice period (Goldman-Rakic 1995). A subset of neurons in LPFC encode the target location throughout the delay period by exhibiting sustained high activity to only a specific target location, with decreasing activity to more distant location constituting a spatial memory field (**Figure 2C**) (Goldman-Rakic 1995, Funahashi et al. 1989, Fuster 1973). Neurons in LPFC can also be tuned to visual objects during memory-based object recognition tasks (Rainer et al. 1998, Rao et al. 1997, Wilson et al. 1993). In addition, neurons in LPFC encode categories irrespective of their precise sensory appearance. In one study, monkeys had to categorize pictures to either belonging to the cat or dog category, while stimuli were systematically morphed between those categories (Freedman et al. 2001). Neurons in LPFC reflected category membership of the stimulus rather than their visual appearance (Freedman et al. 2001). Neurons in LPFC encode the magnitude of items in a visual display, irrespective of sensory appearance (Nieder 2002). Numerosity stimuli were controlled for visual appearance, density, total covered area, and other features. The neurons showed characteristic tuning curves, with decreasing activity for more distant numerosities, and broader tuning curves for larger numerosities (Nieder and Miller 2003). Thus, neuronal activity matched behavioral properties in agreement with Weber's law, reflecting both numerical distance and numerical magnitude effects (Nieder and Miller 2003, Nieder and Merten 2007).

**Behavioral rules** In a classic test assessing the ability to switch between task rules, the Wisconsin card sorting test (WCST), subjects are required to sort a test item to an existing card deck based on either the color or the shape of the test item. The rules ("sort color" or "sort shape") change after a couple of trials without explicit instructing. Subjects have to adjust their behavior based on the feedback after every trial (correct or wrong). Patients with PFC damage have difficulties switching between these rules (Milner 1963). Monkeys can perform the WCST, too, and functional imaging studies suggest that the LPFC is involved in switching between task rules (Nakahara et al. 2002). Lesion studies

in monkeys suggest a specific role for LPFC in maintaining task rules, whereas other prefrontal and frontal areas are specifically involved in error monitoring and updating rules (Buckley et al. 2009). In addition, neurons in LPFC represent task rules (Mansouri 2006).

An alternative approach is explicitly cueing the rule currently in effect, which also requires rule representation and rule switching but a lesser demand in error monitoring (Stoet and Snyder 2009). In one study, monkeys had to report if two successively presented pictures were the same or different depending on a cue that instructed the monkeys which rule they had to use (Wallis et al. 2001). Neurons in LPFC reflected the abstract behavioral rule, irrespective of the actual pictures that were shown. Using rule-switching tasks, similar results have been reported for a number of different rules (Hoshi et al. 2000, Asaad et al. 2000, Genovesio et al. 2005). Even abstract arithmetic rules, such as “greater than” and “less than” comparisons, are encoded by LPFC neurons (Bongard and Nieder 2010, Vallentin et al. 2012, Eiselt and Nieder 2013). In these tasks, monkeys were required to report if a test numerosity, i. e. the number of items in a visual display, was larger or smaller than a preceding sample item, based on a rule cue indicating which rule was currently in effect. Neurons in LPFC encoded the abstract arithmetic rule irrespective of the numerosities or the sensory appearance of the rule cues. The PFC’s involvement in applying rules is supported by patients with prefrontal lesions, who show impairments retrieving task context (Chapados and Petrides 2015), as well as lesioned animals that show impairments in learning rules (Petrides 1985).

**Goal values** Neurons in PFC reflect the amount of expected reward in situations where monkeys were cued about the amount or quality of reward they would receive after finishing a task (Watanabe 1996, Kennerley et al. 2009, Wallis and Miller 2003, Roesch and Olson 2003). In LPFC, where also working memory signals are present, information about the amount of expected reward modulated visual working memory (Amemori and Sawaguchi 2006) and spatial working memory signals (Kennerley et al. 2009, Kobayashi et al. 2002, Leon and Shadlen 1999, Wallis and Miller 2003, Watanabe et al. 2005). In accordance with LPFC’s role in executive control, neurons in LPFC encoded the monkey’s future response in addition to information about reward size, whereas other PFC areas were only encoding reward size (Wallis and Miller 2003). Thus, the LPFC likely integrates information about goal values expressed by the expected reward with cognitive information to enable goal-directed executive control (Watanabe 2007).

### 1.2.3. Models of prefrontal cortex functions

Despite the variety of specific executive functions, PFC models generalize mechanisms describing how PFC might achieve these functions (Miller and Cohen 2001, Miller and Wallis 2009). According to these models, which rely on the conceptual framework of ex-

ecutive functions discussed previously, context cues can activate PFC populations representing rules or other goal-relevant information (**Figure 3A**). Because they are connected to PFC populations encoding sensory information, which generalizes to information from memories, both populations together can bias the selection of a particular action, which is distinct from the selection of another action when a different context activates a different population of PFC neurons. In this model, connections between neurons and populations are reinforced if the outcome is rewarding, likely mediated by dopamine signaling (Miller and Cohen 2001, Miller and Wallis 2009).

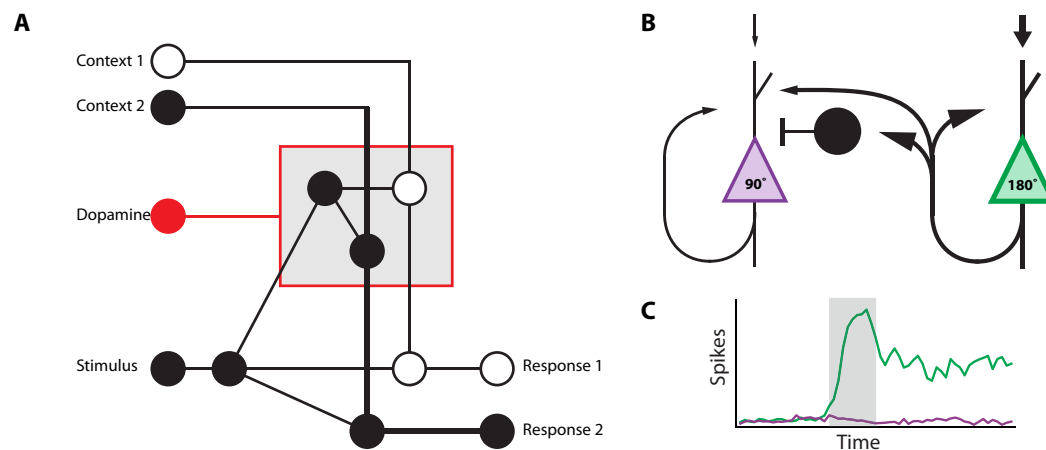


**Figure 3: Models of prefrontal cortex functions.** **A:** Context-specific cues from the environment activate specific PFC populations (grey box) that together with sensory signals relevant for behavior trigger the selection of particular actions. Through conditional associations, a different context can lead to the selection of a different action. PFC networks are influenced by dopamine (red). Circles represent neuronal population, lines connections between populations. After Miller and Cohen (2001). **B:** Schematic model architecture used in computational models of PFC networks. Pyramidal cells (triangles) are tuned to specific spatial directions and have recurrent excitatory connections and connections to GABA-ergic interneurons (circle), which project to pyramidal cells. If one selective pool is stimulated (180°), sustained working memory activity is mediated by recurrent NMDA connections and lateral inhibition through interneurons, which suppress population selective for other directions and dominate during spontaneous activity states with low firing rates. Note that axonal subcellular target regions are largely unknown and ignored in this schematic. Architecture from Goldman-Rakic et al. (2000), Brunel and Wang (2001), and Durstewitz et al. (2000b). **C:** Neurons in the network can switch from a stable spontaneous activity state with low firing rate to a stable high-activity state with high firing rate after transient stimulation (gray box) of a selective subpopulation (green population in **B** selective for 180°). Own simulation with network parameters from Brunel and Wang (2001).

Within PFC, the integration of a variety of goal-related information across time requires a sustained signal, which is most obvious during working memory processing. Based on anatomical evidence and electrophysiological studies, Goldman-Rakic (1995) proposed a network architecture to implement working memory (**Figure 3B**). This architecture has been used to build biologically-plausible computational models describing how PFC networks might implement working memory processes (Durstewitz et al. 2000b, Brunel and Wang 2001, Constantinidis and Wang 2004). The network architec-

ture relies on excitatory recurrent connections mediated mainly by  $\alpha$ -amino-3-hydroxy-5-methyl-4-isoxazolepropionic acid (AMPA) and *N*-Methyl-D-aspartate (NMDA) receptors. NMDA receptors have long postsynaptic currents, which allow for integrating activity over longer timescales. In addition, inhibitory connections from  $\gamma$ -Aminobutyric acid-(GABA-)ergic interneurons to pyramidal cells balance the excitatory drive, shaping selective responses of pyramidal cells by inhibition, which is also supported by electrophysiological studies (Rao et al. 2000, Constantinidis et al. 2002). These attractor networks show two stable states: a spontaneous, low activity state dominated by inhibitory currents and a persistent, high activity state of a subset of pyramidal cells with strong recurrent excitatory connections dominated by NMDA currents (Brunel and Wang 2001, Wang 1999). The persistent activity state is stable even without external stimulation. These models were used to describe spatial (Constantinidis and Wang 2004, Durstewitz et al. 2000b, Compte et al. 2000) and object working memory (Brunel and Wang 2001) processes in PFC.

Experimental evidence supports the predicted prominent role of NMDA receptors in mediating the sustained high-activity state as blocking NMDA receptors impaired sustained responses (Wang et al. 2013, Seamans et al. 2003). The power of attractor networks models is further demonstrated by their ability to generalize to a number of other functions for executive control. The same model architecture has been applied to problems in perceptual decision-making (Wang 2002, 2008), reward-based decision-making (Deco et al. 2013), and the learning of category representations (Engel et al. 2015). In addition, they allow for investigating neuromodulation in cortical networks. By changing synaptic conductances in the model, mechanisms for dopamine modulation of prefrontal networks have been proposed (Durstewitz et al. 2000a, Brunel and Wang 2001).

### 1.3. Dopamine modulation of executive control

#### 1.3.1. Dopamine systems in the brain

Dopamine belongs to the catecholamines together with epinephrine and norepinephrine (Björklund and Lindvall 1984). Several nuclei in the brain stem contain dopaminergic neurons, with the largest assembly of dopaminergic neurons found in the mesencephalic dopamine system of the primate brain (Felten and Sladek 1983). It consists of the cell groups A8, A9 and A10 (Felten and Sladek 1983, Williams and Goldman-Rakic 1998). The area A8 lies dorsal to the lateral part of the substantia nigra. A9 corresponds to the substantia nigra pars compacta and A10 to the ventral tegmental area of the mesencephalon. Humans and macaques have less than 400,000 dopaminergic neurons (Stark and Pakkenberg 2004), which project to many subcortical and cortical areas exerting a widespread control of brain function, characteristic of a neuromodulator (Björklund

and Lindvall 1984). Three main subdivisions of the mesencephalic dopamine system can be distinguished. The mesostriatal pathway projects to the basal ganglia and has an important role in the voluntary execution of movement (Obeso et al. 2008). The mesolimbic pathway projects to a variety of structures belonging to the limbic system and has been extensively studied with respect to its function in motivation, learning, and addiction (Wise 2009, 2004). Finally, the mesocortical pathway projects mainly to the frontal lobe and modulates cognitive functions such as working memory (Seamans and Yang 2004). Dopamine acts on five different dopamine receptors D<sub>1</sub>–D<sub>5</sub>, which are G protein coupled receptors modulating intracellular signaling cascaded rather than producing postsynaptic currents directly (Jackson and Westlind-Danielsson 1994, Seamans and Yang 2004). Based on structural and pharmacological similarities, these receptors fall into two main receptor types, the D1-like receptor family (D1R) with subtypes D<sub>1</sub> and D<sub>5</sub> and the D2-like receptor family (D2R) with subtypes D<sub>2</sub>, D<sub>3</sub> and D<sub>4</sub> (Jackson and Westlind-Danielsson 1994, Seamans and Yang 2004).

### 1.3.2. The mesocortical dopamine system

Dopaminergic projections to the cortex can be separated into two parallel systems (Williams and Goldman-Rakic 1998): Projections that originate mainly from A10 innervate the anterior cingulate cortex (area 24) and medial frontal areas (areas 14 and 32) in both primates and rodents, which is often assigned to the mesolimbic pathway. In addition, primates developed a distinct mesoprefrontal dopamine system projecting particularly to dorsal and lateral areas of the PFC (areas 12/47, 9/46, and 9). This pathway originates from the area A8 and A9 and to a lesser extent from A10, thus from more lateral parts of the midbrain dopamine system, establishing a medial-to-lateral projection topography (**Figure 4A**) (Williams and Goldman-Rakic 1998). Compared to other cortical areas, the PFC exhibits the highest dopamine concentrations and synthesis rates (Brown et al. 1979).

Within primate PFC, dopaminergic fibers innervate both pyramidal cells and interneurons forming synaptic contacts with somas, dendritic shafts, and dendritic spines (Goldman-Rakic et al. 1989, Smiley and Goldman-Rakic 1993). Contacts with spines on pyramidal cells establish synaptic triads with the postsynaptic neuron receiving another, presumably glutamatergic input (Goldman-Rakic et al. 1989). Dopamine receptors are located postsynaptically on dendritic spines (Bergson et al. 1995), but even more often found extrasynaptically (Smiley et al. 1994), suggesting that dopamine controls cortical information processing via diffusion in the neuropil (volume transmission) (Zoli et al. 1998).

D1Rs are expressed in all cortical layers in primate LPFC and are about 10-fold more abundant than D2Rs (Lidow et al. 1991). D2Rs, in contrast, have low expression rates in most layers showing highest expression rates in layer V (Lidow et al. 1991, 1998).

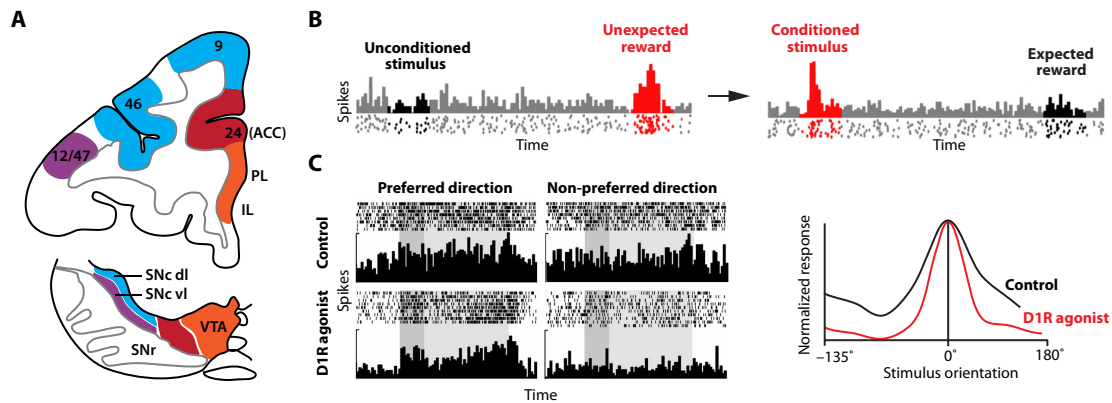


**Figure 4: Dopamine modulation of PFC.** **A:** Mesocortical dopamine projections show a ventromedial-dorsolateral projection topography, where medial dopamine neurons project to medial frontal areas and lateral dopamine neurons project to PFC and LPFC. ACC, anterior cingulate cortex; PL, prelimbic cortex; IL, infralimbic cortex; VTA, ventral tegmental area; SNc, substantia nigra pars compacta; SNr, substantia nigra pars reticulata; dl, dorsolateral; vl, ventrolateral. Modified from Ranganath and Jacob (2015) with data compiled from Williams and Goldman-Rakic (1998). **B:** Dopamine neurons fire phasic bursts in response to unexpected reward (left) and to reward predicting cues (right), thus signaling reward prediction errors. Modified from Bromberg-Martin et al. (2010). **C:** Application of D1R agonists in LPFC enhances spatial tuning primarily by inhibiting responses to non-preferred spatial directions. Left, single neuron example; right, population tuning curve. Modified from Vijayraghavan et al. (2007).

D1Rs and D2Rs are expressed in both pyramidal cells and interneurons (de Almeida and Mengod 2010, Smiley et al. 1994, Mrzljak et al. 1996, Muly et al. 1998) suggesting that dopamine modulates both excitatory and inhibitory synaptic transmission.

### 1.3.3. Dopamine physiology

#### Dopamine signal

In monkeys, dopamine neurons respond with short, phasic bursts of activity when presented with appetitive stimuli, such as food or fruit juice (Schultz 1986, Schultz and Romo 1990, Romo and Schultz 1990). These responses are independent of the different types of appetitive stimuli and occur in the majority of recorded dopamine neurons. Remarkably, after classical conditioning of an unconditioned stimulus with a reward, dopamine neurons shift their phasic activation from the time of reward delivery to the time of presentation of the conditioned stimulus (**Figure 4B**) (Ljungberg et al. 1992). Dopamine neurons are not active during the delay between conditioned stimulus and reward delivery (Ljungberg et al. 1991). In addition, unexpected omission of reward leads to a suppression of dopamine neuron activity. The peak activity of dopamine bursts is correlated with the expected amount of reward (Tobler et al. 2005). These findings lead to the theory that dopamine neurons signal the reward prediction error

used for reinforcement learning (Schultz et al. 1997, Schultz 2006, 1998).

More recent experiments revealed that some dopamine neurons also respond to aversive stimuli, which seem to belong to a specific subset of dopamine neurons located in dorsolateral parts of the substantia nigra (Matsumoto and Hikosaka 2009). In addition, neurons in dorsolateral substantia nigra were activated by behaviorally relevant visual stimuli needed to solve a visual search task requiring working memory, whereas ventromedial dopamine neurons represented reward prediction errors (Matsumoto and Takada 2013). These findings suggest that dopamine may convey distinct signals serving different functions along the dorsolateral-medioventral axis (Matsumoto and Takada 2013), with ventromedial dopamine neurons carrying reward prediction error signals and dorsolateral dopamine neurons carrying saliency signals (Bromberg-Martin et al. 2010). Remarkably, dopamine neurons in the dorsolateral midbrain project specifically to LPFC (Williams and Goldman-Rakic 1998), which indicates that the saliency signal conveyed by dopamine neurons during cognitive tasks modulates LPFC networks mediating executive control.

Reward signals and cognitive signals converge in the PFC, and reward signals likely modulate cognitive signals relevant for executive control such as working memory (Watanabe 2007). However, it remains unclear if dopamine mediated reward signals modulate memory signals directly. Given that dopamine neurons seem to carry distinct signals (Schultz 2007, Bromberg-Martin et al. 2010), it is conceivable that PFC signals about reward and working memory signals are distinctly modulated by dopamine.

### **Dopamine receptor mechanisms of action in prefrontal cortex**

**D1R mechanisms** D1Rs and D2Rs have been demonstrated to modulate the responsiveness of PFC neurons via a variety of cellular mechanisms, of which only the most prominent ones can be introduced here (Seamans and Yang 2004). D1R stimulation shows an overall inhibitory effect on PFC neurons *in vivo* (Vijayraghavan et al. 2007, Williams and Goldman-Rakic 1995). This inhibition might be mediated by amplifying inhibitory post-synaptic currents in pyramidal cells (Trantham-Davidson et al. 2004) or weakening non-NMDA-glutamatergic responses (Seamans et al. 2001a). At the same time, D1R stimulation shows a specific excitatory effect by potentiating only NMDA-evoked responses *in vitro* (Seamans et al. 2001a, Tseng and O'Donnell 2004).

**D2R mechanisms** D2R stimulation, oppositely, shows an overall excitatory effect *in vivo* (Wang et al. 2004a). This excitatory effect might be mediated by a decrease of GABA-evoked inhibitory currents in pyramidal cells (Seamans et al. 2001b, Trantham-Davidson et al. 2004). On the other hand, D2Rs have been demonstrated to show inhibitory effects, too. D2Rs decrease NMDA-evoked responses in pyramidal cells via interneurons (Tseng

and O'Donnell 2004) and increase interneuron excitability (Zhong and Yan 2016).

Together, D1Rs and D2Rs show both excitatory and inhibitory effects when investigated in isolation *in vitro*. However, D1Rs and D2Rs seem to differentially modulate synaptic currents in distinct cell types.

### 1.3.4. Dopamine modulation of prefrontal cortex functions

#### Visual signals and attention

**Stimulus detection** During the detection of faint stimuli, PFC neurons signal the choice of the animal about presence or absence of the stimulus, i. e. the monkeys' subjective percept rather than physical stimulus intensity (de Lafuente and Romo 2005, 2006, Merten and Nieder 2012). Recordings from midbrain dopamine neurons during stimulus detection revealed that dopamine activity reflects perceived stimulus intensity, too, rather than physical stimulus intensity, since dopamine neurons were only active when the animals successfully detected the stimulus (de Lafuente and Romo 2011). Remarkably, the latency of dopamine neurons reflecting the animals choice matched the latency of choice signals in frontal cortex, lacking behind visual signals in sensory cortex (de Lafuente and Romo 2012). These findings suggest that dopamine might prepare its higher-order target areas for the processing of incoming signals (Redgrave and Gurney 2006, de Lafuente and Romo 2011). However, it remains unknown if dopamine modulates visual signals in PFC directly, which would be a prediction from this hypothesis.

**Attentional processing** Noudoost and Moore (2011a) manipulated dopamine signaling in FEF while monkeys could choose a target by making a saccade in a free-choice task. Both D1R and D2R manipulation increased target selection towards the location in space, where the receptive fields of the manipulated site was. In addition, only D1R manipulation changed visual signals in V4 resembling effects observed after shifting spatial attention towards the receptive field (Noudoost and Moore 2011a, Reynolds et al. 2000). Based on the distribution of prefrontal dopamine receptors, Noudoost and Moore (2011b) suggested that only D1Rs modulate visual signals in V4 possibly by intracortical connection from superficial layers in FEF, while D2Rs modulate target selection by sub-cortical connections from deep layers. These findings support the idea that dopamine mediates the attention-dependent modulation of visual signals also observed in visual cortices (Arsenault et al. 2013). The source of this attentional signals is likely the PFC (Clark and Noudoost 2014), given that dopamine signaling in frontal cortex modulates neuronal activity in visual cortices (Noudoost and Moore 2011a,b). However, it remains unclear if dopamine also modulates visual signals in PFC directly, which as discussed above are clearly present in PFC.



### Working memory modulation

**Role of D1R** First direct evidence for an involvement of dopamine in cortical functions was found by depleting dopamine in PFC, which lead to an impairment of working memory that could partially be rescued by pharmacologically increasing dopamine levels (Brozoski et al. 1979). Blocking D1Rs impairs spatial working memory performance in studies using the ODR task (Sawaguchi and Goldman-Rakic 1991, 1994) and in visual working memory tasks in humans (Müller et al. 1998). Stimulating D1Rs improves working memory performances in dopamine depleted animals, but not controls (Arnsten et al. 1994), supporting the notion that the effects of D1R activation in PFC is dose-dependent following an inverted-U response curve, where sub- or supra-optimal D1R activation is detrimental for working memory performance (Arnsten 2011). This dose-dependency has been found in LPFC neurons. When stimulating D1Rs of LPFC neurons during an ODR task using micro-iontophoresis, the tuning of the neurons' memory fields is enhanced at an optimal dose (**Figure 4C**), following an inverted-U response curve with little stimulation having no effect and large stimulation having detrimental effects on tuning (Vijayraghavan et al. 2007). Blocking prefrontal D1Rs impairs spatial memory fields (Sawaguchi 2001), but has also been reported to improve spatial tuning of LPFC neurons (Williams and Goldman-Rakic 1995).

**Role of D2R** D2R modulation of working memory has been less clear. D2R stimulation has been shown to influence working memory performance in monkeys and humans by increasing or decreasing performance (Arnsten et al. 1995, Gibbs and D'Esposito 2005, Von Huben et al. 2006, Mehta et al. 2001), depending on the subject's baseline performance (Clark and Noudoost 2014). Blocking D2Rs often produced no effects on working memory performance (Sawaguchi and Goldman-Rakic 1994), but has also been shown to impair working memory performance in monkeys (Von Huben et al. 2006) and humans (Mehta et al. 2004, Clark and Noudoost 2014). However, electrophysiological studies failed to find any effects on spatial mnemonic activity during the delay period in ODR tasks after stimulating or blocking D2Rs in LPFC (Wang et al. 2004a, Williams and Goldman-Rakic 1995).

**Conclusion** Together, evidence from human and animal studies show a strong involvement of D1Rs in working memory processing. The lack of physiological evidence of D2R modulation on spatial mnemonic processing (Wang et al. 2004a) lead to the view that D2Rs seem to be less involved in modulating working memory processing, despite behavioral evidence that suggest an involvement of D2Rs in working memory, too (Arnsten 2011, Seamans and Yang 2004, Clark and Noudoost 2014).

## **Behavioral flexibility**

**Animal studies** Evidence for an involvement of D1Rs in executive functions other than working memory mainly comes from animal behavioral studies. In rodent studies assessing behavioral flexibility, rats learned to enter a specific arm in a maze based on either a spatial strategy (e.g., “turn right”) or on a visual strategy (e.g., “select arm with visual cue”) (Floresco and Magyar 2006). Blocking D1Rs impairs flexibly switching between the different response strategies, without impairing learning of the strategies (Ragozzino 2002, Floresco and Magyar 2006). An even stronger influence was reported by blocking D2Rs, which lead to an impaired performance by increasing perseverative errors, i.e. rats maintained the same response strategy and needed much more trials to shift their strategy (Floresco and Magyar 2006, Floresco et al. 2006). Similarly, depleting dopamine in PFC impaired learning new cue-reward associations in marmoset monkeys (Crofts et al. 2001). Recently, Puig and Miller (2012) trained macaque monkeys to form associations between arbitrary visual items and saccade directions. After a sample item and a delay period, monkeys were required to make a saccade towards right or left depending on the item shown before. Blocking D1Rs in PFC impaired the monkey’s ability to learn new associations while not strongly affecting selecting familiar associations (Puig and Miller 2012). Blocking D2Rs impaired learning new associations, too (Puig and Miller 2015). In addition, blocking D2R increased perseverative errors, which was not observed for blocking D1Rs (Puig and Miller 2015). Further, blocking either D1Rs or D2Rs reduced neural signatures of associations encoding the upcoming response in LPFC (Puig and Miller 2012, 2015).

**Human studies** In humans, D1R availability in human PFC is positively correlated with flexibly shifting between rules during the WCST (Takahashi et al. 2008, 2012). Blocking D2Rs impaired shifting between response strategies in a variation of the WCST, in which subjects had to learn new visual discriminations based on different stimulus dimensions (Mehta et al. 1999). Stimulating D2Rs improved performance of subjects in a WCST (Kimberg et al. 1997) and increased functional imaging signals in frontal cortex during rule switching (Stelzel et al. 2013). These findings lead to the conclusion that cognitive flexibility is mainly mediated by D2Rs (Klanker et al. 2013).

**Conclusion** Together, primarily behavioral evidence suggests a complementary role for both D1Rs and D2Rs in mediating behavioral flexibility with a specific role of D2Rs in switching behavioral strategies (Floresco and Magyar 2006, Floresco 2013). However, cellular mechanisms of dopamine modulation of neuronal signals underlying executive functions beyond working memory are lacking.

### 1.3.5. Models of dopamine modulation of prefrontal cortex

**Qualitative models** Based on models of PFC network architecture and electrophysiological evidence about D1R modulation of prefrontal neurons, Goldman-Rakic et al. (2000) proposed a network architecture describing how D1R might modulate PFC networks to mediate the observed changes in spatial tuning during working memory, which proposes a gating mechanism of excitatory input to both pyramidal cells and interneurons. Later, Arnsten (2011) and Arnsten et al. (2012) proposed a model, in which D1Rs primarily modulate lateral connections by reducing excitatory input from pyramidal neurons with opposite tuning or increasing inhibition from interneurons to pyramidal cells (Figure 5A) based on their finding that D1R stimulation primarily reduced responses to nonpreferred spatial directions (Vijayraghavan et al. 2007).

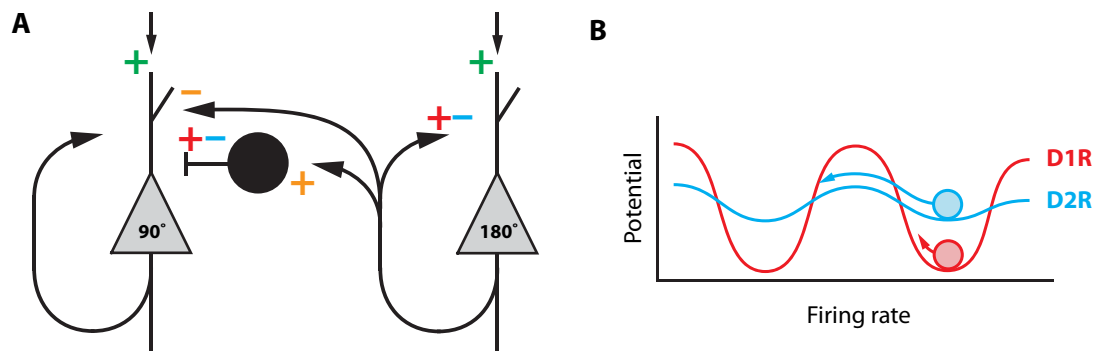


**Figure 5: Models of dopamine modulation of prefrontal cortex.** **A:** Same basic model architecture as in Figure 3B. Dopamine modulates PFC networks by changing synaptic conductances in the model. Orange, proposed D1R effect on sculpting PFC representations by decreasing lateral excitatory connections or increasing interneuron excitability (Arnsten 2011). Red, proposed D1R modulation by computational models suggesting an increase in recurrent NMDA currents and an increase in GABA currents (Durstewitz et al. 2000a). Blue, proposed D2R modulation by computational models opposite from D1R modulation (Durstewitz and Seamans 2008). Green, proposed gating mechanism by dopamine (Cohen et al. 1996). **B:** Dual-state theory of D1R/D2R activation in PFC proposing a D1R-dominated state with stable, i. e. deep basin attractors and a D2R-dominated state with flexible, i. e. shallow basin attractors. After Rolls et al. (2008).

**Computational models for D1R** Using biologically-plausible attractor models of PFC networks based primarily on *in vitro* results from primate and rodent studies, Durstewitz et al. (2000a) proposed a model in which D1R stimulation enhances the stability of PFC representations by increasing neuronal responses to preferred rules and at the same decreasing spontaneous activity, together increasing the neurons' selectivity during working memory (Figure 5A). This effect was mediated first by an increase of GABA currents, which decreased the spontaneous activity of pyramidal cells. Second, sustained high-activity states, were enhanced by increasing NMDA currents in the model

(Durstewitz and Seamans 2002, Brunel and Wang 2001). This model is in agreement with early electrophysiological studies (Williams and Goldman-Rakic 1995, Sawaguchi 2001). However, the proposed mechanism by which D1R enhances working memory tuning relies primarily on the increase of recurrent excitatory connections mediated by NMDA-receptors, which is the opposite mechanism proposed by Arnsten (2011) and Arnsten et al. (2012) discussed above. It remains to be resolved if the model can explain a reduction in responses to nonpreferred directions, without changing responses to preferred directions as reported by Vijayraghavan et al. (2007).

**Dual-state theory of prefrontal cortex dopamine function** Based on the finding that D2Rs show some *in vitro* effects opposite from D1Rs, which are mainly a D2R-mediated decrease and a D1R-mediated increase in GABA responses, Seamans et al. (2001b) and Seamans and Yang (2004) proposed a conceptual framework for dopamine modulation of prefrontal networks. In this framework, PFC networks are either in a D1R-dominated state, in which an increase in recurrent excitation and a decrease in spontaneous activity stabilizes current representations in working memory. Conversely, a D2R-dominated state reduces inhibition in the networks allowing for fluctuations between representations, rendering PFC networks more flexible and enabling switching between different representations in accordance with the role of D2Rs in mediate behavioral flexibility (**Figure 5B**). These states might be controlled in time: dopamine might first support dynamic updating of prefrontal representations via a D2R-dominated state, and subsequently stabilize a limited amount of representations via a D1R-dominated state, shutting down irrelevant representations and safeguarding representations from distractors (Seamans et al. 2001b, Seamans and Yang 2004). This idea has been translated into biologically-plausible network models using the same architecture as before, incorporating a proposed D1R and D2R modulation (Durstewitz and Seamans 2008). For D1Rs, the same modulation as proposed before stabilizes prefrontal representations (Durstewitz et al. 2000a, Durstewitz and Seamans 2002). For D2Rs, the opposite mechanism of decreasing GABA currents and increasing NMDA currents in the model produced unstable representations with spontaneous transitions between spontaneous and high-activity states (Durstewitz and Seamans 2008).

**Attractor hypothesis of schizophrenia** The dual-state theory of prefrontal cortex dopamine function has been linked to clinical symptoms of schizophrenia, forming the attractor hypothesis of schizophrenia (Rolls et al. 2008). In this model, excessive D2R activation produces unstable representations in PFC leading to positive symptoms such as hallucinations and intrusion of thought (Mueser and McGurk 2004). Accordingly, blocking D2Rs is the common mechanism of all antipsychotic drugs used to treat positive symptoms of schizophrenia (Seeman 2002).

**Gating model of dopamine** The attractor model is in agreement with another view of dopamine functions, in which the short-lived phasic dopamine signal gates sensory input to PFC (**Figure 5A**) (Cohen et al. 1996, 2002). This idea is supported by properties of dopamine neurons, which exhibit short-latency signals in response to salient events. In a functional imaging study, D'Ardenne et al. (2012) found that LPFC encoding of context was correlated with the amount of phasic activation of midbrain dopamine areas suggesting that dopamine gates the updating of prefrontal working memory representations. Further, dopamine neurons fire phasic bursts in response to faint stimuli in a detection task and show no response if the animals failed to detect the stimulus (de Lafuente and Romo 2012, 2011).

**Conclusion** Together, models about dopamine functions in PFC suggest that dopamine gates representations in PFC and subsequently controls the stability of prefrontal sustained representations by balancing D1R/D2R activation. For D1R, the models are supported by electrophysiological studies in monkeys reporting a D1R-mediated modulation of working memory processes. However, the models also predict a prominent D2R modulation of sustained responses in PFC, which has not been reported *in vivo*. In particular, the models predict that the ratio of D1R/D2R activation controls dynamic properties of prefrontal networks when representations are updated.

#### 1.4. Open questions

**Box 1. Open questions about dopamine modulation of executive functions addressed in my thesis.**

1. What are the cellular basis and mechanisms of dopamine modulation of executive functions beyond working memory?
  - (i) Visual signals relevant for perceptual detections
  - (ii) Behavioral rules
2. What is the precise role of D2Rs in working memory processing?
3. Is there physiological evidence for predictions by computational models about dopamine's role in stabilizing representations?
4. Does dopamine modulate reward signals and cognitive signals by a common mechanism?

Based on the key features of executive functions, PFC, and dopamine discussed in the previous sections, I want to highlight some of the main questions that we need to address to understand dopamine's role in modulating executive functions in PFC

**(Box 1).** These questions emerge from the lack of studies investigating how dopamine modulates physiological underpinnings in the PFC.

First, electrophysiological studies almost exclusively used the ODR task to investigate working memory. However, as discussed above, executive functions comprise a much larger range of specific abilities not previously addressed, such as behavioral rules and perceptual decisions. In addition, the ODR task has severe limitations in interpreting the sustained activity during memory delay, which might be attributed to motor processing (Markowitz et al. 2015, Takeda and Funahashi 2004) or attentional processing (Lebedev et al. 2004) due to constraints in task design. Second, the role of D2Rs has been neglected, although behavioral, clinical and computational evidence suggest a strong involvement of D2Rs in working memory and executive control. Third, there is a gap between physiological data and computational models, which propose a strong role of both D1R and D2R in modulation PFC neurons and networks by controlling the stability of prefrontal representations. Finally, it is unclear if dopamine signals about expected reward and dopamine modulation of cognitive signals, which are both present in PFC, share common properties or if both systems are modulated independently.

In my thesis, I want to address these questions by training macaque monkeys on tasks requiring executive control, recording from single neurons in LPFC and pharmacologically stimulating and blocking dopamine receptors using micro-iontophoresis. In addition, I want to use computational models to test if predictions from dopamine mechanisms of action apply to my experimental data and, reversely, test concepts proposed by existing models to my experimental data.

---

## 2. Main results

### 2.1. Statement of contributions

This thesis comprises 5 publications, which are summarized in the following sections and in **Box 2**. The individual publications and manuscripts can be found in **Part II**.

1. Jacob\*, S. N., **Ott\***, T., Nieder, A. (2013). Dopamine regulates two classes of primate prefrontal neurons that represent sensory signals. *Journal of Neuroscience* **33**(34):13724–34. (\*shared first-authorship)

I trained the monkeys and performed electrophysiological recordings together with S. N. Jacob. I analyzed the data together with S. N. Jacob. I wrote the paper with S. N. Jacob and A. Nieder.

2. **Ott, T.**, Jacob, S. N., Nieder, A. (2014). Dopamine receptors differentially enhance rule coding in primate prefrontal cortex neurons. *Neuron* **84**(6):1317–1328.

I designed the task with A. Nieder. I trained the monkeys and performed all electrophysiological recordings. I analyzed the data. I wrote the paper with A. Nieder. S. N. Jacob provided analysis tools and edited the manuscript.

3. **Ott, T.**, Nieder, A. (under review). Dopamine D2 receptors enhance population dynamics in prefrontal working memory circuits.

I designed the task with A. Nieder. I trained the monkeys and performed all electrophysiological recordings. I analyzed the data. I wrote the paper with A. Nieder.

4. **Ott, T.**, Stein, A. M., Nieder, A. (in preparation). Dopamine D1 and D2 receptors oppositely modulate reward signals in primate prefrontal cortex neurons.

I designed the task with A. Nieder. I trained the first monkey and supervised training of the second monkey, which was mainly trained by A. M. Stein. I performed electrophysiological recordings with A. M. Stein. I analyzed the data. I wrote the manuscript with A. Nieder.

5. Hage, S. R., **Ott, T.**, Eiselt, A.-K., Jacob, S. N., Nieder, A. (2014). Ethograms indicate stable well-being during prolonged training phases in rhesus monkeys used in neurophysiological research. *Laboratory Animals* **48**(1):82–7.

S. R. Hage and A. Nieder designed the study. I contributed to the study by collecting the majority of the behavioral data for focal sampling. Together with S. R. Hage, A.-K. Eiselt and S. N. Jacob, I collected behavioral data for statistical sampling. S. R. Hage analyzed the data and wrote the paper with A. Nieder. I helped in editing the manuscript.

## **2.2. Dopamine modulation of visual signals**

Dopamine modulates executive functions, which rely on the integrity of PFC. Midbrain dopamine neurons fire phasic bursts in response to salient sensory events and predict the detection of faint sensory stimuli. Thus, it has been hypothesized that dopamine acts as a gate allowing for updating prefrontal representations. In PFC, dopamine has been shown to modulate working memory responses of single neurons. However, it is unknown if dopamine controls visual information in PFC that precede memory representations. Here we tested the hypothesis that prefrontal dopamine modulates visual representations needed for perceptual decisions.

We trained two macaque monkeys to detect faint visual stimuli on a screen. Monkeys had to decide about the presence or absence of the visual stimulus to make a correct choice and receive a reward. We simultaneously recorded single neurons in LPFC while applying dopamine to the vicinity of recorded neurons using micro-iontophoresis with custom-made electrode-pipette combinations.

We found that dopamine distinctly modulated two classes of LPFC neurons. One group of neurons was quickly inhibited by dopamine and showed short latencies to visual stimuli. Representation of visual stimuli was retained despite prominent inhibition, which led to an increase in signal-to-noise ratio. This group consisted mainly of narrow-spiking, putative interneurons. The second group was slowly excited by dopamine and showed longer response latencies to visual stimuli. In this class of neurons, encoding of visual stimuli was improved by reducing response variability. This class consisted exclusively of broad-spiking, putative pyramidal cells.

In conclusion, prefrontal dopamine regulated two distinct LPFC populations with distinct properties. The observed effects support the idea that dopamine gates sensory input to PFC and subsequently improves sensory representations needed for perceptual decisions. Thus, dopamine might control the flow of information in PFC shaping how PFC initiates appropriate behavior in response to sensory changes in the environment.

## **2.3. D1R and D2R modulation of behavioral rules**

Applying rules is a key function of executive control enabling goal-directed behavior. By guiding behavior in novel situations, rules enable behavioral flexibility and rapid learning. Neurons in LPFC signal rules relevant to solve a task. Midbrain dopamine neurons strongly innervate PFC modulating flexible behavior. However, the cellular basis for dopamine modulation of rules remains unknown.

In this study, we trained two macaque monkeys to flexibly switch between two behavioral rules. Monkeys had to remember a sample numerosity, i. e. the amount of dots in a visual display, during a delay period to choose if a test stimulus was larger (“larger than” rule) or smaller (“smaller than” rule) than the sample stimulus based on the rule



currently in effect to get a reward. The rule was cued by either a visual or a gustatory stimulus in the delay period between sample and test item presentation to dissociate neuronal responses signaling the abstract rule from responses correlating with sensory features of the rule cue. We recorded 384 randomly selected single neurons in LPFC and simultaneously applied dopamine receptor targeting drugs at the vicinity of the recorded neurons using micro-iontophoresis.

We determined neurons encoding the abstract numerical rule by a significant main factor of rule without an interaction of rule and rule cue modality during the delay period using analysis of variance (ANOVA). About 17% of all recorded neurons (64/384) encoded abstract numerical rules, with similar numbers preferring the “smaller than” rule or the “larger than” rule. D1R stimulation slightly inhibited the spontaneous firing rate of the neurons. At the same time, D1R stimulation increased responses for the preferred rule in the delay period, increasing the neurons’ selectivity for numerical rules. Oppositely, blocking D1Rs increased spontaneous activity impaired encoding of numerical rules. D2R stimulation increased rule coding, too, although by a distinct mechanism. After applying D2R agonists, spontaneous activity was slightly increased, while responses to the non-preferred rule were decreased, thus increasing the neurons’ selectivity for numerical rules. Thus, D1R and D2R both increase rule coding by dif-

**Box 2. Main results of the studies included in my thesis.**

1. Dopamine modulated visual signals in LPFC in two distinct classes of neurons.
  - (i) Dopamine inhibited narrow-spiking neurons increasing signal-to-noise ratio of visual signals with short latencies.
  - (ii) Dopamine excited broad-spiking neurons reducing variability of visual signals with longer latencies.
2. D1R and D2R modulated neuronal rule signals in LPFC by complementary mechanisms.
  - (i) D1R reduced spontaneous activity and enhanced responses of preferred rules.
  - (ii) D2R increased spontaneous activity and reduced responses of non-preferred rules.
3. D2R modulated working memory representations in LPFC.
  - (i) D2R stimulation enhanced working memory signals on single neuron and population levels.
  - (ii) D2R stimulation increased dynamic properties of neuronal networks.
  - (iii) Computational models suggest that interneuron-to-pyramidal signaling underlies the observed effects.
4. D1R and D2R oppositely modulated reward expectancy signals in LPFC neurons.

ferential mechanisms. Drug application left behavioral performance of the monkeys unchanged, but slightly increased reaction times.

In conclusion, our results suggest a complementary mechanism for D1Rs and D2Rs in modulation executive functions in LPFC. D1R and D2R show opposite mechanisms in modulation spontaneous activity. At the same time, both enhance numerical rule coding of LPFC neurons by distinct mechanisms. These results might provide a cellular basis for D1R and D2R stimulation of executive control.

#### **2.4. D2R modulation of working memory**

Working memory, which is the ability to briefly retain and manipulate information in mind, is key function of executive control. Sustained activity in LPFC is considered the neuronal substrate of working memory. Dopamine neurons innervate LPFC modulating spatial working memory performance. Stimulating or blocking D1Rs in LPFC modulates the spatial tuning of neurons during the delay period of spatial working memory tasks. However, D2R manipulation failed to show any modulation of sustained mnemonic activity during spatial working memory. This is surprising, given behavioral, clinical, and computational evidence suggesting a strong role of D2Rs in modulating sustained activity underlying working memory.

Here we tested if D2Rs modulate feature-based working memory of the number of items in a display, i. e. the numerosity information. We trained two macaque monkeys to perform a memory-guide rule switching task, in which the monkeys had to remember a sample numerosity during a memory delay period to indicate in the subsequent test phase if a test numerosity was larger or smaller than the sample numerosity based on the rule currently in effect. We tested a range of sample numerosities to assess neuronal selectivity of sample numerosities during the memory delay period. We recorded 310 randomly selected single neurons in LPFC and simultaneously applied dopamine receptor targeting drugs at the vicinity of the recorded neurons using micro-iontophoresis.

We identified single units selectively encoding the sample numerosities during the memory delay using an ANOVA with significant main effect of sample numerosity. Neurons showed a characteristic tuning with a high firing rate for their preferred numerosity and lower firing rates for more distant numerosities. After D2R stimulation, the neurons' tuning curve was steeper, enhancing working memory representations for numerosities. To assess if coding measures translate to the population level, we analyzed population responses using regression analysis. Similarly, D2R stimulation increased the population code for working memory. Next, we tested if predictions from computational models about the role of D2Rs in rendering prefrontal representations more flexible by using principal component analysis to quantify dynamic properties of neuronal populations. D2R stimulation increased the dynamic responses of LPFC neurons during the transition from sample to memory representations. In contrast, D1R manip-

ulation did not systematically change working memory representations, but decreased the dynamic properties of LPFC populations.

Finally, we tested a biologically-plausible computational model of prefrontal networks to test if predictions about D2R mechanisms of action from *in vitro* studies apply to our experimental findings. Decreasing GABA signaling from interneurons to pyramidal cells and increasing interneuron excitability qualitatively reproduced our experimental findings, i. e. increased spontaneous activity and coding selectivity.

These results suggest a prominent modulation of feature-based working memory representations by D2Rs in LPFC. Computational modeling proposed a potential mechanism of action, suggesting that D2Rs modulate working memory primarily by acting on interneuron-to-pyramidal signaling. In addition, our results are in agreement with models postulating that D2Rs increase dynamic properties of prefrontal populations.

## 2.5. D1R and D2R modulation of reward signals

During executive control, different types of information have to be integrated to enable goal-directed behavior. Both information about expected rewards that signal goal values and working memory information are encoded by LPFC neurons, where there are integrated. For example, expected reward size modulates working memory processing in LPFC neurons. Dopamine strongly innervates LPFC neurons modulating executive control and working memory processing. However, it remains unknown if dopamine modulates working memory processing directly, or through the modulation of reward signals, which leads to differential predictions about dopamine modulation of reward signals in PFC.

Here we examined how dopamine receptors modulate reward expectancy signals of LPFC neurons. We trained macaque monkeys on a reward-modulated working memory task, in which a reward cue at the beginning of each trial predicted the amount of reward for a correct choice at the end of a trial. Monkeys had to remember visual items during a delay period to match it with a test item in the subsequent test phase. We recorded from 256 single units in LPFC while simultaneously stimulating D1Rs or D2Rs using micro-iontophoresis.

Information about the expected reward modulated the monkey's behavior. A larger expected reward increased the percentage of correct trials, decreased reaction times and decreased the percentage of trials aborted by the animals. We identified LPFC neurons signaling the expected reward size by an ANOVA with significant main effect reward size. A large proportion, about one third, of LPFC neurons carried information about reward size. D1R stimulation did not change information about reward size in the cue period following reward cue presentations. However, D1R stimulation impaired reward expectancy coding during the delay period preceding sample presentation. In contrast, D2R stimulation improved reward expectancy coding during both cue period and delay

period. As reported previously, D1R stimulation decreased the neurons' spontaneous activity. This change in baseline activity was correlated with D1R modulation of reward expectancy coding during both cue and delay periods. In contrast, D2R stimulation increased spontaneous activity, which was not correlated with D2R stimulation induced changes in coding quality.

In conclusion, D1R and D2R stimulation oppositely modulated reward signals in LPFC neurons. D1R modulation was opposite as found in previous studies for working memory and rule coding. These results suggest that opposite mechanisms described for D1R and D2R modulation dominate the modulation of reward signals in LPFC and suggest a complex interaction between dopamine control of reward signals and executive functions in LPFC.

### 2.6. Impact of prolonged training on behavioral well-being of rhesus monkeys

Macaque monkeys are widely used in neurophysiological studies including all studies for my thesis. These studies rely on operant conditioning techniques to train a large variety of cognitively demanding tasks. Behavioral tasks requiring executive control involving the PFC are particularly demanding and require extensive training of the animals. During training and recording, the animals' psychological well-being has to be ensured.

Here S. R. Hage et al. defined objective behavioral criteria to measure the psychological well-being of seven macaque monkeys during behavioral training protocols. We defined a set of behavioral categories logged during a combination of two sampling protocols to assess the monkeys' behavior. First, we focally sampled behavior continuously for 30 min directly after behavioral training sessions. Second, we used statistical scan sampling collecting instantaneous samples every hour during the day. These data were compared by S. R. Hage between two behavioral training protocols. The first training protocol (long break) consisted of 12 consecutive training days followed by 9 consecutive days without training and free access to both water and food. During training days, water intake was restricted to training sessions and food was delivered *ad libitum*. The second training protocol (short break) consisted of 12 consecutive training days with restricted water intake and 2 subsequent days without training and free access to food and water.

We found no systematic differences in the monkeys' behavior during training that followed a short break compared to training that followed a long break. Behavioral sampling revealed typical behaviors during the day, for example peak activity after training and decreasing activity in late afternoon. However, this pattern was not affected by the differences in training protocol. Further, extensive feeding and foraging behavior following training sessions revealed by continuous sampling did not change after a long or a short break. Importantly, we observed no abnormal behavior such as pacing.

---

These results suggest that the monkeys' psychological well-being can be guaranteed during training periods without long breaks. Prolongation of the daily working schedule does not act as a stressor as the animals are likely well habituated to the training schedule.

### **3. Discussion**

#### **3.1. Dopamine modulates a variety of signals relevant for executive control**

##### **3.1.1. Visual signals**

Dopamine stimulation differentially modulated two distinct classes of LPFC neurons. The two classes showed different characteristics in their response to sensory stimuli, suggesting that dopamine modulates cortical visual signals via two distinct modes of operation.

##### **Inhibition by dopamine**

Dopamine-mediated inhibition was characterized by a reduction in general firing rate of the neurons, without changing the magnitude of visual representations. This type of modulation resembles a subtraction, which is an additive shift in response levels retaining encoding properties and increasing signal-to-noise levels (Silver 2010). Control over sensory signals by subtraction mediates response normalization offering a major computational advantage (Carandini and Heeger 2012). Inhibition can adaptively rescale the input to a neuron to match its dynamic range (Mitchell and Silver 2003) and therefore maximize information transmission (Brenner et al. 2000).

These results support the gating model of dopamine, in which dopamine is hypothesized to filter sensory input to cortex (Cohen et al. 1996, 2002). Mechanistically, gating could be realized by modulating the dendritic arbor in input layers (Durstewitz et al. 2000a, Gao et al. 2003). One major argument supporting the gating mechanism is the presence of a precisely timed signal, which mediates gating of sensory inputs. Neurons inhibited by dopamine showed rapid modulation by dopamine, rendering them ideal recipients of rapid, phasic dopamine signals relayed to PFC (Redgrave et al. 2008). Further, mean visual response latencies of inhibited neurons was about 165 ms, closely following the mean latency of phasic dopamine bursts after visual stimulation of about 120 ms (Dommert et al. 2005) and dopamine response latencies following the detection of somatosensory stimuli of about 150 ms (de Lafuente and Romo 2012). Thus, dopamine might reinforce or block signals reaching the PFC and mediate the updating of behaviorally relevant signals in PFC (D'Ardenne et al. 2012) increasing the cortical signal-to-noise ratio (Servan-Schreiber et al. 1990).

In visual cortex, subtractive shifts in neuronal firing rates is mediated by somatostatin-(SOM-)expressing, dendrite-targeting interneurons (Wilson et al. 2012). Dopamine has been shown to increase inhibitory signaling from non-fast-spiking, dendrite-targeting interneurons to pyramidal cells (Gao et al. 2003). Thus, this mechanism might drive the observed inhibition in the subset of broad-spiking cells inhibited by dopamine, which are putative pyramidal cells (Mitchell et al. 2007, Connors and Gutnick 1990). All narrow-spiking, putative interneurons were inhibited by dopamine. Given the important role of interneurons in cortical information flow (Rao et al. 2000, Constantinidis et al. 2002), interneurons constitute an ideal target by which dopamine could mediate rapid gating.

#### **Excitation by dopamine**

In neurons excited by dopamine, neuronal firing rates were increased in proportion to baseline activity, indicating a multiplicative gain (Silver 2010). Gain modulation by dopamine has been proposed by computational models as a mechanism by which cortical networks might increase signal detection performance (Servan-Schreiber et al. 1990, Thurley et al. 2008), which we also observed at a single neuron level. Further, in neurons excited by dopamine, dopamine induced a reduction in trial-to-trial variability of neuronal spike counts. Together, these results resemble effects on neuronal firing properties described following the allocation of attention towards a neurons' receptive field (McAdams and Maunsell 1999, Noudoost and Moore 2011a). Thus, dopamine might similarly enhance relevant PFC signals as if allocating attention to these signals (Noudoost and Moore 2011b), controlling the selection of relevant information.

Neuronal response latencies to visual stimuli were considerably longer in neurons excited by dopamine, on average about 100 ms longer than for neurons inhibited by dopamine. Further, dopamine only slowly induced the observed changes in neurons excited by dopamine. Thus, dopamine might exert differential control on cortical neurons by distinct temporal profiles (Schultz 2007). Dopamine-excited neurons could be influenced by tonic dopamine signals, which are controlled by anatomically distinct pathways (Floresco 2013). In the PFC, tonic signals might primarily be mediated by high-affinity dopamine receptors located extra-synaptically (Grace et al. 2007).

In visual cortex, gain modulation was reported to be mediated by parvalbumin-(PV-)expressing, soma-targeting interneurons (Wilson et al. 2012). Dopamine has been shown to decrease inhibitory signaling from fast-spiking, soma-targeting interneurons (Gao et al. 2003). This modulation might drive the excitation observed in broad-spiking, putative pyramidal cells, by dis-inhibiting pyramidal cell firing.

## Conclusion

Together, these results suggest that dopamine controls two distinct cortical populations. Differential modulation might be mediated by an inhomogeneous receptor distribution present in PFC (Noudoost and Moore 2011b). Possibly, differential distributions of D1Rs and D2Rs at the level of cell types, cortical layers, and subcellular location establish heterogeneous dopamine modulation profiles.

### 3.1.2. Rule signals

Stimulation of D1R or D2R enhanced neuronal representations of numerical rules by distinct physiological mechanisms. Stimulating D1Rs decreased spontaneous activity and at the same time increased responses to the neurons' preferred rule. In contrast, stimulating D2Rs increased spontaneous activity while decreasing responses to non-preferred rules, thus also increasing rule coding.

### D1R modulation of rule coding

We observed a D1R-mediated inhibition of overall neuronal firing rates. D1R-induced inhibition of LPFC neurons was repeatedly reported by previous *in vivo* studies (Vijayraghavan et al. 2007, Williams and Goldman-Rakic 1995). Mechanistically, this can be explained either by *in vitro* studies reporting that D1R stimulation reducing the efficacy of excitatory neurotransmission in PFC (Gao et al. 2001) and weakens non-NMDA-glutamatergic responses (Seamans et al. 2001a). Further, D1Rs have been shown to enhance inhibitory post-synaptic currents (IPSCs) in pyramidal cells (Trantham-Davidson et al. 2004), thus modulating interneuron-to-pyramidal signaling. At the same time, D1R stimulation induced an increase in neuronal responses to the preferred rule during sustained rule-related activity in the delay period. D1R-induced excitatory effects might be mediated by an increase in NMDA-evoked responses observed *in vitro* (Seamans et al. 2001a, Tseng and O'Donnell 2004).

The bidirectional modulation, i. e. a decrease in spontaneous activity and an increase in sustained activity, was proposed by computational models implementing previously described D1R modulation of synaptic currents (Durstewitz et al. 2000a). In these models, an increase in GABA-conductances from interneuron-to-pyramidal cells and an increase in recurrent NMDA conductances qualitatively matches our experimental results (Brunel and Wang 2001), increasing the selectivity of sustained high-activity states. Thus, our data strongly supports these models. Experimental predictions from the same computational models have been positively tested by manipulating NMDA receptors in LPFC, which modulated sustained activity during working memory (Wang et al. 2013).

Our results provide a possible cellular basis for the role of D1R in mediating behavioral flexibility. Blocking prefrontal D1Rs in monkeys impairs learning of new association rules and reduces corresponding neural selectivity to learned saccade directions (Puig and Miller 2012). In rodent studies, blocking D1Rs impairs flexibly switching between different response strategies (Ragozzino 2002, Floresco and Magyar 2006). Similarly, D1R availability in human PFC is positively correlated with flexibly shifting between rules in a WCST (Takahashi et al. 2008, 2012).

#### **D2R modulation of rule coding**

We found a D2R-mediated increase in overall firing rates. D2R-induced excitation of LPFC neurons has been reported by previous *in vivo* studies (Wang et al. 2004a, Wang and Goldman-Rakic 2004). *In vitro* studies have shown that D2Rs decrease IPSCs in pyramidal cells (Seamans et al. 2001b, Trantham-Davidson et al. 2004), thus decreasing interneuron-to-pyramidal signaling leading to a dis-inhibition of pyramidal cells. At the same time, D2R stimulation reduced neuronal responses to non-preferred rules, thus showing inhibitory effects. Inhibitory effects have been repeatedly reported by *in vitro* studies reporting that D2R stimulation decreases NMDA-evoked responses (Tseng and O'Donnell 2004) and increases inhibition by enhancing interneuron excitability (Zhong and Yan 2016).

These results partly contradict ideas from computational models about the role of D2Rs in modulating sustained activity in PFC (Durstewitz and Seamans 2008, Rolls et al. 2008). In agreement with the models, D2Rs increases network activity through an decrease in GABA-mediated inhibition (Durstewitz and Seamans 2008). However, the models proposed an antagonism between D1Rs and D2Rs, in which D2R stimulation would decrease and de-stabilize sustained activity states (Durstewitz and Seamans 2008). In contrast, we found an increase in selectivity and coding capacity for rule-related sustained activity in PFC neurons.

Our results show that D2Rs modulate the representations of task rules of LPFC neurons thus providing a cellular basis for D2R modulation of executive functions. Blocking prefrontal D2Rs impaired monkeys to learn new association rules and reduced neural selectivity in LPFC to learned saccade directions (Puig and Miller 2015). In agreement with our data, blocking D2Rs increased neuronal responses to non-preferred saccade directions. In addition, monkeys made more perseverative errors indicating that the ability to switch between representations was impaired (Puig and Miller 2015), an effect also observed in rodents (Floresco and Magyar 2006). Similarly, blocking D2Rs impairs shifting between rules in humans (Mehta et al. 1999) and stimulating D2Rs enhances the performance to switch between rules (Kimberg et al. 1997). Thus, our results support the idea that D2Rs mediate behavioral flexibility (Klanker et al. 2013).



## Conclusion

Together, our results show that D1R and D2R cooperatively modulate the processing of numerical rules underlying executive control in LPFC neurons. D1R and D2R show opposite mechanisms as predicted by computational models, but also show complementary mechanisms not described previously. Future theories about dopamine receptor functions in LPFC will have to incorporate these effects.

### 3.1.3. Working memory signals

Stimulating D2Rs enhanced neuronal working memory representations for numerosities on single neuron and population levels in LPFC. In addition, D2R stimulation increased the dynamic properties of prefrontal networks. Computational modeling suggested that D2Rs primarily act by decreasing GABAergic responses in pyramidal cells.

### D2R modulation of working memory

Our results provide a possible cellular basis for D2R modulation of working memory. In animal and human studies, it has been repeatedly shown that D2Rs modulate working memory performance (Clark and Noudoost 2014). However, modulation was often complex, depending on the baseline performance and the age of subjects. This might be contributing to the failure of finding D2R modulation of spatial working memory processes at the neuronal level. Wang et al. (2004a) trained monkeys on a ODR task and recorded neurons from LPFC while manipulation D2Rs. They found no effect of D2Rs on spatial mnemonic processing during the delay period. D2Rs did, however, modulate saccade-related responses during the response phase when monkeys made a saccade towards the target. In contrast, we found a prominent modulation of sustained activity in the delay period during working memory. In our study, monkeys learned to remember the numerosity information of visual displays, thus requiring feature-based working memory. Recordings from LPFC suggest that spatial and feature-based working memory might be represented by anatomically distinct populations (Wilson et al. 1993), although many neurons represent both spatial and visual information (Rao et al. 1997). In addition, the ODR task might reflect mainly motor preparation signals rather than representation of sensory signals (Markowitz et al. 2015, Takeda and Funahashi 2004), since the monkeys know from the onset of the sample location where they have to make a saccade to in the subsequent test phase. Thus, the ODR task might capture specific spatial processing signatures.

Similarly, these differences might explain the lack of effects on working memory processing following D1R manipulation. On the other hand, interpretation of the absence of an effect for D1Rs is limited, because our dataset for analyzing D1R effects on working

memory might have been too small. In addition, D1R show a strong and possibly narrow inverted-U response curve that might be different for D2Rs (Floresco 2013), making additional experiments necessary.

#### **D2R mechanisms of action**

We implemented a biophysically-plausible spiking neural network in which synaptic connections are described on a single neuron level to investigate possible mechanisms of action for D2Rs on working memory processing. Neuromodulation can be investigated by systematically changing synaptic conductances. We constrained possible synaptic modulation of D2Rs by investigating putative D2R targets supported by *in vitro* studies (Seamans et al. 2001b, Zhong and Yan 2016, Trantham-Davidson et al. 2004), which propose a decrease in IPSCs in pyramidal cells and an increase in interneuron excitability. When incorporating this putative D2R modulation in the model, we observed a small increase in spontaneous activity as well as a prominent increase in sustained activity, increasing the neurons' selectivity during working memory. Thus, the model could reproduce two of our major experimental findings.

Our results suggest that primarily interneuron-to-pyramidal signals mediates the enhancement of working memory representations. In agreement, interneurons have been shown to control cortical information flow, shaping neuronal tuning of memory representations (Constantinidis et al. 2002, Rao et al. 2000). In visual cortex, PV-expressing, soma-targeting neurons have been shown to modulate response gain, which might underlie the excitatory mechanisms.

#### **D2R modulation of dynamic response properties**

Since single neuron responses show a high complexity and variability (Rigotti et al. 2013), we explored whether computations in PFC might emerge from the dynamics of populations of neurons (Mante et al. 2013). We described neuronal responses in the framework of dynamical systems in which the activity of neuronal population can be described as a dynamical process revealing shared activity patterns that are prominent in the population response (Cunningham and Yu 2014). This allowed us to study dopamine receptor modulation of PFC network properties.

Computational models about dopamine receptor modulation proposed that D2Rs render PFC networks more flexible, i.e. increase their dynamic response properties (Durstewitz and Seamans 2008, Rolls et al. 2008, Seamans and Yang 2004). We tested this hypothesis by quantifying the dynamic responses of PFC networks using principal component analysis representing the activity of neuronal populations in state space (Harvey et al. 2012). By calculating the rate of change of neuronal trajectories in state

space (Stokes et al. 2013), we quantified the responsiveness of prefrontal networks during sample presentation and working memory. Similar to previous findings, we found that prefrontal networks show high dynamic phases after sample onset and at the beginning of the delay period. During memory delay, prefrontal networks show a more stable response pattern (Stokes et al. 2013). D2R stimulation enhanced the dynamic properties of prefrontal networks by an increase in the speed with which activity patterns changed over time. This enhancement was only observed during high dynamic phases in particular during the transition between visual and mnemonic representations at the beginning of the delay period. Oppositely, D1R stimulation decreased the dynamic properties of PFC networks.

These results support computational models proposing that dopamine receptors control dynamic updating of PFC representations (Durstewitz and Seamans 2008, Rolls et al. 2008, Seamans and Yang 2004). However, they also predict a decrease in selectivity for D2R stimulation during sustained responses. In contrast, we found an increase in selectivity both for single neurons and the population analysis. Future models might be able to reconcile both findings.

## Conclusion

Together, our results suggest a prominent D2R modulation of working memory processing in LPFC. Computational modeling suggests a mechanisms by which D2Rs might modulates PFC networks. Conversely, we tested predictions from existing models and found evidence that D2Rs promote the flexible updating of PFC representations.

### 3.1.4. Reward signals

Single neurons in LPFC represented reward expectancy signals during a working memory task. D1R stimulation decreased representations of reward expectancy, whereas D2R stimulation increased representations of reward expectancy.

### Opposite modulation of reward signals by D1R and D2R

The D1R-induced reduction of sustained reward expectancy signals in LPFC was surprising, given that most studies and our previous work mostly found improvement of the selectivity of sustained responses, or no effects (Vijayraghavan et al. 2007). As in previous studies, we found an overall inhibition of firing rates induced by D1R stimulation, possibly mediated by mechanisms described earlier. Possibly, inhibitory mechanisms dominated the modulation of sustained reward expectancy signals. There are several possible reasons. First, dopamine baseline levels might be higher during encoding of reward expectancy signals, shifting the inverted-U response curve to the left. Second,

neurons signaling expected reward might be modulated by D1R using different mechanisms, which realize opposite D1R and D2R effects. In either case, the results indicate that LPFC populations signaling reward expectancy are differentially impacted by D1Rs as compared to neurons representing working memory.

In contrast, D2R stimulation improved sustained reward expectancy signals, just as it improved sustained working memory and sustained rule-related representations. Thus, D2Rs might modulate a variety of signals relevant for executive control by common mechanisms. In agreement, D2Rs consistently increased spontaneous activity in this and previous studies.

#### **Dependence on baseline modulation**

D1R modulation of reward expectancy signals was correlated with D1R modulation of spontaneous firing rates. These results suggest that D1R-mediated inhibition and the observed decrease in selectivity share a common mechanism. They further suggest that D1R modulation strongly depends on baseline dopamine levels following an inverted-U response curve (Arnsten 2011). In contrast, the modulation by D2Rs was not correlated with changes in baseline. Thus, mechanisms by which D2Rs modulate spontaneous activity might be independent from mechanisms by which D2Rs enhance selectivity for reward signals in LPFC neurons.

#### **Conclusion**

Together, D1Rs and D2Rs modulate reward expectancy signals in LPFC neurons by opposite mechanisms. The different mechanism as compared to the modulation of memory (Wang et al. 2004a, Vijayraghavan et al. 2007) and rule-related signals challenge the idea that reward expectancy signals positively modulate working memory signals requiring further investigation (Kennerley et al. 2009, Leon and Shadlen 1999, Watanabe 2007)

### **3.2. Dopamine receptors show differential modulation of executive control**

#### **3.2.1. Complementary mechanisms for D1R and D2R**

Our results suggest that D1Rs and D2Rs assume complementary roles in modulating cognitive signals relevant for executive control. Both D1R and D2R stimulation increased neuronal coding of numerical rules. Thus, D1Rs and D2Rs likely do not have opposing roles in controlling executive control as postulated by computational studies (Durstewitz and Seamans 2008, Rolls et al. 2008). Instead, our results support evidence that D1Rs and D2Rs cooperatively modulate processes underlying behavioral flexibility (Floresco and Magyar 2006, Floresco 2013).

In rats, blocking either D1R or D2R impairs flexibly switching between different response strategies based on spatial or visual cues (Ragozzino 2002, Floresco et al. 2006). In addition, dopamine levels in PFC increased after learning the initial rule as well as after shifting to the new rule, indicating that prefrontal dopamine is involved in mediating rule shifts (Ragozzino 2002). A causal role for an involvement of prefrontal dopamine in shifting between response strategies has been found in monkeys, where depletion of prefrontal dopamine impaired learning of novel reward-predicting stimulus features (Crofts et al. 2001). Blocking either prefrontal D1R or D2R impaired monkeys to switch between arbitrary stimulus-response associations (Puig and Miller 2012, 2015), suggesting that D1Rs and D2Rs might cooperatively control behavioral flexibility.

Both D1Rs and D2Rs modulate working memory performance in humans and animals (Clark and Noudoost 2014). This modulation is strongly dependent on the subject's baseline performance and genotype associated with dopamine availability (Clark and Noudoost 2014, Robbins and Arnsten 2009), supporting the theory that dopamine modulation of working memory follows a narrow inverted-U response curve, with either too little or too much dopamine impairing working memory (Floresco 2013, Arnsten 2011, Goldman-Rakic et al. 2000). For D1Rs, an inverted-U modulation has been found on neuronal level in LPFC (Vijayraghavan et al. 2007). However, despite the behavioral evidence, D2Rs did not modulate spatial working memory in LPFC (Wang et al. 2004a). Our data resolve these findings, since we found a strong modulation of D2Rs on working memory processes in LPFC. Together, these results suggest that D1Rs and D2Rs have complementary roles for working memory, too. Further studies might resolve the unexpected finding that D1Rs did not modulate working memory representations in our study, which might either reflect differences between spatial and feature-based working memory discussed above, or a shift on the inverted-U response curve between studies.

### 3.2.2. Opposite mechanisms for D1R and D2R

#### Modulation of signal and noise

At the same time, we found several mechanisms by which D1Rs and D2Rs seemed to act oppositely. First, D1R reduced spontaneous activity and D2R increased spontaneous activity, as reported previously (Vijayraghavan et al. 2007, Wang et al. 2004a). Second, D1R increased responses to preferred rules, thus showing an additional excitatory contribution to neuronal firing properties. These results are in agreement with predictions from computational models incorporating *in vitro* results (Durstewitz et al. 2000a, Brunel and Wang 2001). Puig and Miller (2012), however, found that blocking prefrontal D1Rs increased responses to non-preferred associations, and stimulating D1Rs primarily reduced responses to non-preferred spatial locations in an ODR task (Vijayraghavan et al. 2007). Since D1R stimulation reduces baseline activity, too, it is hard to disentangle in-

hibitory from excitatory contributions. Previous studies did not systematically quantify these kinds of contributions, making direct comparisons hard (Puig and Miller 2012, Vijayraghavan et al. 2007). D2Rs, on the other hand, seem to have inhibitory contributions to neuronal firing properties, since D2R stimulation reduced responses to non-preferred rules. In agreement, blocking D2Rs has been reported to increase neural responses to non-preferred associations (Puig and Miller 2015).

Together, D1Rs and D2Rs show opposite mechanisms in modulating spontaneous activity and differential mechanisms in modulation the possible “signal” of cognitive variable (preferred response) and the “noise” of a cognitive variable (non-preferred response). This differential modulation lead to an increase in the neuronal coding capacity for rule representations for both D1R and D2R stimulation. Thus, mechanistically D1Rs and D2Rs seem to have opposing mechanisms, while functionally both receptor types contribute complementarily to executive control.

#### **Modulation of reward signals**

Surprisingly, D1Rs reduced reward expectancy signals in LPFC, while D2Rs enhanced reward expectancy signals. Thus, opposing mechanisms seemed to dominate dopamine receptor modulation of reward signals. For now, it is unclear if reward and working memory or rule signals are independently modulated by dopamine, or if differences in baseline dopamine shifting the inverted-U response curve can account for the observed differences. In either case, the same amount of D1R activation lead to opposite findings for D1Rs on modulating coding of reward signals as compared to rule signals. In contrast, the same amount of D2R activation lead modulation of reward and rule signals in the same direction, indicating that both receptors are characterized by distinct response profiles.

These findings are supported by rodent studies, which reported opposite mechanisms for D1Rs and D2Rs in modulation reward-based decision-making (Floresco 2013). In these studies, rats can chose between a lever press delivering a small certain reward or a lever press delivering a large risky reward, i. e. only with a specific probability. Sensitivity to reward can be investigated by quantifying how many times rats stay with the risky choice after a reward was delivered (win-stay) and how many times rats switched to the lever with certain small reward after no reward was delivered at the risky lever (lose-shift), which can be interpreted as sensitivity to negative feedback. D1R and D2R stimulation oppositely modulated reward sensitivity and negative feedback sensitivity (St. Onge et al. 2011, Floresco 2013). Stimulating D1Rs increased reward sensitivity by increasing win-stay tendencies, whereas D2R stimulation decreased reward sensitivity by decreasing win-stay tendencies promoting switching levers. Negative feedback sensitivity was oppositely modulated by blocking D1Rs or D2R, either increasing or decreasing

lose-shift tendencies, respectively. These findings suggest that decision-making based on reward signals is oppositely modulated by prefrontal dopamine receptors (Floresco 2013).

## Conclusion

Together, complementary as well as opposite mechanism underlie dopamine receptor modulation of executive functions in PFC. These differences might dissociate between distinct types of signals for working memory, behavioral flexibility, and reward-based decision-making.

### 3.3. Models of dopamine modulation suggest specific mechanism of action

#### 3.3.1. Differential modulation of interneurons and pyramidal cells

##### Proposed mechanism of action

Results from previous modeling studies (Durstewitz et al. 2000a, Brunel and Wang 2001, Durstewitz and Seamans 2008) together with our own modeling suggest a specific mechanism of action for D1Rs and D2Rs (**Figure 6A**). For D1Rs, increasing NMDA currents enhances recurrent excitation during sustained responses. At the same time, increasing GABA currents decreases spontaneous activity. These effects proposed by modeling studies are supported by our experimental data for the sustained representation of rules. For working memory, we propose a specific mechanism for D2Rs. Decreasing GABA currents in pyramidal cells increased both spontaneous activity and sustained activity. When this dis-inhibition was balanced by increasing interneuron activity (enhancing AMPA currents on interneurons), spontaneous activity was only slightly elevated, while sustained activity was strongly increased, enhancing the neurons' selectivity.

##### Interneurons and pyramidal cells

Thus, we propose opposite mechanisms of action for D1Rs and D2Rs on modulating interneuron-to-pyramidal signaling, as well as independent mechanisms of action on modulating recurrent excitation (D1R) and interneuron excitability (D2R). The proposed mechanism is based on findings from *in vitro* studies discussed in previous sections. It relies on a differential modulation of pyramidal cells and interneurons by dopamine receptors. Dopamine has been reported to modulate recurrent excitation in pyramidal cells without changing pyramidal-to-interneuron signaling (Gao and Goldman-Rakic 2003). However, dopamine did change interneuron excitability as well as interneuron-to-pyramidal signaling by either decreasing or increasing mechanisms, depending on

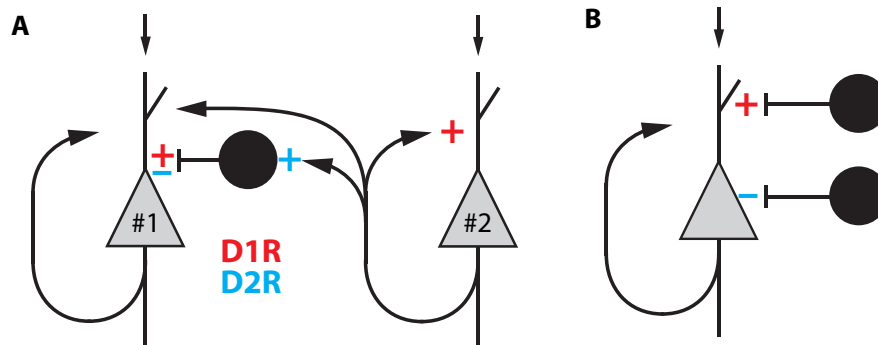


**Figure 6: Proposed dopamine receptor mechanisms of action .** **A:** Same basic model architecture as in **Figure 3B** with pyramidal cell populations selective for two different features (#1 and #2). We propose that D1Rs positively modulate recurrent excitation via NMDA receptors and, at the same time, positively modulate GABA signaling from interneurons to pyramidal cells (red). For D2Rs, we propose that D2Rs negatively modulate GABA signaling and positively modulate interneuron excitability by increasing interneuron AMPA signaling (blue). **B:** Hypothesized dopamine receptor modulation by different interneuron subtypes. We hypothesize that D1Rs modulate interneuron-to-pyramidal signaling in SOM-expressing, non-fast-spiking, dendrite targeting interneurons, possibly mediating gating and a decrease in spontaneous activity. For D2Rs, we hypothesize that D2Rs modulate interneuron-to-pyramidal signaling in PV-expressing, fast-spiking, soma-targeting interneurons, possibly mediating gain modulation. Model mainly based on experiments from Wilson et al. (2012) and Gao et al. (2003).

the interneuron subtype (Gao et al. 2003). Interneuron-to-pyramidal was decreased in fast-spiking, soma-targeting interneurons but increased in non-fast-spiking, dendrite-targeting interneurons. Together with our results, and with studies from rodent cortex (Wilson et al. 2012), it seems likely that the increase in interneuron-to-pyramidal observed in dendrite-targeting interneurons is mediated by D1Rs, whereas the decrease in soma-targeting interneurons is mediated by D2Rs (**Figure 6B**). This differential modulation could be realized by an inhomogeneous subcellular dopamine receptor localization on pyramidal cells (Noudoost and Moore 2011b). It might also unify possible gating mechanisms, which could ideally be mediated by D1Rs on dendrites, mediating subtractive shifts observed during gating of sensory input as well as a decrease in spontaneous activity. Thus, inhibitory effects observed after dopamine application on LPFC neurons are likely mediated by D1Rs. In contrast, excitatory mechanisms observed after dopamine application are likely mediated by D2Rs. D2R modulation resembles a gain modulation, which was reported to be mediated by soma-targeting interneurons (Wilson et al. 2012). However, a pure gain modulation would not result in enhanced coding capacities, as gain also increases noise levels (Servan-Schreiber et al. 1990, Herrero et al. 2008). Thus, an additional inhibitory mechanism possibly mediated by an increase of interneuron excitability, which was observed for rule representations, might contribute to D2R-mediated increase in coding capacities during working memory and rules.

Together, our results suggest that D1Rs and D2Rs differentially modulate pyramidal cells, interneurons, and interneuron subtypes.



### 3.3.2. Modulation of population dynamics

We observed a bidirectional modulation of the dynamic properties of LPFC networks by D1Rs and D2Rs. These findings are in agreement with computational models, which suggest that D1Rs stabilize prefrontal representations, i. e. make them less dynamic, and that D2Rs de-stabilize prefrontal representations, i. e. make them more dynamic (Durstewitz and Seamans 2008, Rolls et al. 2008, Seamans and Yang 2004, Seamans et al. 2001b). The models also predicted that sustained activity in D2R-dominated states would not be stable, and thus show a reduction of selectivity when computing trial-averages. However, we observed an enhancement of selectivity during sustained responses after D2R stimulation. Thus, we propose that D2Rs render prefrontal networks more flexible by increasing dynamic responsiveness of the neurons, but at the same time increase selectivity during sustained responses. At present, it is unknown whether a common mechanism might mediate both properties or, alternatively, if distinct mechanisms drive the observed pattern of responses.

### 3.4. Future directions

Several open questions follow from our results, which results from limitations in studies performed so far.

1. Our hypothesis about the contributions of D1Rs and D2Rs in gating sensory signals needs to be tested empirically. Visual cortical signals could be recorded during application of drugs specifically targeting D1Rs or D2Rs. Based on our results, D1Rs might mediate fast inhibition of short-latency visual signals while retaining coding capacities, while D2Rs might mediate slow excitation of long-latency visual signals enhancing coding capacities.
2. It remains unclear which factors drive the differences in results for studies using the ODR task and our results, in particular for differences between D1R and D2R in modulating working memory activity. It would be helpful to record from LPFC neurons with specific manipulation of D1Rs and D2Rs during a joint spatial and feature-based working memory task. In addition, it would be helpful to systematically alter the drug amount applied to the recording sites to investigate possible drug-response curves, which might be different for different receptors and functions (Floresco 2013). Possibly, D2Rs do not modulate spatial mnemonic signals but only feature-based working memory signals, while D1Rs modulate both types of signals.
3. For reward signals, it needs to be additionally investigated if there is a direct interaction between dopamine receptor modulation of reward signals and working memory signals. This could be done by analyzing the interaction between reward

and memory signals directly. Possibly, reward expectancy modulation of memory signals is dopamine-dependent, arguing for a strong interaction between reward and cognitive signals. Alternatively, dopamine might independently modulate reward and memory signals, supporting the notion that dopamine modulation of cognitive signals is largely independent from the modulation of reward signals (Matsumoto and Takada 2013).

4. Future computational models might need to incorporate different interneuron subtypes (Wang et al. 2004b), which have been shown to differentially exert inhibitory control on pyramidal cells (Lee et al. 2014, Pi et al. 2013). In addition, the role of D1Rs and D2Rs in stabilizing prefrontal representations needs to be resolved.
5. Empirical testing of predictions by computational models might help to test the validity of the models. Specifically, the role of NMDA receptors (Wang et al. 2013), or GABA<sub>A</sub> receptors on sustained responses could be tested. As predictions become increasingly complex, differential dopamine modulation of cortical cell types needs to be addressed. This could be either done using genetic tools or using recent advances in classifying functional cell types using electrophysiological properties (Tripathy et al. 2015). Specifically, low-dosage blockage of GABA<sub>A</sub> receptors should lead to a strong dis-inhibition of pyramidal cells with differential impact during spontaneous and sustained activity.
6. A causal role for specific dopamine receptor modulation of neuronal processes underlying executive function is in many cases still missing. Application of larger drug amounts using pressure ejections or genetic tools might help to establish causal relationships between dopamine modulation of neuronal firing properties and behavior.
7. It remains unclear which signals are precisely carried by dopamine neuron activity. To find out, it would be necessary to record from midbrain dopamine neurons during tasks requiring executive control and to determine the amount of dopamine release within PFC, possibly by micro-dialysis, voltammetry, or genetic markers.

#### 3.5. Conclusion

Our studies provide several novel insights into dopamine modulation of neuronal processes underlying executive functions (**Box 3**). First, we hypothesize that dopamine gates sensory signals reaching LPFC relevant for behavior. Second, we propose that D1Rs and D2Rs cooperatively modulate a variety of executive function including working memory and the representation of task rules mediating behavioral flexibility. On the other hand, D1Rs and D2Rs might oppositely modulate reward-based decision-making. Third, experimental data together with computational modeling propose a

**Box 3. Main conclusions about dopamine functions in LPFC.**

1. Dopamine gates cortical visual signals.
2. D1R and D2R cooperatively modulate a variety of signals mediating executive control.
3. D1R and D2R have opposite as well as complementary dopamine receptor mechanisms.
4. Dopamine receptors control stability and flexibility of cortical networks.

specific mechanism of action for D1Rs and D2Rs comprising opposite as well as complementary dopamine receptor mechanisms. Finally, our results suggest that dopamine receptors mediate flexible updating and subsequent stabilization of representations in prefrontal networks.

Together, dopamine regulates information flow in PFC underlying executive control, biasing top-down signals to select appropriate actions to achieve goals.

---

## Abbreviations

AMPA	$\alpha$ -amino-3-hydroxy-5-methyl-4-isoxazolepropionic acid
ANOVA	Analysis of variance
D1R	Dopamine D1-like receptors
D2R	Dopamine D2-like receptors
FEF	Frontal eye field
GABA	$\gamma$ -Aminobutyric acid
LPFC	Lateral prefrontal cortex
MDNT	Mediodorsal nucleus of the thalamus
NMDA	<i>N</i> -Methyl- <i>D</i> -aspartate
ODR	Oculo-motor delayed response
PFC	Prefrontal cortex
PV	Parvalbumin
SOM	Somatostatin
WCST	Wisconsin card sorting test

---

**References**

- Amemori, K.-i. and Sawaguchi, T. (2006). Contrasting effects of reward expectation on sensory and motor memories in primate prefrontal neurons. *Cerebral Cortex* **16**(7):1002–1015.
- Arnsten, A. F. T. (2009). Stress signalling pathways that impair prefrontal cortex structure and function. *Nature Reviews Neuroscience* **10**(6):410–22.
- Arnsten, A. F. T. (2011). Catecholamine influences on dorsolateral prefrontal cortical networks. *Biological Psychiatry* **69**(12):e89–99.
- Arnsten, A. F. T., Cai, J. X., Murphy, B. L. and Goldman-Rakic, P. S. (1994). Dopamine D1 receptor mechanisms in the cognitive performance of young adult and aged monkeys. *Psychopharmacology (Berl.)* **116**(2):143–151.
- Arnsten, A. F. T., Cai, J. X., Steere, J. C. and Goldman-Rakic, P. S. (1995). Dopamine D2 receptor mechanisms contribute to age-related cognitive decline: the effects of quinpirole on memory and motor performance in monkeys. *Journal of Neuroscience* **15**(5 Pt 1):3429–39.
- Arnsten, A. F. T. and Li, B.-M. (2004). Neurobiology of executive functions: Catecholamine influences on prefrontal cortical functions. *Biological Psychiatry* **57**(11):1377–1384.
- Arnsten, A. F. T., Wang, M. J. and Paspalas, C. D. (2012). Neuromodulation of thought: flexibilities and vulnerabilities in prefrontal cortical network synapses. *Neuron* **76**(1):223–239.
- Arsenault, J. T., Nelissen, K., Jarraya, B. and Vanduffel, W. (2013). Dopaminergic reward signals selectively decrease fMRI activity in primate visual cortex. *Neuron* **77**(6):1174–1186.
- Asaad, W. F., Rainer, G. and Miller, E. K. (2000). Task-specific neural activity in the primate prefrontal cortex. *Journal of Neurophysiology* **84**(1):451–9.
- Baddeley, A. (2012). Working memory: theories, models, and controversies. *Annual Review of Psychology* **63**(1):1–29.
- Badre, D. and D'Esposito, M. (2009). Is the rostro-caudal axis of the frontal lobe hierarchical? *Nature Reviews Neuroscience* **10**(9):659–669.
- Bechara, a., Damasio, H. and Damasio, a. R. (2000). Emotion, decision making and the orbitofrontal cortex. *Cerebral cortex* **10**(3):295–307.
- Bergson, C., Mrzljak, L., Smiley, J. F., Pappy, M., Levenson, R. and Goldman-Rakic, P. S. (1995). Regional, cellular, and subcellular variations in the distribution of D1 and D5 dopamine receptors in primate brain. *Journal of Neuroscience* **15**(12):7821–36.
- Björklund, A. and Lindvall, O. (1984). Dopamine-containing systems in the CNS. In A. Björklund and T. Hkfelt, eds., *Handbook of Chemical Neuroanatomy. Vol 2: Classical Transmitters in the CNS, Part I.*, Amsterdam: Elsevier Science, pages 55–122.

- Bongard, S. and Nieder, A. (2010). Basic mathematical rules are encoded by primate prefrontal cortex neurons. *Proceedings of the National Academy of Sciences of the United States of America* **107**(5):2277–82.
- Brenner, N., Bialek, W., Steveninck, R. D. R. V. and de Ruyter van Steveninck, R. (2000). Adaptive rescaling maximizes information transmission. *Neuron* **26**(3):695–702.
- Bromberg-Martin, E. S., Matsumoto, M. and Hikosaka, O. (2010). Dopamine in motivational control: rewarding, aversive, and alerting. *Neuron* **68**(5):815–834.
- Brown, R. M., Crane, A. M. and Goldman, P. S. (1979). Regional distribution of monoamines in the cerebral cortex and subcortical structures of the rhesus monkey: concentrations and in vivo synthesis rates. *Brain Research* **168**(1):133–50.
- Brozoski, T. J., Brown, R. M., Rosvold, H. E. and Goldman, P. S. (1979). Cognitive deficit caused by regional depletion of dopamine in prefrontal cortex of rhesus monkey. *Science* **205**(4409):929–932.
- Brunel, N. and Wang, X.-j. J. (2001). Effects of neuromodulation in a cortical network model of object working memory dominated by recurrent inhibition. *Journal of Computational Neuroscience* **11**(1):63–85.
- Buckley, M. J., Mansouri, F. a., Hoda, H., Mahboubi, M., Browning, P. G. F., Kwok, S. C., Phillips, A. and Tanaka, K. (2009). Dissociable components of rule-guided behavior depend on distinct medial and prefrontal regions. *Science* **325**(5936):52–58.
- Cantlon, J. F. and Brannon, E. M. (2006). Shared system for ordering small and large numbers in monkeys and humans. *Psychological Science* **17**(5):401–6.
- Cantlon, J. F. and Brannon, E. M. (2007). Basic math in monkeys and college students. *PLoS Biology* **5**(12):2912–2919.
- Carandini, M. and Heeger, D. J. (2012). Normalization as a canonical neural computation. *Nature Reviews Neuroscience* **13**(1):51–62.
- Chapados, C. and Petrides, M. (2015). Ventrolateral and dorsomedial frontal cortex lesions impair mnemonic context retrieval. *Proceedings of the Royal Society B: Biological Sciences* **282**(1801):20142555–20142555.
- Clark, K. L. and Noudoost, B. (2014). The role of prefrontal catecholamines in attention and working memory. *Frontiers in Neural Circuits* **8**(33):1–19.
- Cohen, J. D., Braver, T. S. and Brown, J. W. (2002). Computational perspectives on dopamine function in prefrontal cortex. *Current Opinion in Neurobiology* **12**(2):223–229.
- Cohen, J. D., Braver, T. S. and O’Reilly, R. C. (1996). A computational approach to prefrontal cortex, cognitive control and schizophrenia: recent developments and current challenges. *Philosophical Transactions of the Royal Society B: Biological Sciences* **351**:1515–1527.
- Compte, A., Brunel, N., Goldman-Rakic, P. S. and Wang, X. J. (2000). Synaptic mechanisms and network dynamics underlying spatial working memory in a cortical network model. *Cerebral Cortex* **10**:910–23.

- Connors, B. W. and Gutnick, M. J. (1990). Intrinsic firing patterns of diverse neocortical neurons. *Trends in Neurosciences* **13**(3):99–104.
- Constantinidis, C., Franowicz, M. N. and Goldman-Rakic, P. S. (2001). The sensory nature of mnemonic representation in the primate prefrontal cortex. *Nature Neuroscience* **4**(3):311–6.
- Constantinidis, C. and Wang, X.-J. (2004). A neural circuit basis for spatial working memory. *The Neuroscientist* **10**(6):553–565.
- Constantinidis, C., Williams, G. V. and Goldman-Rakic, P. S. (2002). A role for inhibition in shaping the temporal flow of information in prefrontal cortex. *Nature Neuroscience* **5**(2):175–180.
- Crofts, H. S., Dalley, J. W., Collins, P., Denderen, J. C. V., Everitt, B. J., Robbins, T. W., Roberts, A. C. and Van Denderen, J. C. (2001). Differential effects of 6-OHDA lesions of the frontal cortex and caudate nucleus on the ability to acquire an attentional set. *Cerebral Cortex* **11**(11):1015–1026.
- Cunningham, J. P. and Yu, B. M. (2014). Dimensionality reduction for large-scale neural recordings. *Nature Neuroscience* **17**(11):1500–1509.
- Curtis, C. E. and D’Esposito, M. (2003). Persistent activity in the prefrontal cortex during working memory. *Trends in Cognitive Sciences* **7**(9):415–423.
- D’Ardenne, K., Eshel, N., Luka, J., Lenartowicz, A., Nystrom, L. E., Cohen, J. D. and Ardenne, K. D. (2012). Role of prefrontal cortex and the midbrain dopamine system in working memory updating. *Proceedings of the National Academy of Sciences of the United States of America* **109**(49):19900–19909.
- de Almeida, J. and Mengod, G. (2010). D2 and D4 dopamine receptor mRNA distribution in pyramidal neurons and GABAergic subpopulations in monkey prefrontal cortex: implications for schizophrenia treatment. *Neuroscience* **170**(4):1133–1139.
- de Lafuente, V. and Romo, R. (2005). Neuronal correlates of subjective sensory experience. *Nature Neuroscience* **8**(12):1698–1703.
- de Lafuente, V. and Romo, R. (2006). Neural correlate of subjective sensory experience gradually builds up across cortical areas. *Proceedings of the National Academy of Sciences of the United States of America* **103**(39):14266–14271.
- de Lafuente, V. and Romo, R. (2011). Dopamine neurons code subjective sensory experience and uncertainty of perceptual decisions. *Proceedings of the National Academy of Sciences of the United States of America* **108**(49):19767–71.
- de Lafuente, V. and Romo, R. (2012). Dopaminergic activity coincides with stimulus detection by the frontal lobe. *Neuroscience* **218**:181–184.
- Deco, G., Rolls, E. T., Albantakis, L. and Romo, R. (2013). Brain mechanisms for perceptual and reward-related decision-making. *Progress in Neurobiology* **103**:194–213.
- Deco, G. and Romo, R. (2008). The role of fluctuations in perception. *Trends in Neurosciences* **31**(11):591–598.

- Dommett, E., Coizet, V., Blaha, C. D. C., Martindale, J., Lefebvre, V., Walton, N., Mayhew, J. E. W., Overton, P. G. and Redgrave, P. (2005). How visual stimuli activate dopaminergic neurons at short latency. *Science* **1476**(2005):1476–1479.
- Durstewitz, D. and Seamans, J. K. (2002). The computational role of dopamine D1 receptors in working memory. *Neural Networks* **15**(4-6):561–572.
- Durstewitz, D. and Seamans, J. K. (2008). The dual-state theory of prefrontal cortex dopamine function with relevance to catechol-o-methyltransferase genotypes and schizophrenia. *Biological Psychiatry* **64**(9):739–749.
- Durstewitz, D., Seamans, J. K. and Sejnowski, T. J. (2000a). Dopamine-mediated stabilization of delay-period activity in a network model of prefrontal cortex. *Journal of Neurophysiology* **83**(3):1733–1750.
- Durstewitz, D., Seamans, J. K. and Sejnowski, T. J. (2000b). Neurocomputational models of working memory. *Nature neuroscience* **3 Suppl**(November):1184–1191.
- Eiselt, A.-K. and Nieder, A. (2013). Representation of abstract quantitative rules applied to spatial and numerical magnitudes in primate prefrontal cortex. *Journal of Neuroscience* **33**(17):7526–7534.
- Engel, T. a., Chaisangmongkon, W., Freedman, D. J. and Wang, X.-J. (2015). Choice-correlated activity fluctuations underlie learning of neuronal category representation. *Nature Communications* **6**:6454.
- Felten, D. L. and Sladek, J. R. (1983). Monoamine distribution in primate brain V. Monoaminergic nuclei: anatomy, pathways and local organization. *Brain Research Bulletin* **10**(2):171–284.
- Floresco, S. B. (2013). Prefrontal dopamine and behavioral flexibility: Shifting from an "inverted-U" toward a family of functions. *Frontiers in Neuroscience* **7**(62):1–12.
- Floresco, S. B. and Magyar, O. (2006). Mesocortical dopamine modulation of executive functions: beyond working memory. *Psychopharmacology (Berl.)* **188**(4):567–585.
- Floresco, S. B., Magyar, O., Ghods-Sharifi, S., Vexelman, C. and Tse, M. T. L. (2006). Multiple dopamine receptor subtypes in the medial prefrontal cortex of the rat regulate set-shifting. *Neuropsychopharmacology* **31**(2):297–309.
- Freedman, D., Riesenhuber, M., Poggio, T. and Miller, E. (2001). Categorical representation of visual stimuli in the primate prefrontal cortex. *Science* **291**(5502):312–6.
- Funahashi, S., Bruce, C. J. and Goldman-Rakic, P. S. (1989). Mnemonic coding of visual space in the monkey's dorsolateral prefrontal cortex. *Journal of Neurophysiology* **61**(2):331–349.
- Fuster, J. (2008). *The prefrontal cortex*. London: Academic Press, 4th edition.
- Fuster, J. M. (1973). Unit activity in prefrontal cortex during delayed-response performance: neuronal correlates of transient memory. *Journal of Neurophysiology* **36**(1):61–78.



- Gao, W.-J. and Goldman-Rakic, P. S. (2003). Selective modulation of excitatory and inhibitory microcircuits by dopamine. *Proceedings of the National Academy of Sciences of the United States of America* **100**(5):2836–2841.
- Gao, W.-J., Krimer, L. S. and Goldman-Rakic, P. S. (2001). Presynaptic regulation of recurrent excitation by D1 receptors in prefrontal circuits. *Proceedings of the National Academy of Sciences of the United States of America* **98**(1):295–300.
- Gao, W.-J., Wang, Y. and Goldman-Rakic, P. S. (2003). Dopamine modulation of perisomatic and peridendritic inhibition in prefrontal cortex. *Journal of Neuroscience* **23**(5):1622–1630.
- Genovesio, A., Brasted, P. J., Mitz, A. R. and Wise, S. P. (2005). Prefrontal cortex activity related to abstract response strategies. *Neuron* **47**(2):307–320.
- Gibbs, S. E. B. and D’Esposito, M. (2005). Individual capacity differences predict working memory performance and prefrontal activity following dopamine receptor stimulation. *Cognitive, Affective & Behavioral Neuroscience* **5**(2):212–221.
- Gold, J. I. and Shadlen, M. N. (2007). The neural basis of decision making. *Annual Review of Neuroscience* **30**:535–574.
- Goldman-Rakic, P. S. (1988). Topography of cognition: parallel distributed networks in primate association cortex. *Annual Review of Neuroscience* **11**:137–156.
- Goldman-Rakic, P. S. (1995). Cellular basis of working memory. *Neuron* **14**(3):477–485.
- Goldman-Rakic, P. S., Leranth, C., Williams, S. M., Mons, N. and Geffard, M. (1989). Dopamine synaptic complex with pyramidal neurons in primate cerebral cortex. *Proceedings of the National Academy of Sciences of the United States of America* **86**(22):9015–9.
- Goldman-Rakic, P. S., Muly, E. C. and Williams, G. V. (2000). D1 receptors in prefrontal cells and circuits. *Brain Research Reviews* **31**(2-3):295–301.
- Grace, A. a., Floresco, S. B., Goto, Y. and Lodge, D. J. (2007). Regulation of firing of dopaminergic neurons and control of goal-directed behaviors. *Trends in Neurosciences* **30**(5):220–227.
- Hage, S. R., Ott, T., Eiselt, A.-K., Jacob, S. N. and Nieder, A. (2014). Ethograms indicate stable well-being during prolonged training phases in rhesus monkeys used in neurophysiological research. *Laboratory Animals* **48**(1):82–7.
- Harvey, C. D., Coen, P. and Tank, D. W. (2012). Choice-specific sequences in parietal cortex during a virtual-navigation decision task. *Nature* **484**(7392):62–68.
- Herrero, J. L., Roberts, M. J., Delicato, L. S., Gieselmann, M. a., Dayan, P. and Thiele, A. (2008). Acetylcholine contributes through muscarinic receptors to attentional modulation in V1. *Nature* **454**(7208):1110–1114.
- Hoshi, E., Shima, K. and Tanji, J. (2000). Neuronal activity in the primate prefrontal cortex in the process of motor selection based on two behavioral rules. *Journal of Neurophysiology* **83**(4):2355–2373.

- Hussar, C. R. and Pasternak, T. (2009). Flexibility of sensory representations in prefrontal cortex depends on cell type. *Neuron* **64**(5):730–743.
- Hussar, C. R. and Pasternak, T. (2013). Common rules guide comparisons of speed and direction of motion in the dorsolateral prefrontal cortex. *Journal of Neuroscience* **33**(3):972–86.
- Jackson, D. M. and Westlind-Danielsson, A. (1994). Dopamine receptors: molecular biology, biochemistry and behavioural aspects. *Pharmacology & Therapeutics* **64**(2):291–370.
- Jacob, S. N., Ott, T. and Nieder, A. (2013). Dopamine regulates two classes of primate prefrontal neurons that represent sensory signals. *Journal of Neuroscience* **33**(34):13724–34.
- Kennerley, S. W., Dahmubed, A. F., Lara, A. H. and Wallis, J. D. (2009). Neurons in the frontal lobe encode the value of multiple decision variables. *Journal of Cognitive Neuroscience* **21**(6):1162–1178.
- Kimberg, D. Y., D’Esposito, M. and Farah, M. J. (1997). Effects of bromocriptine on human subjects depend on working memory capacity. *Neuroreport* **8**(16):3581–3585.
- Klanker, M., Feenstra, M. and Denys, D. (2013). Dopaminergic control of cognitive flexibility in humans and animals. *Frontiers in Neuroscience* **7**(201):1–24.
- Kobayashi, S., Lauwereyns, J., Koizumi, M., Sakagami, M. and Hikosaka, O. (2002). Influence of reward expectation on visuospatial processing in macaque lateral prefrontal cortex. *Journal of Neurophysiology* **87**(3):1488–1498.
- Lebedev, M. a., Messinger, A., Kralik, J. D. and Wise, S. P. (2004). Representation of attended versus remembered locations in prefrontal cortex. *PLoS Biology* **2**(11).
- Lee, A., Gee, S., Vogt, D., Patel, T., Rubenstein, J. and Sohal, V. (2014). Pyramidal neurons in prefrontal cortex receive subtype-specific forms of excitation and inhibition. *Neuron* **81**(1):61–68.
- Lee, D., Seo, H. and Jung, M. W. (2012). Neural basis of reinforcement learning and decision making. *Annual Review of Neuroscience* **35**:287–308.
- Leon, M. I. and Shadlen, M. N. (1999). Effect of expected reward magnitude on the response of neurons in the dorsolateral prefrontal cortex of the macaque. *Neuron* **24**(2):415–425.
- Lidow, M. S., Goldman-Rakic, P. S., Gallager, D. W. and Rakic, P. (1991). Distribution of dopaminergic receptors in the primate cerebral cortex: quantitative autoradiographic analysis using [3H]raclopride, [3H]spiperone and [3H]SCH23390. *Neuroscience* **40**(3):657–671.
- Lidow, M. S., Wang, F., Cao, Y. and Goldman-Rakic, P. S. (1998). Layer V neurons bear the majority of mRNAs encoding the five distinct dopamine receptor subtypes in the primate prefrontal cortex. *Synapse* **28**(1):10–20.

- Ljungberg, T., Apicella, P. and Schultz, W. (1991). Responses of monkey mid-brain dopamine neurons during delayed alternation performance. *Brain Research* **567**(2):337–341.
- Ljungberg, T., Apicella, P. and Schultz, W. (1992). Responses of monkey dopamine neurons during learning of behavioral reactions. *Journal of Neurophysiology* **67**(1):145–163.
- Mansouri, F. a. (2006). Prefrontal cell activities related to monkeys' success and failure in adapting to rule changes in a Wisconsin Card Sorting Test analog. *Journal of Neuroscience* **26**(10):2745–2756.
- Mante, V., Sussillo, D., Shenoy, K. V. and Newsome, W. T. (2013). Context-dependent computation by recurrent dynamics in prefrontal cortex. *Nature* **503**:78–84.
- Markowitz, D. A., Curtis, C. E., Pesaran, B. and Goldberg, M. E. (2015). Multiple component networks support working memory in prefrontal cortex. *Proceedings of the National Academy of Sciences of the United States of America* **112**(35):11084–11089.
- Matsumoto, M. and Hikosaka, O. (2009). Two types of dopamine neuron distinctly convey positive and negative motivational signals. *Nature* **459**(7248):837–41.
- Matsumoto, M. and Takada, M. (2013). Distinct representations of cognitive and motivational signals in midbrain dopamine neurons. *Neuron* **79**(5):1011–1024.
- McAdams, C. J. and Maunsell, J. H. (1999). Effects of attention on the reliability of individual neurons in monkey visual cortex. *Neuron* **23**(4):765–73.
- Mehta, M. a., Manes, F. F., Magnolfi, G., Sahakian, B. J. and Robbins, T. W. (2004). Impaired set-shifting and dissociable effects on tests of spatial working memory following the dopamine D2 receptor antagonist sulpiride in human volunteers. *Psychopharmacology (Berl.)* **176**(3-4):331–342.
- Mehta, M. a., Sahakian, B. J., McKenna, P. J. and Robbins, T. W. (1999). Systemic sulpiride in young adult volunteers simulates the profile of cognitive deficits in Parkinson's disease. *Psychopharmacology (Berl.)* **146**(2):162–174.
- Mehta, M. A., Swanson, R., Ogilvie, A. D., Sahakian, B. and Robbins, T. W. (2001). Improved short-term spatial memory but impaired reversal learning following the dopamine D2 agonist bromocriptine in human volunteers. *Psychopharmacology (Berl.)* **159**:10–20.
- Merten, K. and Nieder, A. (2012). Active encoding of decisions about stimulus absence in primate prefrontal cortex neurons. *Proceedings of the National Academy of Sciences of the United States of America* **109**(16):6289–6294.
- Miller, E. K. and Cohen, J. D. (2001). An integrative theory of prefrontal cortex function. *Annual Review of Neuroscience* **24**:167–202.
- Miller, E. K., Freedman, D. J. and Wallis, J. D. (2002). The prefrontal cortex: categories, concepts and cognition. *Philosophical Transactions of the Royal Society B: Biological Sciences* **357**(1424):1123–1136.

- Miller, E. K. and Wallis, J. D. (2009). Executive function and higher-order cognition : definition and neural substrates. In L. R. Squire, ed., *Encyclopedia of Neuroscience*, Academic Press, volume 4, pages 99–104.
- Milner, B. (1963). Effects of different brain lesions of card sorting. *Archives of Neurology* **9**:90–100.
- Mitchell, J. F., Sundberg, K. A. and Reynolds, J. H. (2007). Differential attention-dependent response modulation across cell classes in macaque visual area V4. *Neuron* **55**(1):131–141.
- Mitchell, S. J. and Silver, R. A. (2003). Shunting inhibition modulates neuronal gain during synaptic excitation. *Neuron* **38**(3):433–445.
- Mrzljak, L., Bergson, C., Pappy, M., Huff, R., Levenson, R. and Goldman-Rakic, P. S. (1996). Localization of dopamine D4 receptors in GABAergic neurons of the primate brain. *Nature* **381**(6579):245–8.
- Mueser, K. T. and McGurk, S. R. (2004). Schizophrenia. *Lancet* **363**(9426):2063–2072.
- Müller, U., von Cramon, D. Y. and Pollmann, S. (1998). D1- versus D2-receptor modulation of visuospatial working memory in humans. *Journal of Neuroscience* **18**(7):2720–8.
- Muly, E. C., Szigeti, K. and Goldman-Rakic, P. S. (1998). D1 receptor in interneurons of macaque prefrontal cortex: distribution and subcellular localization. *Journal of Neuroscience* **18**(24):10553–10565.
- Nakahara, K., Hayashi, T., Konishi, S. and Miyashita, Y. (2002). Functional MRI of macaque monkeys performing a cognitive set-shifting task. *Science* **295**(5559):1532–1536.
- Nieder, A. (2002). Representation of the quantity of visual items in the primate prefrontal cortex. *Science* **297**(5587):1708–1711.
- Nieder, A. (2005). Counting on neurons: the neurobiology of numerical competence. *Nature Reviews Neuroscience* **6**(3):177–90.
- Nieder, A. and Merten, K. (2007). A labeled-line code for small and large numerosities in the monkey prefrontal cortex. *Journal of Neuroscience* **27**(22):5986–5993.
- Nieder, A. and Miller, E. K. (2003). Coding of cognitive magnitude: Compressed scaling of numerical information in the primate prefrontal cortex. *Neuron* **37**(1):149–157.
- Nieder, A. and Miller, E. K. (2004). A parieto-frontal network for visual numerical information in the monkey. *Proceedings of the National Academy of Sciences of the United States of America* **101**(19):7457–7462.
- Noudoost, B. and Moore, T. (2011a). Control of visual cortical signals by prefrontal dopamine. *Nature* **474**(7351):372–375.
- Noudoost, B. and Moore, T. (2011b). The role of neuromodulators in selective attention. *Trends in Cognitive Sciences* **15**(12):585–591.

- Obeso, J. A., Rodríguez-Oroz, M. C., Benitez-Temino, B., Blesa, F. J., Guridi, J., Marin, C. and Rodriguez, M. (2008). Functional organization of the basal ganglia: therapeutic implications for Parkinson's disease. *Movement Disorders* **23 Suppl 3**:S548–59.
- Ott, T., Jacob, S. N. and Nieder, A. (2014). Dopamine receptors differentially enhance rule coding in primate prefrontal cortex neurons. *Neuron* **84**(6):1317–1328.
- Ott, T. and Nieder, A. (submitted). Dopamine D2 receptors enhance population dynamics in primate prefrontal working memory circuits. *Under review*.
- Ott, T., Stein, A. M. and Nieder, A. (in preparation). Dopamine D1 and D2 receptors oppositely modulate reward signals in primate prefrontal cortex neurons. *In preparation*.
- Petrides, M. (1985). Deficits in non-spatial conditional associative learning after periarculate lesions in the monkey. *Behavioural Brain Research* **16**:95–101.
- Petrides, M. (2000). The role of the mid-dorsolateral prefrontal cortex in working memory. *Experimental Brain Research* **133**(May):44–54.
- Petrides, M. (2005). Lateral prefrontal cortex: architectonic and functional organization. *Philosophical Transactions of the Royal Society B: Biological Sciences* **360**(1456):781–795.
- Petrides, M. and Pandya, D. N. (1999). Dorsolateral prefrontal cortex: comparative cytoarchitectonic analysis in the human and the macaque brain and corticocortical connection patterns. *European Journal of Neuroscience* **11**(3):1011–1036.
- Petrides, M., Tomaiuolo, F., Yeterian, E. H. and Pandya, D. N. (2012). The prefrontal cortex: Comparative architectonic organization in the human and the macaque monkey brains. *Cortex* **48**(1):46–57.
- Pi, H.-J., Hangya, B., Kvitsiani, D., Sanders, J. I., Huang, Z. J. and Kepecs, A. (2013). Cortical interneurons that specialize in disinhibitory control. *Nature* **503**(7477):521–4.
- Puig, M. V. and Miller, E. K. (2012). The role of prefrontal dopamine D1 receptors in the neural mechanisms of associative learning. *Neuron* **74**(5):874–886.
- Puig, M. V. and Miller, E. K. (2015). Neural substrates of dopamine D2 receptor modulated executive functions in the monkey prefrontal cortex. *Cerebral Cortex* **25**(9):2980–2987.
- Ragozzino, M. E. (2002). The effects of dopamine D(1) receptor blockade in the prelimbic-infralimbic areas on behavioral flexibility. *Learning & Memory* **9**(1):18–28.
- Rainer, G., Asaad, W. F. and Miller, E. K. (1998). Selective representation of relevant information by neurons in the primate prefrontal cortex. *Nature* **393**(6685):577–579.
- Ranganath, A. and Jacob, S. N. (2015). Doping the Mind: Dopaminergic Modulation of Prefrontal Cortical Cognition. *The Neuroscientist* (ahead of print): 10.1177/1073858415602850.

- Rao, S. C., Rainer, G. and Miller, E. K. (1997). Integration of what and where in the primate prefrontal cortex. *Science* **276**(5313):821–824.
- Rao, S. G., Williams, G. V. and Goldman-Rakic, P. S. (2000). Destruction and creation of spatial tuning by disinhibition: GABA(A) blockade of prefrontal cortical neurons engaged by working memory. *Journal of Neuroscience* **20**(1):485–494.
- Redgrave, P. and Gurney, K. (2006). The short-latency dopamine signal: a role in discovering novel actions? *Nature Reviews Neuroscience* **7**(12):967–975.
- Redgrave, P., Gurney, K. and Reynolds, J. (2008). What is reinforced by phasic dopamine signals? *Brain Research Reviews* **58**(2):322–339.
- Reynolds, J. H., Pasternak, T. and Desimone, R. (2000). Attention increases sensitivity of V4 neurons. *Neuron* **26**(3):703–714.
- Rigotti, M., Barak, O., Warden, M. R., Wang, X.-J., Daw, N. D., Miller, E. K. and Fusi, S. (2013). The importance of mixed selectivity in complex cognitive tasks. *Nature* **497**:585–90.
- Robbins, T. W. and Arnsten, A. F. T. (2009). The neuropsychopharmacology of fronto-executive function: monoaminergic modulation. *Annual Review of Neuroscience* **32**:267–87.
- Roesch, M. R. and Olson, C. R. (2003). Impact of expected reward on neuronal activity in prefrontal cortex, frontal and supplementary eye fields and premotor cortex. *Journal of Neurophysiology* **90**(3):1766–1789.
- Rolls, E. T., Loh, M., Deco, G. and Winterer, G. (2008). Computational models of schizophrenia and dopamine modulation in the prefrontal cortex. *Nature Reviews Neuroscience* **9**(9):696–709.
- Romo, R. and Schultz, W. (1990). Dopamine neurons of the monkey midbrain: contingencies of responses to stimuli eliciting immediate behavioral reactions. *Journal of Neurophysiology* **63**(3):592–606.
- Salazar, R. F., Dotson, N. M., Bressler, S. L. and Gray, C. M. (2012). Content-specific fronto-parietal synchronization during visual working memory. *Science* **338**(6110):1097–1100.
- Sawaguchi, T. (2001). The effects of dopamine and its antagonists on directional delay-period activity of prefrontal neurons in monkeys during an oculomotor delayed-response task. *Neuroscience Research* **41**(2):115–128.
- Sawaguchi, T. and Goldman-Rakic, P. S. (1991). D1 dopamine receptors in prefrontal cortex: involvement in working memory. *Science* **251**(4996):947–50.
- Sawaguchi, T. and Goldman-Rakic, P. S. (1994). The role of D1-dopamine receptor in working memory: local injections of dopamine antagonists into the prefrontal cortex of rhesus monkeys performing an oculomotor delayed-response task. *Journal of Neurophysiology* **71**(2):515–28.

- Schultz, W. (1986). Responses of midbrain dopamine neurons to behavioral trigger stimuli in the monkey. *Journal of Neurophysiology* **56**(5):1439–1461.
- Schultz, W. (1998). Predictive reward signal of dopamine neurons. *Journal of Neurophysiology* **80**(1):1–27.
- Schultz, W. (2006). Behavioral theories and the neurophysiology of reward. *Annual Review of Psychology* **57**:87–115.
- Schultz, W. (2007). Multiple dopamine functions at different time courses. *Annual Review of Neuroscience* **30**:259–88.
- Schultz, W., Dayan, P. and Montague, P. R. (1997). A neural substrate of prediction and reward. *Science* **275**(5306):1593–9.
- Schultz, W. and Romo, R. (1990). Dopamine neurons of the monkey midbrain: contingencies of responses to stimuli eliciting immediate behavioral reactions. *Journal of Neurophysiology* **63**(3):607–624.
- Seamans, J. K., Durstewitz, D., Christie, B. R., Stevens, C. F., Sejnowski, T. J. and F. S. C. (2001a). Dopamine D1/D5 receptor modulation of excitatory synaptic inputs to layer V prefrontal cortex neurons. *Proceedings of the National Academy of Sciences of the United States of America* **98**(1):301–306.
- Seamans, J. K., Gorelova, N., Durstewitz, D. and Yang, C. R. (2001b). Bidirectional dopamine modulation of GABAergic inhibition in prefrontal cortical pyramidal neurons. *Journal of Neuroscience* **21**(10):3628–38.
- Seamans, J. K., Nogueira, L. and Lavin, A. (2003). Synaptic basis of persistent activity in prefrontal cortex in vivo and in organotypic cultures. *Cerebral Cortex* **13**(11):1242–1250.
- Seamans, J. K. and Yang, C. R. (2004). The principal features and mechanisms of dopamine modulation in the prefrontal cortex. *Progress in Neurobiology* **74**(1):1–58.
- Seeman, P. (2002). Atypical antipsychotics: mechanism of action. *Canadian Journal of Psychiatry* **47**(1):27–38.
- Servan-Schreiber, D., Printz, H. and Cohen, J. D. (1990). A network model of catecholamine effects: gain, signal-to-noise ratio, and behavior. *Science* **249**(4971):892–5.
- Shettleworth, S. J. (2010). *Cognition, evolution, and behavior*. New York: Oxford University Press, 2nd edition.
- Siegel, M., Buschman, T. J. and Miller, E. K. (2015). Cortical information flow during flexible sensorimotor decisions. *Science* **348**(6241):1352–55.
- Silver, R. A. (2010). Neuronal arithmetic. *Nature Reviews Neuroscience* **11**(7):474–489.
- Smiley, J. F. and Goldman-Rakic, P. S. (1993). Heterogeneous targets of dopamine synapses in monkey prefrontal cortex demonstrated by serial section electron microscopy: a laminar analysis using the silver-enhanced diaminobenzidine sulfide (SEDS) immunolabeling technique. *Cerebral Cortex* **3**(3):223–238.

- Smiley, J. F., Levey, A. I., Ciliax, B. J., Goldman-Rakic, P. S. and Ciliax, B. J. (1994). D1 dopamine receptor immunoreactivity in human and monkey cerebral cortex: predominant and extrasynaptic localization in dendritic spines. *Proceedings of the National Academy of Sciences of the United States of America* **91**(12):5720–5724.
- St. Onge, J. R., Abhari, H. and Floresco, S. B. (2011). Dissociable contributions by prefrontal D1 and D2 receptors to risk-based decision making. *Journal of Neuroscience* **31**(23):8625–8633.
- Stark, A. K. and Pakkenberg, B. (2004). Histological changes of the dopaminergic nigrostriatal system in aging. *Cell and Tissue Research* **318**(1):81–92.
- Stelzel, C., Fiebach, C. J., Cools, R., Tafazoli, S. and D’Esposito, M. (2013). Dissociable fronto-striatal effects of dopamine D2 receptor stimulation on cognitive versus motor flexibility. *Cortex* **49**(10):2799–811.
- Stoet, G. and Snyder, L. H. (2009). Neural correlates of executive control functions in the monkey. *Trends in Cognitive Sciences* **13**(5):228–34.
- Stokes, M. G., Kusunoki, M., Sigala, N., Nili, H., Gaffan, D. and Duncan, J. (2013). Dynamic coding for cognitive control in prefrontal cortex. *Neuron* **78**(2):364–375.
- Takahashi, H., Kato, M., Takano, H., Arakawa, R., Okumura, M., Otsuka, T., Kodaka, F., Hayashi, M., Okubo, Y., Ito, H. and Suhara, T. (2008). Differential contributions of prefrontal and hippocampal dopamine D(1) and D(2) receptors in human cognitive functions. *Journal of Neuroscience* **28**(46):12032–8.
- Takahashi, H., Yamada, M. and Suhara, T. (2012). Functional significance of central D1 receptors in cognition: beyond working memory. *Journal of Cerebral Blood Flow and Metabolism* **32**(7):1248–58.
- Takeda, K. and Funahashi, S. (2004). Population vector analysis of primate prefrontal activity during spatial working memory. *Cerebral Cortex* **14**(12):1328–1339.
- Tanji, J. and Hoshi, E. (2008). Role of the lateral prefrontal cortex in executive behavioral control. *Physiological Reviews* **88**(140):37–57.
- Thurley, K., Senn, W. and Lüscher, H.-R. (2008). Dopamine increases the gain of the input-output response of rat prefrontal pyramidal neurons. *Journal of Neurophysiology* **99**(6):2985–97.
- Tobler, P. N., Fiorillo, C. D. and Schultz, W. (2005). Adaptive coding of reward value by dopamine neurons. *Science* **307**(5715):1642–5.
- Tranham-Davidson, H., Neely, L. C., Lavin, A. and Seamans, J. K. (2004). Mechanisms underlying differential D1 versus D2 dopamine receptor regulation of inhibition in prefrontal cortex. *Journal of Neuroscience* **24**(47):10652–9.
- Tripathy, S. J., Burton, S. D., Geramita, M., Gerkin, R. C. and Urban, N. N. (2015). Brain-wide analysis of electrophysiological diversity yields novel categorization of mammalian neuron types. *Journal of Neurophysiology* **113**(10):3474–3489.



- Tseng, K. Y. and O'Donnell, P. (2004). Dopamine-glutamate interactions controlling prefrontal cortical pyramidal cell excitability involve multiple signaling mechanisms. *Journal of Neuroscience* **24**(22):5131–9.
- Vallentin, D., Bongard, S. and Nieder, A. (2012). Numerical rule coding in the prefrontal, premotor, and posterior parietal cortices of macaques. *Journal of Neuroscience* **32**(19):6621–30.
- Vijayraghavan, S., Wang, M., Birnbaum, S. G., Williams, G. V. and Arnsten, A. F. T. (2007). Inverted-U dopamine D1 receptor actions on prefrontal neurons engaged in working memory. *Nature Neuroscience* **10**(3):376–84.
- Viswanathan, P. and Nieder, A. (2013). Neuronal correlates of a visual "sense of number" in primate parietal and prefrontal cortices. *Proceedings of the National Academy of Sciences of the United States of America* **110**(27):11187–92.
- Von Huben, S. N., Davis, S. a., Lay, C. C., Katner, S. N., Crean, R. D. and Taffe, M. a. (2006). Differential contributions of dopaminergic D1- and D2-like receptors to cognitive function in rhesus monkeys. *Psychopharmacology (Berl.)* **188**:586–596.
- Walker, A. E. (1940). A cytoarchitectural study of the prefrontal area of the macaque monkey. *Journal of Comparative Neurology* **73**(1):59–86.
- Wallis, J. D., Anderson, K. C. and Miller, E. K. (2001). Single neurons in prefrontal cortex encode abstract rules. *Nature* **411**(6840):953–6.
- Wallis, J. D. and Miller, E. K. (2003). Neuronal activity in primate dorsolateral and orbital prefrontal cortex during performance of a reward preference task. *European Journal of Neuroscience* **18**(7):2069–2081.
- Wang, M., Vijayraghavan, S. and Goldman-Rakic, P. S. (2004a). Selective D2 receptor actions on the functional circuitry of working memory. *Science* **303**(5659):853–6.
- Wang, M., Yang, Y., Wang, C.-J., Gamo, N. J., Jin, L. E., Mazer, J. a., Morrison, J. H., Wang, X.-J. and Arnsten, A. F. T. (2013). NMDA receptors subserve persistent neuronal firing during working memory in dorsolateral prefrontal cortex. *Neuron* **77**(4):736–49.
- Wang, X. J. (1999). Synaptic basis of cortical persistent activity: the importance of NMDA receptors to working memory. *Journal of Neuroscience* **19**(21):9587–9603.
- Wang, X.-J. (2002). Probabilistic decision making by slow reverberation in cortical circuits. *Neuron* **36**:955–968.
- Wang, X.-J. (2008). Decision making in recurrent neuronal circuits. *Neuron* **60**(2):215–234.
- Wang, X.-J., Tegnér, J., Constantinidis, C. and Goldman-Rakic, P. S. (2004b). Division of labor among distinct subtypes of inhibitory neurons in a cortical microcircuit of working memory. *Proceedings of the National Academy of Sciences of the United States of America* **101**(5):1368–1373.
- Wang, Y. and Goldman-Rakic, P. S. (2004). D2 receptor regulation of synaptic burst firing in prefrontal cortical pyramidal neurons. *Proceedings of the National Academy of Sciences of the United States of America* **101**(14):5093–8.

- Watanabe, M. (1996). Reward expectancy in primate prefrontal neurons. *Nature* **382**(6592):629–32.
- Watanabe, M. (2007). Role of anticipated reward in cognitive behavioral control. *Current Opinion in Neurobiology* **17**(2):213–9.
- Watanabe, M., Hikosaka, K., Sakagami, M. and Shirakawa, S.-I. (2005). Functional significance of delay-period activity of primate prefrontal neurons in relation to spatial working memory and reward/omission-of-reward expectancy. *Experimental Brain Research* **166**(2):263–76.
- Williams, G. V. and Goldman-Rakic, P. S. (1995). Modulation of memory fields by dopamine D1 receptors in prefrontal cortex. *Nature* **376**(6541):572–5.
- Williams, S. M. and Goldman-Rakic, P. S. (1998). Widespread origin of the primate mesofrontal dopamine system. *Cerebral Cortex* **8**(4):321–45.
- Wilson, F. a., Scalaide, S. P. and Goldman-Rakic, P. S. (1993). Dissociation of object and spatial processing domains in primate prefrontal cortex. *Science* **260**(5116):1955–1958.
- Wilson, N. R., Runyan, C. A., Wang, F. L. and Sur, M. (2012). Division and subtraction by distinct cortical inhibitory networks in vivo. *Nature* **488**(7411):343–8.
- Wise, R. a. (2004). Dopamine, learning and motivation. *Nature Reviews Neuroscience* **5**(6):483–94.
- Wise, R. a. (2009). Roles for nigrostriatal—not just mesocorticolimbic—dopamine in reward and addiction. *Trends in Neurosciences* **32**(10):517–24.
- Zhong, P. and Yan, Z. (2016). Distinct Physiological Effects of Dopamine D4 Receptors on Prefrontal Cortical Pyramidal Neurons and Fast-Spiking Interneurons. *Cerebral Cortex* **26**(1):180–191.
- Zoli, M., Torri, C., Ferrari, R., Jansson, A., Zini, I., Fuxe, K. and Agnati, L. F. (1998). The emergence of the volume transmission concept. *Brain Research Reviews* **26**(2-3):136–47.

---

**Part II.**  
**Individual studies**



---

### **Study 1: Dopamine modulation of visual signals**

Jacob\*, S. N., Ott\*, T., Nieder, A. (2013). Dopamine regulates two classes of primate prefrontal neurons that represent sensory signals. *Journal of Neuroscience* **33**(34):13724–34. (\*shared first-authorship)



# Dopamine Regulates Two Classes of Primate Prefrontal Neurons That Represent Sensory Signals

Simon N. Jacob,\* Torben Ott,\* and Andreas Nieder

Animal Physiology, Institute of Neurobiology, University of Tübingen, D-72076 Tübingen, Germany

The lateral prefrontal cortex (PFC), a hub of higher-level cognitive processing, is strongly modulated by midbrain dopamine (DA) neurons. The cellular mechanisms have been comprehensively studied in the context of short-term memory, but little is known about how DA regulates sensory inputs to PFC that precede and give rise to such memory activity. By preparing recipient cortical circuits for incoming signals, DA could be a powerful determinant of downstream cognitive processing. Here, we tested the hypothesis that prefrontal DA regulates the representation of sensory signals that are required for perceptual decisions. In rhesus monkeys trained to report the presence or absence of visual stimuli at varying levels of contrast, we simultaneously recorded extracellular single-unit activity and applied DA to the immediate vicinity of the neurons by micro-iontophoresis. We found that DA modulation of prefrontal neurons is not uniform but tailored to specialized neuronal classes. In one population of neurons, DA suppressed activity with high temporal precision but preserved signal/noise ratio. Neurons in this group had short visual response latencies and comprised all recorded narrow-spiking, putative interneurons. In a distinct population, DA increased excitability and enhanced signal/noise ratio by reducing response variability. These neurons had longer visual response latencies and were composed exclusively of broad-spiking, putative pyramidal neurons. By gating sensory inputs to PFC and subsequently strengthening the representation of sensory signals, DA might play an important role in shaping how the PFC initiates appropriate behavior in response to changes in the sensory environment.

## Introduction

All neuronal systems are subject to neuromodulation, which can profoundly alter the properties of target circuits (Marder, 2012). The primate lateral prefrontal cortex (PFC), a hub of higher-level cognitive functioning (Fuster, 2008; Bongard and Nieder, 2010; Eiselt and Nieder, 2013), receives particularly strong projections from dopamine (DA) neurons in the midbrain (Williams and Goldman-Rakic, 1998; Björklund and Dunnett, 2007). DA neurons fire phasic bursts of action potentials with short latencies of 100–150 ms in response to behaviorally relevant sensory events (Schultz, 1998; Matsumoto and Hikosaka, 2009). Therefore, it has been suggested that DA could prepare its higher-order target areas for the processing of incoming signals (Redgrave and Gurney, 2006; de Lafuente and Romo, 2011). How might DA influence recipient prefrontal neurons to control information relayed to this important cortical structure?

Prefrontal DA regulates many frontal lobe functions, such as set-shifting and behavioral flexibility (Floresco et al., 2006), association learning (Puig and Miller, 2012), and the maintenance of

stimuli in working memory (Brozoski et al., 1979). Much of what is known about the mechanisms of DA action in PFC stems from electrophysiological studies on memory-related activity, i.e., in the absence of sensory stimulation (Williams and Goldman-Rakic, 1995). In rhesus monkeys engaged in a spatial working memory task, PFC neurons active in the delay period of the task showed improved tuning to preferred remembered locations when stimulated with DA receptor agonists (Vijayraghavan et al., 2007). Therefore, it is believed that the principal function of DA in PFC is to strengthen mental representations (Arnsten, 2011).

In contrast, little is known about how DA modulates prefrontal sensory signals that precede and give rise to such sustained activity. Anecdotal evidence indicates that visual stimuli used to cue a target to be remembered are also influenced by DA (Sawaguchi et al., 1990; Williams and Goldman-Rakic, 1995), but quantitative analysis and an in-depth investigation of the cellular mechanisms are lacking. Because phasic DA activity that is time-locked to relevant sensory stimuli seems particularly suited to regulate the representation of these shorter-lived signals, it has been proposed that DA might serve as a gating signal that controls inputs to PFC (Servan-Schreiber et al., 1990; D'Ardenne et al., 2012). By assigning salience to prefrontal sensory inputs, phasic DA could strongly influence subsequent cognitive processing in PFC. Visual signals, for example, are passed through lower-level cortical areas in a feedforward manner and reach the PFC within 100–150 ms (Thorpe and Fabre-Thorpe, 2001). The PFC collects this sensory information to form subjective judgments, such as regarding the presence or absence of sensory stimulation (de Lafuente and Romo, 2006). Recent electrophysiological studies have demonstrated that the physical intensity of tactile and visual

Received Jan. 16, 2013; revised June 10, 2013; accepted July 9, 2013.

Author contributions: S.N.J. and A.N. designed research; S.N.J. and T.O. performed research; S.N.J. and T.O. analyzed data; S.N.J., T.O., and A.N. wrote the paper.

This work was supported by grants from the German Research Foundation [S.N.J. (Grant JA 1999/1-1) and A.N. (Grant NI 618/2-1)]. We thank A. Thiele for technical assistance with electrode fabrication and iontophoresis, K. Merten for help with animal training and data analysis, and S. Hage and C. Zielinski for comments on this manuscript.

\*S.N.J. and T.O. contributed equally to this work.

The authors declare no competing financial interests.

Correspondence should be addressed to Dr. Simon N. Jacob, Department of Psychiatry and Psychotherapy, Charité Berlin, Charitéplatz 1, 10117 Berlin, Germany. E-mail: simon.jacob@charite.de.

DOI:10.1523/JNEUROSCI.0210-13.2013

Copyright © 2013 the authors 0270-6474/13/3313724-11\$15.00/0

stimuli is represented in single neurons of the primate PFC alongside their perceived intensity, i.e., the animal's subjective experience of a stimulus (de Lafuente and Romo, 2005; Merten and Nieder, 2012, 2013).

Here, we investigate in trained rhesus monkeys how DA controls the prefrontal representation of such brief sensory stimuli that must be detected by the animals (Merten and Nieder, 2012, 2013). We found that DA strengthens visual signals by modulating activity in two distinct classes of neurons. Our results suggest that prefrontal DA may play an important role in determining how the PFC orchestrates behavioral responses triggered by sensory events.

## Materials and Methods

### *Surgical procedures*

Two male rhesus monkeys (*Macaca mulatta*) were implanted with a titanium head post and one recording chamber centered over the principal sulcus of the lateral PFC, anterior to the frontal eye fields (right hemisphere in monkey H, right and left hemispheres consecutively in monkey M). Surgery was conducted using aseptic techniques under general anesthesia. Structural magnetic resonance imaging was performed before implantation to locate anatomical landmarks. All experimental procedures were in accordance with the guidelines for animal experimentation approved by the local authority, the Regierungspräsidium Tübingen.

### *Behavioral protocol*

**Task.** The monkeys were trained to report the presence or absence of visual objects flashed at varying contrast levels centered on their perceptual threshold. The animals initiated each experimental trial by grasping a lever and fixating a central fixation target (fixation period). After 500 ms, a stimulus was displayed for 100 ms in half of the trials (stimulus period). In the other half, no stimulus was shown. Both trial types were randomly intermixed. After the delay period (2700 ms), a colored rule cue instructed the monkey how to respond. If a stimulus was presented, a red square cue required the monkey to release the lever within 1000 ms to receive a fluid reward, whereas a blue cue indicated to the monkey to keep holding the lever for 1200 ms. The rule applied in the inverse way if no stimulus was presented.

CORTEX software (National Institute of Mental Health, Bethesda, MD) was used for experimental control and behavioral data acquisition. The animals maintained fixation throughout the fixation, stimulus, and delay periods within 1.75° of visual angle of the central fixation target (ISCAN).

**Visual stimuli.** The stimulus consisted of a gray object (4° of visual angle in diameter) presented at seven levels of contrast close to perceptual threshold, determined individually for each animal (monkey H: 7.3, 8.7, 10.6, 11.6, 19.9, 24.9, and 28.0%; monkey M: 9.1, 9.8, 11.8, 12.5, 14.7, 16.7, and 17.4%), measured with an LS-100 luminance meter (Konica Minolta). The shape of the object was chosen randomly from a set of two objects: hexagon and circle for monkey H; cross and rhomboid for monkey M. The area of the object was kept constant to maintain the same visual contrast across different shapes.

Visual contrasts were determined for each animal individually to yield approximately the same data points on the psychometric curve. To pool data for analysis, visual contrasts were normalized to an ordinal scale of 1–7 (1 corresponding to the lowest and 7 to the highest stimulus contrast presented to each animal, regardless of the actual physical intensity). Salient stimuli analyzed in Figures 3 and 5 denote the three highest contrasts (5–7).

### *Electrophysiology*

In each recording session, up to three electrodes (see below, Iontophoresis) were inserted transdurally using a modified electrical microdrive (NAN Instruments). Neurons were recorded at random; no attempt was made to preselect neurons according to particular response properties. Signal acquisition, amplification, filtering, and digitalization were accomplished with the MAP system (Plexon). Waveform separation was performed offline (Offline Sorter; Plexon).

### *Iontophoresis*

DA was applied iontophoretically (MVCS iontophoresis system; npi electronic) using custom-made tungsten-in-glass electrodes flanked by two pipettes each (Thiele et al., 2006). Electrode impedances were 1–3 M $\Omega$  (measured at 500 Hz; Omega Tip Z; World Precision Instruments). Pipette resistances depended on the pipette opening diameter, drug, and solvent used. Typical resistances were 15–50 M $\Omega$  (full range, 15–150 M $\Omega$ ). Pilot *in vitro* experiments (DA iontophoresis into NaCl, concentrations quantified by HPLC) determined the smallest holding current that ensured good retention without accumulation of dead space and thus allowed for rapid delivery of DA after switching to ejection currents. Retention currents were –7 to –10 nA. Ejection currents for DA (200 mM in double-distilled water, pH 4.0 with HCl; Sigma-Aldrich) were +25–100 nA (median, +50 nA). Control experiments with 0.9% NaCl, pH 7, used +50 nA. Ejection currents were chosen to match the values reported to be maximally effective, i.e., in the peak range of the inverted-U function (Sawaguchi, 2001; Vijayraghavan et al., 2007). DA currents were varied only during experiments to determine whether the ratio of inhibition/excitation depended on the applied concentration. Otherwise, we did not attempt to investigate dosage effects.

One pipette per electrode was filled with DA solution, and the other contained 0.9% NaCl. Electrode impedance and pipette resistance were measured after each recording session. DA was applied continuously for 12–15 min, depending on the number of trials completed correctly by the animal. The first block was always the control condition. Given the fast DA application verified by HPLC (see above), we did not automatically exclude data at the current switching points.

### *Data analyses*

Data analysis was performed with MATLAB (Mathworks). None of the reported analyses depended on the exact choice of trials to include or time windows to analyze. Repeating analyses with a different choice of parameters yielded comparable results.

**Excitability modulation.** Neurons stimulated with DA were excluded from additional analysis if their baseline (fixation period) discharge rates were <1 Hz in the control or DA phase. Baseline firing rates of each neuron were pooled for the control condition and the DA condition and compared with a rank-sum test (Mann–Whitney *U* test). If the median firing rate in the DA condition was significantly ( $p < 0.05$ , two-sided test) larger than in the control condition, the neuron was classified as excited, and if the median was lower, the neuron was classified as inhibited by DA.

**Receiver operating characteristic analyses.** Neuronal coding strength was quantified using receiver operating characteristic (ROC) analysis (Green and Swets, 1966). The area under the ROC curve (auROC) is a nonparametric measure of the discriminability of two distributions. It denotes the probability with which an ideal observer can tell apart a meaningful signal from a noisy background. Values of 0.5 indicate no separation, and values of 1 signal perfect discriminability. The auROC takes into account both the difference between distribution means as well as their widths and is therefore a more suitable indicator of signal quality than other, simpler measures of signal/noise ratio (Servan-Schreiber et al., 1990; Parker and Newsome, 1998; Herrero et al., 2008).

**Stimulus-responsive neurons.** A two-way ANOVA was calculated with main factors stimulus contrast (salient/absent) and iontophoresis condition (control/DA) using firing rates after stimulus presentation (300 ms time window aligned to the individual response latency of the neuron; see below), including correct trials only. Neurons with a significant stimulus main effect ( $p < 0.05$ ) were classified as stimulus responsive. Salient stimulation was defined as the three highest visual contrasts.

Except for the analysis in Figure 7*b* (see below), visual response latencies were calculated using sliding ROC analysis with a window size of 50 ms, step of 1 ms. For each window, we calculated the auROC by comparing the firing rates between correct salient stimulus trials (hits) and correct absent stimulus trials (correct rejections). To test whether the auROC was significantly different from 0.5, bootstrapping was used to construct 999 resamples by randomly sampling the data with replacement and maintaining the original number of trials per condition. The latency of a neuron was defined as the time after stimulus onset but no



later than 500 ms, when the auROC exceeded the 95% confidence interval of the bootstrapped data for 50 consecutive windows. The response latency was determined separately for the control and DA conditions. If no value could be determined, a default latency corresponding to the median response latency of all neurons in the respective condition was used (228 and 217 ms for the control and DA conditions, respectively). The choice of these parameters ensured that the analysis window (see below, Neuronal signal metrics) covered the stimulus response in all neurons.

To directly compare visual response latencies between the population of inhibited and excited stimulus encoding neurons (see Fig. 7*b*), response latency was defined as two consecutive significant auROC values using a window size of 50 ms, step of 10 ms. This choice of parameters was more sensitive to the actual onset of the stimulus response so that latencies were reliably determined in all stimulus neurons (i.e., no default latencies were used).

For single-cell spike density histograms, the average firing rate in salient trials and trials without visual stimulation (correct trials only) was smoothed with a Gaussian kernel (bin width of 150 ms, step of 1 ms). For the population responses, activity was normalized, averaged, and smoothed with the same Gaussian kernel. Responses were normalized by subtracting the mean baseline firing rate in the control condition and dividing by the SD of the baseline firing rates in the control condition.

Stimulus responses calculated using sliding ROC analysis (window size of 300 ms, step of 50 ms) quantified the discriminability between the firing rate distributions of correct salient trials and correct rejection trials.

**Neuronal signal metrics.** All analyses were performed using data from a 300 ms window aligned to individual visual response latencies. This ensured that stimulus responses were adequately captured in all neurons. To distinguish between additive and multiplicative operations, the difference between the mean firing rate in hit trials and correct rejections was divided by the mean baseline firing rate for all (normalized) contrasts and both iontophoresis conditions (Vijayraghavan et al., 2007). Neuro-metric curves were determined by calculating the auROC between discharge rates in hit trials and correct rejections for all (normalized) visual contrasts. Neuronal variability was quantified by the Fano factor (FF), i.e., the ratio of trial-by-trial spike count variance and mean spike count (Churchland et al., 2010).

To determine whether DA modulated a signal metric, multiple linear regression analysis was applied to the population data (Merten and Nieder, 2012). Linear functions were fitted to the factors normalized visual contrast and iontophoresis condition (control and DA) using the model for the signal metric ( $S$ ):  $S = a_{-0} + a_{-stim} \times STIM + a_{-ion} \times ION$ , where  $a_{-stim}$  and  $a_{-ion}$  are the coefficients that quantify the signal metric dependence on the normalized stimulus contrast (STIM) and the iontophoresis condition (ION). To assess DA effects on the analyzed signal metric,  $p$  values for the factor iontophoresis condition were used ( $t$  statistics for the coefficient  $a_{-ion}$ ).

DA modulation of neuronal variability was also quantified by multiple linear regression analysis. Linear functions were fitted to the relationship between mean spike count of each contrast and neuron (COUNT) and variance of the spike count of each contrast and neuron (VAR) separately for each iontophoresis condition (ION), i.e., control and DA. An interaction term was included to analyze changes in the slope of the linear functions induced by DA ( $VAR \times ION$ ). The model term was  $COUNT = a_{-0} + a_{-var} \times VAR + a_{-ion} \times ION + a_{-int} \times VAR \times ION$ .  $p$  values for the interaction term  $a_{-int}$  were used to assess DA effects on neuronal variability.

**Kinetics of excitability.** Exponential functions were fitted to the baseline firing rates of all trials recorded within 6 min of switching to the ejection current (temporal resolution of one trial, i.e., one data point per 5 s). Neurons with bad fits (e.g., fitted parameters out of bounds;  $n = 1$  inhibited cell,  $n = 4$  excited cells) were excluded from additional analysis. If several DA phases were recorded, baseline firing rates were aligned to all instances of switching to the ejection current and averaged using bins of 5 s. The amplitude of DA modulation was estimated by the mean baseline firing rate in the first or second half of the DA condition for inhibited and excited neurons, respectively. The time course of the base-

line firing rate (FR) was expressed as  $FR = A \times (1 - \exp(-x/\tau))$ , where  $A$  is the estimated amplitude and  $\tau$  the parameter fitted using nonlinear least squares. The population time course was calculated by averaging the normalized baseline discharge rates from all trials recorded within 6 min before and after switching to DA application using bins of 5 s and smoothed with a Gaussian kernel (width of 10 s, step of 5 s).

**Extracellular action potential waveforms.** Recorded single units were categorized into narrow-spiking (NS) and broad-spiking (BS) neurons, i.e., putative interneurons and pyramidal cells, using a linear classifier ( $k$ -means,  $k = 2$ , squared Euclidean distance) (Diester and Nieder, 2008). For each single unit, the template waveform was extracted with the Plexon Offline sorter. Only neurons with a downward voltage deflection followed by an upward peak were included. Units with a minimum outside 200–400  $\mu$ s or a maximum before 300  $\mu$ s after reaching the initial threshold were excluded ( $n = 3$  of 60 units). Waveforms were normalized by their difference between maximum and minimum voltage deflection and aligned to their minimum. Units in the cluster with the smaller mean spike width constituted the population of NS neurons, and units in the cluster with the larger mean spike width constituted the BS neurons. Interdependence between modulation type (excited or inhibited by DA) and waveform type was tested with Fisher's exact test.

## Results

To determine how DA regulates sensory signals in PFC, we presented brief flashes of visual stimuli at varying contrasts to two rhesus macaque monkeys (*Macaca mulatta*). The animals were trained to detect the stimuli and report their subjective perceptual judgment about the presence or absence of visual stimulation (Merten and Nieder, 2012) (Fig. 1*a*). The rule-based task design ensured that neuronal activity in the delay period after the stimulus was free of preparatory motor signals. While the monkeys performed this task, we recorded single units from the lateral PFC. During recordings, trial blocks without pharmacological manipulation (control) alternated with blocks in which DA was applied to the vicinity of the recorded cells by micro-iontophoresis (Fig. 1*b*). As expected, we did not observe changes in the monkeys' behavior as a consequence of micro-iontophoretic drug application (Fig. 1*c,d*), because transmitter application with this method is very focal (Herz et al., 1969).

### Two classes of DA-sensitive prefrontal neurons

We recorded 110 neurons that entered the analysis (60 neurons from monkey M, 50 neurons from monkey H). Application of DA influenced the excitability of prefrontal neurons. We compared fixation period activity in the control condition with the DA condition (rank-sum test,  $p < 0.05$ ; Fig. 2*a*). DA suppressed discharge rates in 32 neurons (DA-inhibited neurons; single-neuron example in Fig. 2*b*). Activity increased in 28 neurons (DA-excited neurons; single-neuron example in Fig. 2*c*). Discharge rates were unaffected in 50 neurons (DA-unmodulated neurons; data not shown). The changes in excitability were independent of the iontophoretically applied DA dosage. The proportion of DA-inhibited to DA-excited neurons was not altered when the cell counts were determined separately for lower (+25–50 nA) and higher (+75–100 nA) ejection currents (23:22 versus 9:6, respectively; Fisher's exact test,  $p = 0.8$ ). None of the physiological parameters analyzed in the following changed in DA-unmodulated cells. This indicates that the effects reported for DA-excited and DA-inhibited neurons were not the result of nonspecific electrical currents.

Inhibitory and excitatory DA effects showed different time courses in the two groups of neurons. In a representative inhibited neuron, DA-mediated suppression of spiking activity was fast and reversed equally rapidly (Fig. 2*b*). In a typical excited neuron, DA caused much slower, undulating changes in firing

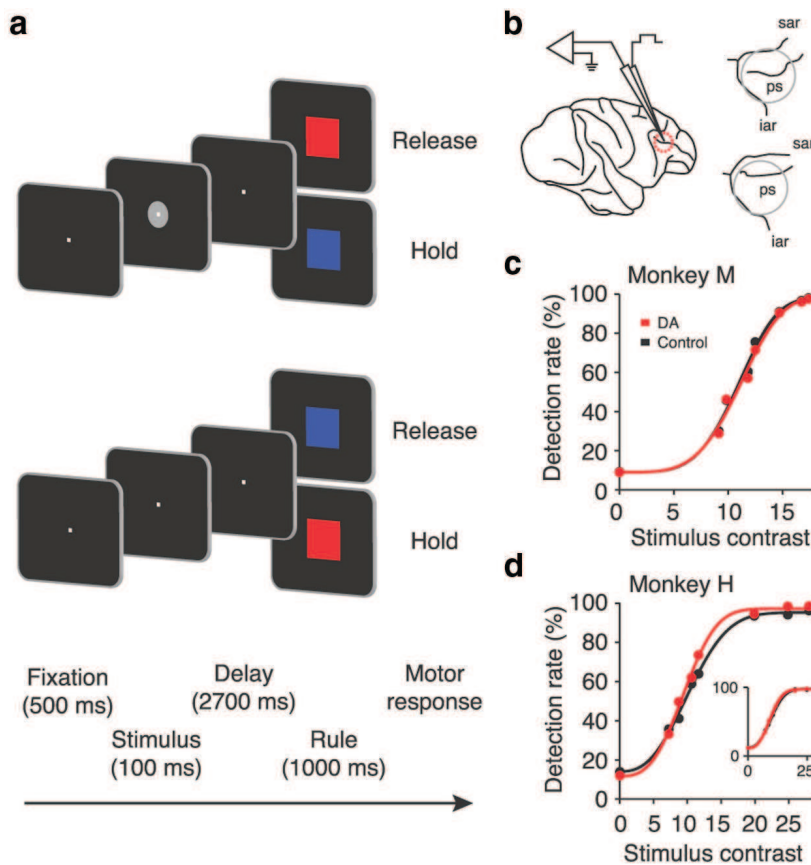


**Figure 1.** Behavioral protocol and electrophysiological recordings with micro-iontophoresis. *a*, Stimulus detection task requiring the monkeys to report whether a visual stimulus had been presented. A visual stimulus of varying contrast levels was flashed for 100 ms in 50% of trials (top). In the other 50%, a blank screen was shown (bottom). *b*, Left, Lateral view of a rhesus monkey brain depicting the location of extracellular neuronal recording and DA iontophoresis in the principal sulcus region of the PFC. Right, Anatomical reconstruction of the recording locations in monkey M (top) and monkey H (bottom). *c*, Psychometric curves with Weibull fits for monkey M ( $n = 31$  sessions). Data for control and DA conditions were pooled across sessions. *d*, Conventions as in *c* for monkey H ( $n = 26$  sessions). The slight difference in performance between control and DA trials in monkey H was attributable to decreased performance at the start of each session (“warm-up” phenomenon; always the control condition) and not the result of DA application. The inset shows psychometric curves for monkey H with the first 5 min (~5%) of each session omitted. ps, Principal sulcus; sar, superior arcuate sulcus; iar, inferior arcuate sulcus.

rates (Fig. 2*c*). These effects were confirmed at the population level (Fig. 2*d,e*): inhibition was precisely time-locked to DA application, whereas DA-mediated excitation reached maximum levels only much later. The rate of change in excitability after DA application was quantified by fitting exponential curves to the temporal profile of neuronal activity. The distribution of time constants suggested categorical differences in the rate of change rather than a gradual transition [mean time constants of  $8.9 \pm 2.1$  s (median, 3.7 s) and  $221.9 \pm 37.1$  s (median, 190 s) for DA-inhibited and DA-excited neurons, respectively; rank-sum test,  $p < 0.001$ ; Figure 2*f,g*]. Control experiments with NaCl application verified that the rapid reduction in excitability was absent during this sham condition and thus not the result of positive ejection currents ( $n = 13$  neurons; Fisher’s exact test comparing with DA condition,  $p < 0.05$ ).

#### Neuron-class-specific modulation of visual responses by DA

We hypothesized that the categorical changes in excitability might reflect differences in how sensory information is represented in these groups of neurons and how it is modulated by DA. Forty-four percent ( $n = 14$ ), 36% ( $n = 10$ ), and 34% ( $n = 17$ ) of DA-inhibited, DA-excited, and DA-unmodulated neurons, respectively, responded to salient visual stimuli [highest three con-

trasts; two-way ANOVA with main effects stimulus (salient/absent) and experimental condition (control/DA), main effect of stimulus,  $p < 0.05$ ; Fig. 2*a*]. A representative DA-inhibited neuron encoded salient visual stimuli with a clear increase in activity in both the control (Fig. 3*a*) and DA (Fig. 3*b*) conditions. Inhibitory DA effects were reversible and subsided when DA application was discontinued (Fig. 3*c*). In contrast, the stimulus response was marginal in an example DA-excited neuron (Fig. 3*d*) but increased markedly after DA was applied (Fig. 3*e*). Again, these changes were clearly reversible (Fig. 3*f*).

These single-cell effects were verified at the population level. Across all DA-inhibited cells, DA induced an offset in activity but preserved the spike rate difference between trials with salient stimuli and no stimulation (Fig. 3*g,h*). However, DA-excited neurons increased stimulus coding based on spike rate differences between trials with salient and absent stimuli (Fig. 3*i,j*).

We further characterized how DA modulated neuronal excitability. For all contrast levels and neurons, we normalized the stimulus-evoked change in firing rate ( $\Delta R_s$ ; difference between mean activity in trials with and without visual stimulation, calculated in a 300 ms window after stimulus presentation) to baseline activity in the fixation period. Data are presented separately for DA-inhibited and DA-excited neurons in both iontophoresis conditions (Fig. 4*a,b*). In DA-inhibited cells, DA subtracted response levels: the normalized  $\Delta R_s$  increased after DA application, i.e., the firing rate difference between trials with and without stimulation was retained at lower baseline firing rates (multiple linear regression, factor iontophoresis condition,  $p < 0.01$ ; Fig. 4*a*).

In DA-excited cells, DA increased gain: there was no change in normalized  $\Delta R_s$  with DA, i.e., the firing rate difference increased in proportion to the baseline (multiple linear regression, factor iontophoresis condition,  $p = 0.5$ ; Fig. 4*b*).

#### Prefrontal DA enhances visual coding strength in excited neurons

We quantified the capacity of the neurons to discriminate between present and absent visual stimulation, i.e., their coding strength or signal/noise ratio. We compared spike rates in these two conditions by calculating the auROC derived from signal detection theory (Green and Swets, 1966). auROC values of 0.5 indicate no discriminability, and values of 1 indicate signal perfect discriminability. For the representative DA-inhibited neuron from Figure 3, *a* and *b*, auROC values increased considerably after the presentation of salient stimuli, but they were unaffected by DA application (Fig. 5*a*). These time courses were confirmed in the population of DA-inhibited neurons (Fig. 5*b*). DA did not induce systematic changes in auROC values in this class of cells (seven neurons increased, seven neurons decreased; mean

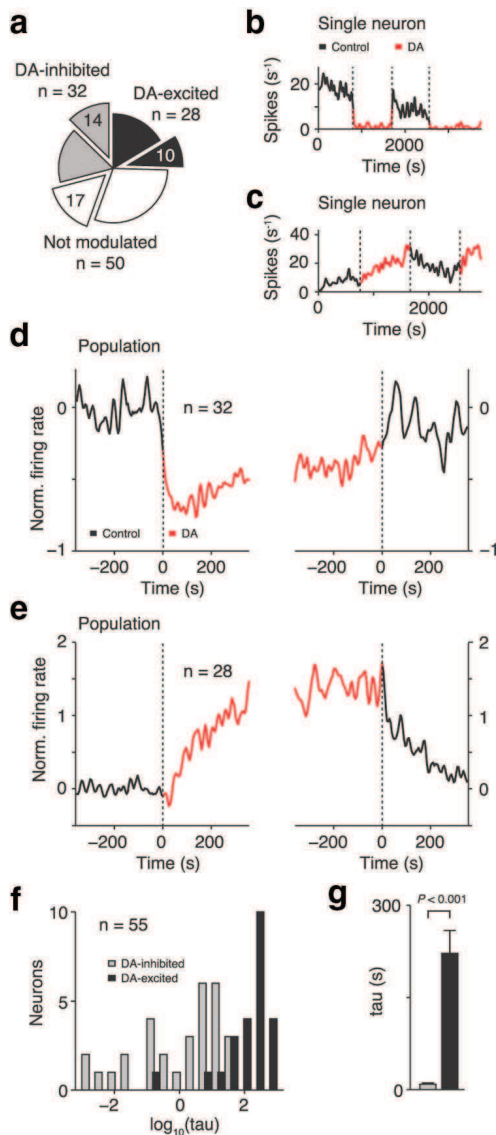


**Figure 2.** Kinetics of DA modulation in inhibited and excited neurons. **a**, Total number of neurons excited, inhibited, or not modulated by DA together with number of stimulus coding neurons in each group (blown out pie sections). **b–e**, Time courses of responses to DA. Baseline (fixation period) firing rates of an example DA-inhibited (**b**) and DA-excited (**c**) neuron stimulated repeatedly with DA over the course of  $\sim 1$  h. Population mean baseline activity of DA-inhibited (**d**) and DA-excited (**e**) neurons aligned to onset (left) and termination (right) of DA application. Inhibition by DA was fast, whereas excitation by DA occurred on longer time-scales. **f**, Frequency distribution of time constants ( $\tau$ ) of exponential fits to single-cell data (baseline activity aligned to DA onset). Five neurons with bad fits were excluded and are not shown (see Materials and Methods). **g**, Mean time constants in the two classes of DA-sensitive neurons. Error bars indicate SEM across neurons.

$\Delta$ auROC pooled across contrasts,  $-0.0102 \pm 0.0143$ ; signed-rank test,  $p = 0.5$ ). Mean population auROC values for individual stimuli tended to increase as a function of stimulus contrast and did not change when DA was applied (multiple linear regression; factor contrast,  $p = 0.12$ ; factor iontophoresis condition;  $p = 0.6$ ; Fig. 5c). Thus, DA did not affect visual coding strength in DA-inhibited neurons.

In contrast, DA significantly improved the stimulus coding quality of DA-excited neurons. Figure 5d shows the time course of the example DA-excited cell from Figure 3, d and e. Stimulus-evoked auROC values increased in this neuron under the influence of DA. This time course was confirmed in the population of DA-excited neurons (Fig. 5e). The increase in auROC values was

very consistent across all DA-excited single cells (eight neurons increased, one neuron unchanged, one neuron decreased; mean  $\Delta$ auROC pooled across contrasts,  $+0.0748 \pm 0.0258$ ; signed-rank test,  $p < 0.05$ ). Mean population auROC values, separated into individual contrasts, increased as a function of stimulus contrast and were significantly higher with DA compared with the control condition (multiple linear regression; factor contrast,  $p < 0.001$ ; factor iontophoresis condition;  $p < 0.001$ ; Fig. 5f). No changes were induced by DA in DA-unmodulated neurons (multiple linear regression; factor contrast,  $p < 0.001$ ; factor iontophoresis condition;  $p = 0.14$ ; data not shown). These results demonstrate that prefrontal DA does not uniformly modify visual coding strength but selectively enhances the capacity to discriminate stimuli from background in the class of DA-excited neurons.

### Prefrontal DA reduces neuronal variability in excited neurons

To investigate which mechanisms could give rise to the strengthening of cortical processing by DA, we determined whether a reduction in neuronal noise (discharge rate variability; Shadlen and Newsome, 1998) might be a contributing factor as hypothesized frequently (Winterer and Weinberger, 2004; Durstewitz and Seamans, 2008; Rolls et al., 2008). To do so, we analyzed the correlation between mean spike counts after stimulus presentation (correct trials) and spike count variance across trials for all neurons in a given class. For quasi-Poisson spiking processes, the data should cluster along the first diagonal (McAdams and Maunsell, 1999). This was the case for DA-inhibited neurons under both control and DA conditions (multiple linear regression, interaction term,  $p = 0.64$ ; Fig. 6a). On a single-cell level, no systematic DA effects on response variability were observed as measured by FF (spike count variance divided by mean; seven neurons increased, seven neurons decreased; mean  $\Delta$ FF pooled across contrasts,  $-0.1498 \pm 0.1709$ ; signed-rank test,  $p = 0.63$ ). Mean population FFs for each contrast were unchanged in DA-inhibited neurons after application of DA (multiple linear regression; factor iontophoresis condition,  $p = 0.31$ ; Fig. 6b).

In contrast to the findings for DA-inhibited neurons, trial-to-trial variability decreased significantly in DA-excited neurons under the influence of DA (multiple linear regression, interaction term,  $p < 0.01$ ; Fig. 6c). The FF reduction was consistent across single cells (eight neurons decreased, two neurons increased; mean  $\Delta$ FF pooled across contrasts,  $-0.391 \pm 0.1931$ ; signed-rank test,  $p < 0.05$ ). Mean population FFs, separated into individual contrasts, were significantly reduced by DA compared with the control condition (multiple linear regression, factor iontophoresis condition;  $p < 0.05$ ; Fig. 6d). No changes were induced in DA-unmodulated neurons (multiple linear regression; factor iontophoresis condition;  $p = 1.0$ ; data not shown). Thus, DA rendered prefrontal processing more reliable by reducing noise at the level of DA-excited neurons.

### Inhibition and excitation control distinct prefrontal processing stages

To further characterize the two DA-responsive neuron classes, we analyzed the extracellular action potential waveforms of the cells. Electrophysiological recordings have suggested that longer waveforms might be primarily associated with pyramidal cells (BS neurons), whereas shorter waveforms could be more typical of interneurons (NS neurons) (Henze et al., 2000; Diester and Nieder, 2008; Hussar and Pasternak, 2009; Vigneswaran et al., 2011). We calculated the average normalized waveform for each single

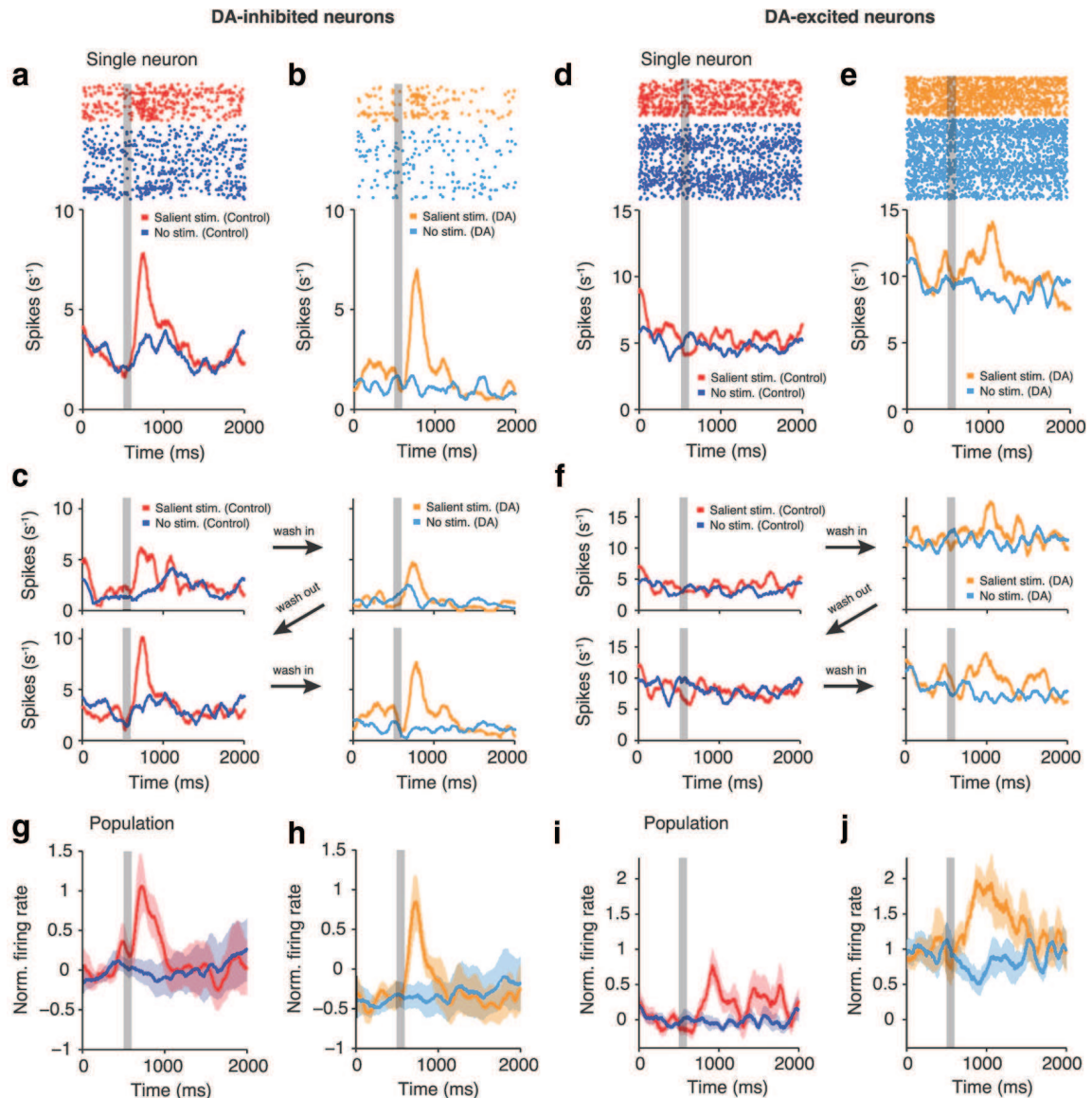


**Figure 3.** DA modulation of prefrontal visual signals is neuron-class specific. *a, b*, Responses of an example DA-inhibited neuron to salient (highest 3 contrasts) and absent visual stimuli in the control (*a*) and DA (*b*) conditions. Activity is aligned to the start of a trial (fixation period). The gray shaded area marks the stimulus presentation. Top, Dot raster plot; bottom, spike density histogram. Visual coding is preserved at shifted response levels. *c*, Sequence of control and DA periods in the same example DA-inhibited neuron. DA-mediated effects are reversible. *d–f*, Conventions as in *a–c* for an example DA-excited neuron. Visual responses are enhanced by DA. *g, h*, Population mean responses of DA-inhibited neurons in control (*g*) and DA (*h*) trials. *i, j*, Conventions as in *g* and *h*, for DA-excited neurons. Shaded areas in *g–j* indicate SEM across neurons.

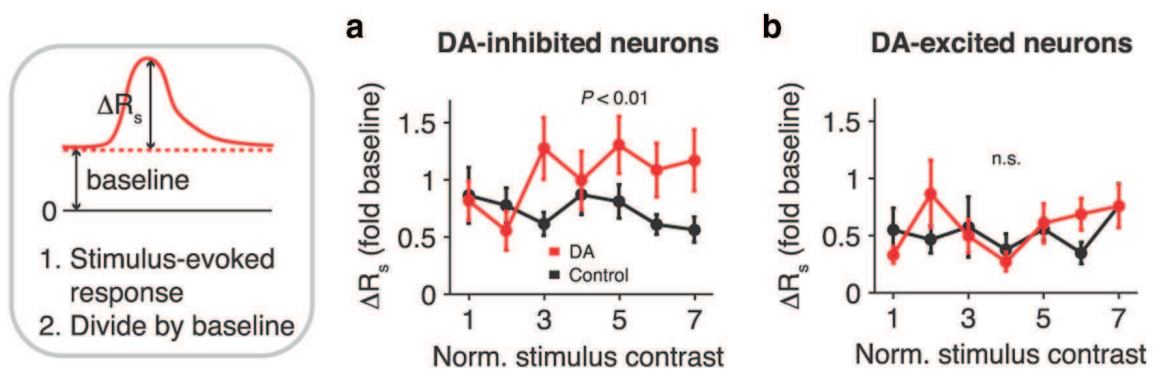


**Figure 4.** Subtraction and multiplication of activity in DA-inhibited and DA-excited neurons. *a*, Stimulus-evoked change in firing rate normalized to baseline activity in the fixation period, computed as shown by schematic on the left, for DA-inhibited neurons under control and DA conditions. Shifts to larger values indicate that DA offsets activity (additive operation), i.e., the firing rate difference is retained at lower baseline firing rates (subtraction). The animals' perceptual threshold (on the rising slope of the psychometric function; Fig. 1*c,d*) corresponds to normalized stimulus contrasts 1–4. *b*, Conventions as in *a* for DA-excited neurons. Superimposed curves indicate that DA increases gain (multiplicative operation), i.e., the firing rate difference increases in proportion to baseline firing rates. Error bars indicate SEM across neurons.

neuron and used a linear classifier to objectively separate BS from NS cells. BS and NS waveforms were distributed differently in the classes of DA-excited and DA-inhibited neurons (Fisher's exact test,  $p < 0.05$ ; Fig. 7*a*). All stimulus-encoding DA-excited cells were BS neurons (putative pyramidal neurons,  $n = 10$ ). In contrast, there were equal numbers of BS and NS cells (putative interneurons) in the class of stimulus-responsive DA-inhibited neurons ( $n = 7$  each). Thus, in the group of DA-inhibited neurons, there were more putative interneurons than to be expected by their frequency in neocortex (20–30%; Markram et al., 2004), and there were significantly more putative pyramidal cells in the class of DA-excited neurons. Interestingly, all stimulus encoding putative interneurons that were responsive to DA were inhibited ( $n = 7$ ). The same pattern was found when all DA-responsive neurons were analyzed (DA-excited neurons: 22 BS, 3 NS; DA-inhibited neurons: 17 BS, 15 NS;  $p < 0.01$ ). In accord with the strongly biased distribution of putative interneurons toward DA-inhibited cells, baseline firing rates under control conditions were higher in this group of neurons compared with DA-excited cells, although the difference did not reach significance ( $8.3 \pm 1.4$  vs  $5.4 \pm 0.8$  spikes/s for DA-inhibited and DA-excited neurons, respectively; rank-sum test,  $p = 0.13$ ). In the instances in which multiple DA-modulated neurons were recorded at the same electrode (12 of 45 electrodes), we more often recorded cells from the same class than from different classes (eight vs four electrodes, respectively). These results support the notion that DA-mediated changes in excitability were characteristic of distinct neuronal populations.

We finally explored whether DA-inhibited and DA-excited neurons might be involved at different stages of prefrontal sensory processing. Under control conditions, prefrontal neurons that were inhibited by DA encoded visual signals significantly earlier than DA-excited neurons (mean stimulus response latency,  $165 \pm 18$  and  $261 \pm 27$  ms for DA-inhibited and DA-excited neurons, respectively; rank-sum test,  $p < 0.05$ ; Fig. 7*b*; see also Figs. 3*g,i*, 5*b,e*). DA-inhibited neurons were driven more strongly by sensory input: under control conditions, visual coding strength was higher in this population compared with DA-excited cells across all contrasts (multiple linear regression; factor neuron class,  $p < 0.001$ ; Fig. 7*c*).

Closer inspection of the population spike density histograms of DA-excited neurons revealed that activity after omission of a stimulus was not a simple continuation of activity in the fixation period when DA had been applied (Fig. 3, compare *i, j*). To examine whether DA-excited neurons represented not just physical stimulus intensity but possibly a processing stage more remote from sensory input, we compared baseline activity in the fixation period with firing rates in trials without stimulation, calculated in the same 300 ms analysis window as previously (Fig. 7*d*). A deviation

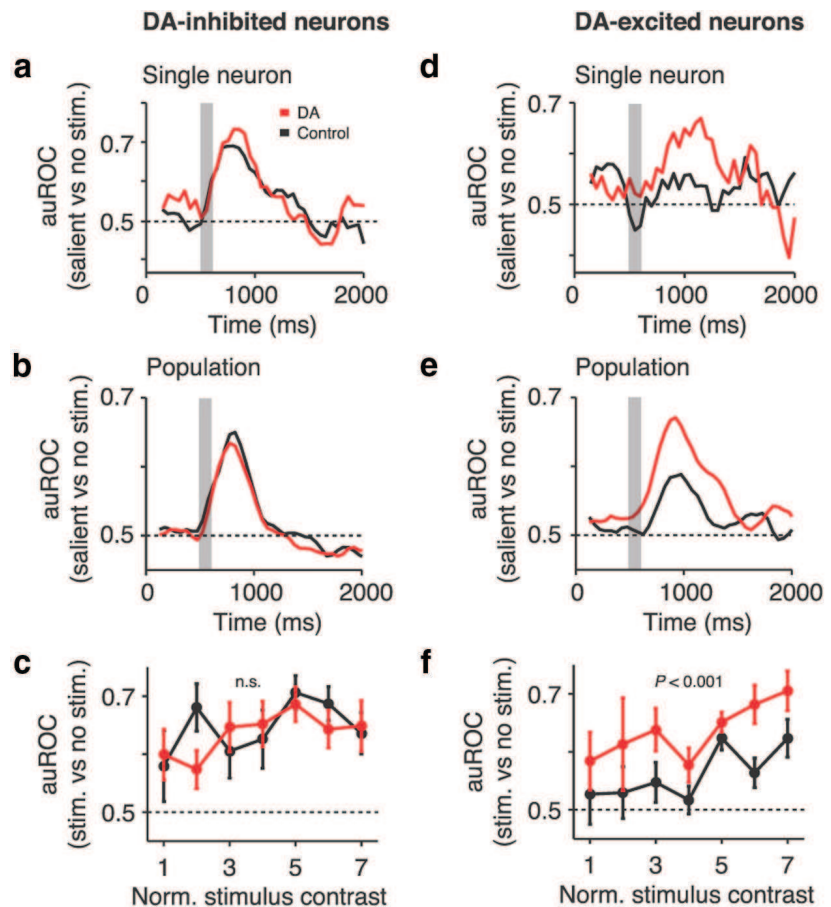


**Figure 5.** Prefrontal DA enhances visual coding in excited neurons. *a*, Sliding window analysis of visual coding strength (auROC values for salient vs absent visual stimulation) for the example DA-inhibited neuron from Figure 3, *a* and *b*, in correct control and DA trials. Data are aligned to the start of a trial (fixation period). The gray shaded area marks the stimulus presentation. *b*, Population mean auROC time course of DA-inhibited neurons in correct control and DA trials. *c*, Population mean auROC values of DA-inhibited neurons for individual contrasts in correct control and DA trials. DA does not change coding strength in the population of DA-inhibited neurons. *d–f*, Conventions as in *a–c* for the example DA-excited neuron from Figure 3, *d* and *e* (*d*) and the population of DA-excited neurons (*e, f*). DA strengthens visual coding in the class of DA-excited neurons. Error bars indicate SEM across neurons.

from zero could suggest that absent stimulation was not encoded as a “default” condition (i.e., a continuation of baseline activity; to be expected for sensory-driven neurons) but instead actively in a potentially more advanced processing step. In DA-inhibited neurons, there were no significant differences between baseline activity and activity after the omission of a stimulus in either control or DA conditions (signed-rank test,  $p = 0.39$  and  $p = 0.54$ , respectively; signed-rank test for difference between control and DA conditions,  $p = 0.95$ ; Fig. 7*d*, left). However, in DA-excited neurons, DA application disclosed a deflection from baseline in trials without visual stimulation that was not evident under control conditions (signed-rank test,  $p = 0.19$  and  $p < 0.01$ , for control and DA conditions, respectively; signed-rank test for difference between control and DA conditions,  $p < 0.01$ ; Fig. 7*d*, right). This result suggests that the absence of visual stimulation was represented differently in the two DA-responsive neuron classes.

## Discussion

We report here that DA regulates the representation of sensory information in the primate PFC. We found that prefrontal DA affects two distinct neuronal populations involved in visual coding. DA controlled neurons with short visual response latencies

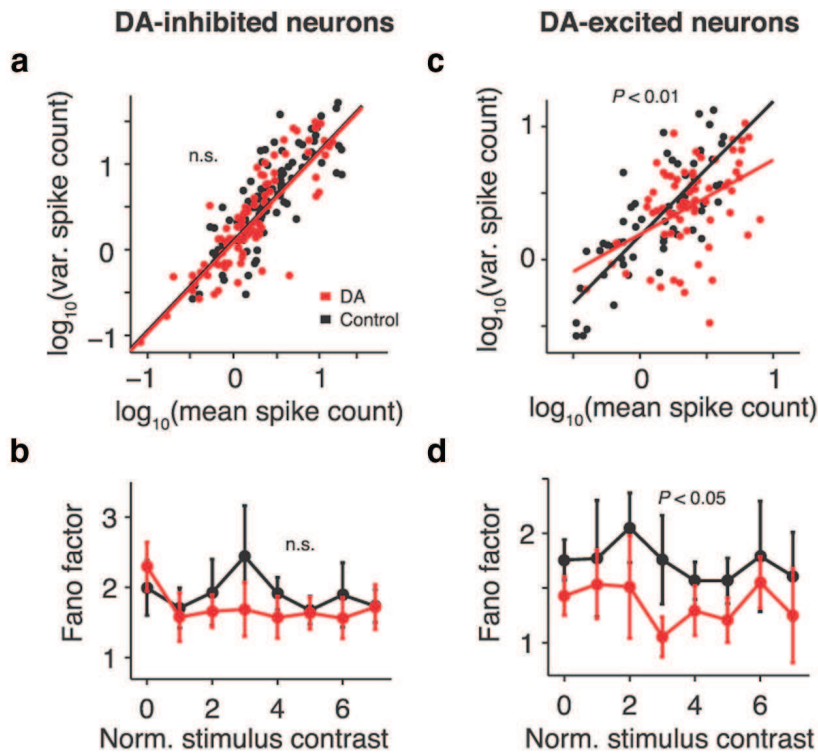


**Figure 6.** Prefrontal DA reduces response variability in excited neurons. **a**, Mean spike count after stimulus presentation versus spike count variance across trials for DA-inhibited neurons. Each data point represents one neuron and stimulus contrast. Straight lines indicate fits to data. **b**, FFs (spike count variance divided by mean) for all stimulus contrasts in DA-inhibited cells. No changes in response variability are observed after DA application. **c**, **d**, Conventions as in **a** and **b** for DA-excited neurons. The slope of the fitted line is significantly smaller in DA trials compared with control conditions. DA reduces response variability across all contrasts in DA-excited cells. Error bars indicate SEM across neurons.

by suppressing neuronal activity. In neurons with longer response latencies, DA acted as an excitatory modulator and strengthened the representation of visual inputs.

### Modes of operation

Inhibition was implemented principally in the form of a subtractive shift in response levels [additive operation (Silver, 2010); Figs. 3*g,h*, 4*a*], whereas excitation in the second population resulted from an increase in gain [multiplicative operation (Silver, 2010); Figs. 3*i,j*, 4*b*]. In the rodent visual cortex, subtraction is induced by dendrite-targeting interneurons, whereas somatargeting interneurons regulate gain (Wilson et al., 2012). *In vitro* experiments in the ferret PFC have demonstrated that these classes of interneurons are modulated by DA (Gao et al., 2003). Thus, DA would subtract activity by modulating dendrites and increase gain by controlling the soma (Yang and Seamans, 1996). Our results now suggest that subtraction and multiplication by DA target not the same prefrontal neuron but instead early and late, possibly functionally specialized, processing stages, respectively (Fig. 7).

### DA-inhibited neurons

Control over sensory inputs by inhibition and subtraction of response levels offers a major computational advantage, namely response normalization (Carandini and Heeger, 2012). Inhibitory conductances can adaptively rescale the input of a neuron to match its dynamic range (Mitchell and Silver, 2003) and therefore maximize information transmission (Brenner et al., 2000; Fairhall et al., 2001). Our data indicate that DA afferents to the

PFC might constitute an important pathway to fine-tune and facilitate downstream processing.

DA could also filter distracting, non-preferred signals by modulating neurotransmission at the dendritic arbor of input layer neurons (“gating”) (Durstewitz et al., 2000; Gao et al., 2003). Neurons extracting behaviorally relevant information from a multitude of competing signals would necessarily show temporally precise modulation. Given their rapid responsiveness to DA (Fig. 2*f,g*), DA-inhibited neurons would be ideal recipients of the phasic signals, e.g., prediction errors, DA neurons relay to the PFC (Redgrave et al., 2008). With a mean stimulus response latency of 165 ms (Fig. 7*b*), these cells closely follow the discharge of midbrain DA neurons that typically occurs between 100 and 150 ms (Dommett et al., 2005; de Lafuente and Romo, 2012). Therefore, DA-inhibited neurons are maximally active at peak extracellular DA concentrations (Schultz, 2007). Thus, DA might reinforce or block signals reaching the PFC and segregate important from distracting information (Servan-Schreiber et al., 1990; D’Ardenne et al., 2012). Interestingly, we found that all putative interneurons were inhibited by DA (Fig. 7*a*). Interneurons are thought to play an important role in the control of information flow in cortex (Constantinidis et

al., 2002) and would constitute an ideal target for rapid gating by DA.

At present, the cellular mechanisms by which DA could mediate fast inhibition are unclear (Seamans and Yang, 2004). Inhibitory DA effects are generally reported on longer timescales as a result of technical constraints, such as bath application of dopaminergic drugs. It is also conceivable that the applied DA binds to non-dopaminergic receptors, such as adrenergic receptors, especially at higher concentrations. Ionophoresis is nonquantitative and generally does not provide reliable assessments of the drug concentrations reaching individual neurons. Therefore, additional experiments are required to resolve the issue of pharmacological specificity as well as to determine whether the observed decrease in excitability is indeed the result of phasic, time-locked signaling or generated by longer-lasting mechanisms.

In behaving nonhuman primates, neuronal inhibition has been identified as an important mechanism by which DA affects prefrontal signal processing. DA suppresses neuronal activity in spatially tuned prefrontal neurons engaged in memory-guided saccade tasks and enhances tuning for the remembered saccade target location (“sculpting inhibition”; Williams and Goldman-Rakic, 1995; Vijayraghavan et al., 2007; Arnsten, 2011). Because subtraction sharpens stimulus selectivity, i.e., tuning (Wilson et al., 2012), we propose that the spatially tuned cells described previously belong to the class of DA-inhibited neurons identified here. Although the ROC measures we used are well suited for analyzing binary yes–no, e.g., stimulus present–absent decisions (Green and Swets, 1966), we did not detect an increase in signal/noise ratio as defined by the auROC in DA-inhibited neurons

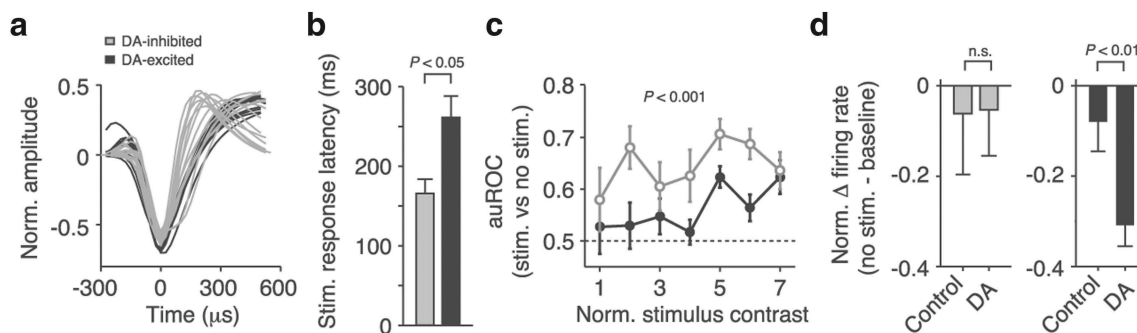


**Figure 7.** DA modulates distinct prefrontal processing stages. *a*, Normalized average waveforms of stimulus-encoding DA-inhibited and DA-excited neurons. All DA-excited cells were BS neurons, and NS neurons were all inhibited by DA. *b*, Visual response latencies of DA-inhibited and DA-excited neurons under control conditions. DA-inhibited neurons encode visual signals significantly earlier. *c*, Visual coding strength of DA-inhibited and DA-excited neurons under control conditions (auROC values comparing firing rates between trials with and without visual stimulation). DA-inhibited neurons are driven more strongly by visual stimulation across all contrast levels. *d*, Normalized difference between baseline activity in the fixation period and activity after omission of a stimulus. Firing rates were identical in DA-inhibited neurons in both control and DA trials. In DA-excited neurons, absence of visual stimulation induced a deflection from baseline when DA had been applied. Error bars indicate SEM across neurons.

(Fig. 5*a–c*). Other response characteristics that are not adequately captured by signal detection theory, e.g., sharpening of tuning curves, might nevertheless create advantages for cortical processing. We also considered the possibility that inhibited neurons were the result of higher intrinsic DA tone and excited neurons were subject to lower DA levels. However, this is unlikely because the ratio of inhibition to excitation was independent of iontophoretic DA dosage, and we did not observe more inhibited neurons at higher DA currents. More experiments tapping different behavioral demands are needed to determine whether the benefits conveyed by DA-induced inhibition lie primarily in rescaling and gating inputs to PFC or whether DA can also affect signal strength per se at this stage.

#### DA-excited neurons

In DA-excited neurons, stimulus responses increased in proportion to baseline activity, indicating a multiplicative increase in gain (Servan-Schreiber et al., 1990; Thurley et al., 2008; Figs. 3*i,j*, 4*b*). Although the strength of sensory inputs was unchanged in DA-inhibited neurons, DA selectively increased signal/noise ratio in excited cells (Fig. 5*d–f*). In addition, stimuli were encoded more reliably because trial-to-trial variability dropped (Fig. 6*c,d*). All three effects closely resemble changes in visual signals observed in visual cortex when attention is allocated in a top-down manner (McAdams and Maunsell, 1999; Mitchell et al., 2007; Noudoost and Moore, 2011*a*). In other words, prefrontal DA may act as a pharmacological spotlight, directing “attention” toward relevant sensory inputs and enhancing their representation at the level of DA-excited neurons (Brunel and Wang, 2001; Noudoost and Moore, 2011*b*). Interestingly, DA-induced excitation occurred on considerably longer timescales than inhibition (Fig. 2*f,g*). Therefore, it is unlikely that the amplification of stimulus coding could be controlled on a trial-by-trial basis in these neurons. DA-excited neurons might not serve the purpose of a flexible, rapidly responsive gate for sensory signals but instead reflect a later processing stage more remote from early sensory inputs. In support of this idea, our analysis of extracellular waveforms did not reveal any putative interneurons in this group of cells but exclusively putative pyramidal neurons (Fig. 7*a*). Also, DA-excited neurons processed visual inputs almost 100 ms later than DA-inhibited neurons (Fig. 7*b*). They were driven less strongly by visual stimuli (Fig. 7*c*) and encoded absent stimulation actively by a deflection in baseline firing instead of passively as a default condition like DA-inhibited neurons (Fig. 7*d*). This transient de-

pression of activity could reflect, for example, an anticipatory response and contributed to the improved discriminability of stimulus and background in these neurons. In any case, it suggests that DA-excited neurons were not truthful encoders of the physical properties of visual stimuli but might constitute an additional step in the goal-directed evaluation of sensory signals.

Although application of transmitters with micro-iontophoresis is very focal (Herz et al., 1969; Hupé et al., 1999), we cannot exclude that the slower response kinetics in DA-excited neurons were attributable to the fact that DA had to diffuse to a different cortical layer before indirectly taking effect on this class of cells. Another possibility is that DA-excited neurons are modulated not by phasic DA but by tonic transmitter release. Compared with DA neuron bursting, little is known about the function of tonic DA signaling (Floresco et al., 2003). It is thought to reflect increased activity in populations of DA neurons and causes an elevation mainly of extrasynaptic transmitter. Tonic extracellular DA levels do not reach the high levels found in the synaptic cleft and might modulate primarily high-affinity extrasynaptic DA receptors on presynaptic terminals (Grace et al., 2007). We presently do not know the cellular receptors that are involved in generating the effects reported here. Therefore, additional studies will have to address whether DA-excited neurons differ from DA-inhibited cells, for example, in their modulation by the two DA receptor families found in PFC, the  $D_1R$  and  $D_2R$ , or other catecholamine receptors (Seamans and Yang, 2004; Wang et al., 2004; Noudoost and Moore, 2011*a*). Differences in the cellular and molecular composition of prefrontal DA-sensitive neurons could allow for targeted modulation of specific cortical signals by DA (Noudoost and Moore, 2011*b*). For example, in the frontal eye fields, behavioral effects of DA on attentional processing depend on whether injections were made in supragranular or infragranular layers that are characterized by distinct DA receptor profiles (Noudoost and Moore, 2011*a*). We now find that DA-sensitive neurons in more anterior lateral PFC are heterogeneous with regard to the sensory information they carry and how they are modulated by DA. Adding to previous studies, our experiments suggest that the timing and strength of DA neurotransmission could have a strong influence on how this modulatory signal is received and processed in PFC.

#### Implications for mental diseases

DA is strongly linked to neuropsychiatric diseases that involve the frontal lobes, such as attention-deficit hyperactivity disorder or

schizophrenia (Arnsten, 2011). By strengthening sensory inputs, prefrontal DA could be a critical factor in resolving ambiguous sensory events or maintaining the focus of attention. It is tempting to speculate that the observed DA effects could help safeguard the healthy mind, e.g., from hallucinations and intrusions of thought that are characteristic of these mental diseases (Winterer and Weinberger, 2004; Rolls et al., 2008; Fletcher and Frith, 2009). For example, it is frequently hypothesized that the symptom relief conveyed by antipsychotic drugs targeting the DA system, in particular the D<sub>2</sub>R, results from the fact that they decrease noise in prefrontal circuits (Winterer and Weinberger, 2004; Rolls et al., 2008). Our experiments now provide evidence on a cellular level that DA indeed controls neuronal variability in the primate brain.

In conclusion, we have demonstrated that DA neuromodulation in PFC is not uniform but tailored to functionally specialized neurons in the prefrontal processing stream (Arnsten et al., 2012). By controlling sensory inputs to the PFC, DA could be a powerful determinant of how the primate brain uses these signals to generate intelligent behavior in interactions with its sensory environment.

## References

- Arnsten AF (2011) Catecholamine influences on dorsolateral prefrontal cortical networks. *Biol Psychiatry* 69:e89–e99. [CrossRef Medline](#)
- Arnsten AF, Wang MJ, Paspalas CD (2012) Neuromodulation of thought: flexibilities and vulnerabilities in prefrontal cortical network synapses. *Neuron* 76:223–239. [CrossRef Medline](#)
- Björklund A, Dunnett SB (2007) Dopamine neuron systems in the brain: an update. *Trends Neurosci* 30:194–202. [CrossRef Medline](#)
- Bongard S, Nieder A (2010) Basic mathematical rules are encoded by primate prefrontal cortex neurons. *Proc Natl Acad Sci U S A* 107:2277–2282. [CrossRef Medline](#)
- Brenner N, Bialek W, de Ruyter van Steveninck R (2000) Adaptive rescaling maximizes information transmission. *Neuron* 26:695–702. [CrossRef Medline](#)
- Brozoski TJ, Brown RM, Rosvold HE, Goldman PS (1979) Cognitive deficit caused by regional depletion of dopamine in prefrontal cortex of rhesus monkey. *Science* 205:929–932. [CrossRef Medline](#)
- Brunel N, Wang XJ (2001) Effects of neuromodulation in a cortical network model of object working memory dominated by recurrent inhibition. *J Comput Neurosci* 11:63–85. [CrossRef Medline](#)
- Carandini M, Heeger DJ (2012) Normalization as a canonical neural computation. *Nat Rev Neurosci* 13:51–62. [CrossRef Medline](#)
- Churchland MM, Yu BM, Cunningham JP, Sugrue LP, Cohen MR, Corrado GS, Newsome WT, Clark AM, Hosseini P, Scott BB, Bradley DC, Smith MA, Kohn A, Movshon JA, Armstrong KM, Moore T, Chang SW, Snyder LH, Lisberger SG, Priebe NJ, et al. (2010) Stimulus onset quenches neural variability: a widespread cortical phenomenon. *Nat Neurosci* 13:369–378. [CrossRef Medline](#)
- Constantinidis C, Williams GV, Goldman-Rakic PS (2002) A role for inhibition in shaping the temporal flow of information in prefrontal cortex. *Nat Neurosci* 5:175–180. [CrossRef Medline](#)
- D'Ardenne K, Eshel N, Luka J, Lenartowicz A, Nystrom LE, Cohen JD (2012) Role of prefrontal cortex and the midbrain dopamine system in working memory updating. *Proc Natl Acad Sci U S A* 109:19900–19909. [CrossRef Medline](#)
- de Lafuente V, Romo R (2005) Neuronal correlates of subjective sensory experience. *Nat Neurosci* 8:1698–1703. [CrossRef Medline](#)
- de Lafuente V, Romo R (2006) Neural correlate of subjective sensory experience gradually builds up across cortical areas. *Proc Natl Acad Sci U S A* 103:14266–14271. [CrossRef Medline](#)
- de Lafuente V, Romo R (2011) Dopamine neurons code subjective sensory experience and uncertainty of perceptual decisions. *Proc Natl Acad Sci U S A* 108:19767–19771. [CrossRef Medline](#)
- de Lafuente V, Romo R (2012) Dopaminergic activity coincides with stimulus detection by the frontal lobe. *Neuroscience* 218:181–184. [CrossRef Medline](#)
- Diester I, Nieder A (2008) Complementary contributions of prefrontal neuron classes in abstract numerical categorization. *J Neurosci* 28:7737–7747. [CrossRef Medline](#)
- Dommett E, Coizet V, Blaha CD, Martindale J, Lefebvre V, Walton N, Mayhew JE, Overton PG, Redgrave P (2005) How visual stimuli activate dopaminergic neurons at short latency. *Science* 307:1476–1479. [CrossRef Medline](#)
- Durstewitz D, Seamans JK (2008) The dual-state theory of prefrontal cortex dopamine function with relevance to catechol-*o*-methyltransferase genotypes and schizophrenia. *Biol Psychiatry* 64:739–749. [CrossRef Medline](#)
- Durstewitz D, Seamans JK, Sejnowski TJ (2000) Dopamine-mediated stabilization of delay-period activity in a network model of prefrontal cortex. *J Neurophysiol* 83:1733–1750. [Medline](#)
- Eiselt AK, Nieder A (2013) Representation of abstract quantitative rules applied to spatial and numerical magnitudes in primate prefrontal cortex. *J Neurosci* 33:7526–7534. [CrossRef Medline](#)
- Fairhall AL, Lewen GD, Bialek W, de Ruyter Van Steveninck RR (2001) Efficiency and ambiguity in an adaptive neural code. *Nature* 412:787–792. [CrossRef Medline](#)
- Fletcher PC, Frith CD (2009) Perceiving is believing: a Bayesian approach to explaining the positive symptoms of schizophrenia. *Nat Rev Neurosci* 10:48–58. [CrossRef Medline](#)
- Floresco SB, West AR, Ash B, Moore H, Grace AA (2003) Afferent modulation of dopamine neuron firing differentially regulates tonic and phasic dopamine transmission. *Nat Neurosci* 6:968–973. [CrossRef Medline](#)
- Floresco SB, Magyar O, Ghods-Sharifi S, Vexelman C, Tse MT (2006) Multiple dopamine receptor subtypes in the medial prefrontal cortex of the rat regulate set-shifting. *Neuropsychopharmacology* 31:297–309. [CrossRef Medline](#)
- Fuster JM (2008) *The prefrontal cortex*, Ed 4. London: Academic.
- Gao WJ, Wang Y, Goldman-Rakic PS (2003) Dopamine modulation of perisomatic and peridendritic inhibition in prefrontal cortex. *J Neurosci* 23:1622–1630. [Medline](#)
- Grace AA, Floresco SB, Goto Y, Lodge DJ (2007) Regulation of firing of dopaminergic neurons and control of goal-directed behaviors. *Trends Neurosci* 30:220–227. [CrossRef Medline](#)
- Green DM, Swets JA (1966) *Signal detection theory and psychophysics*. New York: Wiley.
- Henze DA, Borhegyi Z, Csicsvari J, Mamiya A, Harris KD, Buzsáki G (2000) Intracellular features predicted by extracellular recordings in the hippocampus in vivo. *J Neurophysiol* 84:390–400. [Medline](#)
- Herrero JL, Roberts MJ, Delicato LS, Gieselmann MA, Dayan P, Thiele A (2008) Acetylcholine contributes through muscarinic receptors to attentional modulation in V1. *Nature* 454:1110–1114. [CrossRef Medline](#)
- Herz A, Ziegglängsberger W, Färber G (1969) Microelectrophoretic studies concerning the spread of glutamic acid and GABA in brain tissue. *Exp Brain Res* 9:221–235. [Medline](#)
- Hupé JM, Chouvet G, Bullier J (1999) Spatial and temporal parameters of cortical inactivation by GABA. *J Neurosci Methods* 86:129–143. [CrossRef Medline](#)
- Hussar CR, Pasternak T (2009) Flexibility of sensory representations in prefrontal cortex depends on cell type. *Neuron* 64:730–743. [CrossRef Medline](#)
- Marder E (2012) Neuromodulation of neuronal circuits: back to the future. *Neuron* 76:1–11. [CrossRef Medline](#)
- Markram H, Toledo-Rodriguez M, Wang Y, Gupta A, Silberberg G, Wu C (2004) Interneurons of the neocortical inhibitory system. *Nat Rev Neurosci* 5:793–807. [CrossRef Medline](#)
- Matsumoto M, Hikosaka O (2009) Two types of dopamine neuron distinctly convey positive and negative motivational signals. *Nature* 459:837–841. [CrossRef Medline](#)
- McAdams CJ, Maunsell JH (1999) Effects of attention on the reliability of individual neurons in monkey visual cortex. *Neuron* 23:765–773. [CrossRef Medline](#)
- Merten K, Nieder A (2012) Active encoding of decisions about stimulus absence in primate prefrontal cortex neurons. *Proc Natl Acad Sci U S A* 109:6289–6294. [CrossRef Medline](#)
- Merten K, Nieder A (2013) Comparison of abstract decision encoding in the monkey prefrontal cortex, the presupplementary and cingulate motor areas. *J Neurophysiol* 110:19–32. [CrossRef Medline](#)
- Mitchell JF, Sundberg KA, Reynolds JH (2007) Differential attention-dependent response modulation across cell classes in macaque visual area V4. *Neuron* 55:131–141. [CrossRef Medline](#)



- Mitchell SJ, Silver RA (2003) Shunting inhibition modulates neuronal gain during synaptic excitation. *Neuron* 38:433–445. CrossRef Medline
- Noudoost B, Moore T (2011a) Control of visual cortical signals by prefrontal dopamine. *Nature* 474:372–375. CrossRef Medline
- Noudoost B, Moore T (2011b) The role of neuromodulators in selective attention. *Trends Cogn Sci* 15:585–591. CrossRef Medline
- Parker AJ, Newsome WT (1998) Sense and the single neuron: probing the physiology of perception. *Annu Rev Neurosci* 21:227–277. CrossRef Medline
- Puig MV, Miller EK (2012) The role of prefrontal dopamine D1 receptors in the neural mechanisms of associative learning. *Neuron* 74:874–886. CrossRef Medline
- Redgrave P, Gurney K (2006) The short-latency dopamine signal: a role in discovering novel actions? *Nat Rev Neurosci* 7:967–975. CrossRef Medline
- Redgrave P, Gurney K, Reynolds J (2008) What is reinforced by phasic dopamine signals? *Brain Res Rev* 58:322–339. CrossRef Medline
- Rolls ET, Loh M, Deco G, Winterer G (2008) Computational models of schizophrenia and dopamine modulation in the prefrontal cortex. *Nat Rev Neurosci* 9:696–709. CrossRef Medline
- Sawaguchi T (2001) The effects of dopamine and its antagonists on directional delay-period activity of prefrontal neurons in monkeys during an oculomotor delayed-response task. *Neurosci Res* 41:115–128. CrossRef Medline
- Sawaguchi T, Matsumura M, Kubota K (1990) Catecholaminergic effects on neuronal activity related to a delayed response task in monkey prefrontal cortex. *J Neurophysiol* 63:1385–1400. Medline
- Schultz W (1998) Predictive reward signal of dopamine neurons. *J Neurophysiol* 80:1–27. Medline
- Schultz W (2007) Multiple dopamine functions at different time courses. *Annu Rev Neurosci* 30:259–288. CrossRef Medline
- Seamans JK, Yang CR (2004) The principal features and mechanisms of dopamine modulation in the prefrontal cortex. *Prog Neurobiol* 74:1–58. CrossRef Medline
- Servan-Schreiber D, Printz H, Cohen JD (1990) A network model of catecholamine effects: gain, signal-to-noise ratio, and behavior. *Science* 249:892–895. CrossRef Medline
- Shadlen MN, Newsome WT (1998) The variable discharge of cortical neurons: implications for connectivity, computation, and information coding. *J Neurosci* 18:3870–3896. Medline
- Silver RA (2010) Neuronal arithmetic. *Nat Rev Neurosci* 11:474–489. CrossRef Medline
- Thiele A, Delicato LS, Roberts MJ, Gieselmann MA (2006) A novel electrode-pipette design for simultaneous recording of extracellular spikes and iontophoretic drug application in awake behaving monkeys. *J Neurosci Methods* 158:207–211. CrossRef Medline
- Thorpe SJ, Fabre-Thorpe M (2001) Seeking categories in the brain. *Science* 291:260–263. CrossRef Medline
- Thurley K, Senn W, Lüscher HR (2008) Dopamine increases the gain of the input-output response of rat prefrontal pyramidal neurons. *J Neurophysiol* 99:2985–2997. CrossRef Medline
- Vigneswaran G, Kraskov A, Lemon RN (2011) Large identified pyramidal cells in macaque motor and premotor cortex exhibit “thin spikes”: implications for cell type classification. *J Neurosci* 31:14235–14242. CrossRef Medline
- Vijayraghavan S, Wang M, Birnbaum SG, Williams GV, Arnsten AF (2007) Inverted-U dopamine D1 receptor actions on prefrontal neurons engaged in working memory. *Nat Neurosci* 10:376–384. CrossRef Medline
- Wang M, Vijayraghavan S, Goldman-Rakic PS (2004) Selective D2 receptor actions on the functional circuitry of working memory. *Science* 303:853–856. CrossRef Medline
- Williams GV, Goldman-Rakic PS (1995) Modulation of memory fields by dopamine D1 receptors in prefrontal cortex. *Nature* 376:572–575. CrossRef Medline
- Williams SM, Goldman-Rakic PS (1998) Widespread origin of the primate mesofrontal dopamine system. *Cereb Cortex* 8:321–345. CrossRef Medline
- Wilson NR, Runyan CA, Wang FL, Sur M (2012) Division and subtraction by distinct cortical inhibitory networks in vivo. *Nature* 488:343–348. CrossRef Medline
- Winterer G, Weinberger DR (2004) Genes, dopamine and cortical signal-to-noise ratio in schizophrenia. *Trends Neurosci* 27:683–690. CrossRef Medline
- Yang CR, Seamans JK (1996) Dopamine D1 receptor actions in layers V–VI rat prefrontal cortex neurons in vitro: modulation of dendritic-somatic signal integration. *J Neurosci* 16:1922–1935. Medline



---

## **Study 2: Dopamine receptor modulation of rule signals**

**Ott, T., Jacob, S. N., Nieder, A. (2014).** Dopamine receptors differentially enhance rule coding in primate prefrontal cortex neurons. *Neuron* **84**(6):1317–1328.



# Dopamine Receptors Differentially Enhance Rule Coding in Primate Prefrontal Cortex Neurons

Torben Ott,<sup>1</sup> Simon Nikolas Jacob,<sup>1,2</sup> and Andreas Nieder<sup>1,\*</sup>

<sup>1</sup>Animal Physiology, Institute of Neurobiology, Auf der Morgenstelle 28, University of Tübingen, 72076 Tübingen, Germany

<sup>2</sup>Present address: Department of Psychiatry and Psychotherapy, Charité Universitätsmedizin Berlin, Charitéplatz 1, 10117 Berlin, Germany

\*Correspondence: andreas.nieder@uni-tuebingen.de

<http://dx.doi.org/10.1016/j.neuron.2014.11.012>

## SUMMARY

Flexibly applying abstract rules is a hallmark feature of executive functioning represented by prefrontal cortex (PFC) neurons. Prefrontal networks are regulated by the neuromodulator dopamine, but how dopamine modulates high-level executive functions remains elusive. In monkeys performing a rule-based decision task, we report that both dopamine D1 and D2 receptors facilitated rule coding of PFC neurons, albeit by distinct physiological mechanisms. Dopamine D1 receptor stimulation suppressed neuronal firing while increasing responses to the preferred rule, thereby enhancing neuronal rule coding. D2 receptor stimulation, instead, excited neuronal firing while suppressing responses to the nonpreferred rule, thus also enhancing neuronal rule coding. These findings highlight complementary modulatory contributions of dopamine receptors to the neuronal circuitry mediating executive functioning and goal-directed behavior.

## INTRODUCTION

Flexibly applying abstract rules is a hallmark feature of executive functioning represented by the activity of prefrontal cortex (PFC) neurons (Wallis et al., 2001; Miller and Cohen, 2001). The PFC receives particularly strong projections from dopamine neurons in the midbrain (Björklund and Dunnett, 2007) that regulate frontal lobe functions (Robbins and Arnsten, 2009). Prefrontal dopamine is essential for spatial working memory (Brozoski et al., 1979; Sawaguchi and Goldman-Rakic, 1991) and the learning of associations and rules (Crofts et al., 2001; Puig and Miller, 2012; Puig and Miller, 2014).

On a cellular level, dopamine influences PFC neurons via the D1 (D1R) and the D2 receptor (D2R) families (Lidow et al., 1998; de Almeida and Mengod, 2010). Prefrontal D1Rs modulate spatial working memory performance (Sawaguchi and Goldman-Rakic, 1991; Müller et al., 1998). In rhesus monkeys engaged in a spatial working memory task, PFC neurons active in the delay period of the task showed improved tuning to preferred remembered locations when stimulated with D1R agonists (Vijayraghavan et al., 2007) and showed impaired tuning when D1Rs were blocked (Sawaguchi, 2001). Interestingly,

blocking D1Rs has also been reported to improve spatial tuning (Williams and Goldman-Rakic, 1995), complicating the current understanding of D1Rs in spatial coding. While an impact of D1Rs on modulating spatial working memory processes in the PFC is established (Arnsten, 2011), the precise role of D1Rs in modulating cognitive signals remains elusive.

D2Rs, on the other hand, do not modulate spatial persistent mnemonic-related activity in the PFC (Sawaguchi and Goldman-Rakic, 1994; Wang et al., 2004). Instead, D2Rs selectively modulate neuronal activities associated with memory-guided saccades in oculomotor delayed-response tasks (Wang et al., 2004). In addition, rodent studies suggest that D2Rs are involved in flexible behavior. Blockade of D2Rs impairs the ability of rats to switch between different response strategies (Floresco and Magyar, 2006). In humans, D2R stimulation increases blood-oxygen-level-dependent activity in the PFC when flexibly switching between rules (Stelzel et al., 2013). Both prefrontal D1Rs and D2Rs are critical for learning new association rules. Blocking D1Rs or D2Rs impairs neural selectivity to learned saccade directions (Puig and Miller, 2012; Puig and Miller, 2014). This suggests a cooperative role for D1Rs and D2Rs in modulating cognitive flexibility (Puig and Miller, 2014).

We hypothesized that both D1Rs and D2Rs play a crucial role in regulating rule-guided decision-making, a hallmark feature of executive control and central to flexible behavior. Executive control is required for processing numbers and quantity information according to abstract principles, or rules, of how to structure, process, and evaluate numerical information. PFC neurons represent these semantic aspects of numerical quantities (Nieder et al., 2002; Nieder, 2012, 2013; Viswanathan and Nieder, 2013; Jacob and Nieder, 2014) and quantitative rules (Bongard and Nieder, 2010; Vallentin et al., 2012; Eiselt and Nieder, 2013). Here, we therefore studied the activity of individual PFC neurons in rhesus monkeys required to flexibly switch between “greater than”/“less than” rules. By selectively activating or blocking D1Rs or D2Rs in the PFC, we report that dopamine modulates the neuronal coding of abstract rules through both receptor families by distinct physiological mechanisms.

## RESULTS

To determine if and how the dopaminergic system modulates abstract rule coding in the PFC, we trained two macaque monkeys to apply numerical rules to numerosities and to flexibly switch between the rules based on cues shown during each trial

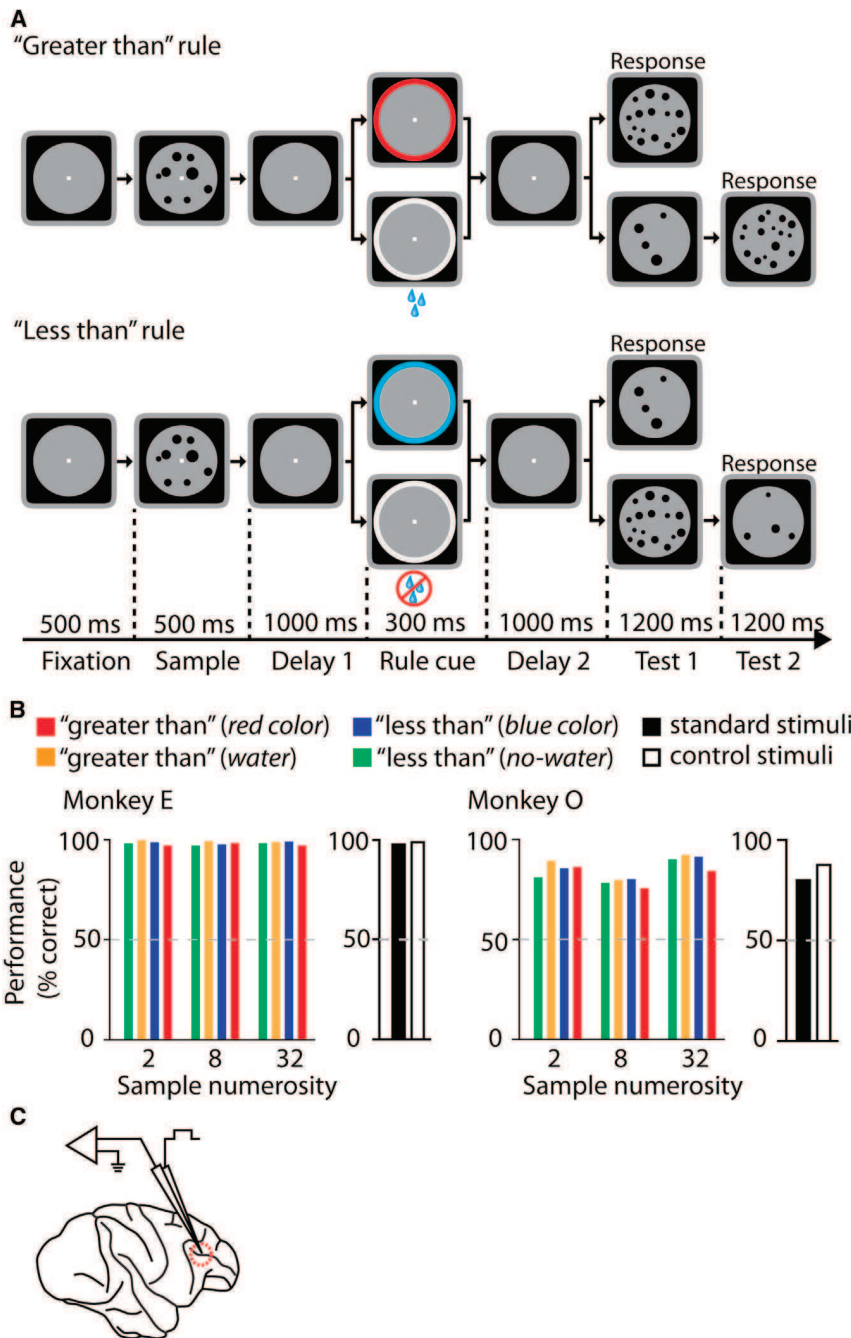


**Figure 1. Numerical Rule Switching Task and Behavioral Performance**

(A) Task protocol. The monkeys compared numbers of dots (numerosities) by applying the numerical rules "greater than" or "less than." The "greater than" rule required the monkeys to release a lever (response) if the first test display showed more dots than the sample display, whereas the "less than" rule required a lever release if the number of items in the first test display was smaller compared to the sample display. For each trial, the rule to apply ("greater than" versus "less than") was indicated by a cue that was presented in the delay between sample and test stimuli. To dissociate the neural activity related to the physical properties of the cue from the rule that it signified, two distinct cues from different sensory modalities were used to indicate the same rule, whereas cues signifying different rules were from the same modality. Because the animals needed information about the numerosity of the test 1 display to prepare a motor response, preparatory motor activation was excluded during the delay 2 phase.

(B) Performance (% correct trials) of the two monkeys for each sample numerosity and for each rule cue. Performance was equal in trials with standard stimuli (black) and control trials (white) using stimuli with equal dot area and density (see [Experimental Procedures](#)). Dotted line indicates chance performance (50%).

(C) Lateral view of a rhesus monkey brain depicting the location of extracellular neuronal recording and iontophoresis in the principal sulcus region of the PFC.

ple-item dot displays. Average correct performances were 98% for monkey E and 85% for monkey O (Figure 1B).

We recorded 384 randomly selected single neurons from the lateral PFC of two macaque monkeys (246 from monkey E, 138 from monkey O) (Figure 1C) performing the rule-switching task. To directly assess the impact of dopamine receptor targeting agents, control conditions without drug application alternated with drug conditions in each recording session. In each session, we tested one of three different substances that selectively targeted the D1R or the D2R: the

D1R agonist SKF81297, the D1R antagonist SCH23390, and the D2R agonist quinpirole. Physiological NaCl solution was used as control.

Rule-selective neurons were identified based on a significant main effect of the behavioral rule on the discharge rate in the delay 2 period using a four-way ANOVA (with main factors iontophoresis condition [control/drug], sample numerosity ["2"/"8"/"32"], behavioral rule ["greater than"/"less than"], and rule-cue modality [red/blue versus water/no-water];  $p < 0.05$ ). To ensure that neuronal responses varied with the rule rather than

(Bongard and Nieder, 2010; Eiselt and Nieder, 2013) (see Figure 1A for protocol and details). Rule-related activity was investigated in the delay 2 period, after the behavioral rule was indicated via the rule cues, but before the monkeys could prepare a motor plan. Simultaneous neuronal recordings and micro-iontophoretic drug application started after the monkeys had learned to proficiently apply the "greater than"/"less than" rules, irrespective of the absolute values of the three sample numerosities ("2," "8," or "32"), the two rule-cue modalities (red/blue versus water/no-water), and the visual appearance of the multi-

**Table 1. Numbers of Recorded Neurons with Each Drug and Respective Number of Rule-Selective Neurons, Selective for “Greater Than” or “Less Than” Rules**

Drug	Total Neurons	Rule-Selective (Greater/Less)
SKF81297 (D1R agonist)	123	20 (12/8)
SCH23390 (D1R antagonist)	112	18 (8/10)
Quinpirole (D2R agonist)	79	16 (7/9)
NaCl	70	10 (7/3)
Sum	384	64

with the rule cue, we excluded neurons that showed a significant interaction of the main factors rule and rule-cue modality. A total of 17% (64/384) of all tested neurons encoded abstract numerical rules (Table 1) and entered subsequent analyses. A similar number of neurons preferred the “greater than” rule (34 neurons with higher discharge for the “greater than” rule) and the “less than” rule (30 neurons exhibiting higher response rates for the “less than” rule).

#### D1Rs and D2Rs Modulated Single Neurons Encoding Abstract Numerical Rules

The coding properties of rule-selective neurons were modulated by drugs targeting either D1Rs or D2Rs. Figure 2A shows a “less than”-rule-selective neuron that differentiated more between “greater than” and “less than” rules (irrespective of rule-cue modalities) after stimulation with D1R agonist SKF81297 (Figure 2A). In contrast, blocking the D1R with SCH23390 strongly reduced rule selectivity of a different neuron that preferred the “greater than” rule in control conditions (Figure 2C). When targeting the D2Rs, rule selectivity was also affected. Stimulation of the D2R with quinpirole increased selectivity in a “less than”-rule-selective neuron (Figure 2E).

To analyze population responses, the responses of neurons classified as “greater than”- or “less than”-rule-selective neurons were normalized and averaged. Stimulating the D1R with SKF81297 increased the differentiation between the preferred rule (red trace) and the nonpreferred rule (blue trace) in the population of rule-selective neurons tested with SKF81297 (Figure 2B) by increasing the mean difference in normalized discharge rates ( $\Delta R = +0.37 \pm 0.12$  [SEM],  $p = 0.01$ ,  $n = 20$ , Wilcoxon test). Conversely, blocking the D1R with SCH23390 significantly reduced the rule selectivity of rule-selective neurons recorded with SCH23390 (Figure 2D;  $\Delta R = -0.17 \pm 0.05$ ,  $p = 0.01$ ,  $n = 18$ , Wilcoxon test). Stimulating the D2R with quinpirole also increased the differentiation between the preferred rule and the nonpreferred rule in the population of all rule-selective neurons recorded with quinpirole (Figure 2F;  $\Delta R = +0.29 \pm 0.078$ ,  $p = 0.001$ ,  $n = 16$ , Wilcoxon test). After terminating iontophoretic drug application, neuronal rule selectivity returned to the same levels as prior to the first drug application, i.e., the drug effects washed out (see Figures S1A, S1C, S1E, and S1G; see Supplemental Information available online). Iontophoretic application of NaCl did not change rule-selective responses (Figures S2A and S2B,  $p = 0.1$ ,  $n = 10$ , Wilcoxon test), confirming drug-specific effects.

#### D1R and D2R Stimulation Enhanced Abstract Rule Coding of PFC Neurons

We characterized the quality of rule coding for each rule-selective neuron (identified by the ANOVA) during control and drug conditions by determining the area under the receiver operator characteristic (AUROC) (see Experimental Procedures) using the discharge rates in the same analysis window as for the ANOVA. Stimulating the D1R increased the coding strength (AUROCs) in 75% (15/20) of all rule-selective neurons tested with SKF81297 (Figure 3A; mean  $\Delta$ AUROC =  $+0.080 \pm 0.023$  [SEM],  $p = 0.004$ ,  $n = 20$ , Wilcoxon test). In contrast, blocking the D1R with SCH23390 decreased the AUROCs in 83% (15/18) of the rule-selective neurons, thus impairing rule coding (Figure 3C;  $\Delta$ AUROC =  $-0.044 \pm 0.016$ ,  $p = 0.01$ ,  $n = 18$ , Wilcoxon test). Stimulation of the D2R with quinpirole also increased the AUROCs in almost all rule-selective neurons (88%, or 14/16) (Figure 3E,  $\Delta$ AUROC =  $+0.050 \pm 0.012$ ,  $p = 0.002$ ,  $n = 16$ , Wilcoxon test). After terminating iontophoretic drug application, AUROCs returned to the same levels as prior to the first drug application phase, i.e., the drug effects washed out (Figures S1B, S1D, S1F, S1H; Supplemental Information). Iontophoretic application of NaCl did not change AUROCs and thus left rule coding unaffected (Figure S2C;  $p = 0.8$ ,  $n = 10$ , Wilcoxon test). In summary, both D1R and D2R activation facilitated rule coding in the PFC.

We used a sliding ROC analysis to assess the time course of rule coding after rule-cue presentation and throughout the entire delay 2 period (Figures 3B, 3D, and 3F). In general, coding quality increased during the delay 2 period. D1R stimulation with SKF81297 caused a more prominent increase of AUROCs compared to control conditions, particularly in the second half of the delay 2 period (Figure 3B, left panel). The average latency of rule coding, defined as the time to the first significant rule coding from delay 2 onset (see Experimental Procedures), did not change after D1R stimulation (Figure 3B; right panel, mean  $\Delta$ latency =  $90 \text{ ms} \pm 103 \text{ ms}$  [SEM],  $p = 0.6$ , Wilcoxon test testing  $\Delta$ latency against zero). Blocking D1Rs with SCH23390 impaired AUROCs during the delay period (Figure 3D, left panel) but left the average latency unchanged (Figure 3D; right panel,  $\Delta$ latency =  $-13 \text{ ms} \pm 75 \text{ ms}$ ,  $p = 0.8$ , Wilcoxon test). Stimulating D2Rs with quinpirole resulted in elevated AUROCs in particular in the second half of the delay phase (Figure 3F, left panel), while not changing average latency (Figure 3F, right panel,  $\Delta$ latency =  $-93 \text{ ms} \pm 50 \text{ ms}$ ,  $p = 0.3$ , Wilcoxon test). Thus, the temporal profile during the delay 2 period was not modulated by dopamine receptor stimulation.

#### D1Rs and D2Rs Differentially Modulated Preferred and Nonpreferred Rule-Related Activity

To investigate whether the dopaminergic system differentially modulates neuronal responses to the preferred and the nonpreferred rule, we calculated a drug modulation index (MI). The MI indicated if discharges to the preferred and/or nonpreferred rule were modulated by the drug, in comparison to the baseline (see Experimental Procedures). Stimulating the D1R with SKF81297 specifically increased neuronal responses to the preferred rule (mean MI =  $+0.35 \pm 0.13$  [SEM],  $p = 0.01$ , Wilcoxon

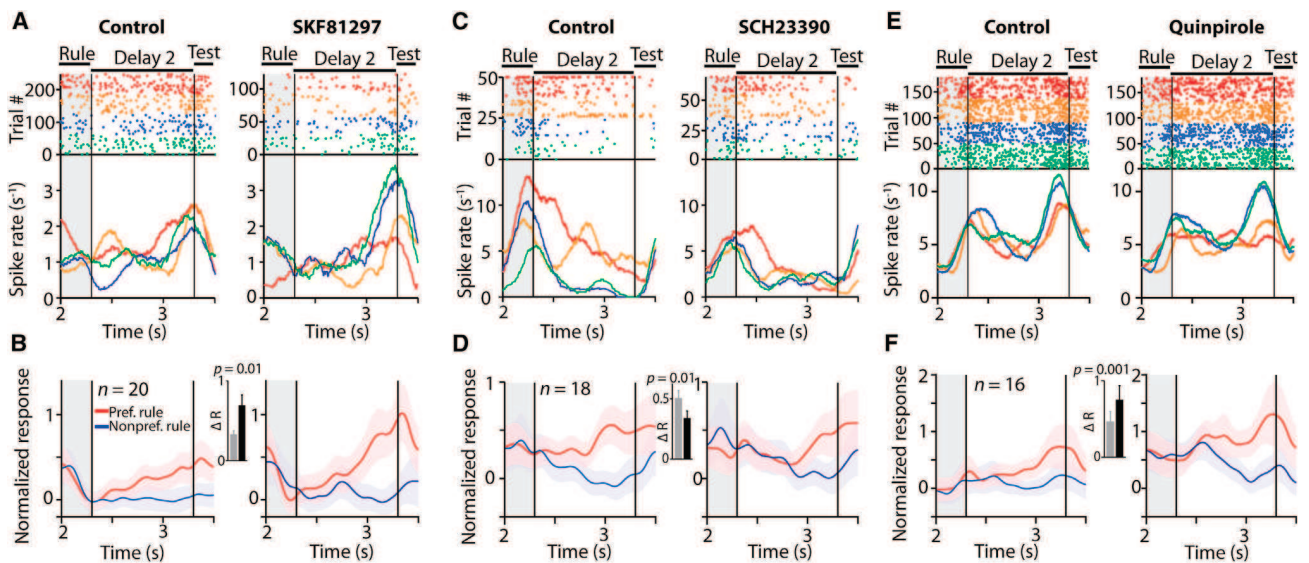


**Figure 2. Modulation of Rule-Selective Neurons by Dopamine Receptors**

(A) Dot raster and PSTH of a single neuron recorded during control conditions (left panel) and after application of SKF81297 (right panel) from the time of rule-cue presentation (gray shaded area). After D1R stimulation, the neuron responded more strongly to the “less than” rule (blue and green trace) as compared to the “greater than” rule (red and orange trace). (C) Same conventions as in (A), showing a single neuron modulated by SCH23390. Blocking the D1R reduced rule-related neuronal responses. (E) Same conventions as in (A), showing a single neuron that was modulated by quinpirole. Stimulating the D2R enhanced rule-related neuronal responses. (B, D, and F) Averaged normalized responses of all rule-selective neurons recorded with the three drugs for the preferred rule (red trace) and the nonpreferred rule (blue trace) during control conditions (left panels) and drug conditions (right panels). Insets show differences in normalized responses  $\Delta R$  between the preferred and the nonpreferred rule for control conditions (gray bars) and drug conditions (black bars). Error bars represent SEMs,  $n$  denotes sample size,  $p$  values of Wilcoxon tests.

test against zero MI), but not to the nonpreferred rule (MI =  $+0.015 \pm 0.090$ ,  $p = 0.9$ ) (Figure 4A;  $p = 0.01$  Wilcoxon test between MIs for the preferred and nonpreferred rules). Consequently, blocking the D1R with SCH23390 reduced neuronal responses to the preferred rule (MI =  $-0.23 \pm 0.083$ ,  $p = 0.02$ ), while leaving neuronal responses to the nonpreferred rule unaffected (MI =  $-0.057 \pm 0.071$ ,  $p = 0.9$ ) (Figure 4B;  $p = 0.01$ ). In contrast, stimulating the D2R with quinpirole reduced neuronal responses to the nonpreferred rule (MI =  $-0.13 \pm 0.071$ ,  $p = 0.02$ ), but not to the preferred rule (MI =  $+0.015 \pm 0.060$ ,  $p = 0.3$ ) (Figure 4C;  $p = 0.03$ ), thus enlarging the differentiation between the preferred and nonpreferred rule as witnessed in previous analysis (Figure 2F).

Differences in the modulation indices could be caused by changes of the discharge rates or by changes in the variability of neuronal discharges. We therefore computed the Fano factor as a measure of the trial-by-trial variability of neuronal discharges (Nawrot et al., 2008). None of the tested drugs changed the Fano factors in the baseline period (Figures S3A–S3D; Supplemental Information) or the delay 2 period for either preferred or nonpreferred rules (Figures S3E–S3H; Supplemental Information). This confirms that changes in rule-related firing rates (relative to the overall firing rates) rather than changes in discharge variability drive the changes in modulation indices.

Taken together, stimulation of both D1Rs and D2Rs improved rule selectivity, but in distinct ways: D1Rs specifically modulated the neuronal responses to the preferred rule (but not to the

nonpreferred rule); D2Rs, on the other hand, modulated neuronal response to the nonpreferred rule (but not to the preferred rule).

#### D1R Stimulation Enhanced Numerosity Coding Strength

Because the monkeys were required to apply rules to numerosities, we also analyzed whether prefrontal dopamine receptors might modulate the encoding of numerical values. We quantified the coding strength of the numerical value in numerosity-selective neurons during the sample period by comparing responses to preferred and nonpreferred sample numerosities. D1R stimulation increased AUROCs of numerosity-selective neurons tested with SKF81297, significantly enhancing sample numerosity coding (Figure 5A; mean  $\Delta$ AUROC =  $+0.04 \pm 0.02$  [SEM],  $n = 28$ ,  $p = 0.02$ , Wilcoxon test). Blocking D1Rs with SCH23390 did not significantly modulate AUROCs (Figure 5C;  $\Delta$ AUROC =  $+0.001 \pm 0.02$ ,  $n = 13$ ,  $p = 0.7$ , Wilcoxon test). D2R stimulation with quinpirole did not systematically change AUROCs (Figure 5E;  $\Delta$ AUROC =  $+0.02 \pm 0.03$ ,  $n = 22$ ,  $p = 0.6$ , Wilcoxon test). Thus, D1R stimulation modulated sample numerosity coding, while D2R stimulation did not.

To study these effects in more detail, we separately analyzed drug impact on the responses to the preferred and nonpreferred numerosity. Application of SKF81297 did not modulate neuronal responses to nonpreferred (mean MI =  $-0.8 \pm 0.4$  [SEM],  $p = 0.2$ , Wilcoxon test against zero MI) or preferred



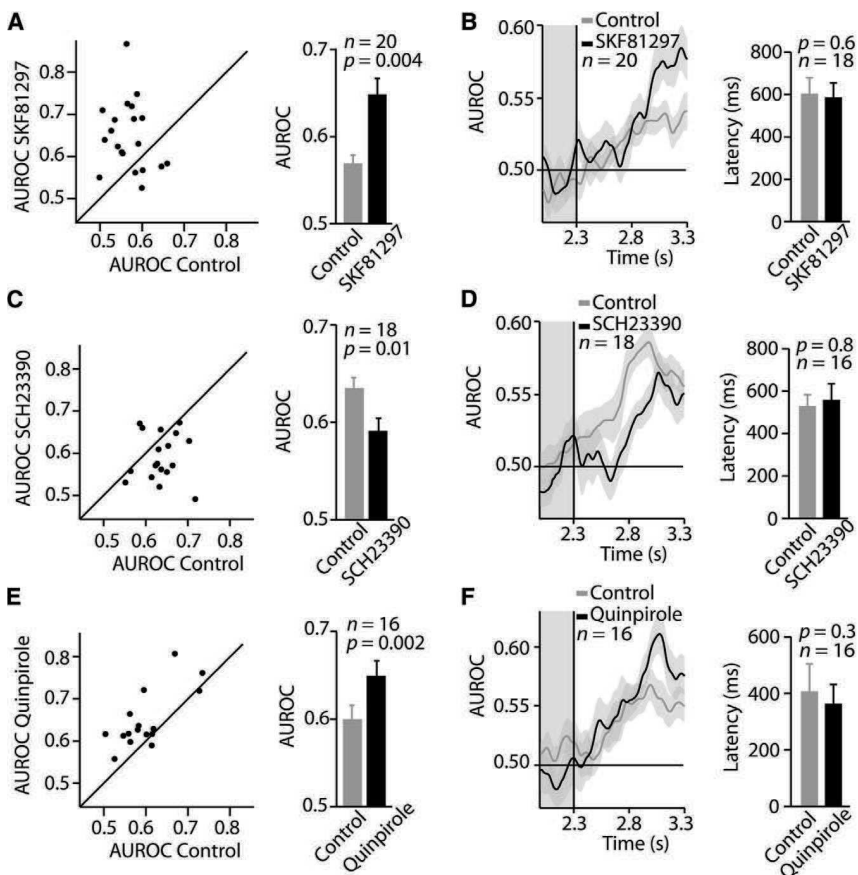


**Figure 3. Modulation of Neuronal Rule Coding by Dopamine Receptors**

(A) Distribution of AUROCs in control conditions and after application of SKF81297 (left panel, each dot corresponds to one neuron). SKF81297 increased AUROCs compared to control conditions in almost all rule-selective neurons. The mean AUROC was increased (right panel) by SKF81297 (black bar) compared to control conditions (gray bar). (B) Sliding ROC analysis showing the temporal evolution of rule coding from rule-cue onset during the delay 2 period (left panel). Gray shaded box corresponds to rule-cue presentation. The latency of rule coding was unchanged (right panel). (C) Same conventions as in (A), showing that SCH23390 reduced AUROCs. (D) Same conventions as in (B) for SCH23390. (E) Same conventions as in (A), showing that quinpirole increased AUROCs. (F) Same conventions as in (B) for quinpirole. Error bars represent SEMs, *n* denotes sample size, *p* values of Wilcoxon tests.

( $MI = -0.8 \pm 0.4$ ,  $p = 0.2$ ) sample numerosities alone (Figure 5B;  $p = 0.4$ , Wilcoxon test between MIs for nonpreferred and preferred sample numerosities). Application of SCH23390 increased neuronal responses to nonpreferred sample numerosities ( $MI = +1.6 \pm 0.8$ ,  $p = 0.02$ ), but also tended to increase responses to preferred sample numerosities ( $MI = +1.3 \pm 0.6$ ,  $p = 0.07$ ), thus resulting in no coding differences (Figure 5D;  $p = 0.7$ ). Application of quinpirole did not modulate neuronal responses to nonpreferred ( $MI = +0.3 \pm 0.3$ ,  $p = 0.2$ ) or preferred ( $MI = +0.7 \pm 0.7$ ,  $p = 0.3$ ) sample numerosities (Figure 5F;  $p = 0.5$ ). In sum, sample coding was not modulated by specific changes of neuronal responses to preferred or nonpreferred sample numerosities.

#### D1Rs and D2Rs Modulated Baseline Activity in Opposite Directions

D1Rs and D2Rs modulated baseline discharge rates (during the fixation period) of the population of all neurons. SKF81297 slightly decreased baseline discharge rates (Figure 6A;  $\Delta FR = -0.27$  Hz,  $p = 0.04$ ,  $n = 123$ , Wilcoxon test), and SCH23390 mildly increased baseline activity (Figure 6B;  $\Delta FR = +0.75$  Hz,  $p = 0.05$ ,  $n = 112$ , Wilcoxon test), whereas quinpirole enhanced baseline rates (Figure 6C;  $\Delta FR = +1.1$  Hz,  $p = 10^{-5}$ ,  $n = 79$ , Wilcoxon test). No baseline modulation was found after applying NaCl solution as a control (Figure 6D;  $\Delta FR = +0.060$  Hz,  $p = 0.5$ ,  $n = 70$ , Wilcoxon test). Figure 6E displays the average time courses

of drug-influenced baseline activity that differed significantly (Figure 6F;  $p = 10^{-7}$ , Kruskal-Wallis test). Dopamine receptor manipulation did not change neuronal trial-by-trial variability measured by the Fano factor (Nawrot et al., 2008) in the baseline period (Figures S3A–S3D; Supplemental Information). In sum, stimulating D1Rs inhibited neurons, while blocking D1Rs excited neurons. Strong excitation was observed after stimulating D2Rs.

#### Dopaminergic Modulation of Behavior

Next, we asked if modulation of prefrontal dopamine receptors influenced the monkeys' behavior. Since monkeys did not show any switch costs (Figure S4; Supplemental Information) consistent with findings reported in task-switching paradigms (Stoet and Snyder, 2009), we focused our behavioral analysis on changes in performance and reaction times. Iontophoretic drug application is highly focal (Herz et al., 1969), and most primate studies that iontophoretically applied drugs to the cortex did not report any behavioral changes (Williams and Goldman-Rakic, 1995; Sawaguchi, 2001; Wang et al., 2004, 2013; Vijayraghavan et al., 2007). However, small modulations of reaction times were reported in some studies (Herrero et al., 2008, 2013). Due to extensive training, behavioral performance was at ceiling levels (see Figure 1) and did not change after drug application (Figure 7A;  $p > 0.1$  for all drugs, Wilcoxon test over recording sessions). However, drug application slightly modulated behavioral reaction times (Figure 7B). Stimulating D1Rs with SKF81297 increased reaction times ( $\Delta RT = +3.2$  ms,  $p = 0.004$ , Mann-Whitney U test). Accordingly, blocking D1Rs with SCH23390 decreased reaction times ( $\Delta RT = -2.8$  ms,  $p = 0.03$ , Mann-Whitney U test). Stimulating D2Rs with quinpirole increased reaction times ( $\Delta RT = +1.8$  ms,

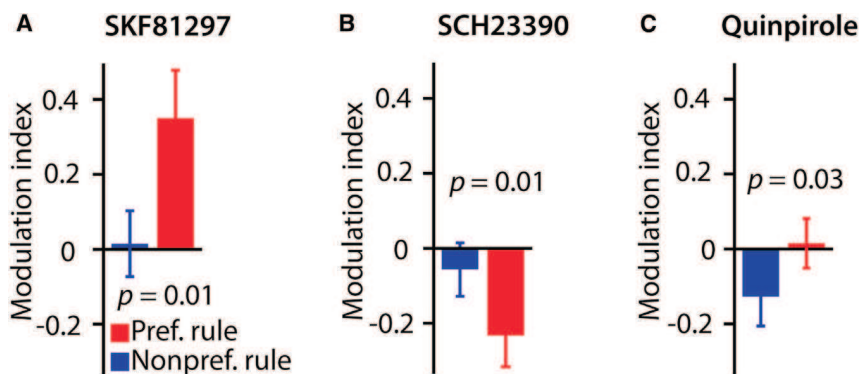


**Figure 4. Differential Modulation of Preferred and Nonpreferred Rule-Related Activity by D1Rs and D2Rs**

(A) SKF81297 enhanced the modulation indices for the preferred rule (red bar), but not the nonpreferred rule (blue bar).

(B and C) Same conventions as in (A), showing that SCH23390 reduced modulation indices for the preferred rule, whereas quinpirole reduced modulation indices for the nonpreferred rule. Error bars represent SEMs, *n* denotes sample size, *p* values of Wilcoxon tests.

$p = 0.04$ , Mann-Whitney U test). As a control, application of NaCl did not produce changes in reaction times ( $\Delta RT = -0.1$  ms,  $p = 0.3$ , Mann-Whitney U test). Thus, manipulation of both prefrontal D1Rs and D2Rs produced changes in the monkeys' behavior.

## DISCUSSION

Our findings highlight that dopaminergic input to the PFC is essential for mediating executive functions. We show that D1Rs and D2Rs assume complementary roles in enhancing neuronal representations of rule-guided decision-making at the microcircuit level. D1R stimulation suppresses neuronal baseline firing while enhancing the neurons' responses to the preferred rule. D2R stimulation, on the other hand, excites neuronal baseline firing while suppressing responses to the nonpreferred rule. Thus, two distinct physiological mechanisms that are dissociable at the dopamine receptor level modulate rule coding in the PFC.

### Modulation of Rule-Related Activity via D1Rs

D1Rs have been demonstrated to modulate the responsiveness of PFC neurons via a variety of cellular mechanisms (Seamans and Yang, 2004). We find that D1R activation suppresses neuronal baseline activity of PFC neurons. Mechanistically, this can be explained either by D1R stimulation reducing the efficacy of excitatory neurotransmission in PFC slices (Gao et al., 2001), amplifying inhibitory currents (Trantham-Davidson et al., 2004), or weakening non-NMDA-glutamatergic responses (Seamans et al., 2001). A predominantly inhibitory effect on PFC neurons has also been reported in studies iontophoretically applying D1R agonists in the PFC of monkeys engaged in a spatial working memory task (Vijayraghavan et al., 2007). This inhibition enhanced the neurons' spatial selectivity in the memory period of the task, "sculpting" their spatial memory fields (Arnsten, 2011). In agreement with this finding, blockade of D1Rs has been shown to impair spatial memory fields (Sawaguchi, 2001) (but see also Williams and Goldman-Rakic, 1995, for opposite findings). At the same time, D1R stimulation increases excitability of PFC neurons in vitro by potentiating NMDA-evoked responses (Seamans et al., 2001; Tseng and O'Donnell, 2004). Together, these findings lead to the proposal that D1R stimulation enhances

NMDA-dependent persistent activity in prefrontal networks and reduces baseline activity by controlling recurrent glutamatergic connections (Seamans and Yang, 2004; Durstewitz and Seamans, 2008; Wang et al., 2013). Our results are in agreement with this model because we find D1R stimulation to increase the neurons' sustained responses to the preferred rule while generally suppressing baseline activity. In contrast, previous studies reported that prefrontal D1Rs primarily modulate neural responses to remembered nonpreferred spatial directions (Vijayraghavan et al., 2007) or neural responses to nonpreferred associations (Puig and Miller, 2012). These findings might reflect differences in spatial and cognitive coding in the PFC. Blocking D1Rs decreased the neurons' sustained responses to the preferred rule while generally enhancing baseline activity. Thus, physiological activation of D1Rs is necessary to maintain rule coding in the PFC.

While prefrontal D1Rs modulate working memory in monkeys (Sawaguchi and Goldman-Rakic, 1991, 1994) and humans (Müller et al., 1998; McNab et al., 2009), emerging evidence also suggests a broader role of D1Rs in prefrontal functions. Blocking prefrontal D1Rs in monkeys impairs learning of new association rules and reduces corresponding neural selectivity to learned saccade directions (Puig and Miller, 2012). In rodent studies, blocking D1Rs impairs flexibly switching between different response strategies (Ragozzino, 2002; Floresco and Magyar, 2006). Similarly, D1R availability in human PFC is positively correlated with flexibly shifting between rules in a Wisconsin card sorting test (Takahashi et al., 2008; Takahashi et al., 2012). By strengthening rule signals in the PFC, our results provide a possible cellular basis for a role of D1Rs in flexible decision-making. Thus, our findings further argue for a role of D1Rs beyond working memory (Floresco and Magyar, 2006), including cognitive control processing such as rule-based decision-making.

### Modulation of Rule-Related Activity via D2Rs

Our data demonstrate a D2R-mediated excitation of PFC cells. Consistently, D2R-mediated excitation was reported by in vitro studies showing that D2Rs increase excitability of PFC cells by decreasing postsynaptic inhibitory currents (Trantham-Davidson et al., 2004) as well as with in vivo studies (Wang and Goldman-Rakic, 2004). In behaving monkeys, iontophoretic D2R stimulation in PFC predominantly excited neurons when

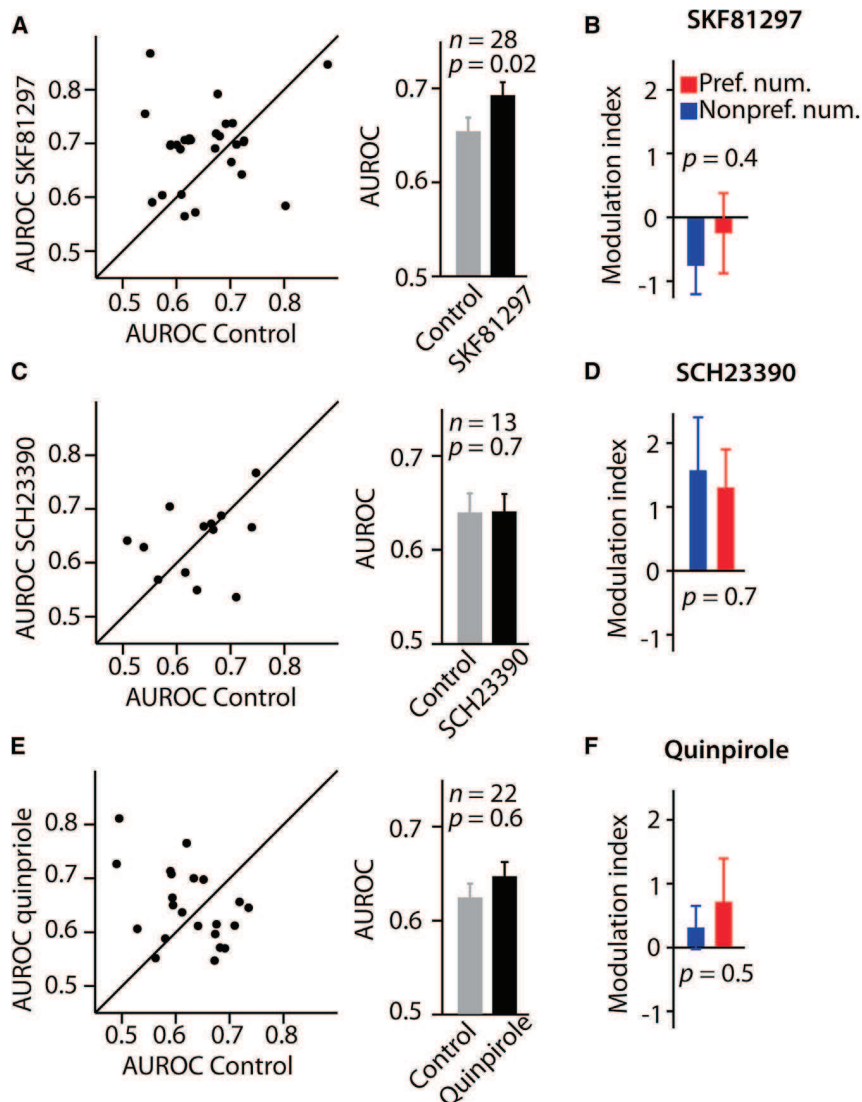


**Figure 5. Modulation of Numerosity Coding Strength by Dopamine Receptors**

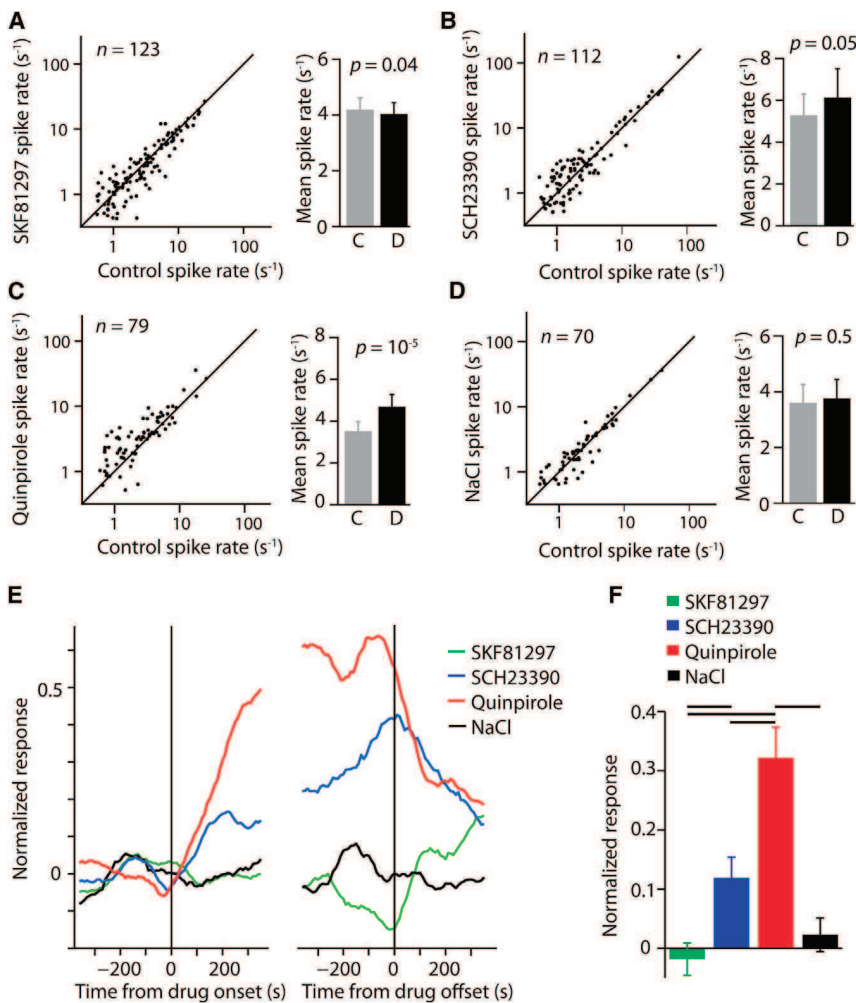
(A) Distribution of AUROCs in control conditions and after application of SKF81297 (left panel, each dot corresponds to one neuron) during the sample period. The mean AUROC was increased (right panel) by SKF81297 (black bar) compared to control conditions (gray bar). (B) Modulation index for nonpreferred (blue bar) and preferred (red bar) responses during the sample period induced by SKF81297. (C) Same conventions as in (A) for SCH23390. (D) Same conventions as in (B) for SCH23390. (E) Same conventions as in (A) for quinpirole, showing no modulation of sample preference. (F) Same conventions as in (B) for quinpirole. Error bars represent SEMs, n denotes sample size, p values of Wilcoxon tests.

monkeys made a saccade toward a remembered location (Wang et al., 2004). Sustained activity during the spatial memory period of the task, however, was not affected (Wang et al., 2004). The authors thus concluded that D2R manipulation has little or no effect on the persistent mnemonic-related activity (Wang et al., 2004). Consistent with these physiological results, D2R manipulation does not produce changes in spatial working memory performance in monkeys (Sawaguchi and Goldman-Rakic, 1994) or humans (Müller et al., 1998).

We show here, however, that a different type of sustained activity, namely rule-selective responses during a delay period, is indeed influenced by D2Rs. D2R stimulation enhances rule coding by suppressing responses to the nonpreferred rule while leaving responses to the preferred rule unchanged. This relative suppression of responses to the nonpreferred rule might be mediated by specific inhibitory D2R actions in prefrontal neurons reported by several *in vitro* studies (Tseng and O'Donnell, 2004). Our findings are in agreement with a recent study showing that

blocking prefrontal D2Rs in monkeys impairs learning of new association rules and reduces neural selectivity for the learned saccade direction particularly for the nonpreferred direction (Puig and Miller, 2014). Furthermore, blocking D2Rs increased preservation errors, thus impairing behavioral flexibility (Puig and Miller, 2014). In addition, rodent studies suggest that D2Rs modulate behavioral flexibility and decision-making (Floresco and Magyar, 2006). After blocking D2Rs in the PFC, rats were impaired in switching between different response strategies (Floresco et al., 2006), and blocking D2Rs impaired set-shifting in humans (Mehta et al., 1999). Stimulating D2Rs increased BOLD signals in frontal cortex during rule switching in humans (Stelzel et al., 2013) and improved performance of monkeys in a delayed response

task (Arnsten et al., 1995). Thus, our finding that D2R activation enhances rule coding in the PFC provides a cellular basis for D2R modulation of cognitive functions. Our results highlight that D2Rs—while not being involved in spatial mnemonic processing—do play an important role during flexible decision-making. Consistent with the electrophysiological findings, both D1R and D2R stimulation caused changes in the monkeys' behavior in the same direction. The monkeys needed slightly longer to respond after D1R and D2R stimulation, whereas blocking D1Rs mildly decreased reaction times. The magnitude of the effect was comparable to previous studies reporting changes in reaction times after iontophoretic drug application (Herrero et al., 2008, 2013). Prolonged reaction times during D1R and D2R stimulation might reflect the increased stability in rule coding in the PFC. In addition to cognitive variables, prefrontal dopamine receptors also modulate motor-related signals (Wang et al., 2004). While we did not investigate motor-related



influences, we speculate that our pharmacological interventions also affected motor selection signals. The precise mechanisms by which manipulation of prefrontal dopamine receptors affects behavior surely require further investigation.

### D1R Modulation of Coding Strength to Sample Numerosity

Midbrain dopamine neurons fire phasic bursts in response to behaviorally relevant sensory events (Schultz, 1998; Matsumoto and Hikosaka, 2009; de Lafuente and Romo, 2012). In the PFC, dopamine enhances visual signals (Jacob et al., 2013), possibly gating neuronal representations of relevant stimuli (D'Ardenne et al., 2012). Consistently, we found that D1R stimulation enhanced neuronal representation of sample numerosity that is needed to solve numerical tasks (Nieder, 2012, 2013; Jacob and Nieder, 2014). Thus, D1Rs might mediate dopamine's function of supporting the detection of relevant sensory events (Redgrave et al., 2008; de Lafuente and Romo, 2011). Together with studies demonstrating D1R modulation of spatial working memory processes (Williams and Goldman-Rakic, 1995; Sawaguchi, 2001; Vijayraghavan et al., 2007) and associative learning (Puig and Miller, 2012), prefrontal D1Rs are also involved in mul-

tipale prefrontal functions and at different time scales (Schultz, 2007). In contrast, D2Rs did not modulate numerosity coding strength, just as it did not modulate spatial working memory processes (Wang et al., 2004), although D2Rs modulate neural signatures of associative learning (Puig and Miller, 2014). Therefore, prefrontal D2Rs might assume a more specific role in cognitive processing.

### Complementary Roles of D1Rs and D2Rs in Behavioral Flexibility

We find that D1Rs and D2Rs modulated spontaneous firing in opposite directions, with D1Rs and D2Rs strengthening rule coding in complementary ways. This is consistent with the idea that the ratio between D1R and D2R activation determines excitability in prefrontal networks (Seamans and Yang, 2004). In recent monkey experiments, both prefrontal D1Rs and D2Rs influenced saccadic target selection (Noudoost and Moore, 2011a) possibly underlying attentional processes (Noudoost and Moore, 2011b; Clark and Noudoost, 2014), while only D1Rs seemed to control cortical visual signals. Interestingly, dopamine depletions impair not only spatial working memory (Brozoski et al., 1979) but also the learning of rules in monkeys (Crofts et al., 2001). Both prefrontal D1R and D2R activation contribute to learning new associative rules, suggesting a cooperative role in cognitive flexibility of both receptor families (Puig and Miller, 2012, 2014). This is in agreement with the finding that midbrain dopamine neurons signal the cognitive component

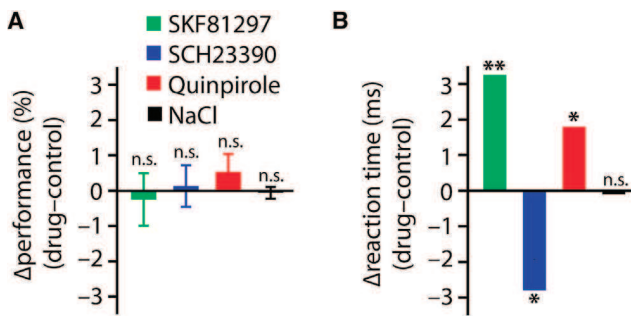


**Figure 7. Drug Effects on the Monkeys' Behavior**

(A) Difference in performance (% correct trials) between control and drug conditions. Error bars represent SEMs over recording sessions. n.s., not significant (Wilcoxon test,  $p > 0.05$ ).

(B) Difference in mean normalized reaction times between control and drug conditions pooled over all recording sessions. n.s., not significant ( $p > 0.05$ ), \* $p < 0.05$ , \*\* $p < 0.01$  (Mann-Whitney U test).

of a task (Stefani and Moghaddam, 2006; Matsumoto and Takada, 2013) and are correlated with the monkeys' decisions (de Lafuente and Romo, 2011). Complementary roles of D1Rs and D2Rs for behavioral flexibility are thus present in both primates and rodents (Floresco and Magyar, 2006; Takahashi et al., 2012; Floresco, 2013; Puig and Miller, 2014). Our data extend these findings and show that dopamine influences executive functions in the PFC through both D1Rs and D2Rs, enhancing rule-based decision-making. These findings might contribute to interpreting drug effects in psychiatric disorders with disturbed prefrontal dopamine signaling (Arnsten, 2011; Winterer and Weinberger, 2004).

## EXPERIMENTAL PROCEDURES

### Animals and Surgical Procedures

Two male rhesus monkeys (*Macaca mulatta*) were implanted with a titanium head post and one recording chamber centered over the principal sulcus of the lateral PFC, anterior to the frontal eye fields (right hemispheres in both monkeys). Surgery was conducted using aseptic techniques under general anesthesia. Structural magnetic resonance imaging was performed before implantation to locate anatomical landmarks. All experimental procedures were in accordance with the guidelines for animal experimentation approved by the authority, the Regierungspräsidium Tübingen, Germany.

### Task

Monkeys learned to flexibly perform numerical "greater than" versus "less than" comparisons. They initiated a trial by grasping a lever and maintaining central fixation on a screen. After a pure fixation period (500 ms), a sample stimulus (500 ms) cued the animals for the reference numerosity (i.e., number of dots) they had to remember for a brief time interval. The first memory interval (delay 1, 1,000 ms) was followed by a rule cue (300 ms) that instructed the monkeys to select either a larger number of dots ("greater than" rule) or a smaller number of dots ("less than" rule) than the sample numerosity in the subsequent test phase. The test phase was preceded by a second delay (delay 2, 1,000 ms) requiring the monkeys to assess the rule at hand for the subsequent choice. In the following test 1 phase, the monkeys had to release the lever in a "greater than" trial, if the number of items in the test display was larger than the number of items in the sample display (match trial), or to keep holding the lever for another 1,200 ms until the appearance of a second test display (test 2), if the number of items in the test display was smaller than the number of items in the sample display (nonmatch trial). In a "less than" trial,

these conditions were reversed. Monkeys got a liquid reward for a correct choice. Thus, only test 1 required a decision; test 2 was used so that a behavioral response was required in each trial, ensuring that the monkeys were paying attention during all trials. Because both sample and test numerosities varied randomly, the monkeys could only solve the task by assessing the numerosity of the test display relative to the three possible numerosities of the sample display together with the appropriate rule in any single trial. To test a range of numerosities, both monkeys were presented with numerosities 2 (smaller test numerosity = 1, larger test numerosity = 4), 8 (4:16), and 32 (16:64). For any sample numerosity, test numerosities were either larger or smaller with equal probability ( $p = 0.5$ ). Because the monkeys' numerosity discrimination performance obeys the Weber-Fechner law (Nieder and Miller, 2003), numerosities larger than a sample numerosity need to be numerically more distant than numerosities smaller than the sample numerosity to reach equal discriminability. Based on this design, any test numerosity (except the smallest and largest used) served as test numerosities for different sample numerosities, thus precluding the animals from learning systematic relations between numerosities.

To prevent the animals from exploiting low-level visual cues (e.g., dot density, total dot area), a standard numerosity protocol (with dot sizes and positions pseudorandomized) and a control numerosity protocol (with equal total area and average density of all dots within a trial) were each presented in 50% of the trials in a pseudorandomized fashion. To dissociate the rule-related cellular responses from responses to the sensory features of the rule cue, each rule was signified by two different rule cues in two different sensory modalities: a red circle ("greater than" rule, red color) or a white circle with a drop of water ("greater than" rule, water) signified the rule "greater than." The "less than" rule was cued by a blue circle ("less than" rule, blue color) or a white circle with no water ("less than" rule, no water). We showed in previous studies that monkeys generalize the numerical principles "greater than" and "less than" to numerosities they had never seen before (Bongard and Nieder, 2010; Eiselt and Nieder, 2013). Before each session, the displays were generated anew using MATLAB (Mathworks). Trials were randomized and balanced across all relevant features ("greater than" and "less than" rules, rule-cue modalities, sample numerosities, standard and control stimuli, match and nonmatch trials). Monkeys had to keep their gaze within  $1.75^\circ$  of the fixation point from the fixation interval up to the onset of the first test stimulus (monitored with an infrared eye-tracking system; ISCAN, Burlington, MA).

### Electrophysiology and Iontophoresis

Extracellular single-unit recording and iontophoretic drug application were performed as described previously (Jacob et al., 2013). In each recording session, up to three custom-made tungsten-in-glass electrodes flanked by two pipettes each were inserted transdurally using a modified electrical microdrive (NAN Instruments). Single neurons were recorded at random; no attempt was made to preselect the neurons to any task-related activity or based on drug effects. Signal acquisition, amplification, filtering, and digitalization were accomplished with the MAP system (Plexon). Waveform separation was performed offline (Offline Sorter; Plexon). Drugs were applied iontophoretically (MVCS iontophoresis system; npi electronic) using custom-made tungsten-in-glass electrodes flanked by two pipettes each (Jacob et al., 2013; Thiele et al., 2006). Electrode impedance and pipette resistance were measured after each recording session. Electrode impedances were 0.8–3 M $\Omega$  (measured at 500 Hz; Omega Tip Z; World Precision Instruments). Pipette resistances depended on the pipette opening diameter, drug, and solvent used. Typical resistances were 15–50 M $\Omega$  (full range, 12–160 M $\Omega$ ). As in previous experiments (Jacob et al., 2013), we used retention currents of  $-7$  nA to hold the drugs in the pipette during control conditions. The ejection current for SKF81297 (10 mM in double-distilled water [pH 4.0] with HCl; Sigma-Aldrich) was +15 nA, the ejection current for SCH23390 (10 mM in double-distilled water [pH 4.0] with HCl; Sigma-Aldrich) was +25 nA, and the ejection current for quinpirole (10 mM in double-distilled water [pH 4.0] with HCl; Sigma-Aldrich) was +40 nA. In control experiments with 0.9% physiological NaCl (pH 4.0) with HCl, the ejection current was +25 nA. We did not investigate dosage effects and chose ejection currents to match the values reported to be maximally effective, i.e., in the peak range

of the “inverted-U function” (Wang et al., 2004; Vijayraghavan et al., 2007). One pipette per electrode was filled with drug solution (either SKF81297, SCH23390, quinpirole, or NaCl), and the other always contained 0.9% NaCl. In each recording session, control conditions using the retention current alternated with drug conditions using the ejection current. Drugs were applied continuously for 12–15 min (drug conditions), depending on the number of trials completed correctly by the animal. Each control or drug application block consisted of 72 correct trials to yield sufficient trials for analysis. The first block (12–15 min) was always the control condition. Given that iontophoretic drug application is fast and can quickly modulate neuronal firing properties (Jacob et al., 2013), we did not exclude data at the current switching points.

## Data Analyses

### Rule-Selective Neurons

All well-isolated recorded single units with a baseline spike rate above 0.5 Hz (determined in the 500 ms fixation period preceding sample presentation) entered the analyses. Neurons were not included based on drug effects. We calculated a four-way ANOVA for each neuron to determine if a neuron's response was correlated with the numerical rules. We used spike rates in a 600 ms window beginning 500 ms after offset of the rule-cue, i.e., in the second half of the delay 2 period. We chose this window because previous studies found the most prominent rule coding during this period (Bongard and Nieder, 2010; Eisele and Nieder, 2013). The main factors were iontophoresis condition (control conditions/drug conditions), sample numerosity (“2”/“8”/“32”), rule to apply (“greater than”/“less than”) and the rule-cue modality (red/blue versus water/no-water). We identified rule-selective neurons by a significant main factor of the rule that the monkeys had to apply ( $p < 0.05$ ). To ensure that neuronal responses varied with the abstract numerical rules rather than with the rule cues, we excluded neurons with a significant interaction of the main factors rule and rule-cue modality ( $p < 0.05$ ). Since the monkeys' behavior did not show any differences for standard and control stimuli (Figure 1), and because we have shown previously that neuronal responses in the PFC do not differentiate between standard and control stimuli (Bongard and Nieder, 2010; Eisele and Nieder, 2013), we pooled over standard and control stimuli trials. A similar number of neurons preferred the “greater than” (34 neurons) and the “less than” rule (30 neurons), and neurons in the PFC encode both numerical rules about equally well (Bongard and Nieder, 2010; Eisele and Nieder, 2013). In general, nine trials was the minimum number of trials in one of the four rule conditions for a neuron to enter the analyses. The maximum number was 70 trials per rule condition, with an average of 25 trials per one of the four rule conditions (i.e., the average neuron was recorded for 200 trials: four rule conditions for control and drug conditions, respectively).

### Single-Cell and Population Responses

For plotting single-cell spike density histograms, the average firing rate in trials with one of the four different rule-cues (correct trials only) was smoothed with a Gaussian kernel (bin width of 200 ms, steps of 1 ms). For the population responses, trials with rule cues signifying the same numerical rule were pooled. A neuron's preferred rule was defined as the numerical rule yielding the higher average spike rate in the analysis window used for the ANOVA. The nonpreferred rule was defined as the numerical rule resulting in lower average spike rate. Neuronal activity was normalized by subtracting the mean baseline firing rate in the control condition and dividing by the standard deviation of the baseline firing rates in the control condition. For population histograms, normalized activity was averaged and smoothed with a Gaussian kernel (bin width of 200 ms, step of 1 ms). To quantify a neuron's selectivity to its preferred rule, we calculated the difference  $\Delta R$  between the normalized response to the preferred and the nonpreferred rule in the same analysis window used for the ANOVA.

### Receiver Operating Characteristic Analysis

Rule-coding quality was quantified using receiver operating characteristic (ROC) analysis derived from Signal Detection Theory (Green and Swets, 1966). The AUROC is a nonparametric measure of the discriminability of two distributions. It denotes the probability with which an ideal observer can tell apart a meaningful signal from a noisy background. Values of 0.5 indicate no separation, and values of 1 signal perfect discriminability. The AUROC takes into account both the difference between distribution means as well as their

widths and is therefore a suitable indicator of signal quality. We used AUROCs to quantify the quality of numerical rule coding. We calculated the AUROC for each neuron using the spike rate distributions of the preferred and the nonpreferred rule in the same analysis window used for the ANOVA. Sliding ROC analysis was performed from rule-cue onset until the end of the delay 2 period with overlapping 100 ms windows stepped in 10 ms increments. For each window, we calculated the AUROC comparing spike rates for the preferred and nonpreferred rule. We performed a permutation test for each window, estimating the null distribution of AUROCs by randomly relabeling trials to the preferred or nonpreferred group with 999 repetitions. Latency of rule coding was defined as the time of the first of three consecutive significant windows in the permutation test ( $p < 0.05$ , two-sided) beginning from the onset of the delay 2 period. Four neurons were excluded from the analysis, because no latency could be computed for both control and drug conditions.

### Drug Modulation Index

To quantify if a drug specifically modulated the discharge of a neuron to the preferred or the nonpreferred rule, we calculated a drug MI for each drug and neuron separately for the preferred and the nonpreferred rule. The MI was computed by first subtracting the mean baseline spike rate (500 ms fixation period preceding sample presentation) from each trial separately for control and drug conditions and dividing by the standard deviation of baseline spike rates to account for general shifts in baseline spike rates induced by the drugs (see Figure 6). Next, we calculated the MI for the preferred rule defined as the difference between the mean response to the preferred rule in the drug condition and the mean response to the preferred rule in the control condition for each neuron and drug. The MI for the nonpreferred rule was calculated in the same way. Thus, the MI reflects the amount by which the drug modulates the preferred or the nonpreferred rule, respectively, in comparison to the neuron's baseline activity.

### Analysis of Sample Numerosity Modulation

We calculated a two-way ANOVA with main factors sample numerosity (sample numerosities “2,” “8,” “32”) and iontophoresis condition (control or drug condition) in the sample phase, a 500 ms window beginning 100 ms after sample onset (Bongard and Nieder, 2010) and selected sample-selective neurons with a significant main effect of sample numerosity ( $p < 0.05$ ). The preferred sample numerosity was defined as the numerosity yielding the highest spike rate, the nonpreferred sample item was defined as the numerosity yielding the lowest spike rate in the sample phase. AUROCs were calculated using the distribution of spike rates for preferred and nonpreferred numerosities in the same analysis window. Modulation indices were calculated in the same analysis window and calculated as described for rule-selective neurons.

### Modulation of Neuronal Baseline Activity

Baseline spike rates (500 ms fixation period preceding sample presentation) were normalized for each neuron by subtracting the mean baseline spike rate in control conditions and dividing by the standard deviation of baseline spike rates in control conditions. Thus, the mean normalized activity in control conditions is by definition zero. The amplitude of drug modulation is then given by the mean normalized activity in drug conditions. We assessed the time course of baseline modulation throughout one block (12–15 min) of drug administration by aligning normalized baseline activity to the time point when the iontophoretic drug application was switched on and off, respectively. We used bins of 10 s (about the time of two trials) to average the population activity and smoothed the population time course with a Gaussian kernel (width of 60 s).

### Behavioral Modulation by Drug Application

Behavioral performance was calculated for each recording session for control and drug conditions and compared using a paired Wilcoxon test ( $n = 63$  for SKF81297,  $n = 50$  for SCH23390,  $n = 39$  for quinpirole, and  $n = 27$  for NaCl). Behavioral reaction times were normalized for each recording session by subtracting the mean reaction time for the respective recording session from each reaction time (Herrero et al., 2013). Normalized reaction times were pooled over recording sessions for control and drug conditions and compared with a Mann-Whitney U test ( $n = 4,886$ ,  $n = 4,778$  for control and SKF81297 conditions;  $n = 5,234$ ,  $n = 4,998$  for control and SCH23390 conditions;  $n = 2,995$ ,  $n = 3,830$  for control and quinpirole conditions;  $n = 2,912$ ,  $n = 2,914$  for control and NaCl conditions). Only correct match trials were used.

## SUPPLEMENTAL INFORMATION

Supplemental Information includes four figures and can be found with this article at <http://dx.doi.org/10.1016/j.neuron.2014.11.012>.

## AUTHOR CONTRIBUTIONS

T.O. designed and performed experiments, analyzed data, and wrote the manuscript; S.N.J. designed experiments and provided analytical tools; A.N. designed experiments and wrote the paper.

## ACKNOWLEDGMENTS

This work was supported by grants from the German Research Foundation (DFG) to S.N.J. (JA 1999/1-1) and to A.N. (NI 618/5-1).

Accepted: November 4, 2014

Published: December 4, 2014

## REFERENCES

- Arnsten, A.F.T. (2011). Catecholamine influences on dorsolateral prefrontal cortical networks. *Biol. Psychiatry* 69, e89–e99.
- Arnsten, A.F.T., Cai, J.X., Steere, J.C., and Goldman-Rakic, P.S. (1995). Dopamine D2 receptor mechanisms contribute to age-related cognitive decline: the effects of quinpirole on memory and motor performance in monkeys. *J. Neurosci.* 15, 3429–3439.
- Björklund, A., and Dunnett, S.B. (2007). Dopamine neuron systems in the brain: an update. *Trends Neurosci.* 30, 194–202.
- Bongard, S., and Nieder, A. (2010). Basic mathematical rules are encoded by primate prefrontal cortex neurons. *Proc. Natl. Acad. Sci. USA* 107, 2277–2282.
- Brozoski, T.J., Brown, R.M., Rosvold, H.E., and Goldman, P.S. (1979). Cognitive deficit caused by regional depletion of dopamine in prefrontal cortex of rhesus monkey. *Science* 205, 929–932.
- Clark, K.L., and Noudoost, B. (2014). The role of prefrontal catecholamines in attention and working memory. *Front. Neural Circuits* 8, 33.
- Crofts, H.S., Dalley, J.W., Collins, P., Van Denderen, J.C., Everitt, B.J., Robbins, T.W., and Roberts, A.C. (2001). Differential effects of 6-OHDA lesions of the frontal cortex and caudate nucleus on the ability to acquire an attentional set. *Cereb. Cortex* 11, 1015–1026.
- D'Ardenne, K., Eshel, N., Luka, J., Lenartowicz, A., Nystrom, L.E., and Cohen, J.D. (2012). Role of prefrontal cortex and the midbrain dopamine system in working memory updating. *Proc. Natl. Acad. Sci. USA* 109, 19900–19909.
- de Almeida, J., and Mengod, G. (2010). D2 and D4 dopamine receptor mRNA distribution in pyramidal neurons and GABAergic subpopulations in monkey prefrontal cortex: implications for schizophrenia treatment. *Neuroscience* 170, 1133–1139.
- de Lafuente, V., and Romo, R. (2011). Dopamine neurons code subjective sensory experience and uncertainty of perceptual decisions. *Proc. Natl. Acad. Sci. USA* 108, 19767–19771.
- de Lafuente, V., and Romo, R. (2012). Dopaminergic activity coincides with stimulus detection by the frontal lobe. *Neuroscience* 218, 181–184.
- Durstewitz, D., and Seamans, J.K. (2008). The dual-state theory of prefrontal cortex dopamine function with relevance to catechol-o-methyltransferase genotypes and schizophrenia. *Biol. Psychiatry* 64, 739–749.
- Eiselt, A.-K., and Nieder, A. (2013). Representation of abstract quantitative rules applied to spatial and numerical magnitudes in primate prefrontal cortex. *J. Neurosci.* 33, 7526–7534.
- Floresco, S.B. (2013). Prefrontal dopamine and behavioral flexibility: shifting from an “inverted-U” toward a family of functions. *Front. Neurosci.* 7, 62.
- Floresco, S.B., and Magyar, O. (2006). Mesocortical dopamine modulation of executive functions: beyond working memory. *Psychopharmacology (Berl.)* 188, 567–585.
- Floresco, S.B., Magyar, O., Ghods-Sharifi, S., Vexelman, C., and Tse, M.T.L. (2006). Multiple dopamine receptor subtypes in the medial prefrontal cortex of the rat regulate set-shifting. *Neuropsychopharmacology* 31, 297–309.
- Gao, W.J., Krimer, L.S., and Goldman-Rakic, P.S. (2001). Presynaptic regulation of recurrent excitation by D1 receptors in prefrontal circuits. *Proc. Natl. Acad. Sci. USA* 98, 295–300.
- Green, D.M., and Swets, J.A. (1966). *Signal Detection Theory and Psychophysics*. (New York: Wiley).
- Herrero, J.L., Roberts, M.J., Delicato, L.S., Gieselmann, M.A., Dayan, P., and Thiele, A. (2008). Acetylcholine contributes through muscarinic receptors to attentional modulation in V1. *Nature* 454, 1110–1114.
- Herrero, J.L., Gieselmann, M.A., Sanayei, M., and Thiele, A. (2013). Attention-induced variance and noise correlation reduction in macaque V1 is mediated by NMDA receptors. *Neuron* 78, 729–739.
- Herz, A., Zieglgänsberger, W., and Färber, G. (1969). Microelectrophoretic studies concerning the spread of glutamic acid and GABA in brain tissue. *Exp. Brain Res.* 9, 221–235.
- Jacob, S.N., and Nieder, A. (2014). Complementary roles for primate frontal and parietal cortex in guarding working memory from distractor stimuli. *Neuron* 83, 226–237.
- Jacob, S.N., Ott, T., and Nieder, A. (2013). Dopamine regulates two classes of primate prefrontal neurons that represent sensory signals. *J. Neurosci.* 33, 13724–13734.
- Lidow, M.S., Wang, F., Cao, Y., and Goldman-Rakic, P.S. (1998). Layer V neurons bear the majority of mRNAs encoding the five distinct dopamine receptor subtypes in the primate prefrontal cortex. *Synapse* 28, 10–20.
- Matsumoto, M., and Hikosaka, O. (2009). Two types of dopamine neuron distinctly convey positive and negative motivational signals. *Nature* 459, 837–841.
- Matsumoto, M., and Takada, M. (2013). Distinct representations of cognitive and motivational signals in midbrain dopamine neurons. *Neuron* 79, 1011–1024.
- McNab, F., Varrone, A., Farde, L., Jucaite, A., Bystritsky, P., Forssberg, H., and Klingberg, T. (2009). Changes in cortical dopamine D1 receptor binding associated with cognitive training. *Science* 323, 800–802.
- Mehta, M.A., Sahakian, B.J., McKenna, P.J., and Robbins, T.W. (1999). Systemic sulpiride in young adult volunteers simulates the profile of cognitive deficits in Parkinson's disease. *Psychopharmacology (Berl.)* 146, 162–174.
- Miller, E.K., and Cohen, J.D. (2001). An integrative theory of prefrontal cortex function. *Annu. Rev. Neurosci.* 24, 167–202.
- Müller, U., von Cramon, D.Y., and Pollmann, S. (1998). D1- versus D2-receptor modulation of visuospatial working memory in humans. *J. Neurosci.* 18, 2720–2728.
- Nawrot, M.P., Boucsein, C., Rodriguez Molina, V., Riehle, A., Aertsen, A., and Rotter, S. (2008). Measurement of variability dynamics in cortical spike trains. *J. Neurosci. Methods* 169, 374–390.
- Nieder, A. (2012). Supramodal numerosity selectivity of neurons in primate prefrontal and posterior parietal cortices. *Proc. Natl. Acad. Sci. USA* 109, 11860–11865.
- Nieder, A. (2013). Coding of abstract quantity by ‘number neurons’ of the primate brain. *J. Comp. Physiol. A Neuroethol. Sens. Neural Behav. Physiol.* 199, 1–16.
- Nieder, A., and Miller, E.K. (2003). Coding of cognitive magnitude: compressed scaling of numerical information in the primate prefrontal cortex. *Neuron* 37, 149–157.
- Nieder, A., Freedman, D.J., and Miller, E.K. (2002). Representation of the quantity of visual items in the primate prefrontal cortex. *Science* 297, 1708–1711.
- Noudoost, B., and Moore, T. (2011a). Control of visual cortical signals by prefrontal dopamine. *Nature* 474, 372–375.
- Noudoost, B., and Moore, T. (2011b). The role of neuromodulators in selective attention. *Trends Cogn. Sci.* 15, 585–591.

- Puig, M.V., and Miller, E.K. (2012). The role of prefrontal dopamine D1 receptors in the neural mechanisms of associative learning. *Neuron* *74*, 874–886.
- Puig, M.V., and Miller, E.K. (2014). Neural substrates of dopamine D2 receptor modulated executive functions in the monkey prefrontal cortex. *Cerebral Cortex*. Published online May 9, 2014. <http://dx.doi.org/10.1093/cercor/bhu096>.
- Ragozzino, M.E. (2002). The effects of dopamine D(1) receptor blockade in the prefrontal-infralimbic areas on behavioral flexibility. *Learn. Mem.* *9*, 18–28.
- Redgrave, P., Gurney, K., and Reynolds, J. (2008). What is reinforced by phasic dopamine signals? *Brain Res. Brain Res. Rev.* *58*, 322–339.
- Robbins, T.W., and Arnsten, A.F.T. (2009). The neuropsychopharmacology of fronto-executive function: monoaminergic modulation. *Annu. Rev. Neurosci.* *32*, 267–287.
- Sawaguchi, T. (2001). The effects of dopamine and its antagonists on directional delay-period activity of prefrontal neurons in monkeys during an oculomotor delayed-response task. *Neurosci. Res.* *41*, 115–128.
- Sawaguchi, T., and Goldman-Rakic, P.S. (1991). D1 dopamine receptors in prefrontal cortex: involvement in working memory. *Science* *251*, 947–950.
- Sawaguchi, T., and Goldman-Rakic, P.S. (1994). The role of D1-dopamine receptor in working memory: local injections of dopamine antagonists into the prefrontal cortex of rhesus monkeys performing an oculomotor delayed-response task. *J. Neurophysiol.* *71*, 515–528.
- Schultz, W. (1998). Predictive reward signal of dopamine neurons. *J. Neurophysiol.* *80*, 1–27.
- Schultz, W. (2007). Multiple dopamine functions at different time courses. *Annu. Rev. Neurosci.* *30*, 259–288.
- Seamans, J.K., and Yang, C.R. (2004). The principal features and mechanisms of dopamine modulation in the prefrontal cortex. *Prog. Neurobiol.* *74*, 1–58.
- Seamans, J.K., Durstewitz, D., Christie, B.R., Stevens, C.F., and Sejnowski, T.J. (2001). Dopamine D1/D5 receptor modulation of excitatory synaptic inputs to layer V prefrontal cortex neurons. *Proc. Natl. Acad. Sci. USA* *98*, 301–306.
- Stefani, M.R., and Moghaddam, B. (2006). Rule learning and reward contingency are associated with dissociable patterns of dopamine activation in the rat prefrontal cortex, nucleus accumbens, and dorsal striatum. *J. Neurosci.* *26*, 8810–8818.
- Stelzel, C., Fiebach, C.J., Cools, R., Tafazoli, S., and D'Esposito, M. (2013). Dissociable fronto-striatal effects of dopamine D2 receptor stimulation on cognitive versus motor flexibility. *Cortex* *49*, 2799–2811.
- Stoet, G., and Snyder, L.H. (2009). Neural correlates of executive control functions in the monkey. *Trends Cogn. Sci.* *13*, 228–234.
- Takahashi, H., Kato, M., Takano, H., Arakawa, R., Okumura, M., Otsuka, T., Kodaka, F., Hayashi, M., Okubo, Y., Ito, H., and Suhara, T. (2008). Differential contributions of prefrontal and hippocampal dopamine D(1) and D(2) receptors in human cognitive functions. *J. Neurosci.* *28*, 12032–12038.
- Takahashi, H., Yamada, M., and Suhara, T. (2012). Functional significance of central D1 receptors in cognition: beyond working memory. *J. Cereb. Blood Flow Metab.* *32*, 1248–1258.
- Thiele, A., Delicato, L.S., Roberts, M.J., and Gieselmann, M.A. (2006). A novel electrode-pipette design for simultaneous recording of extracellular spikes and iontophoretic drug application in awake behaving monkeys. *J. Neurosci. Methods* *158*, 207–211.
- Trantham-Davidson, H., Neely, L.C., Lavin, A., and Seamans, J.K. (2004). Mechanisms underlying differential D1 versus D2 dopamine receptor regulation of inhibition in prefrontal cortex. *J. Neurosci.* *24*, 10652–10659.
- Tseng, K.Y., and O'Donnell, P. (2004). Dopamine-glutamate interactions controlling prefrontal cortical pyramidal cell excitability involve multiple signaling mechanisms. *J. Neurosci.* *24*, 5131–5139.
- Vallentin, D., Bongard, S., and Nieder, A. (2012). Numerical rule coding in the prefrontal, premotor, and posterior parietal cortices of macaques. *J. Neurosci.* *32*, 6621–6630.
- Vijayraghavan, S., Wang, M., Birnbaum, S.G., Williams, G.V., and Arnsten, A.F.T. (2007). Inverted-U dopamine D1 receptor actions on prefrontal neurons engaged in working memory. *Nat. Neurosci.* *10*, 376–384.
- Viswanathan, P., and Nieder, A. (2013). Neuronal correlates of a visual “sense of number” in primate parietal and prefrontal cortices. *Proc. Natl. Acad. Sci. USA* *110*, 11187–11192.
- Wallis, J.D., Anderson, K.C., and Miller, E.K. (2001). Single neurons in prefrontal cortex encode abstract rules. *Nature* *411*, 953–956.
- Wang, Y., and Goldman-Rakic, P.S. (2004). D2 receptor regulation of synaptic burst firing in prefrontal cortical pyramidal neurons. *Proc. Natl. Acad. Sci. USA* *101*, 5093–5098.
- Wang, M., Vijayraghavan, S., and Goldman-Rakic, P.S. (2004). Selective D2 receptor actions on the functional circuitry of working memory. *Science* *303*, 853–856.
- Wang, M., Yang, Y., Wang, C.-J., Gamo, N.J., Jin, L.E., Mazer, J.A., Morrison, J.H., Wang, X.-J., and Arnsten, A.F.T. (2013). NMDA receptors subserve persistent neuronal firing during working memory in dorsolateral prefrontal cortex. *Neuron* *77*, 736–749.
- Williams, G.V., and Goldman-Rakic, P.S. (1995). Modulation of memory fields by dopamine D1 receptors in prefrontal cortex. *Nature* *376*, 572–575.
- Winterer, G., and Weinberger, D.R. (2004). Genes, dopamine and cortical signal-to-noise ratio in schizophrenia. *Trends Neurosci.* *27*, 683–690.



Neuron, Volume 84

**Supplemental Information**

**Dopamine Receptors Differentially Enhance  
Rule Coding in Primate Prefrontal Cortex Neurons**

Torben Ott, Simon N. Jacob, and Andreas Nieder

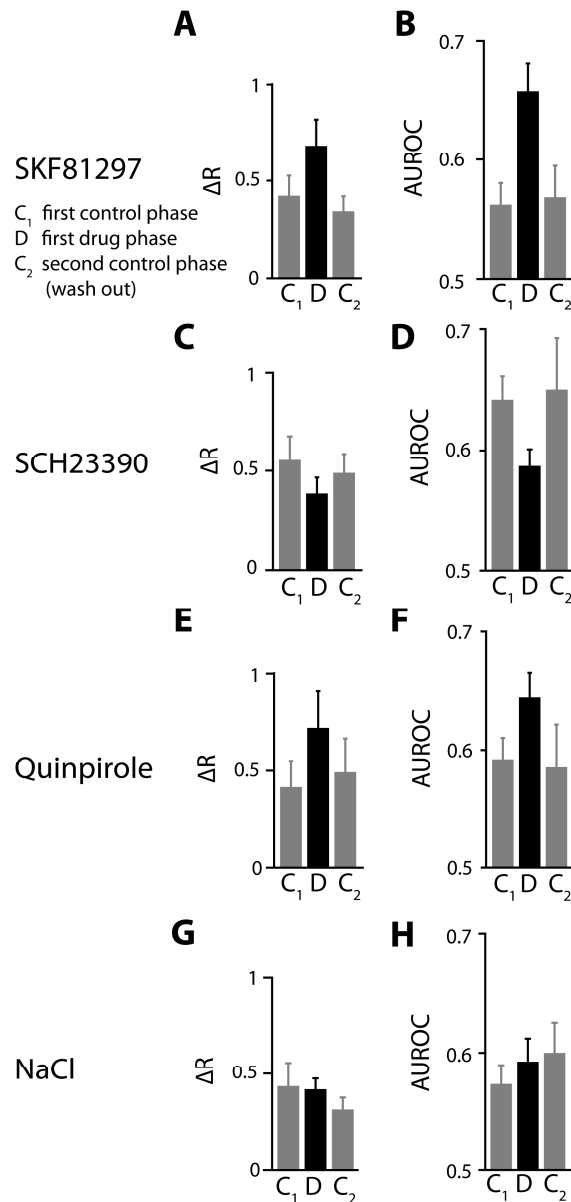


**Figure S1 (Related to Figure 2 and 3)** Drug wash-in and wash-out effects. **(A)** Difference of normalized neuronal responses between the preferred and nonpreferred rule ( $\Delta R$ ) in the first control phase of a recording session (C<sub>1</sub>), the first SKF81297 application phase (D) and the second control phase of a recording session, i.e., the wash-out phase after ending SKF81297 application (C<sub>2</sub>). SKF81297-induced increase of  $\Delta R$ s was evident in the first drug phase and disappeared in the second control phase, when drug application was discontinued, i.e., the drug effect washed out and there was no difference between the first and second control phase ( $p = 0.8$ , Wilcoxon test between the first and second control phase). **(B)** Same conventions as in (A) for AUROCs. Application of SKF81297 increased the AUROCs in the first drug phase, and the AUROCs returned to levels prior to drug application in the second control phase ( $p = 0.9$ ). **(C–F)** Same conventions as in (A–B), showing recovery of drug effects for SCH23390 ( $p = 0.9$  and  $p = 0.8$  for  $\Delta R$ s and AUROCs between control phases, respectively) and quinpirole ( $p = 0.4$  and  $p = 0.9$  for  $\Delta R$ s and AUROCs between control phases, respectively). **(G–H)** Same conventions as in (A–B), showing that control experiments using NaCl did not produce changes in  $\Delta R$  or AUROCs between control and NaCl-application phases ( $p = 0.5$  and  $p = 0.3$  for  $\Delta R$ s and AUROCs between control phases, respectively). Error bars represent SEMs.

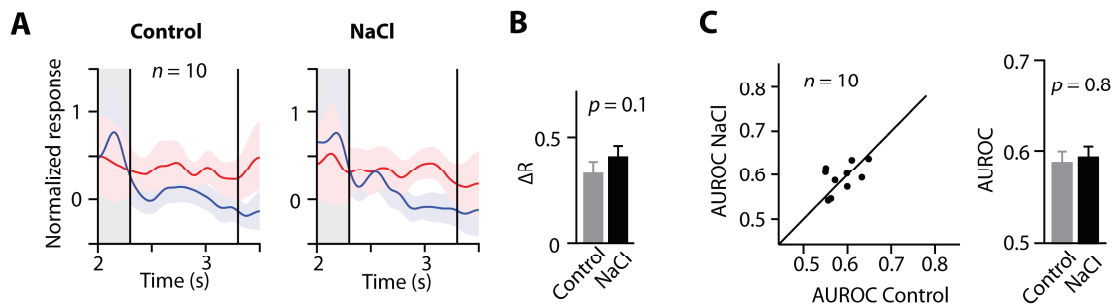


**Figure S2 (Related to Figure 2 and 3)** Physiological NaCl-solution did not produce changes in rule coding. **(A)** Normalized population response of all rule-selective neurons (determined as described above using a four-way ANOVA) recorded with NaCl for the preferred rule (*red trace*) and the nonpreferred rule (*blue trace*) during control conditions (*left panel*) and after application of NaCl (*right panel*). **(B)** Mean difference of normalized responses ( $\Delta R$ ) between the preferred and the nonpreferred rule for control conditions (*grey bar*) and NaCl conditions (*black bar*).  $\Delta R$ s were not significantly affected by NaCl application (modulation of  $\Delta R = 0.081 \pm 0.035$ ,  $p = 0.1$ , Wilcoxon test). **(C)** Distribution of AUROCs in control conditions and NaCl conditions (*left panel*, each dot corresponds to one neuron). Mean AUROCs in control conditions (*right panel*, *grey bar*) and NaCl conditions (*black bar*) were not significantly different ( $\Delta \text{AUROC} = 0.0060 \pm 0.011$ ,  $p = 0.5$ ). Consequently, the effects of iontophoretic drug application on numerical rule coding reported in this study are specifically caused by the respective drugs. Error bars represent SEMs,  $n$  denotes sample size,  $p$ -values of Wilcoxon tests.

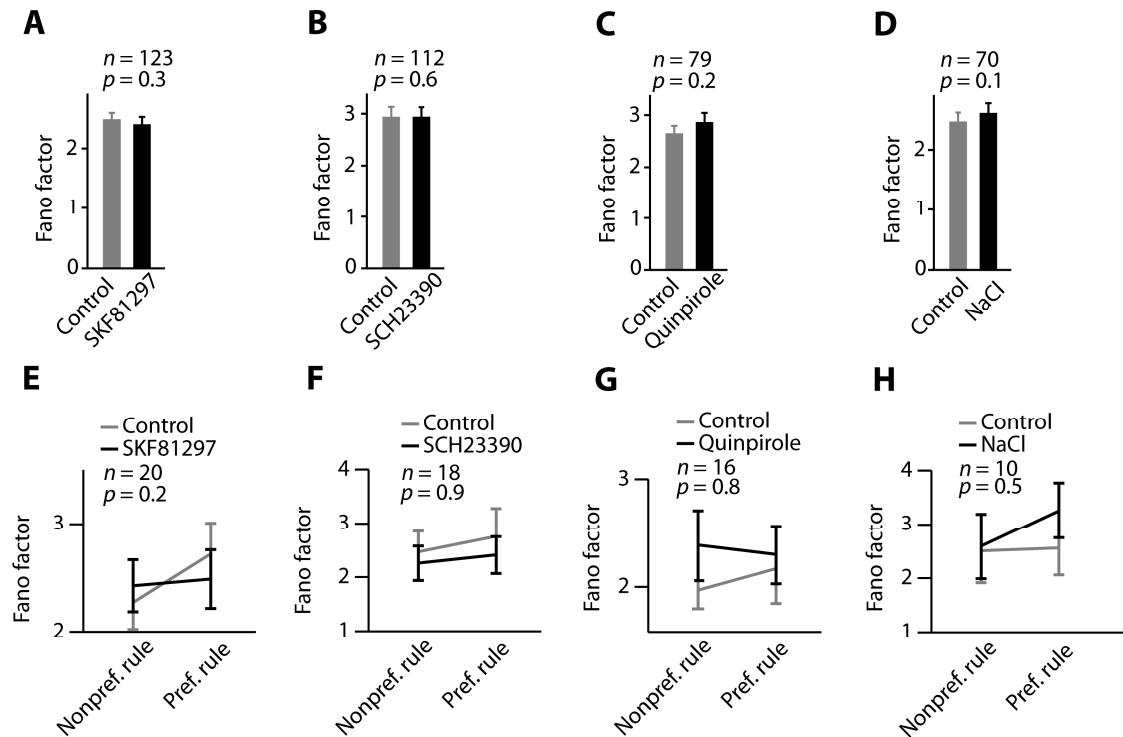


**Figure S3 (Related to Figure 4)** Dopamine receptors did not modulate Fano factors. **(A)–(D)** We calculated the Fano factor, defined as the ratio of variance of spike counts and mean of spike counts in a given analysis window, as a measure of neuronal trial-by-trial variability (Nawrot et al., 2008). Fano factors in baseline period (500 ms fixation period preceding sample presentation) during control and drug conditions were not significantly different ( $p > 0.1$  for all comparisons, Wilcoxon test). **(E)–(H)** Fano factors of rule-selective neurons during the delay 2 period (same analysis windows as for the analysis of rule-selectivity), separated for preferred and nonpreferred rule presentation, were not significantly different between control and drug conditions ( $p > 0.2$  for all comparisons, Wilcoxon test). Error bars represent SEMs, n denotes sample size, p-values of Wilcoxon tests.

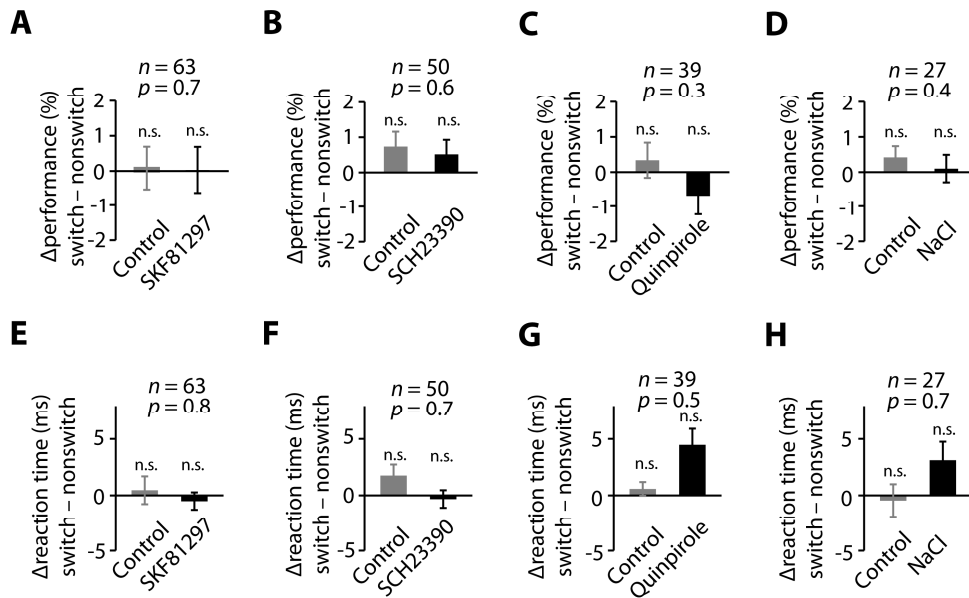


**Figure S4 (Related to Figure 7)** Absence of behavioral switch costs. **(A)–(D)** Switch costs measured by a difference in performance (% correct trials) in trials requiring monkeys to switch the rule compared to the previous trials (switch trials, i.e. in “greater than” trials succeeding “less than” trials and vice versa) and in trials in which monkeys applied the same rule as in the previous trial (nonswitch trials, i.e. in “greater than” trials succeeding “greater than” trials, the same for “less than” trials). The average switch costs were determined over all recording sessions for the different drugs in control and drug conditions. Performance did not differ between switch and nonswitch trials ( $p > 0.3$  for all comparisons, Wilcoxon test comparing average performance of switch and nonswitch trials across recording sessions). Drug application did not produce changes in switch costs for either drug ( $p > 0.5$  for all drugs, Wilcoxon test comparing switch costs for control and drug conditions over recording sessions). **(E)–(H)** Switch costs measured by a difference in reaction times on switch and nonswitch trials. The switch costs were averaged over all recording sessions for the different drugs in control and drug conditions. Reaction times did not differ between switch and nonswitch trials ( $p > 0.4$  for all comparisons, Wilcoxon test comparing average reaction times in switch and nonswitch trials over recording sessions), and the difference in reaction times between switch and nonswitch trials was not modulated by either drug ( $p > 0.3$  for all drugs, Wilcoxon test comparing switch costs for control and drug conditions over recording sessions). Thus, we observed no behavioral switch costs during the rule switching task, which is typical for monkeys engaged in task-switching paradigms (Stoet and Snyder, 2009). Error bars represent SEMs, n denotes sample size, p-values of Wilcoxon tests comparing control and drug condition, n.s. non-significant Wilcoxon tests comparing switch costs against zero difference.



---

### **Study 3: Dopamine D2 receptor modulation of working memory signals**

**Ott, T., Nieder, A.** (under review). Dopamine D2 receptors enhance population dynamics in prefrontal working memory circuits.





# **Dopamine D2 receptors enhance population dynamics in primate prefrontal working memory circuits**

Torben Ott and Andreas Nieder\*

Animal Physiology, Institute of Neurobiology, Auf der Morgenstelle 28, University of Tübingen, 72076 Tübingen, Germany

\* To whom correspondence should be addressed:

E-mail: [andreas.nieder@uni-tuebingen.de](mailto:andreas.nieder@uni-tuebingen.de)

## **Abstract**

Working memory is associated with persistent activity in the prefrontal cortex (PFC). The neuromodulator dopamine, which is released by midbrain neurons projecting into the frontal lobe, influences PFC neurons and networks via the dopamine D1 (D1R) and the D2 receptor (D2R) families. Although behavioral, clinical, and computational evidence suggest an involvement of D2Rs in working memory, a neuronal explanation is missing. We report an enhancement of persistent working memory responses of PFC neurons after iontophoretically stimulating D2Rs in monkeys memorizing the number of items in a display. D2R activation improved working memory representation at the population level and increased population dynamics during the transition from visual to mnemonic representations. Computational modeling suggests that D2Rs act by modulating interneuron-to-pyramidal signaling. By increasing the network's response dynamics, D2Rs might put PFC networks in a more flexible state and enhance the neurons' working memory coding, thereby controlling dynamic cognitive control.

## **Introduction**

The persistent activation of prefrontal cortex (PFC) neurons in the absence of external stimulation is considered a neuronal correlate of working memory, which is the ability to briefly retain and manipulate information in mind (Fuster, 2008). During working memory, stimuli are processed flexibly from moment to moment depending on the behavioral context and current goals mediating cognitive control (Baddeley, 2012). Working memory, and executive control functions in general, are influenced by midbrain dopamine neurons that project to PFC. There, dopamine affects PFC neurons via the dopamine D1 receptor (D1R) and D2 receptor (D2R) families (Robbins and Arnsten, 2009).

While D1Rs have been shown to modulate working memory and other executive functions on both behavioral (Müller et al., 1998; Noudoost and Moore, 2011; Puig and Miller, 2012; Sawaguchi and Goldman-Rakic, 1991) and neuronal level (Ott et al., 2014; Puig and Miller, 2012; Vijayraghavan et al., 2007; Williams and Goldman-Rakic, 1995), the role of D2Rs has been less clear. Behaviorally, D2Rs stimulation can improve working memory performance in primates (Gibbs and D'Esposito, 2005; Von Huben et al., 2006; Mehta et al., 2001) and D2Rs are involved in cognitive flexibility and attention (Floresco and Magyar, 2006; Noudoost and Moore, 2011; Puig and Miller, 2015; Stelzel et al., 2013). Clinical evidence suggests a prominent role of D2Rs in psychiatric diseases characterized by disturbed executive control and psychosis (Rolls et al., 2008; Winterer and Weinberger, 2004). Supported by computational modeling studies, D2Rs were hypothesized to increase cognitive flexibility by putting PFC working memory networks in a flexible state (Durstewitz

and Seamans, 2008; Rolls et al., 2008) enabling dynamic cognitive control (Cools, 2015; Stokes et al., 2013).

Despite this evidence, a neuronal correlate of D2R influence on working memory signals is lacking. In a previous single-cell study in monkeys required to memorize the location of saccade targets, D2R manipulation had a strong impact on eye movement-related discharges, but no effect on the preceding persistent spatial working memory signal (Wang et al., 2004a). So far, the underlying physiological basis for D2Rs modulation of working memory is still unknown.

We hypothesized that D2Rs modulate persistent working memory activity in PFC neurons and networks. Therefore, we trained two macaque monkeys to remember visual items that represented different numerosities, thus involving feature-based working memory processing as opposed to spatial working memory (Jacob and Nieder, 2014; Nieder, 2002; Viswanathan and Nieder, 2013). By combining single unit recordings with iontophoretic drug application and computational modeling, we show that D2R stimulation indeed increases working memory coding at the single neuron level and enhances the response dynamics of prefrontal networks.

## Results

We trained monkeys to memorize the number of items over a brief delay period ('memory delay' in **Figure 1A**) in a delayed response task (Bongard and Nieder, 2010; Ott et al., 2014). The monkeys had to assess the number of dots shown on a sample display, and maintain this sample numerosity in working memory during the delay period. Next, a rule cue was presented that instructed the monkeys to respond to a subsequent test display showing either more or less dots than the sample display. Thus, the delay phase after sample presentation constituted a pure working memory period (devoid of motor preparation) which allowed for investigation of neuronal working memory processes.

While the monkeys performed this task with varying numerosities and rules proficiently (**Figure 1B,C**), we recorded 310 randomly selected single neurons from the lateral PFC of two macaque monkeys (**Figure 1D**). To directly assess the impact of dopamine receptor targeting agents on neuronal working memory activity, each neuron was recorded both without drug application (*control condition*) and while stimulating dopamine receptor agents at the vicinity of the recorded neurons using micro-iontophoresis (*drug condition*) (Jacob et al., 2013; Thiele et al., 2006). Control conditions alternated with drug conditions in each recording session. In each session we tested one of three different substances that selectively targeted the D2R or the D1R: The D2R was assessed in 76 neurons by applying the D2R agonist quinpirole. The D1R was tested in 82 neurons using the D1R-agonist SKF81297, and in 85 neurons using the D1R-antagonist SCH23390. To verify drug-specific effects, 67 neurons were recorded using normal saline. In general, D2R stimulation

slightly increased the neuron's spiking activity, while D1R stimulation slightly decreased neuronal activity (Ott et al., 2014).

We identified single units selectively encoding the sample numerosities during the memory delay (delay 1; see **Figure 1A**) using a 2-way-ANOVA with main factors sample numerosity ("2", "8", "32") and drug condition (control, pharmacological application). Many neurons were tuned to one of the presented numerosities in the delay period (Jacob and Nieder, 2014; Nieder, 2002). A representative delay-selective unit (**Figure 2A**) showed characteristic tuning for one of the sample numerosities, i.e. a higher discharge rate for their preferred numerosity ("2" in this neuron) and increasingly lower discharge rates for more distant numerosities.

After D2R stimulation with quinpirole, response differences of the same neuron to different memorized numerosities were increased, enhancing neuronal selectivity and tuning curve (**Figure 2B**). To analyze averaged responses and tuning curves of the entire population of selective neurons, we ordered each neuron's delay-selective discharges to the three presented numerosities by its respective preferred, intermediate preferred and least preferred numerosity. A comparison of the population averaged spike rates in the control (**Figure 2C**) and drug conditions (**Figure 2D**), showed enhanced differentiation of the responses to the three memorized numerosities during D2R stimulation, and a steepening of the population averaged tuning curves (**Figure 2D**).

### **D2R stimulation enhanced working memory coding at the single neuron level**

To quantify the neuronal delay selectivity across time, we defined a sliding tuning index (TI) (**Figure 3A**) (see **Experimental Procedures**). The TI was significantly

enhanced by D2R stimulation (**Figure 3D**) (TI = +0.11 mean  $\pm$ 0.04 SEM,  $p = 0.01$ , signed rank test). As a measure of effect size, we derived the percentage of explained variance (PEV,  $\omega^2$ ) by the variable 'numerosity' across time for all selective neurons, calculated using a sliding ANOVA (**Figure 3B**) (see **Experimental Procedures**). The PEV also increased after D2R stimulation (**Figure 3E**) ( $\Delta$ PEV = +0.06 $\pm$ 0.02,  $p = 0.01$ , signed rank test). To quantify coding quality, we compared discharge rates of the neuron's preferred and least preferred sample numerosity by calculating the area under the receiver operating characteristic (AUROC) across time (**Figure 3C**). D2R stimulation significantly increased AUROCs in the delay period ( $\Delta$ AUROC = +0.11 $\pm$ 0.03,  $p = 0.003$ , signed rank test), indicating an enhancement of the neurons' working memory coding capacities (**Figure 3F**). This enhancement was observed for all comparisons between the most, intermediate and least preferred numerosity (**Figure S1**). The same significant effects were observed when analyzing all (delay-selective or not) neurons recorded with the D2R agonist ( $n = 76$ ) (**Figure S2**).

The identical comparisons of working memory responses were performed with pharmacological D1R stimulation or blockage, respectively. However, we found no differences in coding capacities when applying the D1R-agonist SKF81297 (**Figure S3A-H**) or the D1R-antagonist SCH23390 (**Figure S4A-H**). The effect of pharmacological manipulation was confirmed through application of saline (NaCl) which did not result in any coding changes (**Figure S5A-H**). Thus, D2R stimulation, but not D1R stimulation, improves memory-delay selectivity for quantities at the single neuron level.

## **D2R stimulation enhanced working memory coding at the population level**

To describe numerosity representation at the population level, we used linear regression disentangling general drug-induced shifts of neuronal activity from neuronal activity explained by numerosity (Mante et al., 2013). By modeling interactions between drug and sample numerosity, we defined numerosity-related axes for control and drug conditions and projected the population response of all 76 neurons tested with the D2R-agonist onto these axes. This provided an estimate of the numerosity representation during working memory at the population level for control and drug conditions (see **Experimental Procedures**).

Relative to the control condition (**Figure 4A**), D2R stimulation prominently increased numerosity representation by the neuronal population during the entire delay period (**Figure 4B**). We quantified the selectivity between numerosities responses by calculating the distance between state trajectories (in **Figure 4A** and **B**) for all sample combinations. Compared to control conditions (**Figure 4C**), stimulation of D2Rs enhanced discrimination between numerosities in the delay period (**Figure 4D**). Average trajectory differences increased after D2R stimulation (**Figure 4E**) (change in mean  $\Delta$ trajectory =  $+1.1 \pm 0.19$ ,  $p = 0.001$ , bootstrapping). Moreover, the regression weights for the task variable 'numerosity' were increased by D2R stimulation, as witnessed by a positive interaction term (**Figure 4F**, mean interaction term =  $+0.021 \pm 0.006$ ,  $p = 0.003$ , signed rank test). We confirmed the results of the regression analysis by using shuffled data and cross-validation (**Figure S6**). To confirm that overall drug-induced shifts in spiking activity cannot explain the results, we simulated data applying the same strength of numerosity coding and the same amount of drug-induced shifts in overall spiking activity



(**Figure S6**). These controls verified that general changes in network activity did not drive specific D2R modulation of working memory.

Again, we found no significant differences in population analyses for neurons tested with the D1R-agonist (**Figure S3I-J**) or D1R-antagonist (**Figure S4I-J**). Application of saline (NaCl) did not produce any effects (**Figure S5I-J**). Thus, D2R-stimulation enhanced the neuronal population's representation of numerosities in the memory delay period.

### **Dopamine receptors modulated the PFC network's response dynamics**

To assess neuronal population's response dynamics, we analyzed population responses of all recorded 76 neurons tested for D2R-effects by representing the population single-unit activity in a low-dimensional space using principal component analysis (PCA, see **Experimental Procedures**), extracting shared activity patterns prominent in the population response (Harvey et al., 2012). Population activity represented by the first three principal components (PCs) showed prominent shifts in population activity after sample onset and at the beginning of the memory delay period as a function of numerosities (**Figure 5A**). After stimulating D2Rs with quinpirole, population activity followed similar trajectories, but showed improved differentiation between different numerosities (**Figure 5B**). Discrimination between numerosity representations, quantified by the Euclidean distance between population trajectories for all numerosity combinations (**Figure 5C**, see **Experimental Procedures**), was increased by D2R stimulation in the delay period (**Figure 5D**). The mean differences between the

trajectories were significantly higher during D2R-stimulation (**Figure 5E**) (change in mean  $\Delta$ trajectory =  $+0.37 \pm 0.18$ ,  $p = 0.02$ , bootstrapping).

To evaluate population dynamics further, we quantified the speed with which the population trajectories traveled through state space by calculating the average rate of change of state space trajectories (Stokes et al., 2013) (see **Experimental Procedures**). Delay-period onset (and sample onset) induced a rapid acceleration of the population trajectories (**Figure 5F**). The distances traveled by the trajectories were greater after D2R stimulation (**Figure 5F**, bottom inset, change in traveled distance =  $+2.1 \pm 1.3$ ,  $p = 0.04$ , bootstrapping). Velocity decreased during the delay period, indicating a more stable state during working memory (**Figure 5F**, top inset). Thus, D2R stimulation enhanced velocity particularly during the dynamic (i.e. transition) periods of the population activity. As above, we verified PCA analysis by using shuffled data, cross-validation, and simulated data (**Figure S7**). Thus, D2R stimulation increased the neuronal population's response dynamics, enhancing the trajectories' separability in state space.

Interestingly, D1R stimulation (**Figure 6A-B**), but not D1R blockage (**Figure 6C-D**), significantly decreased the population's velocity in state space (change in velocity =  $-2.4 \pm 1.2$ ,  $p = 0.02$ , change in traveled distance =  $-2.4 \pm 1.3$ ,  $p = 0.004$ , bootstrapping, control analyses in **Figure S8**). Application of saline (NaCl) did not produce any effects (**Figure S5K-L**). Thus, D1Rs and D2Rs showed opposite effects on coding stability during transition stages.

### **Computational modeling suggests specific mechanism for D2R modulation**

We enacted a biophysically plausible network attractor model of object working memory (Brunel and Wang, 2001; Goodman and Brette, 2009; Wang, 2002) to investigate possible mechanisms of D2R actions. The model consisted of pyramidal cells and interneurons with recurrent excitatory and recurrent inhibitory connections (**Figure 7A**). These cell types generate attractor networks with stable spontaneous activity states and stable persistent (reverberatory) activity states (**Figure 7B**) modeling information held in working memory (see **Experimental Procedures**). Connections were modeled by excitatory pyramidal-to-pyramidal and pyramidal-to-interneuron AMPA and NMDA glutamatergic synapses, as well as inhibitory interneuron-to-interneuron and interneuron-to-pyramidal GABAergic synapses.

When transiently stimulating one of three selective subsets of pyramidal cells, corresponding to neurons selective for one of the three numerosities, the pyramidal cell population switched from a spontaneous activity state to a stable persistent activity state without further stimulation (**Figure 7B**). *In vitro* studies using prefrontal slices suggest that D2R stimulation decreases responsiveness to GABA in pyramidal cells (Seamans et al., 2001; Trantham-Davidson et al., 2004). We thus studied effects of decreasing the GABA conductance in interneuron-to-pyramidal synapses, which lead to an overall increase in spiking activity that impaired the network's stable spontaneous activity state under only slight decreases of GABA conductances (**Figure 7C**).

D2R stimulation has been shown to modulate interneuron excitability (Zhong and Yan, 2014). We implemented this effect by increasing AMPA conductances in interneurons, leading to an increase in inhibition and to a breakdown of the

network's persistent activity state (**Figure 7D**). However, by combining both modulations, disinhibition of pyramidal cells by decreasing GABA conductances was balanced by increasing AMPA conductances in interneurons, i.e. increasing interneuron excitability. Both spontaneous and persistent activity states remained stable over a larger range (**Figure 7E**). The network showed a small increase in spontaneous activity in addition to a prominent increase of persistent activity, increasing the neurons' selectivity to a sample stimulus during the delay memory period, reproducing our key experimental results.

## **Discussion**

We show that stimulation of prefrontal D2Rs enhanced working memory representations of numerosities both on single neuron and on population levels. D2Rs changed the flexibility of neuronal population activity by increasing the population's response dynamics. By using a computational model of prefrontal networks, we suggest a mechanism by which D2Rs control prefrontal working memory networks.

### **D2R improves feature-based working memory representations**

These results provide a neuronal basis for D2R modulation of working memory in primates and complement reported behavioral effects of D2R manipulation. D2R stimulation has been shown to influence working memory performance in monkeys and humans by increasing or decreasing performance (Arnsten et al., 1995; Gibbs and D'Esposito, 2005; Von Huben et al., 2006; Mehta et al., 2001), depending on the subject's baseline performance (Clark and Noudoost, 2014). In addition, D2Rs play a role in mediating cognitive flexibility (Klanker et al., 2013). Blocking D2Rs impairs the ability of rats to switch between different response strategies (Floresco et al., 2006). In monkeys, blocking prefrontal D2Rs impairs learning of new association rules and reduces neural selectivity for the learned saccade direction (Puig and Miller, 2015), while stimulating D2Rs increased neural selectivity for task rules in the same numerical switching task (Ott et al., 2014).

Despite this behavioral impact, a neuronal correlate of D2R modulation of working memory was lacking so far. In monkeys performing a oculomotor delayed-

response (ODR) task to test spatial working memory, D2Rs did not modulate persistent delay activity (Wang et al., 2004a). However, because the ODR task allows for saccadic motor preparation, many neurons might reflect response-related signals rather than pure working memory representations during the delay (Markowitz et al., 2015; Takeda and Funahashi, 2004). Here, we excluded motor preparation during the delay by forcing the monkeys to make a response-independent and rule-cued decision. Persistent activity in the delay phase thus reflects feature-based working memory representations devoid of motor preparation. In this situation, we find that D2R stimulation robustly enhanced persistent mnemonic activity in PFC neurons, thus resolving the discrepancy between behavioral and neuronal effects. It is also conceivable that feature-based working memory and spatial working memory are distinctly represented by PFC neurons (Wilson et al., 1993).

In contrast to the clear D2R effects, D1R manipulation did not seem to modulate persistent working memory activity in the current study. This was unexpected, given that several studies reported D1R modulation of spatial working memory signals (Vijayraghavan et al., 2007; Williams and Goldman-Rakic, 1995) or D1R modulation of persistent rule-related signals in the same task as used in the present study (Ott et al., 2014). A possible explanation for this discrepancy might be related to the prominent dose-dependency of D1R effects. Reported D1R manipulations followed an inverted-U function and produced varying effects, including an improvement of spatial working memory signals by both stimulating and blocking D1Rs (Vijayraghavan et al., 2007; Williams and Goldman-Rakic, 1995). Thus, effects observed after D1R manipulation seem to heavily depend on the baseline activation of D1Rs. This D1R response function might account for the

differences between our and other studies. Alternatively, or in addition, D1R modulation might differentially modulate spatial (Vijayraghavan et al., 2007; Williams and Goldman-Rakic, 1995) and feature-based (our study) working memory.

### **Putative D2R mechanism involves differential modulation of interneurons and pyramidal cells**

We implemented a biophysically plausible spiking neural network in which synaptic connections are described on a single neuron level. By simulating recurrent excitatory and inhibitory connections, the activity of neurons in the network show characteristic stable attractor states. This approach was successfully used previously to describe working memory and decision-making processes (Constantinidis and Wang, 2004; Durstewitz et al., 2000a; Wang, 2002). Using this model, we propose a mechanism by which D2Rs might act on synaptic transmission to modulate working memory representations. We propose that D2Rs decrease GABAergic synaptic currents in pyramidal cells, thus disinhibiting pyramidal cell firing. In addition, D2R stimulation increases AMPA synaptic currents in interneurons, thereby increasing interneuron excitability. This modulation increased the differentiation between persistent activity and spontaneous activity in the network model, thus enhancing working memory selectivity.

Our model suggests that D2Rs might change interneuron-to-pyramidal signaling by reducing inhibitory postsynaptic currents (IPSCs) mediated by GABA receptors in pyramidal cells (Seamans et al., 2001). Decreased IPSCs disinhibit pyramidal cell

firing and thereby increase the neurons' persistent activity. This disinhibition of pyramidal cells might be balanced by an increase in interneuron excitability (Zhong and Yan, 2014). We constrained possible synaptic modulation by investigating putative D2R targets supported by *in vitro* studies (Seamans et al., 2001; Trantham-Davidson et al., 2004; Zhong and Yan, 2014), although we acknowledge diverse D2R effects found *in vitro* (Seamans and Yang, 2004). The proposed mechanism accounts for two key experimental results of the current study. First, D2R stimulation increased neuronal activity of prefrontal neurons (Ott et al., 2014), which has also been reported by previous studies (Wang and Goldman-Rakic, 2004; Wang et al., 2004a). Second, D2R stimulation increased selectivity of working memory representations. Our findings argue for a strong role of interneurons in maintaining working memory representations. This suggested role of inhibition is supported by *in vivo* recordings showing that cortical inhibition mediated by GABA receptors are crucial for shaping working memory representations (Constantinidis et al., 2002; Rao et al., 2000). This is physiologically plausible since D2Rs are abundantly expressed in PFC interneurons, particularly in parvalbumin-positive interneurons (de Almeida and Mengod, 2010), which have been shown to modulate response gain in rodent cortex (Wilson et al., 2012).

The proposed mechanism assumes that D2Rs influence interneurons and pyramidal cells differentially. This assumption is supported by studies that showed a differential impact of dopamine on pyramidal cells and interneurons (Gao and Goldman-Rakic, 2003). Dopamine excites putative pyramidal cells, whereas it both excites and inhibits putative interneurons (Jacob et al., 2013). Thus,



differential modulation of cortical cell types might be a key mechanism by which dopamine controls cortical networks.

More detailed models might incorporate different types of structured interneuron connections (Wang et al., 2004b) that account for differential roles of cortical interneuron classes in inhibitory control of pyramidal neurons (Lee et al., 2014; Pi et al., 2013) and help to distinguish D2R actions between cortical cell types. Importantly, however, the spiking neural network model provides hypotheses about micro-circuit mechanisms that can now be tested empirically (Wang et al., 2013). Specifically, we hypothesize that experimentally manipulating GABA currents in prefrontal networks might modulate the persistent activity of neurons similarly as observed in the model.

Our results complement studies investigating possible mechanisms of D1Rs (Durstewitz and Seamans, 2008). It has been proposed that D1Rs modulate the network's persistent activity by changing recurrent NMDA conductances (Brunel and Wang, 2001; Durstewitz et al., 2000b), which increases persistent delay activity of single neurons in the model. This result reproduces experimental studies reporting an enhancement of selective response in the delay period of single neurons after D1R stimulation (Ott et al., 2014; Vijayraghavan et al., 2007). Thus, D2Rs and D1Rs might act on prefrontal networks by distinct physiological mechanisms (Ott et al., 2014).

## **Dopamine receptors modulate network dynamics**

Because neuronal responses show high complexity and variability at the single neuron level (Rigotti et al., 2013), we explored whether computations in PFC might emerge from the dynamics of populations of neurons (Mante et al., 2013). We described neuronal responses in the framework of dynamical systems in which the activity of neuronal population can be described as a dynamical process revealing shared activity patterns that are prominent in the population response (Cunningham and Yu, 2014). This allowed us to study dopamine receptor modulation of PFC network properties. D2R activation increased working memory representations of numerosities at the population level independently of general shifts in neuronal activity, suggesting that D2Rs interact with mechanisms generating persistent working memory activity. This working memory representation can be realized through sequence-based circuit dynamics not captured by single neuron analyses but by our state space analysis (Harvey et al., 2012). State space analysis revealed how neuromodulation can change the dynamic properties of neuronal populations. D2R stimulation increased the state space distance between trajectories during working memory. As a consequence, the neuronal system can differentiate more reliably between working memory representations of numerosities.

At the onset of visual stimulation with numerosities as well as during the transition from visual to mnemonic processing during the delay, population responses were characterized by high dynamic phases. These instances of high network dynamics were followed by a more stable phase during working memory. This characteristic response dynamic was similarly observed during flexible decision-making (Stokes et al., 2013). D2R stimulation enhanced the dynamic

responses of PFC populations, thereby enhancing state flexibility in PFC networks. In contrast, D1R stimulation decreased population dynamics, thereby maintaining PFC networks in a more stable state.

These results support computational models which suggest that dopaminergic modulation of prefrontal working memory networks balance stability and flexibility of working memory representations (Durstewitz and Seamans, 2008; Rolls et al., 2008; Seamans and Yang, 2004; Seamans et al., 2001). According to this hypothesis, a D1R-dominated state stabilizes prefrontal representations, whereas a D2R-dominated state destabilizes them enabling switching between different representations thus mediating flexibility. Our results provide experimental evidence that D2Rs control stability and flexibility of prefrontal working memory representations. These results contribute to the idea that excessive cortical D2R activation contributes to psychosis by destabilizing working memory representations in schizophrenic patients (Rolls et al., 2008; Winterer and Weinberger, 2004). Thus, excessive D2R activation might attribute aberrant salience to external events or internal representations, leading to symptoms of psychosis such as sensory hallucinations and intrusions of thought (Kapur, 2003). In conclusion, prefrontal dopamine receptors might mediate dynamic cognitive control (Cools, 2015) by balancing the stability of persistent activity during working memory with the flexibility of prefrontal networks needed for adaptive, goal-directed behavior.

## References

- De Almeida, J., and Mengod, G. (2010). D2 and D4 dopamine receptor mRNA distribution in pyramidal neurons and GABAergic subpopulations in monkey prefrontal cortex: implications for schizophrenia treatment. *Neuroscience* 170, 1133–1139.
- Arnsten, A.F., Cai, J.X., Steere, J.C., and Goldman-Rakic, P.S. (1995). Dopamine D2 receptor mechanisms contribute to age-related cognitive decline: the effects of quinpirole on memory and motor performance in monkeys. *J. Neurosci.* 15, 3429–3439.
- Baddeley, A. (2012). Working Memory: Theories, Models, and Controversies. *Annu. Rev. Psychol.* 63, 1–29.
- Bongard, S., and Nieder, A. (2010). Basic mathematical rules are encoded by primate prefrontal cortex neurons. *Proc. Natl. Acad. Sci. U. S. A.* 107, 2277–2282.
- Brunel, N., and Wang, X.J. (2001). Effects of neuromodulation in a cortical network model of object working memory dominated by recurrent inhibition. *J. Comput. Neurosci.* 11, 63–85.
- Clark, K.L., and Noudoost, B. (2014). The role of prefrontal catecholamines in attention and working memory. *Front. Neural Circuits* 8, 33.
- Constantinidis, C., and Wang, X.-J. (2004). A neural circuit basis for spatial working memory. *Neuroscientist* 10, 553–565.
- Constantinidis, C., Williams, G. V, and Goldman-Rakic, P.S. (2002). A role for inhibition in shaping the temporal flow of information in prefrontal cortex. *Nat. Neurosci.* 5, 175–180.
- Cools, R. (2015). The cost of dopamine for dynamic cognitive control. *Curr. Opin. Behav. Sci.* 4, 1–8.
- Cunningham, J.P., and Yu, B.M. (2014). Dimensionality reduction for large-scale neural recordings. *Nat. Neurosci.* 17, 1500–1509.
- Durstewitz, D., and Seamans, J.K. (2008). The dual-state theory of prefrontal cortex dopamine function with relevance to catechol-o-methyltransferase genotypes and schizophrenia. *Biol. Psychiatry* 64, 739–749.
- Durstewitz, D., Seamans, J.K., and Sejnowski, T.J. (2000a). Neurocomputational models of working memory. *Nat. Neurosci.* 3 *Suppl*, 1184–1191.
- Durstewitz, D., Seamans, J.K., and Sejnowski, T.J. (2000b). Dopamine-mediated stabilization of delay-period activity in a network model of prefrontal cortex. *J. Neurophysiol.* 83, 1733–1750.

- Floresco, S.B., and Magyar, O. (2006). Mesocortical dopamine modulation of executive functions: beyond working memory. *Psychopharmacol.* *188*, 567–585.
- Floresco, S.B., Magyar, O., Ghods-Sharifi, S., Vexelman, C., and Tse, M.T.L. (2006). Multiple dopamine receptor subtypes in the medial prefrontal cortex of the rat regulate set-shifting. *Neuropsychopharmacology* *31*, 297–309.
- Fuster, J. (2008). *The Prefrontal Cortex, Fourth Edition* (London: Academic Press).
- Gao, W.-J., and Goldman-Rakic, P.S. (2003). Selective modulation of excitatory and inhibitory microcircuits by dopamine. *Proc. Natl. Acad. Sci. U.S.A.* *100*, 2836–2841.
- Gibbs, S.E.B., and D’Esposito, M. (2005). Individual capacity differences predict working memory performance and prefrontal activity following dopamine receptor stimulation. *Cogn. Affect. Behav. Neurosci.* *5*, 212–221.
- Goodman, D.F.M., and Brette, R. (2009). The brain simulator. *Front. Neurosci.* *3*, 192–197.
- Harvey, C.D., Coen, P., and Tank, D.W. (2012). Choice-specific sequences in parietal cortex during a virtual-navigation decision task. *Nature* *484*, 62–68.
- Von Huben, S.N., Davis, S. a., Lay, C.C., Katner, S.N., Crean, R.D., and Taffe, M. a. (2006). Differential contributions of dopaminergic D1- and D 2-like receptors to cognitive function in rhesus monkeys. *Psychopharmacology (Berl)*. *188*, 586–596.
- Jacob, S.N., and Nieder, A. (2014). Complementary roles for primate frontal and parietal cortex in guarding working memory from distractor stimuli. *Neuron* *83*, 226–237.
- Jacob, S.N., Ott, T., and Nieder, A. (2013). Dopamine regulates two classes of primate prefrontal neurons that represent sensory signals. *J. Neurosci.* *33*, 13724–13734.
- Kapur, S. (2003). Psychosis as a state of aberrant salience: a framework linking biology, phenomenology, and pharmacology in schizophrenia. *Am. J. Psychiatry* *160*, 13–23.
- Klanker, M., Feenstra, M., and Denys, D. (2013). Dopaminergic control of cognitive flexibility in humans and animals. *Front. Neurosci.* *7*, 201.
- Lee, A., Gee, S., Vogt, D., Patel, T., Rubenstein, J., and Sohal, V. (2014). Pyramidal neurons in prefrontal cortex receive subtype-specific forms of excitation and inhibition. *Neuron* *81*, 61–68.
- Mante, V., Sussillo, D., Shenoy, K. V, and Newsome, W.T. (2013). Context-dependent computation by recurrent dynamics in prefrontal cortex. *Nature* *503*, 78–84.

- Markowitz, D.A., Curtis, C.E., and Pesaran, B. (2015). Multiple component networks support working memory in prefrontal cortex. *Proc. Natl. Acad. Sci. U. S. A.* *112*, 11084–11089.
- Mehta, M.A., Swainson, R., Ogilvie, A.D., Sahakian, B., and Robbins, T.W. (2001). Improved short-term spatial memory but impaired reversal learning following the dopamine D2 agonist bromocriptine in human volunteers. *Psychopharmacology (Berl)*. *159*, 10–20.
- Müller, U., von Cramon, D.Y., and Pollmann, S. (1998). D1- versus D2-receptor modulation of visuospatial working memory in humans. *J. Neurosci.* *18*, 2720–2728.
- Nieder, A. (2002). Representation of the quantity of visual items in the primate prefrontal cortex. *Science*. *297*, 1708–1711.
- Noudoost, B., and Moore, T. (2011). Control of visual cortical signals by prefrontal dopamine. *Nature* *474*, 372–375.
- Ott, T., Jacob, S.N., and Nieder, A. (2014). Dopamine receptors differentially enhance rule coding in primate prefrontal cortex neurons. *Neuron* *84*, 1317–1328.
- Pi, H.-J., Hangya, B., Kvitsiani, D., Sanders, J.I., Huang, Z.J., and Kepecs, A. (2013). Cortical interneurons that specialize in disinhibitory control. *Nature* *503*, 521–524.
- Puig, M.V., and Miller, E.K. (2012). The role of prefrontal dopamine D1 receptors in the neural mechanisms of associative learning. *Neuron* *74*, 874–886.
- Puig, M.V., and Miller, E.K. (2015). Neural substrates of dopamine D2 receptor modulated executive functions in the monkey prefrontal cortex. *Cereb. Cortex* *25*, 2980–2987.
- Rao, S.G., Williams, G. V, and Goldman-Rakic, P.S. (2000). Destruction and creation of spatial tuning by disinhibition: GABA(A) blockade of prefrontal cortical neurons engaged by working memory. *J. Neurosci.* *20*, 485–494.
- Rigotti, M., Barak, O., Warden, M.R., Wang, X.-J., Daw, N.D., Miller, E.K., and Fusi, S. (2013). The importance of mixed selectivity in complex cognitive tasks. *Nature* *497*, 585–590.
- Robbins, T.W., and Arnsten, a F.T. (2009). The neuropsychopharmacology of fronto-executive function: monoaminergic modulation. *Annu. Rev. Neurosci.* *32*, 267–287.
- Rolls, E.T., Loh, M., Deco, G., and Winterer, G. (2008). Computational models of schizophrenia and dopamine modulation in the prefrontal cortex. *Nat. Rev. Neurosci.* *9*, 696–709.

- Sawaguchi, T., and Goldman-Rakic, P.S. (1991). D1 dopamine receptors in prefrontal cortex: involvement in working memory. *Science* 251, 947–950.
- Seamans, J.K., and Yang, C.R. (2004). The principal features and mechanisms of dopamine modulation in the prefrontal cortex. *Prog. Neurobiol.* 74, 1–58.
- Seamans, J.K., Gorelova, N., Durstewitz, D., and Yang, C.R. (2001). Bidirectional dopamine modulation of GABAergic inhibition in prefrontal cortical pyramidal neurons. *J. Neurosci.* 21, 3628–3638.
- Stelzel, C., Fiebach, C.J., Cools, R., Tafazoli, S., and D'Esposito, M. (2013). Dissociable fronto-striatal effects of dopamine D2 receptor stimulation on cognitive versus motor flexibility. *Cortex.* 49, 2799–2811.
- Stokes, M.G., Kusunoki, M., Sigala, N., Nili, H., Gaffan, D., and Duncan, J. (2013). Dynamic coding for cognitive control in prefrontal cortex. *Neuron* 78, 364–375.
- Takeda, K., and Funahashi, S. (2004). Population vector analysis of primate prefrontal activity during spatial working memory. *Cereb. Cortex* 14, 1328–1339.
- Thiele, A., Delicato, L.S., Roberts, M.J., and Gieselmann, M. a (2006). A novel electrode-pipette design for simultaneous recording of extracellular spikes and iontophoretic drug application in awake behaving monkeys. *J. Neurosci. Methods* 158, 207–211.
- Tranaham-Davidson, H., Neely, L.C., Lavin, A., and Seamans, J.K. (2004). Mechanisms underlying differential D1 versus D2 dopamine receptor regulation of inhibition in prefrontal cortex. *J. Neurosci.* 24, 10652–10659.
- Vijayraghavan, S., Wang, M., Birnbaum, S.G., Williams, G. V, and Arnsten, A.F.T. (2007). Inverted-U dopamine D1 receptor actions on prefrontal neurons engaged in working memory. *Nat. Neurosci.* 10, 376–384.
- Viswanathan, P., and Nieder, A. (2013). Neuronal correlates of a visual “sense of number” in primate parietal and prefrontal cortices. *Proc. Natl. Acad. Sci. U. S. A.* 110, 11187–11192.
- Wang, X.-J. (2002). Probabilistic decision making by slow reverberation in cortical circuits. *Neuron* 36, 955–968.
- Wang, Y., and Goldman-Rakic, P.S. (2004). D2 receptor regulation of synaptic burst firing in prefrontal cortical pyramidal neurons. *Proc. Natl. Acad. Sci. U. S. A.* 101, 5093–5098.
- Wang, M., Vijayraghavan, S., and Goldman-Rakic, P.S. (2004a). Selective D2 receptor actions on the functional circuitry of working memory. *Science* 303, 853–856.

- Wang, M., Yang, Y., Wang, C.-J., Gamo, N.J., Jin, L.E., Mazer, J. a, Morrison, J.H., Wang, X.-J., and Arnsten, A.F.T. (2013). NMDA receptors subserve persistent neuronal firing during working memory in dorsolateral prefrontal cortex. *Neuron* 77, 736–749.
- Wang, X.-J., Tegnér, J., Constantinidis, C., and Goldman-Rakic, P.S. (2004b). Division of labor among distinct subtypes of inhibitory neurons in a cortical microcircuit of working memory. *Proc. Natl. Acad. Sci. U. S. A.* 101, 1368–1373.
- Williams, G. V, and Goldman-Rakic, P.S. (1995). Modulation of memory fields by dopamine D1 receptors in prefrontal cortex. *Nature* 376, 572–575.
- Wilson, F. a, Scaldidhe, S.P., and Goldman-Rakic, P.S. (1993). Dissociation of object and spatial processing domains in primate prefrontal cortex. *Science* 260, 1955–1958.
- Wilson, N.R., Runyan, C.A., Wang, F.L., and Sur, M. (2012). Division and subtraction by distinct cortical inhibitory networks in vivo. *Nature* 488, 343–348.
- Winterer, G., and Weinberger, D.R. (2004). Genes, dopamine and cortical signal-to-noise ratio in schizophrenia. *Trends Neurosci.* 27, 683–690.
- Zhong, P., and Yan, Z. (2014). Distinct physiological effects of dopamine D4 receptors on prefrontal cortical pyramidal neurons and fast-spiking interneurons. *Cereb. Cortex* first published online August 21, 2014 doi:10.1093/cercor/bhu190.

### **Acknowledgments**

This work was supported by grants from the German Research Foundation (DFG) to A.N. (NI 618/5-1).

### **Author contributions**

T.O. designed and performed experiments, analyzed data and wrote the paper.  
A.N. designed experiments and wrote the paper.



## Figure legends

### Figure 1. Memory-guided decision-making task and behavioral performance

(A) Memory-guided decision-making task. Monkeys grabbed a bar and fixated a central fixation spot throughout the trial. They had to remember a sample numerosity (number of dots) during the memory delay period (delay 1). After presentation of a rule cue indicating either the “greater than”- or “less than”-rule, the monkeys were required to respond (by releasing the bar) to test-displays showing more or fewer dots, respectively, than the sample numerosity to receive a reward.

(B) Behavioral performance (% correct) for monkey E (*left panels*) and monkey O (*right panels*) for the range of sample numerosities (“2”, “8”, and “32”) as well as for standard and control stimuli.

(C) Example sample stimuli. For each session, new random dot patterns were created, using different patterns for all sample-test combinations.

(D) Recording site located in the right lateral PFC for both monkeys.

### Figure 2. D2R modulation of working memory-selective neurons

(A) Dot-raster histogram (*top*; each dot represents an action potential; colors indicate the three numerosities) and spike-density histograms (*bottom*) of an example neuron. The neuron was tuned to numerosity “2”, with lower activity for more distant numerosities (inset tuning curve in delay 1 period).

(B) After D2R stimulation, the same neuron as in (A) showed enhanced and more selective tuning (layout as in (A)).

(C) Time course of average normalized response of all numerosity-selective delay neurons; trials grouped according to the neurons’ preferred numerosity (inset tuning curve in delay 1 period).

(D) Same neurons as in (C), after D2R stimulation. Population responses were enhanced and tuning was steeper (layout as in (C)).

### Figure 3. D2R stimulation enhanced numerosity coding during working memory at single neuron level

(A) Time-dependent TIs for control (*black*) and drug (*red*) conditions from fixation onset to the end of the delay 1 period.

(B) Time course of PEV ( $\omega^2$ ) (layout as in (A)).

(C) Time course of AUROCs (layout as in (A)).

(D) TIs during the delay period for quinpirole application plotted against TIs in control conditions; each dot corresponds to one single unit, inset shows mean over neurons.

(E) PEV ( $\omega^2$ ) during quinpirole application plotted against PEV in control conditions (layout as in (D)).

(F) AUROCs during quinpirole application plotted against AUROCs in control conditions (layout as in (D)). Gray windows in (A–H) denote analysis window in the delay 1 period. Error bars and colored shaded areas represent standard errors of the mean (SEMs). \*  $p < 0.05$ , \*\*  $p < 0.01$  (signed rank test).

**Figure 4. D2R stimulation enhanced numerosity coding during working memory at population level.**

(A) Population responses projected on the numerosity axes for control conditions. Trajectories represent the time-dependent numerosity evidence control conditions for different numerosities represented by the neuronal population.

(B) Time-dependent numerosity evidence for the same population of neurons under quinpirole (layout as in (A)).

(C) Absolute differences between all pair-wise sample trajectory combinations (see (A)) in control conditions.

(D) Absolute differences between all pair-wise sample trajectory combinations under quinpirole (layout as in (C)).

(E) Mean trajectory difference (i.e., mean of curves in (C and D)) for control conditions (*black*) and drug conditions (*red*). D2R stimulation significantly enhanced mean trajectory difference in the delay 1 period (inset).

(F) Population average regression weights for the factor numerosity in the linear regression model for control and drug conditions (interaction term for sample and drug is either subtracted or added, respectively, see **Experimental Procedures**). Gray shaded areas denote analysis window, error bars represent SEMs (estimated by bootstrapping). \*\*\*  $p < 0.001$ , \*\*  $p < 0.01$  (bootstrapping in (E) and signed rank test in (F)).

**Figure 5. D2R stimulation enhanced response dynamics of prefrontal populations.**

(A) The activity of all recorded neurons ( $n = 76$ ) recorded with D2R stimulation represented in state space by the first three PCs for control conditions.

(B) Same neurons as in (A) represented in state space during quinpirole application

(layout as in A).

(C) Euclidean distance between all pair-wise trajectories (see (A)) for control conditions.

(D) Euclidean distance between all pair-wise trajectories (see (B)) during quinpirole application (layout as in (C)).

(E) Mean trajectory distance (i.e., mean of curves in (C and D)) for control (*black*) and drug (*red*) conditions. D2R stimulation significantly increased trajectory distance in the delay 1 period (inset).

(F) Mean trajectories' velocity, i.e. the rate of change of positions in state space over time, for control (*black*) and drug (*red*) conditions. D2R stimulation increased the population's mean velocity in state space at the beginning of the delay period after sample offset (top inset) as well as the distance travelled by the trajectories through state space (bottom inset). Numbers indicate trial events, 1: fixation onset, 2: sample onset: 3: delay 1 start, 4: delay 1 end (rule cue onset). Gray shaded areas denote analysis windows, error bars represent SEMs (estimated by bootstrapping). \*\*  $p < 0.01$ , \*  $p < 0.05$  (bootstrapping).

### **Figure 6. D1R stimulation decreased response dynamics of prefrontal populations.**

(A) PCA analysis for SKF91297. Same conventions as in Figure 5E for D1R stimulation.

(B) Same conventions as Figure 5F for SKF81297.

(C) PCA analysis for SCH23390. Same conventions as in Figure 5E for blocking D1Rs.

(D) Same conventions as Figure 5F for SCH23390. Gray shaded areas denote analysis windows, error bars represent SEMs (estimated by bootstrapping).

\*\*  $p < 0.01$ , \*  $p < 0.05$  (bootstrapping).

### **Figure 7. Attractor network model for D2R modulation of working memory.**

(A) Within the network, recurrent excitatory connections by AMPA and NMDA receptors are structured in three selective pyramidal cell groups (*colored circles*), characterized by strong recurrent connections within one selective pool  $w_+$  (*thick arrows*) (see **Experimental Procedures**) and weak synaptic connections  $w_-$  between pools (*dashed arrows*) and from non-selective neurons. Other connections have weight  $w = 1$  (*thin arrows*). An interneuron pool is characterized by recurrent GABA connections and interneuron-to-pyramidal GABAergic connections subject to

neuromodulation (C). Pyramidal cells project to interneurons, too (D). External Poisson input is mediated by AMPA receptors. For details see **Experimental Procedures**.

(B) Population activity before and after transient stimulation (*red shaded area*) of the first selective pool (*purple curve*), showing two distinct stable states, a spontaneous activity state before stimulation and a persistent activity state after stimulation.

(C) Simulation under systematic variation of GABA conductances in interneuron-to-pyramidal synapses. Plotted is the spontaneous activity (*closed circles*) before stimulation and the persistent activity after stimulation (*open squares*) of the stimulated selective pool (*purple*), corresponding to a bifurcation diagram (Brunel and Wang, 2001). Note that a decrease in GABA conductance is plotted to the right, since D2R stimulation has been shown to decrease GABA transmission.

(D) Same conventions as in (C) with systematic variation of AMPA conductances from pyramidal cells to interneurons.

(E) Proposed D2R modulation combining both GABA modulation in (C) and AMPA modulation in (D).

### **Figure S1. Pair-wise sample numerosity comparisons.**

(A) D2R stimulation increased AUROCs for preferred and least preferred numerosities for all numerosity-selective neurons.

(B) AUROCs for preferred and intermediate preferred numerosities were increased.

(C) AUROCs for intermediate preferred and least preferred numerosities were increased. Error bars represent SEMs, p-values from signed rank tests.

### **Figure S2. D2R stimulation enhanced numerosity coding during working memory.**

(A) Average normalized response of all recorded neurons recorded with D2R stimulation (n = 76) irrespective of individual numerosity-selectivity for control conditions.

(B) Same neurons as in (A) during D2R stimulation.

(C) Tuning for mean normalized responses in the delay 1 period. The drug induced a general excitation as well as an increase in differentiation between samples.

(D) Time-dependent TI for all neurons recorded with quinpirole.

(E) TIs in delay 1 period during quinpirole application plotted against TIs in control conditions. Each dot corresponds to one neuron.

- (F) Mean TIs of all neurons for control and drug conditions.
- (G) Same conventions as (D) for PEV ( $\omega^2$ ).
- (H) Same conventions as in (E) for PEV ( $\omega^2$ ).
- (I) Same conventions as in (F) for PEV ( $\omega^2$ ).
- (J) Same conventions as in (D) for AUROCs.
- (K) Same conventions as in (E) for AUROCs.
- (L) Same conventions as in (F) for AUROCs. Gray shaded areas denote analysis window in delay 1, error bars and shaded areas represent SEMs, p-values from signed rank tests.

**Figure S3. SKF81297 control did not modulate working memory coding, but decreased population dynamics.**

- (A) Average normalized population response for all numerosity-selective neurons ( $n = 11$ ) recorded with SKF81297 in control conditions.
- (B) Same layout as in (A) during D1R stimulation.
- (C) TIs of selective neurons in delay 1 period obtained during drug application plotted against TIs in control conditions. Each dot corresponds to one neuron.
- (D) Mean TIs over neurons in (C) for control and drug conditions.
- (E) Same conventions as in (C) for PEV ( $\omega^2$ ).
- (F) Same conventions as in (D) for PEV ( $\omega^2$ ).
- (G) Same conventions as in (C) for AUROCs.
- (H) Same conventions as in (D) for AUROCs.
- (I) Regression analysis for all neurons recorded with SKF81297 ( $n = 82$ ). Same conventions as in Figure 4E for SKF81297.
- (J) Same conventions as in Figure 4F for SKF81297. Gray areas denote analysis windows. Error bars and colored areas represent SEMs. p-values of signed rank tests. n.s. not significant ( $p > 0.05$ ) (bootstrapping or signed rank tests).

**Figure S4. SCH22390 control did not modulate working memory processing.**

- (A) Average normalized population response for all numerosity-selective neurons ( $n = 6$ ) recorded with SCH22390 in control conditions.
- (B) Same neurons as in (A) during blocking D1Rs.
- (C) TIs of selective neurons in delay 1 period obtained during drug application plotted against TIs in control conditions. Each dot corresponds to one neuron.
- (D) Mean TIs over neurons in (C) for control and drug conditions.
- (E) Same conventions as in (C) for PEV ( $\omega^2$ ).

- (F) Same conventions as in (D) for PEV ( $\omega^2$ ).
- (G) Same conventions as in (C) for AUROCs.
- (H) Same conventions as in (D) for AUROCs.
- (I) Regression analysis for all neurons recorded with SCH23390 (n = 85). Same conventions as in Figure 4E for SCH23390.
- (J) Same conventions as in Figure 4F for SCH23390. Gray areas denote analysis windows. Error bars and colored areas represent SEMs. p-values of signed rank tests, n.s. not significant ( $p > 0.05$ ) (bootstrapping or signed rank tests).

**Figure S5. NaCl control did not produce any effect.**

- (A) Average normalized population response for all numerosity-selective neurons (n = 8) recorded with saline (NaCl) in control conditions.
- (B) Same neurons as in (A) after NaCl application.
- (C) TIs of selective neurons in delay 1 period obtained during NaCl application plotted against TIs in control conditions. Each dot corresponds to one neuron.
- (D) Mean TIs over neurons in (C) for control and saline conditions.
- (E) Same conventions as in (C) for PEV ( $\omega^2$ ).
- (F) Same conventions as in (D) for PEV ( $\omega^2$ ).
- (G) Same conventions as in (C) for AUROCs.
- (H) Same conventions as in (D) for AUROCs.
- (I) Regression analysis for all neurons recorded with saline (n = 67). Same conventions as in Figure 4E for NaCl application.
- (J) Same conventions as in Figure 4F for NaCl application.
- (K) PCA analysis for NaCl experiments. Same conventions as in Figure 5E for NaCl application.
- (L) Same conventions as Figure 5F for NaCl application. Gray areas denote analysis windows. Error bars and colored areas represent SEMs. p-values of signed rank tests, n.s. not significant ( $p > 0.05$ ) (bootstrapping or signed rank tests).

**Figure S6. Control analyses for regression results (quinpirole).**

- (A) Results (conventions as in Figure 4E) by simulating data using a Poisson process and the same amount of numerosity coding in the delay period as well as the same amount of drug-induced changes in overall spiking activity as in the real data. “Stimulation” with quinpirole (*red*) did not systematically change the difference between trajectories, showing that drug-induced effects cannot be explained by shifts in overall spiking activity.

(B) Simulation results for regression weights (conventions as in Figure 4F) in control (*black*) or “drug” conditions (*red*).

(C) Same conventions as in Figure 4E using only half of the trials for analysis (cross-validation set 1).

(D) Same conventions as in Figure 4F using only half of the trials for analysis (cross-validation set 1).

(E) Same conventions as in Figure 4E using only the other half of the trials for analysis, i.e. not overlapping with data used in (C and D) (cross-validation set 2).

(F) Same conventions as in Figure 4F using only the other half of the trials for analysis, i.e. not overlapping with data used in (C and D) (cross-validation set 2). D2R stimulation shows comparable effects for cross-validation as the results shown in Figure 4. Gray shaded areas denote analysis windows, error bars represent SEMs (estimated by bootstrapping), \*\*\*  $p < 0.001$ , \*  $p < 0.05$ , †  $p < 0.1$ , n.s. not significant ( $p > 0.1$ ) (bootstrapping in (A,C,E) and signed rank in (B,D,F) right panels).

**Figure S7. Control analyses for PCA results (quinpirole).**

(A) Results (conventions as in Figure 5E) by simulating data using a Poisson process and the same amount of numerosity coding in the delay period as well as the same amount of drug-induced changes in overall spiking activity as in the real data. “Stimulation” with quinpirole (*red*) did not systematically change the distance of trajectories (inset), showing that drug-induced effects are not a consequence of a general change in spiking activity.

(B) Conventions as Figure 5F for simulations results.

(C) Same conventions as in Figure 5E using only half of the trials for analysis (cross-validation set 1).

(D) Same conventions as in Figure 5F using only half of the trials for analysis (cross-validation set 1).

(E) Same conventions as in Figure 5E using only the other half of the trials for analysis, i.e. not overlapping with data used in (C and D) (cross-validation set 2).

(F) Same conventions as in Figure 5F using only the other half of the trials for analysis, i.e. not overlapping with data used in (C and D) (cross-validation set 2). D2R stimulation shows comparable effects for cross-validation as the results shown in Figure 5. Gray shaded areas denote analysis windows, error bars represent SEMs (estimated by bootstrapping), \*\*  $p < 0.01$ , \*  $p < 0.05$ , †  $p < 0.1$ , n.s. not significant ( $p > 0.1$ ) (bootstrapping).

**Figure S8. Control analyses for PCA results (SKF81297).**

(A) Results (conventions as in Figure 5E) by simulating data using a Poisson process and the same amount of numerosity coding in the delay period as well as the same amount of drug-induced changes in overall spiking activity as in the real data. “Stimulation” with SKF81297 (*red*) did not systematically change the distance of trajectories (inset), showing that drug-induced effects are not a consequence of a general change in spiking activity.

(B) Conventions as Figure 5F for simulations results.

(C) Same conventions as in Figure 5E using only half of the trials for analysis (cross-validation set 1).

(D) Same conventions as in Figure 5F using only half of the trials for analysis (cross-validation set 1).

(E) Same conventions as in Figure 5E using only the other half of the trials for analysis, i.e. not overlapping with data used in (C and D) (cross-validation set 2).

(F) Same conventions as in Figure 5F using only the other half of the trials for analysis, i.e. not overlapping with data used in (C and D) (cross-validation set 2).

D1R stimulation shows comparable effects for cross-validation as the results shown in Figure 6. Gray shaded areas denote analysis windows, error bars represent SEMs (estimated by bootstrapping), \*\*  $p < 0.01$ , \*  $p < 0.05$ , †  $p < 0.1$ , n.s. not significant ( $p > 0.1$ ) (bootstrapping).



# Experimental Procedures

(partly to be moved to Supplemental Information)

## Animals and surgical procedures

Two male rhesus monkeys (*Macaca mulatta*) were implanted with a titanium head post and one recording chamber centered over the principal sulcus of the lateral PFC, anterior to the frontal eye fields (right hemispheres in both monkeys). Surgery was conducted using aseptic techniques under general anaesthesia. Structural magnetic resonance imaging was performed before implantation to locate anatomical landmarks. All experimental procedures were in accordance with the guidelines for animal experimentation approved by the authority, the Regierungspräsidium Tübingen, Germany.

## Task

Monkeys performed a memory-guided decision-making task, comparing sample numerosities (set sizes) with test numerosities. They initiated a trial by grasping a lever and maintaining central fixation on a screen. After a pure fixation period (500 ms), a sample stimulus (500 ms) cued the animals for the reference numerosity (i.e., number of dots) they had to remember in the subsequent memory delay period (delay 1, 1,000 ms) without numerosities. The first memory interval was followed by a rule-cue (300 ms) that instructed the monkeys to select either a larger number of dots (“greater than” rule) or a smaller number of dots (“less than” rule) than the sample numerosity in the subsequent test phase. The test phase was preceded by a second delay (delay 2, 1,000 ms) requiring the monkeys to assess the rule at hand for the subsequent choice. In the following test 1 phase, the monkeys had to release the lever in a “greater than” trial, if the number of items in the test display was larger than the number of items in the sample display, or to keep holding the lever for another 1,200 ms until the appearance of a second test display (test 2), if the number of items in the test display was smaller than the number of items in the sample display. In a “less than” trial, these conditions were reversed. Monkeys got a liquid reward for a correct choice. Thus, only test 1 required a decision; test 2 was used so that a behavioral response was required in each trial, ensuring that the monkeys were paying attention during all trials. Because both sample and test numerosities var-

ied randomly, the monkeys could only solve the task by assessing the numerosity of the test display relative to the three possible numerosities of the sample display together with the appropriate rule in any single trial. To test a range of numerosities, both monkeys were presented with numerosities 2 (smaller test numerosity = 1, larger test numerosity = 4), 8 (4:16), and 32 (16:64). For any sample numerosity, test numerosities were either larger or smaller with equal probability ( $p = 0.5$ ). Because the monkeys numerosity discrimination performance obeys the Weber–Fechner law (Nieder et al., 2002), numerosities larger than the sample numerosity need to be numerically more distant than numerosities smaller than the sample numerosity to reach equal discriminability. Based on this design, any test numerosity (except the smallest and largest used) served as test numerosities for different sample numerosities, thus preventing the animals from learning systematic relations between numerosities.

To prevent the animals from exploiting low-level visual cues (e.g., dot density, total dot area), a standard numerosity protocol (with dot sizes and positions pseudo-randomized) and a control numerosity protocol (with equal total area and average density of all dots within a trial) were each presented in 50% of the trials in a pseudo-randomized fashion. Each rule was signified by two different rule-cues in two different sensory modalities: a red circle (“greater than” rule, red color) or a white circle with a drop of water (“greater than” rule, water) signified the rule “greater than”. The “less than” rule was cued by a blue circle (“less than” rule, blue color) or a white circle with no water (“less than” rule, no-water). We showed in previous studies that monkeys generalize the numerical principles “greater than” and “less than” to numerosities they had never seen before (Bongard and Nieder, 2010). Before each session, the displays were generated anew using MATLAB (Mathworks). Trials were randomized and balanced across all relevant features (sample numerosities, “greater than” and “less than” rules, rule-cue modalities, standard and control stimuli, match and non-match trials). Monkeys had to keep their gaze within  $1.75^\circ$  of the fixation point from the fixation interval up to the onset of the first test stimulus (monitored with an infrared eye-tracking system; ISCAN, Burlington, MA).

### **Electrophysiology and iontophoresis**

Extracellular single-unit recording and iontophoretic drug application was per-

formed as described previously (Jacob et al., 2013; Ott et al., 2014). In each recording session, up to three custom-made tungsten-in-glass electrodes flanked by two pipettes each were inserted transdurally using a modified electrical micro-drive (NAN Instruments). Single neurons were recorded at random; no attempt was made to preselect the neurons to any task-related activity or based on drug effects. Signal acquisition, amplification, filtering, and digitalization were accomplished with the MAP system (Plexon). Waveform separation was performed offline (Offline Sorter; Plexon). Drugs were applied iontophoretically (MVCS iontophoresis system; npi electronic) using custom-made tungsten-in-glass electrodes flanked by two pipettes each (Thiele et al., 2006; Jacob et al., 2013; Ott et al., 2014). Electrode impedance and pipette resistance were measured after each recording session. Electrode impedances were 0.8–3 M $\Omega$  (measured at 500 Hz; Omega Tip Z; World Precision Instruments). Pipette resistances depended on the pipette opening diameter, drug, and solvent used. Typical resistances were 15–50 M $\Omega$  (full range, 12–160 M $\Omega$ ). As in previous experiments (Jacob et al., 2013; Ott et al., 2014), we used retention currents of  $-7$  nA to hold the drugs in the pipette during control conditions. The ejection current for SKF81297 (10 mM in double-distilled water, pH 4.0 with HCl; Sigma-Aldrich) was  $+15$  nA, the ejection current for SCH23390 (10 mM in double-distilled water, pH 4.0 with HCl; Sigma-Aldrich) was  $+25$  nA, and the ejection current for quinpirole (10 mM in double-distilled water, pH 4.0 with HCl; Sigma-Aldrich) was  $+40$  nA. In control experiments with 0.9 % physiological NaCl, pH 4.0 with HCl, the ejection current was  $+25$  nA. We did not investigate dosage effects and chose ejection currents to match the values reported to be maximally effective, i.e., in the peak range of the ‘inverted-U’ (Wang et al., 2004; Vijayraghavan et al., 2007). One pipette per electrode was filled with drug solution (either SKF81297, SCH23390, quinpirole, or NaCl), and the other always contained 0.9 % NaCl. In each recording session, control conditions using the retention current alternated with drug conditions using the ejection current. Drugs were applied continuously for 12–15 min (drug conditions), depending on the number of trials completed correctly by the animal. Each control or drug application block consisted of 72 correct trials to yield sufficient trials for analysis. The first block (12–15 min) was always the control condition. Given that iontophoretic drug application is fast and can quickly modulate neuronal firing properties (Jacob et al., 2013), we did not exclude data at the

current switching points.

## **Data analysis**

### *Selection criteria*

All well-isolated recorded single units with a baseline spike rate above 0.5 Hz (determined in the 500 ms fixation period preceding sample presentation) and with at least 15 trials for each of the three sample numerosities in each control and drug condition entered all subsequent analyses. Neurons were not included based on drug effects.

### *Numerosity-selective neurons*

We calculated a two-way ANOVA for each neuron to determine if a neuron's response was correlated with sample numerosities in the memory delay period (delay 1), thus representing a numerosity in working memory. We used spike rates in a 800 ms window beginning 200 ms after sample offset, based on previous studies (Bongard and Nieder, 2010). The main factors were numerosity ("2"/"8"/"32") and iontophoresis condition (control conditions/drug conditions). We identified numerosity-selective neurons by a significant main factor of the factor numerosity ( $p < 0.05$ ). Since the monkeys behavior did not show any differences for standard and control stimuli (**Extended Data Fig. 1**), and because we have shown previously that neuronal responses in the PFC do not differentiate between standard and control stimuli (Bongard and Nieder, 2010), we pooled over standard and control stimuli trials.

### *Single-cell and population responses*

For plotting single-cell spike density histograms, the average firing rate in trials with one of the three different sample numerosities (correct trials only) was smoothed with a Gaussian kernel (bin width of 200 ms, step of 1 ms). Tuning curves were constructed by calculating mean spike rates in the same analysis window used for the ANOVA. For the population responses, we defined a neuron's preferred numerosity as the numerosity yielding the higher average spike rate in the analysis window used for the ANOVA, averaging over control and drug trials. Accordingly, the intermediate and least preferred numerosities were defined as the numerosities resulting in lower average spike rates. Neuronal activity was normalized by subtracting the mean baseline firing rate in the control

condition and dividing by the standard deviation of the baseline firing rates in the control condition. For population histograms, normalized activity was averaged and smoothed with a Gaussian kernel (bin width of 200 ms, step of 1 ms). Population tuning curves were calculated as the mean normalized activity for each condition in the same analysis windows used for the ANOVA.

### *Neuronal information about sample numerosities*

We estimated the information a single unit carried about the sample numerosity during working memory by using three different quantifications. Calculations were performed based on spike rates in the delay period using the same analysis window as for the ANOVA. Additionally, we performed sliding window analysis, using spike rates in overlapping 100 ms windows stepped in 10 ms increments from fixation onset to the end of the delay 1 period. First, we defined a tuning index (TI) by subtracting the neurons spike rate to the least preferred sample numerosity from the spike rate of the preferred numerosity and dividing by the sum, i.e.

$$\text{TI} = \frac{\text{FR}_{\text{pref}} - \text{FR}_{\text{leastpref}}}{\text{FR}_{\text{pref}} + \text{FR}_{\text{leastpref}}}. \quad (1)$$

TIs vary between 0 and 1, expressing the relative (rather than absolute) differences in spike rates between sample numerosities, where low values correspond to low numerosity selectivity and high values correspond to high numerosity selectivity. Second, we calculated the percent explained variance (PEV) using  $\omega^2$ , expressing how much of a neurons spike rates can be explained by the sample numerosity (Jacob and Nieder, 2014).  $\omega^2$  is defined as

$$\omega^2 = \frac{\text{SS}_{\text{groups}} - \text{df} \cdot \text{MSE}}{\text{SS}_{\text{total}} + \text{MSE}}, \quad (2)$$

where the individual terms are calculated using a one-way ANOVA using all three sample numerosities as levels (pooled over control and drug condition).  $\text{SS}_{\text{groups}}$  is the sum of squares between groups (sample numerosities),  $\text{SS}_{\text{total}}$  the total sum of squares,  $\text{df}$  the degree of freedoms, and  $\text{MSE}$  the mean squared error. The number of trials in each group was balanced by stratifying the number of trials in each group to the minimum trial number across groups, randomly selecting individual trials. This process was repeated 25 times, and the mean of the stratified values

was taken as the final statistic.  $\omega^2$  is an unbiased, zero-mean statistic when there is no information, while values above zero indicates the variance explained by the sample numerosity (Jacob and Nieder, 2014). Third, sample numerosity coding quality was quantified using receiver operating characteristic (ROC) analysis derived from Signal Detection Theory. The area under the ROC curve (AUROC) is a nonparametric measure of the discriminability of two distributions. It denotes the probability with which an ideal observer can tell apart a meaningful signal from a noisy background. Values of 0.5 indicate no separation, and values of 1 signal perfect discriminability. The AUROC takes into account both the difference between distribution means as well as their widths and is therefore a suitable indicator of signal quality. We used AUROCs to quantify the quality of sample numerosity coding in the memory period. We calculated the AUROC for each neuron using the spike rate distributions of the preferred and the least preferred numerosity in the same analysis window used for the ANOVA.

### *Linear regression analysis*

We used linear regression analysis to estimate the neuronal population coding of numerosities in working memory, disentangling general drug-induced neuronal activity changes and variability of neuronal responses explained by the numerosity that might be mixed both at single neuron level and at the level of principal components (Mante et al., 2013) (see below). By modeling interactions between drug and sample numerosity, we defined numerosity-related axes for control and drug conditions and projected the population response onto these axes, yielding an estimate of the sample representation during working memory at population level for control and drug conditions. We preprocessed single unit data first by stratifying the number of trials in each condition, randomly selecting a fixed amount of trials corresponding to the minimal amount of trials of all conditions. Then we calculated, for each trial, spike rates in a 100 ms window and 50 ms steps from fixation onset to the end of delay 1 period, yielding  $T = 41$  time points, covering the first 2100 ms of each trial. Next, we z-scored spike rates by combining all  $T$  time bins and trials, yielding response vectors  $r_{i,t}$  of length  $N_{trials}$  (total number of trials) for each neuron  $i$  and each time bin  $t$ . Population responses were defined as matrices  $x_s^{con}$  of size  $n \times T$  ( $n$  number of neurons and  $T = 41$  time bins) for each sample numerosity  $s$  and drug condition  $con$  (control or drug), with  $x_s^{con}(i, t)$

( $i = 1, \dots, n$ ;  $t = 1, \dots, T$ ) for each neuron  $i$  and time point  $t$  defined as the mean over trials of  $r_{i,t}$ , containing trials of sample numerosity  $s$  and condition  $con$ .

Then we performed linear regression similar to Mante et al. (2013). For each time bin and neuron, we described the  $i$ -th neuron's response in trial  $j$  at time  $t$  as a linear combination of spike rates depending on numerosity, drug conditions, and, importantly, an interaction between numerosity and drug condition:

$$r_{i,t}(j) = \beta_{i,t}(1) \cdot num(j) + \beta_{i,t}(2) \cdot drug(j) + \beta_{i,t}(3) \cdot num(j) \cdot drug(j) + \beta_{i,t}(4), \quad (3)$$

where  $\beta_{i,t}(k)$  ( $k = 1, \dots, 3$ ) describe how much of the trial-by-trial variability of neuron  $i$  at the point  $t$  depends on the task variable  $k$ .  $\beta_{i,t}(4)$  captures variance independent of task variables and describes differences in responses across time. For numerosities, we set  $num(j)$  to 1, 2, or 3 depending on the numerosity type shown in trial  $j$  (preferred numerosity: 3, intermediate preferred numerosity: 2, least preferred numerosity: 1). We used contrast coding to code the drug condition, i.e. set  $drug(j) = -1$ , if trial  $j$  was a control trial, and  $drug(j) = 1$ , if trial  $j$  was a drug trial. To estimate the regression coefficients  $\beta_{i,t}$ , we constructed a design matrix  $F_i$  of size  $N_{coef} \times N_{trials}$ , where  $N_{coef}$  is the number of coefficients to be estimated ( $N_{coef} = 4$ ) and  $N_{trials}$  the number of total trials of neuron  $i$ . Each row of  $F_i$  contains the values of the coding variables for numerosity, drug, numerosity and drug interactions for each trial  $j$  as described above. The last row consists of ones. The regression coefficients can then be estimated as

$$\beta_{i,t} = (F_i F_i^T)^{-1} F_i^T \cdot r_{i,t}, \quad (4)$$

where  $F_i$  is the design matrix,  $r_{i,t}$  a column vector of length  $N_{trials}$  containing the trial-by-trial spike rates of neuron  $i$  at time point  $t$ , and  $\beta_{i,t}$  is a vector of length  $N_{coef}$  containing the estimated regression coefficients. We performed this calculation for each time point  $t$  and each neuron  $i$ . We then rearranged  $\beta_{i,t}(k)$  ( $k = 1, \dots, 4$ ) to  $\beta_{k,t}(i)$  ( $i = 1, \dots, n$ ), where each  $\beta_{k,t}$  represents a direction in  $n$ -dimensional state space, corresponding to the direction along which the corresponding task variable (i.e., numerosity and drug condition) is represented at the level of neuronal population over time. To estimate numerosity coding, we defined a numerosity related axis (i.e., directions in  $n$ -dimensional state space) for control and drug conditions separately by using the interaction term. For control

conditions,

$$\beta_{num,t}^{control} = \beta_{1,t} - \beta_{3,t}, \quad (5)$$

and for drug conditions

$$\beta_{num,t}^{drug} = \beta_{1,t} + \beta_{3,t}, \quad (6)$$

where each  $\beta_{k,t}$  is a  $n$ -dimensional vector, i.e.  $\beta_{num,t}^{control}$  and  $\beta_{num,t}^{drug}$  are  $n$ -dimensional vectors describing, for each time point  $t$ , directions in state space that correspond to the axis representing numerosity for control and drug conditions, respectively. To define time-independent axes in state space during working memory, we calculated the mean direction in delay 1 period (same analysis window used for the ANOVA, corresponding to time bins  $T_{delay} = 25, \dots, 40, \#T_{delay} = 16$ ) over time, i.e.

$$\beta_{num}^{control} = \frac{\sum_{t \in T_{delay}} \beta_{num,t}^{control}}{\#T_{delay}}, \quad (7)$$

and

$$\beta_{num}^{drug} = \frac{\sum_{t \in T_{delay}} \beta_{num,t}^{drug}}{\#T_{delay}}, \quad (8)$$

each, again,  $n$ -dimensional vectors in state space, describing, time-independently, directions in state space that correspond to the axes representing numerosity for control and drug conditions during working memory. We then projected the neuronal population response  $x_s^{con}$  for each numerosity  $s$  ( $s = 1, 2, 3$ ) and drug condition  $con$  ( $con=control/drug$ ) onto the numerosity axis, yielding estimates of the population's amount of numerosity representation at time point  $t$ . Specifically, we calculated for each numerosity  $s$  the projection as

$$p_s^{control} = \beta_{num}^{control} \cdot x_s^{control}, \quad (9)$$

and

$$p_s^{drug} = \beta_{num}^{drug} \cdot x_s^{drug}, \quad (10)$$

with  $\beta_{num}^{control}$  and  $\beta_{num}^{drug}$  vectors of length  $n$ ,  $x_s^{con}$  ( $s = 1, 2, 3, con=control/drug$ ) matrices of size  $n \times T$  ( $T = 41$  time points), yielding a series of time-dependent projection vectors  $p_s^{con}$  ( $s = 1, 2, 3, con=control/drug$ ) of length  $T$ , quantifying the numerosity evidence for numerosity  $s$  in control and drug conditions.



To assess statistical significance, we calculated the mean  $\Delta p^{con}$  between all pairwise numerosity combinations for control and drug conditions in the delay period (using the same analysis window as used for the ANOVA) and used bootstrapping (with 999 repetitions) to estimate standard errors and confidence intervals. Additionally, we confirmed results by shuffling control and drug data 999 times and estimating confidence intervals for the difference between control and drug conditions from the shuffle data, yielding similar results. We used cross-validation to confirm the above analysis, by computing two independent estimates, using only every second trial in each calculation, i.e. using non-overlapping data. Both estimates yielded comparable results. Additionally, we performed the analysis using simulated data to test if the observed effects are due to simple drug-induced shifts in overall spiking activity. To achieve comparable results, we simulated each neuron by using the same amount of trials for that neuron, the same mean spike rate  $M$  (combining all conditions), the same amount of numerosity coding  $U_s$  for each sample numerosity  $s$  (combining control and drug conditions and using differences to  $M$  for all numerosities in the delay period, same analysis window as used for the ANOVA), and the same amount of drug-induced changes in spiking activity  $D$  (using the mean difference of spike rates for control and drug conditions, combining all numerosity stimuli). We then simulated the neuron's response over time using a Poisson process with a mean spike rate of  $R = M$  during fixation and sample period for all trials in all conditions, and a mean spike rate of  $R_s = M + U_s$  for trials with numerosity  $s$  in control conditions and  $R_s = M + U_s + D$  for drug conditions. We repeated the simulation 1000 times and performed regression analysis in exactly the same way, calculating mean estimates and confidence intervals of all parameters. Confirming our previous results, simulated data showed no systematic differences between control and drug conditions. Thus, the reported results are unlikely a consequence of changes in overall spiking activity but rather induced by interaction between the drug and the numerosity representations not captured by the simulation, i.e. by specific actions of the drug on working memory signals that cannot be produced by general changes in network activity.

### *Principal component analysis*

We performed principal component analysis (PCA) to represent the population

activity of  $n = 76$  single units in a low-dimensional subspace, extracting shared activity patterns prominent in the population response (Cunningham and Yu, 2014). Neuronal population activity at time  $t$  in condition  $c$  can be represented by a  $n$ -dimensional vector in  $n$ -dimensional space, where each dimension corresponds to one single unit (i.e.,  $n = 76$  dimensions). PCA corresponds to a change of basis, where each basis vector is defined by its direction in  $n$ -dimensional space, determining directions of maximal covariance. By using the first three directions capturing the largest amount of variance, or principal components (PCs), neuronal population activity can be represented in 3-dimensional space. We pre-processed single unit data as for regression analysis, stratifying number of trials, binning windows of 100 ms and steps of 50 ms, and z-scoring by combining all trials from all conditions. We then calculated trial-averaged responses by averaging all trials of the same condition, yielding one vector of length  $T = 41$  for each condition  $c$  ( $c = 1, \dots, C$ ) and neuron  $i$  ( $i = 1, \dots, n$ ). As in the previous analyses, we defined  $C = 6$  conditions corresponding to each combination of numerosity (preferred, intermediate preferred, least preferred as defined above) and drug condition (control, drug application). We constructed the  $n$ -dimensional population response  $P$  by considering the activity of all neurons in each time bin and condition as pseudo-simultaneous, yielding a  $TC \times n$  matrix. For PCA, we used MATLAB's `princomp(P)` function to calculate the PCA scores  $S$ , i.e. the neuronal population activity after change of basis. We represented neuronal population activity by using the first three PCs capturing the largest amount of variance in population response, accounting for 42% (for quinpirole data) of the total variance, yielding 3-dimensional trajectories in state space. To quantify the population's discriminability between numerosities, we calculated the Euclidean distance between the population trajectories in state space, using the full  $n$ -dimensional space. The distance  $d$  at each time point  $t$  ( $t = 1, \dots, T$ ) between two trajectories of conditions  $c_1$  and  $c_2$  is defined as

$$d_t(c_1, c_2) = \sqrt{\sum_{i=1}^n (S_{c_1}(t, i) - S_{c_2}(t, i))^2}, \quad (11)$$

where  $S_c$  is sub-matrix of  $S$  containing  $T$  rows of condition  $c$ . This yields time-dependent distance estimates for all three numerosity combinations for control and drug conditions. Distances were normalized to baseline (500 ms fixation pe-

riod preceding sample onset) for control and drug condition by subtracting the mean distance in the baseline period from each time point. Mean distance was the average distance over all sample combinations for control and drug conditions. To assess statistical significance, we calculated the mean distance in the delay 1 period (same analysis window as used for the ANOVA) for all numerosity combinations and used bootstrapping (with 999 repetitions) to estimate standard errors and confidence intervals for control and drug conditions.

To assess the dynamics of neuronal population responses, we calculated the speed by which population trajectories travelled through state space (Stokes et al., 2013). The velocity was defined as the Euclidean distance between two adjacent points in time within the same condition (as opposed to two points at the same time, but from different condition), divided by the time between those points, i.e. 50 ms (since we used  $step = 50$  ms steps). Thus, the velocity  $v$  at time  $t$  of condition  $c$  is given by

$$v_{t,c} = \sqrt{\sum_{i=1}^n (S_c(t, i) - S_c(t + 1, i))^2 \cdot step^{-1}}, \quad (12)$$

yielding a time-dependent instantaneous velocity of neuronal trajectories for each condition  $c$ . As above, we baseline normalized velocities by subtracting the mean velocity in the baseline period. Mean velocity  $v_t$  was the average velocity over all sample numerosities for control and drug conditions. Additionally, we quantified the distance the trajectories travelled through state space by integrating the mean, time-dependent, velocity  $v_t$  over time ( $t = 1, \dots, T - 1$ ), i.e.

$$s = \sum_{t=1}^{T-1} v_t \cdot step. \quad (13)$$

To assess statistical significance, we calculated the mean velocity in the beginning of the delay period (300 ms window starting with sample offset) of all numerosities and used bootstrapping (with 999 repetitions) to estimate standard errors and confidence intervals for control and drug conditions. As above, we confirmed all statistical analyses using shuffled data, yielding comparable statistical results. Additionally, we confirmed PCA analysis cross-validation and simulated data.

### Neuronal network model

Model architecture and descriptions from synaptic currents are taken from Brunel

**Table S1: Parameters of leaky integrate-and-fire neurons.**

Parameter	Pyramidal cells	Interneurons
$V_L$	-70 mV	-70 mV
$V_{thr}$	-50 mV	-50 mV
$V_{reset}$	-55 mV	-55 mV
$C_m$	0.5 nF	0.2 nF
$g_m$	25 nS	20 nS
$\tau_m$	2 ms	1 ms

et al. (2001) and Wang (2002). The cortical network model is characterized by a spontaneous activity state and a persistent activity state, modeling persistent delay activity found during working memory. Persistent activity is largely mediated by recurrent excitatory connections with NMDA synapses, while the spontaneous activity state is dominated by GABA inhibition (Brunel et al., 2001).

The model consists of  $N_E = 2000$  excitatory pyramidal cells and  $N_I = 500$  inhibitory interneurons. The network is fully connected, i.e. each neuron receives  $C_E = N_E = 2000$  excitatory connections from pyramidal cells and  $C_I = N_I = 500$  inhibitory connections from interneurons. Additionally, each neuron receives excitatory Poisson input from  $C_{ext} = 800$  neurons arriving with a mean rate of 3 Hz, corresponding to a background external input to each cell of  $v_{ext} = 2.4$  kHz, independent from cell to cell.

Pyramidal cells and interneurons are described by leaky integrate-and-fire neurons. All parameters were identical to the parameters used by Brunel et al. (2001) (see **Table S1**). Neurons are characterized by a resting potential  $V_L$ , a firing threshold  $V_{thr}$ , a reset potential  $V_{reset}$ , a membrane capacitance  $C_m$ , a membrane leak conductance  $g_m$ , and a refractory period  $\tau_m$ . Below threshold, the membrane potential  $V(t)$  is described by the differential equation

$$C_m \frac{dV(t)}{dt} = -g_m(V(t) - V_L) - I_{syn}(t), \quad (14)$$

where  $I_{syn}(t)$  models the summed synaptic current flowing into the cell. When the membrane potential  $V(t)$  reaches the firing threshold  $V_{thr}$ , the neuron elicits a spike and the membrane potential  $V(t)$  is set to  $V_{reset}$ .

Total synaptic current consists of four components, corresponding to four synapses,

an AMPA current from recurrent excitatory connections, a NMDA current from recurrent excitatory connections, a GABA current from recurrent inhibitory connections, and an AMPA current from external inputs, i.e.

$$I_{syn}(t) = I_{AMPA}(t) + I_{NMDA}(t) + I_{GABA}(t) + I_{AMPA,ext}, \quad (15)$$

where individual currents depend on conductances  $g$  and reversal potentials  $V_E = 0.0$  mV and  $V_I = -70$  mV, i.e.

$$I_{AMPA}(t) = g_{AMPA}(V(t) - V_E) \sum_{j=1}^{C_E} w_j s_j^{AMPA}(t), \quad (16)$$

$$I_{NMDA}(t) = \frac{g_{NMDA}(V(t) - V_E)}{1 + 0.2801e^{-0.062V(t)}} \sum_{j=1}^{C_E} w_j s_j^{NMDA}(t), \quad (17)$$

$$I_{GABA}(t) = g_{GABA}(V(t) - V_I) \sum_{j=1}^{C_I} s_j^{GABA}(t), \quad (18)$$

$$I_{AMPA,ext}(t) = g_{AMPA,ext}(V(t) - V_E) \sum_{j=1}^{C_{ext}} s_j^{AMPA,ext}(t). \quad (19)$$

The sum over  $j$  represents the sum over all synaptic connections formed by presynaptic neuron  $j$ . The dimensionless  $w_j$  describe the synaptic weight of connection  $j$ , allowing for structured connections (see below). The gating variables  $s_j$  describe the time course of the fraction of open channels, depending on a time constant  $\tau$  and the time of a presynaptic spike. For both recurrent and external AMPA, we described  $s_j^{AMPA}$  by

$$\frac{ds_j^{AMPA}(t)}{dt} = -\frac{s_j^{AMPA}(t)}{\tau_{AMPA}} + \sum_k \delta(t - t_j^k), \quad (20)$$

where the sum over  $k$  represents the spike train of presynaptic neuron  $j$ . NMDA channels are described by two differential equations, corresponding to the rise time  $\tau_{NMDA,rise}$  and decay time  $\tau_{NMDA,decay}$ , expressed by

$$\frac{ds_j^{NMDA}(t)}{dt} = -\frac{s_j^{NMDA}(t)}{\tau_{NMDA,decay}} + \alpha x_j(t)(1 - s_j^{NMDA}(t)), \quad (21)$$

**Table S2: Parameters of synaptic equations.**

Synapse	Parameter	Pyramidal cells	Interneurons
AMPA	$g_{AMPA}$	0.02 nS	0.016 nS
	$g_{AMPA,ext}$	2.1 nS	1.62 nS
	$\tau_{AMPA}$	2 ms	2 ms
NMDA	$g_{NMDA}$	0.066 nS	0.052 nS
	$\tau_{NMDA,rise}$	2 ms	2 ms
	$\tau_{NMDA,decay}$	100 ms	100 ms
	$\alpha$	0.5 kHz	0.5 kHz
GABA	$g_{GABA}$	0.52 nS	0.4 nS
	$\tau_{GABA}$	10 ms	10 ms

$$\frac{dx_j(t)}{dt} = -\frac{x_j(t)}{\tau_{NMDA,rise}} + \sum_k \delta(t - t_j^k). \quad (22)$$

GABA channels were described by

$$\frac{ds_j^{GABA}(t)}{dt} = -\frac{s_j^{GABA}(t)}{\tau_{GABA}} + \sum_k \delta(t - t_j^k). \quad (23)$$

All synapses had a latency of 0.5 ms. All equations and parameters used for describing synapses were identical as used by Brunel et al. (2001), using their large simulations, and are listed in **Table S2**. Interneurons are characterized by lower conductances in general, in particular NMDA conductances (**Table S2**).

We structured the network by manipulating the connection weights for excitatory recurrent connections  $w_j$  (Brunel et al., 2001; Wang, 2002). Within the pyramidal cell group, we defined three subgroups that represent a selective group for one stimulus each, i.e. for one numerosity. Each group consisted of a fraction  $f = 0.1$  of the overall population size, i.e. of  $N_{selective} = fN_E = 200$  neurons. Crucially, within one selective group, recurrent excitatory connections had the weight  $w_+ = 1.9 > 1$ , whereas between selective group, weights were set to  $w_- = 1 - f\frac{w_+-1}{1-f} < 1$ , to keep the overall amount excitatory drive constant (Brunel et al., 2001). Connections from selective neurons to neurons in the non-selective group, as well as from selective neurons to interneurons, had the weight  $w_j = 1.0$ . Connections from the non-selective group to the selective group had the weight

$$w_j = w_-.$$

To simulate network activity during the working memory task, we recorded the activity (i.e., time of spikes) of all neurons in the network for three seconds. After a baseline period of one second, we stimulated one of the three selective pyramidal cell groups for 500 ms by increasing the total external input for all neurons in this group by  $\mu = 80$  Hz. Thus, stimulation increased external drive by about 3%. Stimulation was followed by a delay period of 1.5 s, during which the external drive was again the same for all neurons in the network (i.e., no stimulation).

For analysis, we systematically varied specific parameters and conducted simulations using the full network. Simulations were performed with Python and the Brian simulator module (<http://www.briansimulator.org>) (Goodman and Brette, 2009), using integration steps of  $dt = 0.1$  ms. Population activity was calculated by using 50 ms bins. The network's persistent activity was defined as the average population activity of the stimulated selective group during the delay period, using a 1-sec window at the end of the delay phase. Spontaneous activity was defined as the average population activity of the same selective group in a 1-sec window preceding stimulation.

We systematically varied GABA conductances on pyramidal cells only with a range of 5% and AMPA conductances on interneurons only with a range of about 15%. For combined modulation of both conductances, i.e. proposed D2R modulation, we used the same range of values. Explicitly, we multiplied the AMPA conductances with a factor  $f_{AMPA}$  by the artificial D2R modulation index  $M_{D2R}$ , e.g. for  $M_{D2R} = 1.1$ ,  $f_{AMPA} = 1.1$ , corresponding to an increase of AMPA conductances by 10%. GABA conductances were multiplied with factor  $f_{GABA} = c(M_{D2R} - 4.2)$  with constant  $c$  such that for  $M_{D2R} = 1$ ,  $f_{AMPA} = 1$  and  $f_{GABA} = 1$ , e.g. for  $M_{D2R} = 1.1$ ,  $f_{GABA} = 0.97$ , corresponding to a decrease of GABA conductances by 3%.

**Figure 1**

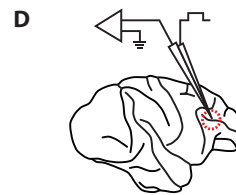
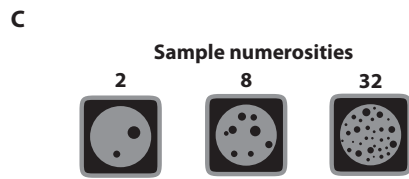
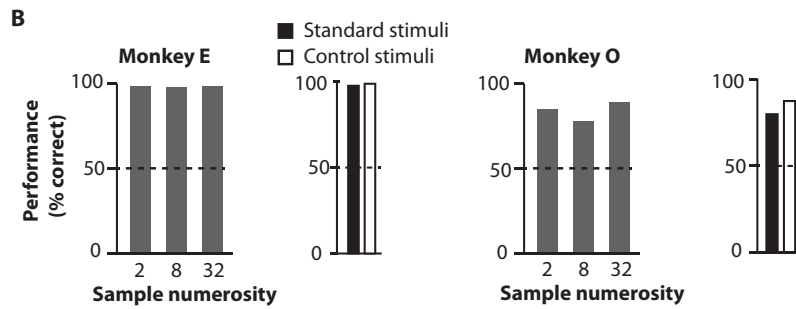
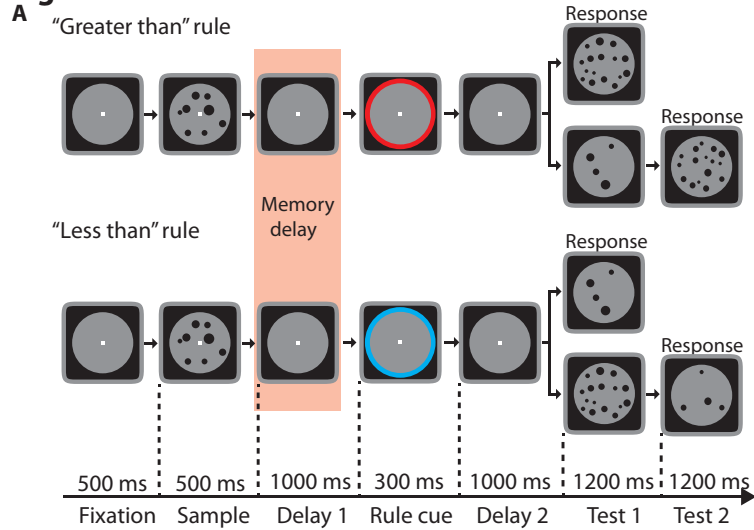


**Figure 2**

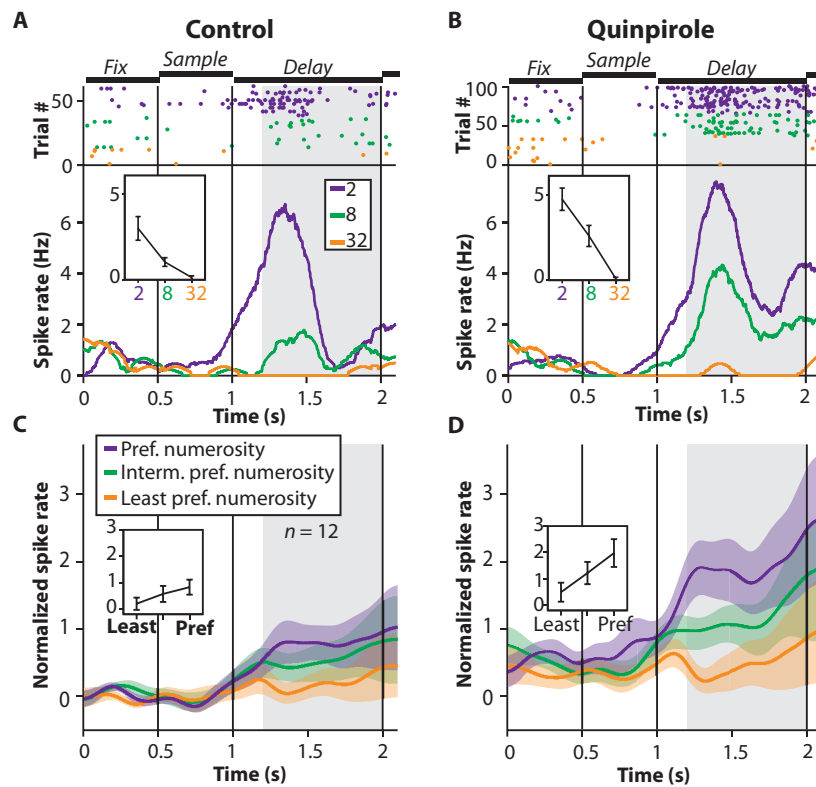




**Figure 3**

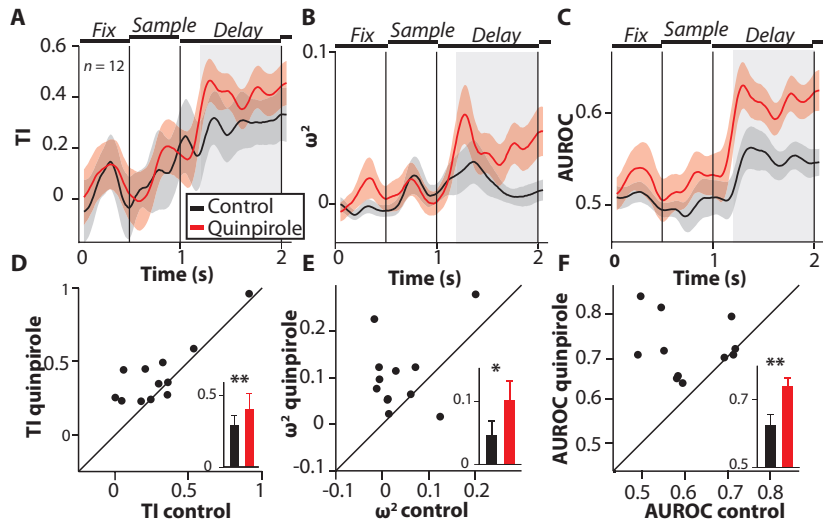


**Figure 4**

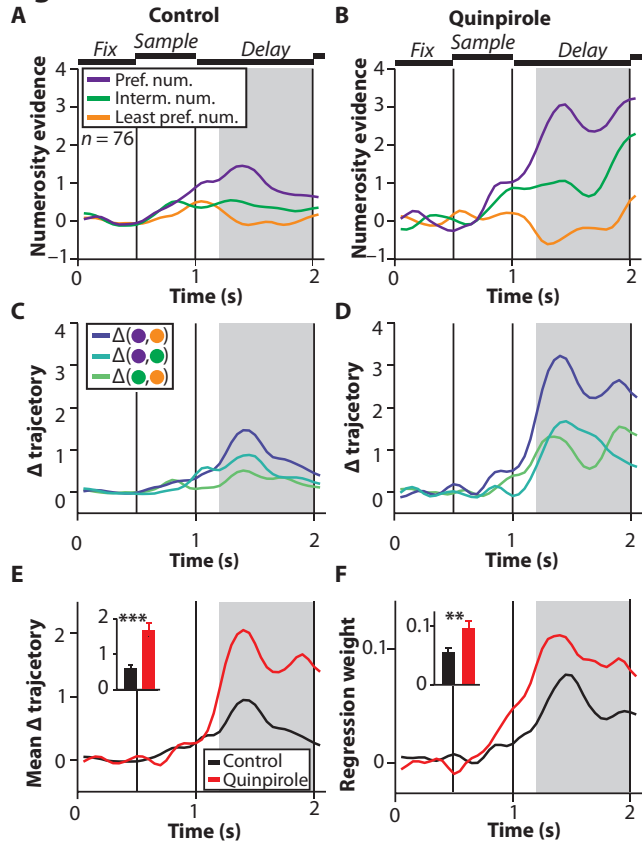


**Figure 5**

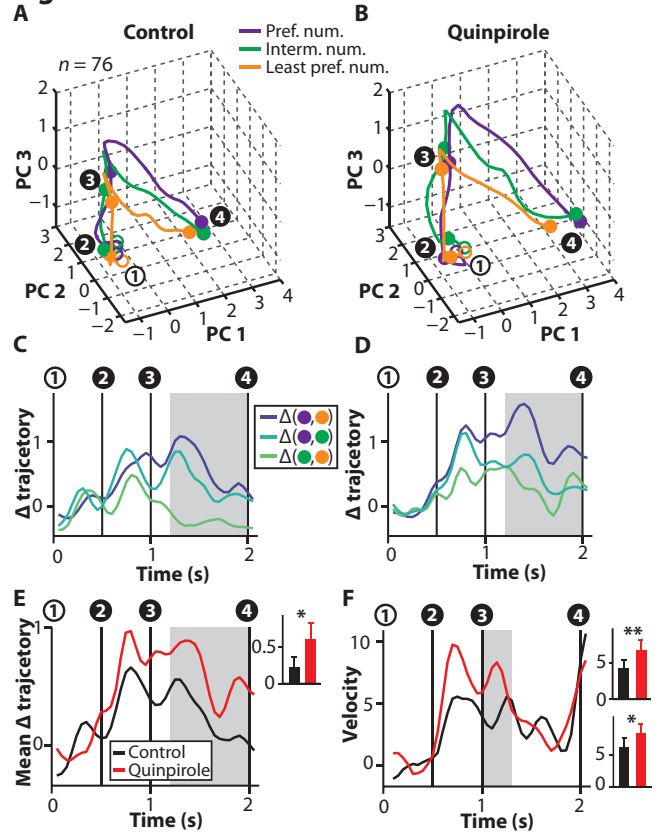


**Figure 6**

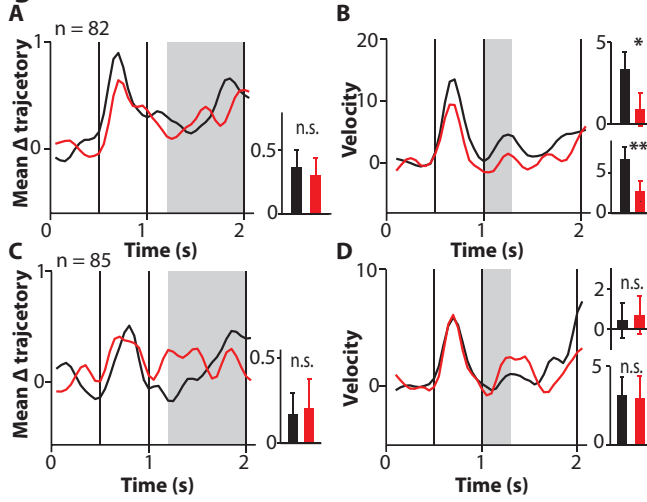


**Figure 7**

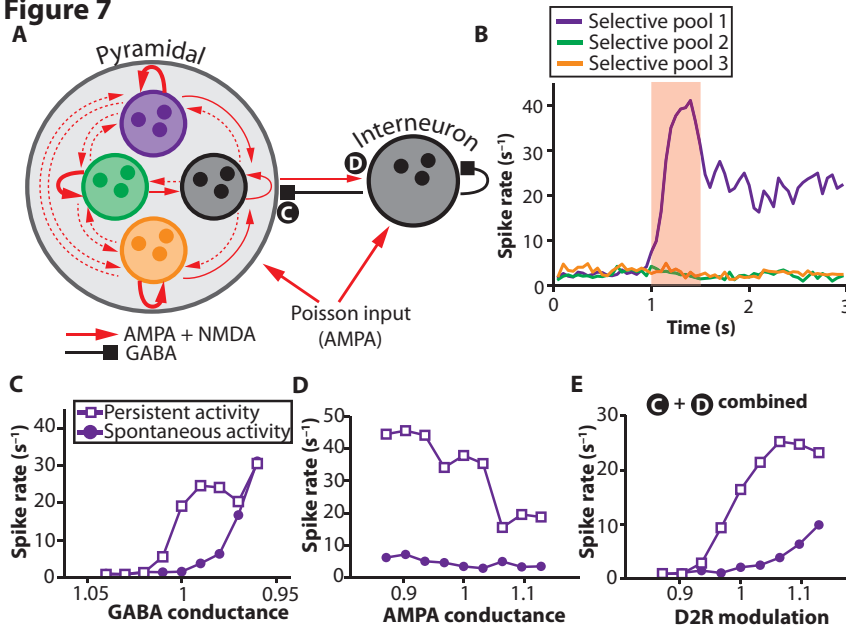


**Figure S1**

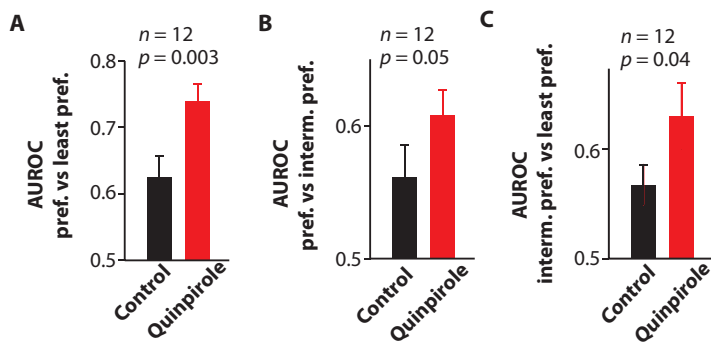


**Figure S2**

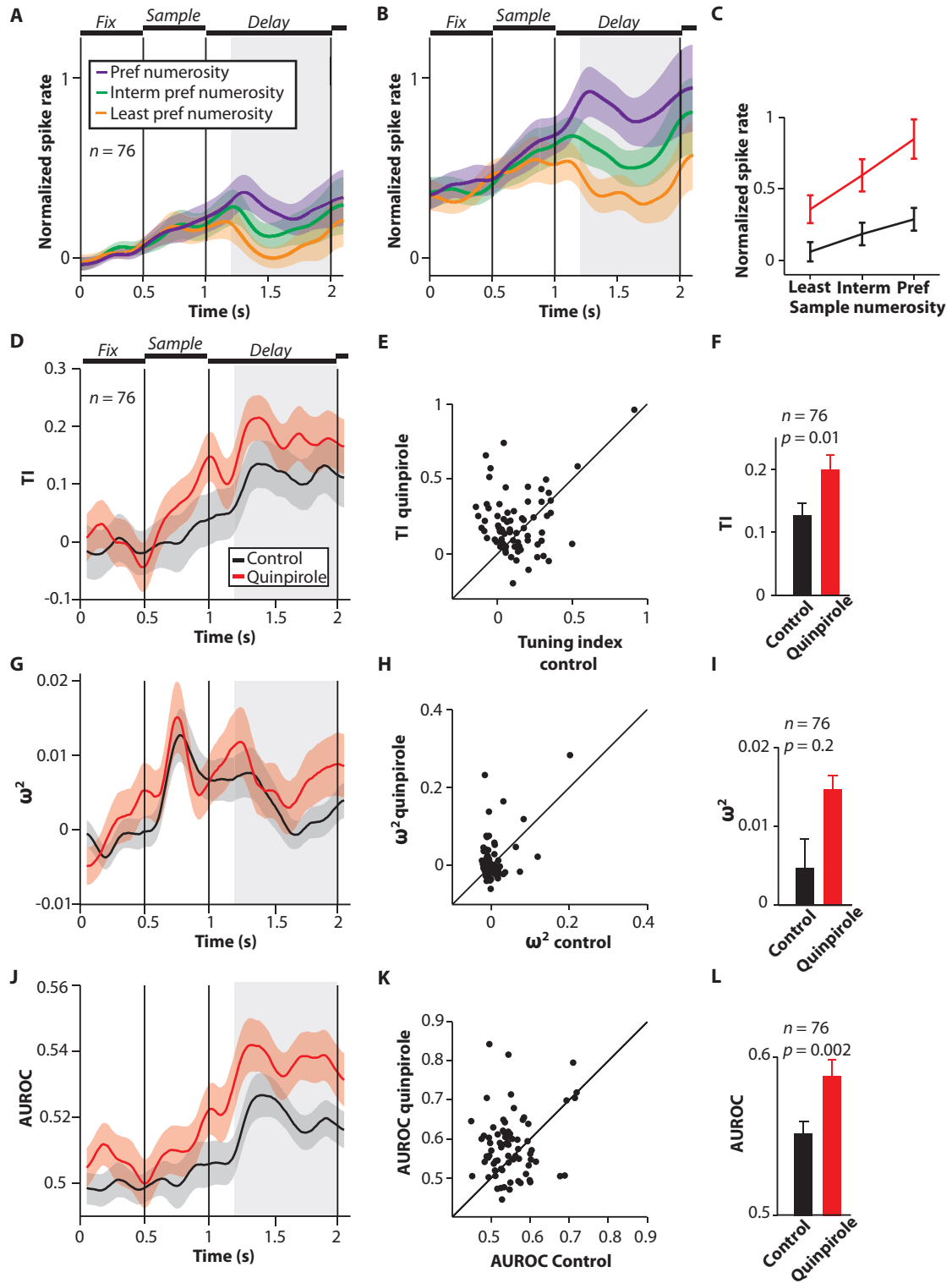


**Figure S3**

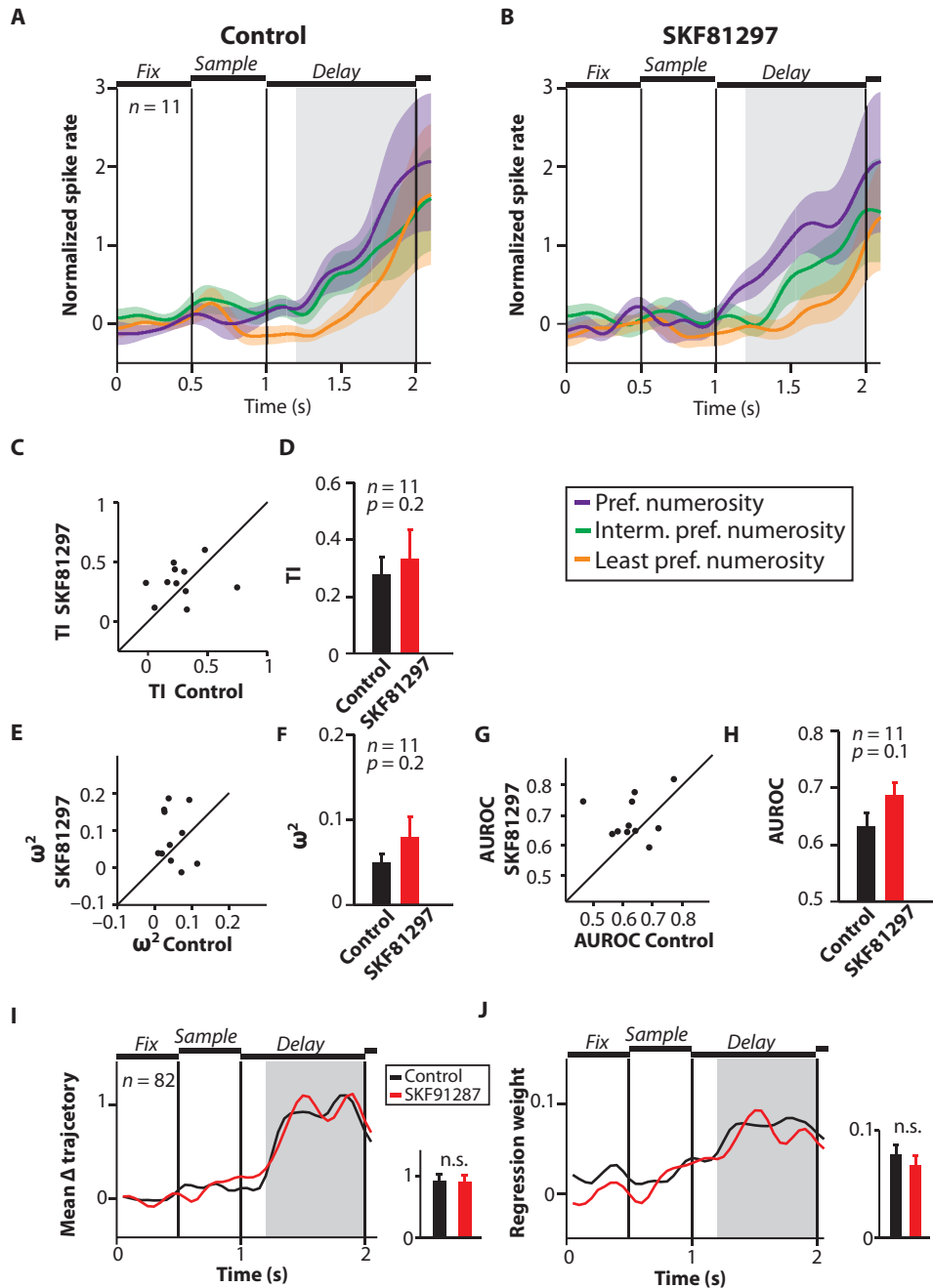


**Figure S4**

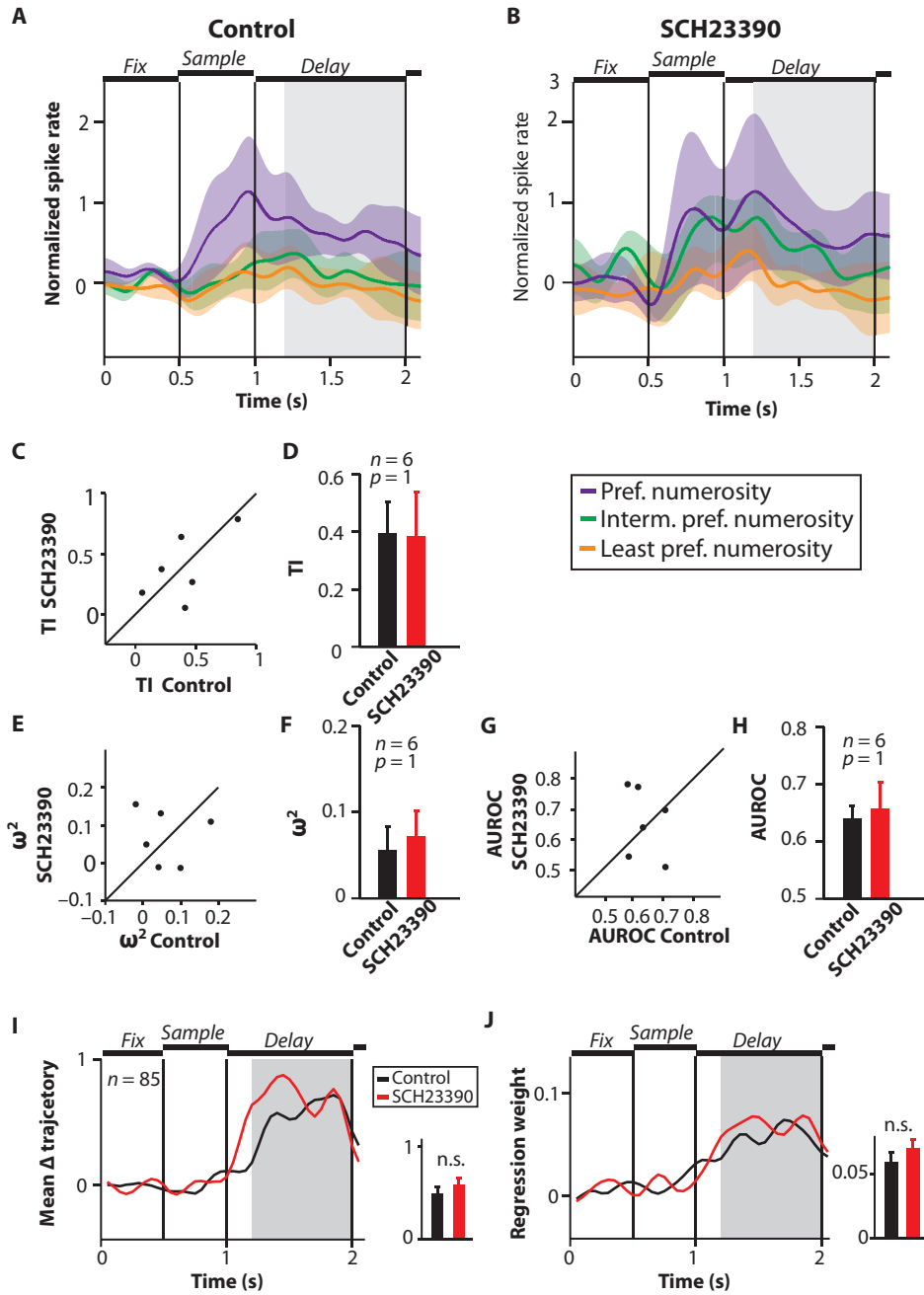


**Figure S5**

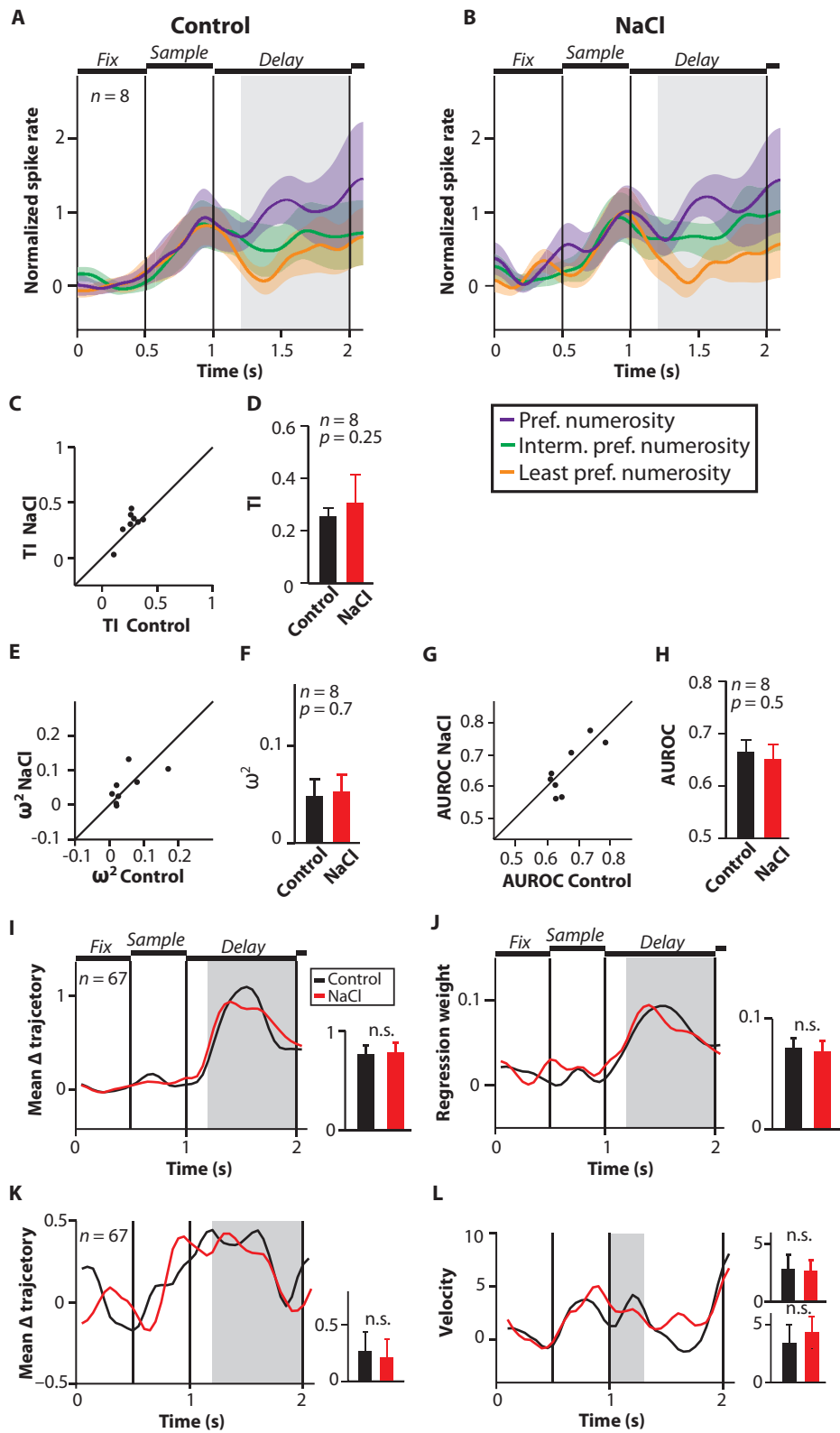
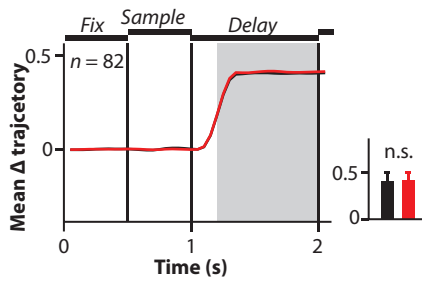


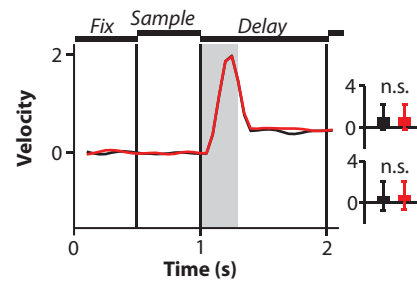


**Figure S8**

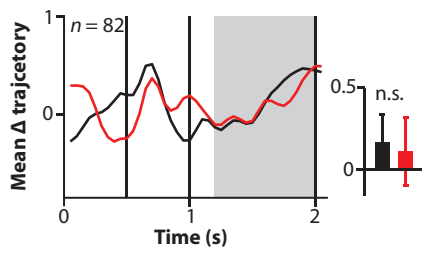
**A Simulation**



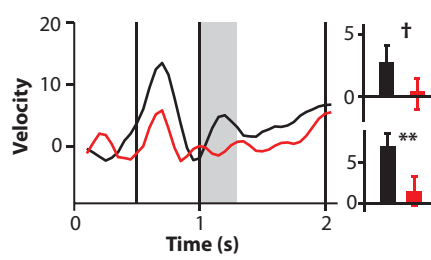
**B**



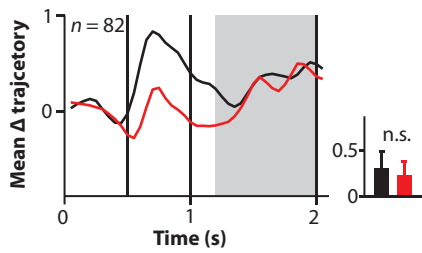
**C Cross-validation Set 1**



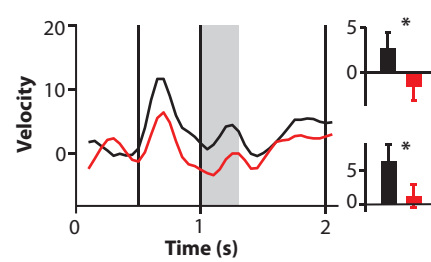
**D**



**E Cross-validation Set 2**



**F**





---

#### **Study 4: Dopamine receptor modulation of reward signals**

**Ott, T., Stein, A. M., Nieder, A.** (in preparation). Dopamine D1 and D2 receptors oppositely modulate reward signals in primate prefrontal cortex neurons.



# **Dopamine D1 and D2 receptors oppositely modulate reward signals in primate prefrontal cortex neurons**

Torben Ott, Anna Marlina Stein & Andreas Nieder\*

Animal Physiology, Institute of Neurobiology, Auf der Morgenstelle 28, University of  
Tübingen, 72076 Tübingen, Germany

\* To whom correspondence should be addressed:

E-mail: [andreas.nieder@uni-tuebingen.de](mailto:andreas.nieder@uni-tuebingen.de)

## **Abstract**

In the prefrontal cortex, different types of information are integrated to enable goal-directed behavior. The dopamine system innervates prefrontal networks, where it modulates information processing relevant for executive control. It remains unclear, however, how other types of information relevant to achieve goals are modulated by dopamine, such as the expected reward additionally represented by prefrontal neurons. Here we trained macaque monkeys on a reward-modulated working memory task, in which a reward cue at the beginning of each trial predicted the amount of reward for a correct choice at the end of a trial. We recorded from single units in the lateral prefrontal cortex while simultaneously stimulating dopamine D1 receptor (D1R) or dopamine D2 receptor (D2R) families using micro-iontophoresis. Stimulating D1Rs did not change responses to the reward cue itself, but impaired representations of reward expectancy during the delay period preceding sample presentation. This modulation depended on the strength of the modulation of spontaneous activity, which was generally inhibited by D1Rs. In contrast, D2R stimulation enhanced representations of reward expectancy signals in both cue and delay periods independently of modulation of spontaneous activity, which was generally excitatory. Thus, dopamine receptors oppositely modulated reward signals in primate prefrontal cortex neurons. These results suggest a distinct modulation of reward signals and cognitive signals by prefrontal dopamine, supporting the hypothesis that dopamine acts via different mechanism to control motivation and cognition.

## **Introduction**

The prefrontal cortex (PFC) mediates executive control functions to guide goal-directed behavior (Miller and Cohen, 2001). Single units in the PFC represent a variety of information related to executive control through persistent activity during behavior, such as working memory (Goldman-Rakic, 1995), categories (Nieder, 2002), and rules (Bongard and Nieder, 2010; Wallis et al., 2001). To achieve goals, other types of information are also relevant. For example, PFC neurons signal the value of goals by representing reward expectancy (Watanabe, 1996). Reward signals modulate cognitive signals in the PFC by increasing the representation of spatial memory signals for larger expected rewards (Amemori and Sawaguchi, 2006; Kennerley and Wallis, 2009; Leon and Shadlen, 1999; Roesch and Olson, 2003). Thus, PFC likely integrates reward signals and cognitive signals to mediate goal-directed behavior (Matsumoto et al., 2003; Watanabe, 2007).

The PFC is strongly innervated by the midbrain dopamine system acting via prefrontal dopamine D1 receptor (D1R) and dopamine D2 receptors (D2R) families (Björklund and Dunnett, 2007). Dopamine neurons fire phasic bursts with short latencies in response to important sensory events (Matsumoto and Hikosaka, 2009; Matsumoto and Takada, 2013; Schultz et al., 1997), in particular to reward predicting stimuli with larger bursts for larger rewards (Tobler et al., 2005). Behaviorally, larger rewards improve performance of monkeys in working memory tasks, reduce abortion of trials and reduce reaction times (Kennerley et al., 2009; Leon and Shadlen, 1999), likely by increasing motivation (Roesch and Olson, 2004). In PFC, dopamine modulates a variety of cognitive control functions (Robbins and Arnsten, 2009), including spatial working memory (Vijayraghavan et al., 2007; Williams and Goldman-Rakic, 1995), the representation of categories in working memory (Ott and Nieder, submitted),

abstract rules (Ott et al., 2014), and associations (Puig and Miller, 2012, 2015) via both D1Rs and D2Rs. D1R stimulation improves tuning of spatial working memory representations (Vijayraghavan et al., 2007) as well as representations of abstract rules (Ott et al., 2014), while blocking D1Rs has mixed effects on spatial working memory representations (Sawaguchi, 2001; Williams and Goldman-Rakic, 1995) and impairs representations of abstract rules in the PFC (Ott et al., 2014). D2R stimulation, on the other hand, improves both working memory representations (Ott and Nieder, submitted) and representations of abstract rules (Ott et al., 2014).

However, it remains unknown if prefrontal dopamine receptors modulate reward signals that are present in the PFC. Hypothetically, dopamine could act primarily on prefrontal reward signals that modulate memory processing, suggesting a common mechanism for dopamine modulation of reward and cognitive signals. Alternatively, dopamine could modulate prefrontal reward and memory signals independently, as suggested by recent recordings from midbrain dopamine neurons reporting that distinct populations of dopamine neurons were active during reward prediction and cognitive control (Matsumoto and Takada, 2013).

Here, we trained two macaque monkeys to perform a reward-modulated working memory task, in which a reward cue predicted the amount of reward the animals received for a correct choice. By specifically stimulating prefrontal D1Rs or D2Rs, we investigated dopamine receptor modulation of reward signals in prefrontal neurons. Contrary from findings for working memory and cognitive control (Ott and Nieder, submitted; Ott et al., 2014; Vijayraghavan et al., 2007), we found an opposite modulation of reward signals by D1Rs and D2Rs, suggesting that dopamine regulation of reward and cognitive signals might be implemented by distinct mechanisms.

## **Methods**

### **Animals and surgical procedures**

Two male rhesus monkeys (*Macaca mulatta*) were implanted with a titanium head post and one recording chamber centred over the principal sulcus of the lateral PFC, anterior to the frontal eye fields (right hemispheres in both monkeys). Surgery was conducted using aseptic techniques under general anaesthesia. Structural magnetic resonance imaging was performed before implantation to locate anatomical landmarks. All experimental procedures were in accordance with the guidelines for animal experimentation approved by the authority, the Regierungspräsidium Tübingen, Germany.

### **Task**

Monkeys learned to perform a reward-modulated working memory task using a delayed matching-to-sample design. They initiated a trial by grasping a lever and maintaining central fixation on a screen. After a pure fixation period (500 ms), a reward cue (300 ms) cued the reward size the monkeys would get for a correct choice at the end of trial. The reward cue was followed by a delay period (delay 1, 1,000 ms) without visual cues. Then a visual sample stimulus was presented (600 ms) that monkeys had to memorize during the subsequent delay period (delay 2, 1,000 ms). After the delay period, a test stimulus was shown, which was either the same visual item as presented during the sample period (match trial, 50 % of trials) or a different visual item (non-match trial, 50 % of trials). To make a correct choice, monkeys were required to release a lever during test 1 only if the same matching stimulus appeared and to keep holding the lever for another 1,000 ms if a non-matching stimulus appeared, which was followed by the test 2 phase showing always a matching stimulus,

during which the monkeys had to release the lever (1,000 ms). Thus, only test 1 required a decision; test 2 was used so that a behavioral response was required in each trial, ensuring that the monkeys were paying attention during all trials. Monkeys got a liquid reward for a correct choice with the amount of liquid determined by the reward cue shown in the beginning of each trial, corresponding to the reward size. We used two reward sizes and two reward cue sets, i.e. 4 different reward cues in total. In the color cue set, a red square indicated a large reward (monkey L 0.8 ml, monkey T 1.0 ml) and a blue square a small reward (monkey L 0.3 ml, monkey T 0.2 ml). Reward sizes were adjusted so that both monkeys showed comparable behavioral performance and effects of cued reward size difference. In the shape set, a gray annulus indicated a large reward and a gray cross indicated a small reward (same reward amount). In each session, we used three new different, randomly selected visual items (downloaded from flickr) as sample stimuli. Each sample stimulus served also as non-matching stimulus and vice versa. Trials were pseudo-randomized and balanced across all relevant features (reward size, reward cue set, sample stimulus, match and non-match trial). Monkeys had to keep their gaze within  $1.75^\circ$  of the fixation point from the fixation interval up to the lever release indicating their choice (monitored with an infrared eye-tracking system; ISCAN, Burlington, MA). If eye fixation was broken during the trial, the trial was aborted followed by a time-out (1,000 ms) and counted as a break trial for behavioral analysis.

### **Electrophysiology and iontophoresis**

Extracellular single-unit recording and iontophoretic drug application was performed as described previously (Jacob et al., 2013; Ott et al., 2014). In each recording session, up to three custom-made tungsten-in-glass electrodes



flanked by two pipettes each were inserted transdurally using a modified electrical microdrive (NAN Instruments). Single neurons were recorded at random; no attempt was made to preselect the neurons to any task-related activity or based on drug effects. Signal acquisition, amplification, filtering, and digitalization were accomplished with the MAP system (Plexon). Waveform separation was performed offline (Offline Sorter; Plexon). Drugs were applied iontophoretically (MVCS iontophoresis system; npi electronic) using custom-made tungsten-in-glass electrodes flanked by two pipettes each (Jacob et al., 2013; Ott et al., 2014; Thiele et al., 2006). Electrode impedance and pipette resistance were measured after each recording session. Electrode impedances were 0.8–3 M $\Omega$  (measured at 500 Hz; Omega Tip Z; World Precision Instruments). Pipette resistances depended on the pipette opening diameter, drug, and solvent used. Typical resistances were 15–50 M $\Omega$  (full range, 12–160 M $\Omega$ ). As in previous experiments (Jacob et al., 2013; Ott et al., 2014), we used retention currents of –7 nA to hold the drugs in the pipette during control conditions. The ejection current for SKF81297 (10 mM in double-distilled water, pH 4.0 with HCl; Sigma-Aldrich) was +15 nA, and the ejection current for quinpirole (10 mM in double-distilled water, pH 4.0 with HCl; Sigma-Aldrich) was +40 nA. We did not investigate dosage effects and chose ejection currents to match the values reported to be maximally effective, i.e., in the peak range of the ‘inverted-U function’ (Ott et al., 2014; Vijayraghavan et al., 2007; Wang et al., 2004). One pipette per electrode was filled with drug solution (either SKF81297 or quinpirole), and the other always contained 0.9 % NaCl. In each recording session, control conditions using the retention current alternated with drug conditions using the ejection current. Drugs were applied continuously for about 12 min (drug conditions), depending on the number of trials completed correctly by the animal. Each control or drug application block consisted of

72 correct trials to yield sufficient trials for analysis. The first block (12 min) was always the control condition. Given that iontophoretic drug application is fast and can quickly modulate neuronal firing properties (Jacob et al., 2013), we did not exclude data at the current switching points.

## Data analyses

*Reward-selective neurons.* All well-isolated recorded single units with a baseline spike rate above 0.5 Hz (determined in the 500 ms fixation period preceding sample presentation) and at least 12 trials in each reward size, reward cue set, and iontophoretic drug application condition (i.e., at least 96 trials in total) entered the analyses. Neurons were not included based on drug effects. We calculated a 3-way ANOVA for each neuron to determine if a neuron's response was correlated with reward expectancy using spike rates in two different analysis periods. The first analysis period, the cue phase, was defined using a 400 ms window beginning 100 ms after reward cue onset. The second analysis period, the delay period, was defined using a 900 ms window beginning 200 ms after sample offset, i.e. non-overlapping with the cue period. Main factors for each ANOVA were reward size (large/small), reward cue set (color set/shape set) and iontophoretic drug condition (control/drug application), including interaction terms. We labelled a neuron as selective for reward expectancy (reward-selective), if it showed a significant main effect of reward size ( $p < 0.05$ ) and no significant main effect of reward cue set ( $p > 0.05$ ) and no interaction between reward size and reward cue set ( $p > 0.05$ ). Thus, we isolated neurons only representing reward expectancy signals. Analysis was independently repeated for the cue and the delay period.

*Single-cell and population responses.* For plotting single-cell spike density histograms, the average firing rate in trials with one of the four different rule-

cues (correct trials only) was smoothed with a Gaussian kernel (bin width of 200 ms, steps of 1 ms) for visual presentation only. For the population responses, trials with rule-cues signifying the same numerical rule were pooled. A neuron's preferred reward size was defined as the reward size (large or small) yielding the higher average spike rate in the analysis windows used for the ANOVAs. The nonpreferred reward size was defined as the reward size resulting in lower average spike rate. Neuronal activity was normalized by subtracting the mean baseline firing rate in the control condition and dividing by the standard deviation of the baseline firing rates in the control condition. For population histograms, normalized activity was averaged and smoothed with a Gaussian kernel (width of 200 ms, step of 1 ms) for visual presentation only.

*Tuning index and receiver operating characteristic analysis.* We quantified the selectivity for reward expectancy for each neuron by calculating a tuning index (TI), defined as the difference in normalized response (normalized as above) between drug and control conditions using spike rates calculated in the same analysis windows as used for the ANOVAs. Rule coding quality was further quantified using receiver operating characteristic (ROC) analysis derived from Signal Detection Theory (Green and Swets, 1966). The area under the ROC curve (AUROC) is a nonparametric measure of the discriminability of two distributions. It denotes the probability with which an ideal observer can tell apart a meaningful signal from a noisy background. Values of 0.5 indicate no separation, and values of 1 signal perfect discriminability. The AUROC takes into account both the difference between distribution means as well as their widths and is therefore a suitable indicator of signal quality (Parker and Newsome, 1998). We used AUROCs to quantify the quality of reward expectancy coding. We calculated the AUROC for each neuron using the spike

rate distributions of the preferred and the nonpreferred reward size in the same analysis windows used for the ANOVAs.

## Results

Two macaque monkeys learned a reward-modulated working memory task, in which they had to memorize a visual item on a screen for a short period of time to report in a subsequent test phase if they had seen the item before (**Figure 1A,B**). A reward cue at the beginning of each trial modulated the monkey's reward expectancy in the delay period preceding the sample item, cueing either a large reward or a small reward for a correct choice at the end of each trial. Two reward cue sets based on color or shape were used to dissociate reward expectancy signals from sensory signals related to cue appearance (**Figure 1C**).

The behavior of both monkeys was modulated by reward expectancy. Behavioral performance, i.e. percentage of correct trials, was slightly lower in trials with small reward expectancy in comparison to trials with large reward expectancy for both monkeys (**Figure 1D,E**,  $\Delta$ performance = 3.1 %  $\pm$  0.3 % (large minus small),  $n = 79$  sessions,  $p < 10^{-6}$ , ANOVA, for monkey L;  $\Delta$ performance = 3.2 %  $\pm$  0.4 %,  $n = 80$ ,  $p < 10^{-5}$  for monkey T) and was not influenced by reward cue set ( $p > 0.2$  for main factor reward cue set or interactions between reward size and reward cue set). The percentage of aborted trials in which monkeys broke eye fixation was larger in trials with small reward expectancy compared to trials with large reward expectancy for both monkeys (**Figure 1F,G**,  $\Delta$ breaks = -17 %  $\pm$  0.9 %,  $n = 79$ ,  $p < 10^{-10}$ , for monkey L;  $\Delta$ breaks = -14 %  $\pm$  1.5 %,  $n = 80$ ,  $p < 10^{-10}$ , for monkey T), and was not influenced by reward cue set ( $p > 0.2$  for all other comparisons). Finally,

reaction times (RTs) of both monkeys were longer in trials with small reward expectancy compared to trials with large reward expectancy (**Figure 1H,I**,  $\Delta RT = -42 \text{ ms} \pm 2 \text{ ms}$ ,  $n = 79$ ,  $p < 10^{-10}$ , for monkey L;  $\Delta RT = -38 \text{ ms} \pm 5 \text{ ms}$ ,  $n = 80$ ,  $p < 10^{-10}$ , for monkey T), again independent of reward cue set ( $p > 0.7$  for all other comparisons). Thus, the monkey's working memory performance was modulated by reward expectancy, indicating that reward expectancy changes the motivational state.

We recorded 256 single units in 159 recording sessions (79 for monkey L, 80 for monkey T) from the lateral PFC of both monkeys (**Table 1**), while the monkeys were performing the task. To directly assess the impact of dopamine receptor targeting agents on neuronal reward expectancy signals, each neuron was recorded both without drug application (*control condition*) and while stimulating dopamine receptor agents at the vicinity of the recorded neurons using micro-iontophoresis (*drug condition*). Control conditions alternated with drug conditions in each recording session. In each session we tested one of two different substances that selectively targeted the D1R or the D2R: The D1R was assessed in 129 neurons by applying the D1R agonist SKF81297. The D2R was tested in 127 neurons using the D2R-agonist quinpirole. In previous experiments, we did not find any effect on neuronal firing properties when applying normal saline (Jacob et al., 2013; Ott et al., 2014). We identified neurons selective for reward expectancy based on two non-overlapping analysis windows, a cue period (400 ms, beginning 100 ms after reward cue onset) and a delay period (900 ms, beginning 200 ms after sample offset), using a 3-way ANOVA with main factors reward size (large/small), reward cue set (color/shape) and iontophoretic drug application (control condition/drug condition). Neurons with a significant main effect of reward size ( $p < 0.05$ ), i.e. neurons that were selective for reward expectancy, were included in

subsequent analyses. To analyze dopamine receptor modulation of pure reward expectancy signals, we excluded neurons with significant main effects of reward cue set or an interaction between reward size and reward cue set ( $p < 0.05$ ).

About one quarter (58/256 neurons) and one third (74/256 neurons) of all recorded neurons were exclusively selective for reward expectancy in cue and delay period, respectively (**Table 1**). Surprisingly, more neurons preferred the small reward size, i.e. had a larger firing rate during trials with small reward expectancy as compared to trials with large reward expectancy (**Table 2**). In the cue period, almost three quarter of reward-selective neurons preferred the small reward, significantly more than predicted by equal distribution (42/58 neurons,  $p = 5 \cdot 10^{-4}$ ,  $\chi^2$  test against equal distribution). In the delay period, numbers were more even with a few more neurons preferring the small reward (45/74 neurons,  $p = 0.06$ ).

### **D2R stimulation, but not D1R stimulation, enhances reward signals in the cue period**

An example neuron selective for reward expectancy during the cue period preferring the large reward was slightly inhibited after D1R stimulation with SKF81297 (**Figure 2A**). Population responses were constructed by pooling trials of both reward cue sets and averaging normalized activity of preferred and nonpreferred reward size, defined as the reward size yielding the larger and lower firing rate, respectively. The population of all reward-selective neurons recorded during sessions with SKF81297 application did not reveal any systematic effect of D1R stimulation on neuronal firing properties (**Figure 2C**). In contrast, D2R stimulation with quinpirole of another neuron selective for small reward expectancy showed a prominent increase in reward selectivity

(**Figure 2B**). This effect was systematically observed for the population activity of all neurons recorded during session with quinpirole application (**Figure 2D**). We quantified the reward selectivity of neurons by calculating a tuning index (TI), defined as the normalized response difference between the preferred and nonpreferred reward size. D1R stimulation did not systematically change TIs during the cue period (**Figure 3A**,  $\Delta\text{TI} = +0.04 \pm 0.09$ ,  $n = 30$ ,  $p = 0.6$ , signed rank test). In contrast, D2R stimulation significantly increased the selectivity for reward expectancy coding, both in neurons preferring small and large reward (**Figure 3B**,  $\Delta\text{TI} = +0.18 \pm 0.07$ ,  $n = 28$ ,  $p = 0.02$ ). In addition, we quantified the coding quality of reward expectancy for each neuron by using the area under the receiver operator characteristic (AUROC) derived from signal detection theory. Values of 0.5 correspond to an absence of coding, large values closer to one indicate strong coding quality. Consistent with the previous results, D1R stimulation with SKF81297 did not systematically change AUROCs in the cue period (**Figure 3C**,  $\Delta\text{AUROC} = +0.01 \pm 0.01$ ,  $n = 30$ ,  $p = 0.2$ , signed rank test). In contrast, D2R stimulation significantly increased AUROCs of all selective neurons in the cue period of both small and large reward preferring neurons (**Figure 3D**,  $\Delta\text{AUROC} = +0.03 \pm 0.01$ ,  $n = 28$ ,  $p = 0.05$ ). Thus, D2R stimulation, but not D1R stimulation, increased reward expectancy coding of single neurons during the cue period.

### **D1R and D2R stimulation have opposite effects on reward signals in the delay period**

During the delay period, stimulating D1Rs with SKF81297 strongly impaired the selectivity of an example neuron selective for small reward expectancy (**Figure 4A**). This effect was consistently observed for all selective neurons recorded in sessions with SKF81297 application, showing that D1R stimulation decreased selectivity for the neurons' preferred reward size (**Figure 4C**). In

contrast, D2R stimulation with quinpirole increased the selectivity for small rewards during the delay period of another single unit (Figure 4B), as also observed for the population of all selective neurons recorded in session with quinpirole application (Figure 4D). Accordingly, SKF81297 decreased TIs during the delay period (**Figure 5A**,  $\Delta\text{TI} = -0.13 \pm 0.06$ ,  $n = 31$ ,  $p = 0.05$ , signed rank test) and quinpirole increased TIs during the delay period in both neurons preferring small and large reward sizes, thus enhancing the neurons' reward selectivity (**Figure 5B**,  $\Delta\text{TI} = +0.14 \pm 0.06$ ,  $n = 43$ ,  $p = 0.007$ ). Coding quality was impaired by D1R stimulation with SKF81297, too, witnessed by a significant decrease in AUROCs (**Figure 5C**,  $\Delta\text{AUROC} = -0.01 \pm 0.005$ ,  $n = 31$ ,  $p = 0.01$ , signed rank test). In contrast, D2R stimulation with quinpirole significantly increased AUROCs in both neurons preferring small and large reward sizes (**Figure 5D**,  $\Delta\text{AUROC} = +0.02 \pm 0.01$ ,  $n = 43$ ,  $p = 0.002$ ), thus enhancing the neurons' coding capacity for reward expectancy. Thus, D1Rs and D2Rs act oppositely on the coding of reward expectancy of single units during the delay period.

### **D1R effect on reward signals depend on baseline modulation**

Finally, we considered the possibility that the modulatory effects of D1Rs and D2Rs are connected to changes in baseline firing rates. As reported previously (Ott et al., 2014), D1R slightly inhibited the neuronal firing, decreasing the neurons' baseline (BL) firing rates (**Figure 6A**,  $\Delta\text{BL} = -0.33 \text{ sp/s} \pm 0.13 \text{ sp/s}$ ,  $n = 129$ ,  $p = 0.008$ , signed rank test). Oppositely, D2Rs increased the neurons' baseline firing rates (**Figure 6D**,  $\Delta\text{BL} = +1.5 \text{ sp/s} \pm 0.29 \text{ sp/s}$ ,  $n = 127$ ,  $p = 10^{-10}$ ). Since our measure of coding quality considers both the distance in the mean and the width between two spike rate distributions, proportional changes of AUROCs cannot be explained by simple additive or multiplicative mechanism that would also scale the noise and thus the width of observed spike rate



distributions (Herrero et al., 2008; Jacob et al., 2013; Parker and Newsome, 1998). To investigate if changes of coding quality are connected to changes of a neuron's baseline firing rate induced by dopamine receptor stimulation, we correlated the drug-induced change in AUROCs with the drug-induced change in baseline firing rates. Interestingly, changes in coding and baseline firing induced by D1R stimulation with SKF81297 were significantly correlated in both the cue (**Figure 6B**,  $R = 0.40$ ,  $n = 30$ ,  $p = 0.03$ , t-statistics) and delay (**Figure 6E**,  $R = 0.36$ ,  $n = 31$ ,  $p = 0.05$ ) period. In contrast, although D2R stimulation with quinpirole in general showed a stronger effect on baseline firing rates, we did not find a correlation between quinpirole-induced changes of coding quality and baseline firing rates in the cue period (**Figure 6C**,  $R = 0.25$ ,  $n = 28$ ,  $p = 0.2$ , t-statistics) or the delay period (**Figure 6F**,  $R = 0.17$ ,  $n = 43$ ,  $p = 0.3$ ). Thus, changes in coding capacity are connected to changes in baseline firing rates for the D1R, but not the D2R.

## Discussion

We report that D1Rs and D2Rs modulate reward expectancy signals in PFC neurons in distinct ways. D1Rs did not systematically change neuronal responses following reward cue presentation, while impairing neuronal representations of reward expectancy during the delay period. This effect depended on D1R modulation of spontaneous activity. In contrast, D2R stimulation enhanced neuronal reward expectancy representations during both cue and delay periods independently of D2R effects on the neurons' baseline activity.

## **Reward expectation modulated behavioral performance**

Explicitly cued differences in reward size that are learned through classical conditioning of an unconditioned stimulus with a reward were reflected in the monkey's behavior. Confirming that the animals followed reward contingencies, larger rewards lead to improved performance, shorter reaction times, and fewer trials that are aborted by the animals, consistent with previous finding that used spatial working memory tasks and reported similar effects using the same behavioral variables (Amemori and Sawaguchi, 2006; Kennerley and Wallis, 2009; Roesch and Olson, 2003). Thus, differences in reward expectancy changed the monkeys performance in the working memory task. We note that this effect could also be attributed to a change in motivation of the animal, since a larger reward leads to a larger motivation (Roesch and Olson, 2004). In this and other task designs, reward expectancy and motivation are interchangeable.

## **Neuronal reward signals and dopamine**

Single neurons in the PFC represented expected reward magnitudes following presentation of the reward cue and during the delay period preceding sample presentations. Neuronal representations of reward expectation in PFC were found in a number of previous studies that reported coding of reward expectation (Kennerley and Wallis, 2009; Kobayashi et al., 2002, 2006; Wallis and Miller, 2003; Watanabe, 1996) or a modulation of prefrontal visual (Amemori and Sawaguchi, 2006) and spatial memory signals by reward expectation (Kennerley and Wallis, 2009; Kobayashi et al., 2002; Lee et al., 2007; Leon and Shadlen, 1999; Roesch and Olson, 2003; Wallis and Miller, 2003; Watanabe et al., 2005). Neuronal responses to the reward cue were fast and strongly modulated by the expected reward size. Given that dopamine neurons

fire phasic bursts in response to salient sensory events (Matsumoto and Hikosaka, 2009; Schultz et al., 1997), in particular graded responses in response to cues predicting expected reward (Tobler et al., 2005), it seems likely that the source of cortical reward signals stem from midbrain dopamine neurons, where reward prediction errors are computed (Eshel et al., 2015). Interestingly, more neurons were selective for small reward expectancies compared to large reward expectancies. This finding was reported previously for PFC neurons (Kennerley and Wallis, 2009) is in agreement to a study that reported higher prefrontal dopamine levels following small reward as compared to large reward predictions (Kodama et al., 2014).

### **D1R modulation of reward signals**

As reported previously, D1R activation slightly suppressed neuronal firing in general (Ott et al., 2014; Vijayraghavan et al., 2007). Surprisingly, activating D1Rs did not systematically modulate reward signals in the cue period. However, there was a significant correlation between reward modulation and baseline modulation in the cue period. Given the narrow inverted-U response curve of D1R effects on neuronal selectivity (Vijayraghavan et al., 2007), systematic changes might have been masked. In the delay period, however, D1R activation systematically decreased neuronal representations of reward expectations. This finding was unexpected, given that the same dose of D1R stimulation increased spatial working memory signals (Vijayraghavan et al., 2007), and representations of visual samples and abstract behavioral rules (Ott et al., 2014). This result suggests that neuronal networks representing reward signals might be modulated distinctly from networks representing cognitive signals, which are also modulated by D1Rs. Blocking prefrontal D1Rs impairs association learning and signals (Puig and Miller, 2012), and modulates

attentional processing (Noudoost and Moore, 2011). This differential modulation could be realized by prefrontal populations with distinct properties, such as a shifted inverted-U curve. Alternatively, dopamine could carry independent signals to modulate reward signals and cognitive signals, as suggested by recent recordings from midbrain dopaminergic neurons reporting that distinct populations of dopaminergic neurons are carrying reward and cognitive signals (Matsumoto and Takada, 2013). Mechanistically, D1-mediated inhibition might be realized by increasing IPSCs in prefrontal pyramidal cells (Seamans et al., 2001a; Trantham-Davidson et al., 2004). However, D1Rs have also been shown an increase in NMDA-evoked responses (Seamans et al., 2001b; Tseng and O'Donnell, 2004), possibly contributing to the D1-mediated enhancement of cognitive signals (Durstewitz and Seamans, 2008; Ott et al., 2014), suggesting that the present findings are dominated by inhibitory effects.

### **D2R modulation of reward signals**

D2R stimulation, on the other hand, improved neuronal reward expectancy coding in both cue and delay periods. This result suggests that D2Rs play a prominent role in regulating prefrontal reward signals. Recently, D2Rs have been reported to modulate variety of prefrontal signals, such as feature-based working memory (Ott and Nieder, submitted) and the representation of abstract behavioral rules (Ott et al., 2014). Furthermore, they play a role in cognitive flexibility. Blocking prefrontal D2Rs impairs learning of new association rules in primates (Puig and Miller, 2015) and impairs rodents in shifting between different response strategies (Floresco and Magyar, 2006). Thus, D2Rs might contribute to the integration of a variety of prefrontal signals carrying both information about rewards and information relevant for executive control, such as working memory, associations, and rules. In addition, D2Rs also seem involved in the behavioral output, as they modulate saccade

signals in PFC (Wang et al., 2004) and influence saccadic target selection in FEF (Noudoost and Moore, 2011). In general, D2Rs slightly increased the neurons' spontaneous activity, as reported previously (Ott et al., 2014; Wang and Goldman-Rakic, 2004; Wang et al., 2004). Mechanistically, excitatory D2R effects might be mediated by decreasing GABAergic responses in pyramidal cells (Seamans et al., 2001a). At the same time, D2Rs have also been shown to increase interneurons' excitability (Zhong and Yan, 2016). Together, these mechanisms might induce an increase in neuronal selectivity during delay periods, as suggested by computational modeling (Ott and Nieder, submitted). Thus, a general mechanism might explain D2R modulation of working memory, abstract, and reward signals in PFC. Interestingly, D2R modulation of reward signals did not correlate with D2R signals of baseline modulation, challenging simple common mechanisms such as gain modulation. Rather, these results suggest a direct interaction of D2Rs with reward encoding mechanisms (Herrero et al., 2008).

### **Opposite modulation of D1Rs and D2Rs of reward signals**

Together, our results show that D1Rs and D2Rs oppositely modulate both spontaneous activity and reward signals in primate PFC neurons. This contrasts effects on cognitive signals subserving executive control, such as working memory (Ott and Nieder, submitted), representations of abstract behavioral rules (Ott et al., 2014), and association learning (Puig and Miller, 2012, 2015) for which D1Rs and D2Rs assume complementary roles in enhancing neuronal information processing. These results suggest that distinct mechanisms in PFC control information processing for executive control and other types of information processing relevant for goal-directed behavior, such as the representations of reward and the value of goals.

## References

- Amemori, K., and Sawaguchi, T. (2006). Contrasting effects of reward expectation on sensory and motor memories in primate prefrontal neurons. *Cereb. Cortex* 16, 1002–1015.
- Björklund, A., and Dunnett, S.B. (2007). Dopamine neuron systems in the brain: an update. *Trends Neurosci.* 30, 194–202.
- Bongard, S., and Nieder, A. (2010). Basic mathematical rules are encoded by primate prefrontal cortex neurons. *Proc. Natl. Acad. Sci. U. S. A.* 107, 2277–2282.
- Durstewitz, D., and Seamans, J.K. (2008). The dual-state theory of prefrontal cortex dopamine function with relevance to catechol-o-methyltransferase genotypes and schizophrenia. *Biol. Psychiatry* 64, 739–749.
- Eshel, N., Bukwich, M., Rao, V., Hemmelder, V., Tian, J., and Uchida, N. (2015). Arithmetic and local circuitry underlying dopamine prediction errors. *Nature* 525, 243–246.
- Floresco, S.B., and Magyar, O. (2006). Mesocortical dopamine modulation of executive functions: beyond working memory. *Psychopharmacol.* 188, 567–585.
- Goldman-Rakic, P.S. (1995). Cellular basis of working memory. *Neuron* 14, 477–485.
- Green, D.M., and Swets, J.A. (1966). *Signal Detection Theory and Psychophysics* (New York: Wiley).
- Herrero, J.L., Roberts, M.J., Delicato, L.S., Gieselmann, M. a, Dayan, P., and Thiele, A. (2008). Acetylcholine contributes through muscarinic receptors to attentional modulation in V1. *Nature* 454, 1110–1114.
- Jacob, S.N., Ott, T., and Nieder, A. (2013). Dopamine regulates two classes of primate prefrontal neurons that represent sensory signals. *J. Neurosci.* 33, 13724–13734.
- Kennerley, S.W., and Wallis, J.D. (2009). Reward-Dependent Modulation of Working Memory in Lateral Prefrontal Cortex. *J. Neurosci.* 29, 3259–3270.
- Kennerley, S.W., Dahmubed, A.F., Lara, A.H., and Wallis, J.D. (2009). Neurons in the frontal lobe encode the value of multiple decision variables. *J. Cogn. Neurosci.* 21, 1162–1178.
- Kobayashi, S., Lauwereyns, J., Koizumi, M., Sakagami, M., and Hikosaka, O. (2002). Influence of reward expectation on visuospatial processing in macaque lateral prefrontal cortex. *J. Neurophysiol.* 87, 1488–1498.
- Kobayashi, S., Nomoto, K., Watanabe, M., Hikosaka, O., Schultz, W., and Sakagami, M. (2006). Influences of rewarding and aversive outcomes on activity in macaque lateral prefrontal cortex. *Neuron* 51, 861–870.

- Kodama, T., Hikosaka, K., Honda, Y., Kojima, T., and Watanabe, M. (2014). Higher dopamine release induced by less rather than more preferred reward during a working memory task in the primate prefrontal cortex. *Behav. Brain Res.* 266, 104–107.
- Lee, D., Rushworth, M.F.S., Walton, M.E., Watanabe, M., and Sakagami, M. (2007). Functional specialization of the primate frontal cortex during decision making. *J. Neurosci.* 27, 8170–8173.
- Leon, M.I., and Shadlen, M.N. (1999). Effect of expected reward magnitude on the response of neurons in the dorsolateral prefrontal cortex of the macaque. *Neuron* 24, 415–425.
- Matsumoto, M., and Hikosaka, O. (2009). Two types of dopamine neuron distinctly convey positive and negative motivational signals. *Nature* 459, 837–841.
- Matsumoto, M., and Takada, M. (2013). Distinct representations of cognitive and motivational signals in midbrain dopamine neurons. *Neuron* 79, 1011–1024.
- Matsumoto, K., Suzuki, W., and Tanaka, K. (2003). Neuronal correlates of goal-based motor selection in the prefrontal cortex. *Science* 301, 229–232.
- Miller, E.K., and Cohen, J.D. (2001). An integrative theory of prefrontal cortex function. *Annu. Rev. Neurosci.* 24, 167–202.
- Nieder, A. (2002). Representation of the quantity of visual items in the primate prefrontal cortex. *Science* (80-. ). 297, 1708–1711.
- Noudoost, B., and Moore, T. (2011). Control of visual cortical signals by prefrontal dopamine. *Nature* 474, 372–375.
- Ott, T., and Nieder, A. (submitted). Dopamine D2 receptors enhance population dynamics in primate prefrontal working memory circuits. Submitted.
- Ott, T., Jacob, S.N., and Nieder, A. (2014). Dopamine receptors differentially enhance rule coding in primate prefrontal cortex neurons. *Neuron* 84, 1317–1328.
- Parker, A.J., and Newsome, W.T. (1998). Sense and the single neuron: probing the physiology of perception. *Annu. Rev. Neurosci.* 21, 227–277.
- Puig, M.V., and Miller, E.K. (2012). The role of prefrontal dopamine D1 receptors in the neural mechanisms of associative learning. *Neuron* 74, 874–886.
- Puig, M.V., and Miller, E.K. (2015). Neural substrates of dopamine D2 receptor modulated executive functions in the monkey prefrontal cortex. *Cereb. Cortex* 25, 2980–2987.
- Robbins, T.W., and Arnsten, A.F.T. (2009). The neuropsychopharmacology of fronto-executive function: monoaminergic modulation. *Annu. Rev. Neurosci.* 32, 267–287.

- Roesch, M.R., and Olson, C.R. (2003). Impact of expected reward on neuronal activity in prefrontal cortex, frontal and supplementary eye fields and premotor cortex. *J. Neurophysiol.* *90*, 1766–1789.
- Roesch, M.R., and Olson, C.R. (2004). Neuronal activity related to reward value and motivation in primate frontal cortex. *Science* (80- ). *304*, 307–310.
- Sawaguchi, T. (2001). The effects of dopamine and its antagonists on directional delay-period activity of prefrontal neurons in monkeys during an oculomotor delayed-response task. *Neurosci. Res.* *41*, 115–128.
- Schultz, W., Dayan, P., and Montague, P.R. (1997). A neural substrate of prediction and reward. *Science* (80- ). *275*, 1593–1599.
- Seamans, J.K., Gorelova, N., Durstewitz, D., and Yang, C.R. (2001a). Bidirectional dopamine modulation of GABAergic inhibition in prefrontal cortical pyramidal neurons. *J. Neurosci.* *21*, 3628–3638.
- Seamans, J.K., Durstewitz, D., Christie, B.R., Stevens, C.F., Sejnowski, T.J., and F, S.C. (2001b). Dopamine D1/D5 receptor modulation of excitatory synaptic inputs to layer V prefrontal cortex neurons. *Proc. Natl. Acad. Sci. U. S. A.* *98*, 301–306.
- Thiele, A., Delicato, L.S., Roberts, M.J., and Gieselmann, M. a (2006). A novel electrode-pipette design for simultaneous recording of extracellular spikes and iontophoretic drug application in awake behaving monkeys. *J. Neurosci. Methods* *158*, 207–211.
- Tobler, P.N., Fiorillo, C.D., and Schultz, W. (2005). Adaptive coding of reward value by dopamine neurons. *Science* (80- ). *307*, 1642–1645.
- Trantham-Davidson, H., Neely, L.C., Lavin, A., and Seamans, J.K. (2004). Mechanisms underlying differential D1 versus D2 dopamine receptor regulation of inhibition in prefrontal cortex. *J. Neurosci.* *24*, 10652–10659.
- Tseng, K.Y., and O'Donnell, P. (2004). Dopamine-glutamate interactions controlling prefrontal cortical pyramidal cell excitability involve multiple signaling mechanisms. *J. Neurosci.* *24*, 5131–5139.
- Vijayraghavan, S., Wang, M., Birnbaum, S.G., Williams, G. V, and Arnsten, A.F.T. (2007). Inverted-U dopamine D1 receptor actions on prefrontal neurons engaged in working memory. *Nat. Neurosci.* *10*, 376–384.
- Wallis, J.D., and Miller, E.K. (2003). Neuronal activity in primate dorsolateral and orbital prefrontal cortex during performance of a reward preference task. *Eur. J. Neurosci.* *18*, 2069–2081.
- Wallis, J.D., Anderson, K.C., and Miller, E.K. (2001). Single neurons in prefrontal cortex encode abstract rules. *Nature* *411*, 953–956.
- Wang, Y., and Goldman-Rakic, P.S. (2004). D2 receptor regulation of synaptic burst firing in prefrontal cortical pyramidal neurons. *Proc. Natl. Acad. Sci. U. S. A.* *101*, 5093–5098.



- Wang, M., Vijayraghavan, S., and Goldman-Rakic, P.S. (2004). Selective D2 receptor actions on the functional circuitry of working memory. *Science* (80-. ). 303, 853–856.
- Watanabe, M. (1996). Reward expectancy in primate prefrontal neurons. *Nature* 382, 629–632.
- Watanabe, M. (2007). Role of anticipated reward in cognitive behavioral control. *Curr. Opin. Neurobiol.* 17, 213–219.
- Watanabe, M., Hikosaka, K., Sakagami, M., and Shirakawa, S.-I. (2005). Functional significance of delay-period activity of primate prefrontal neurons in relation to spatial working memory and reward/omission-of-reward expectancy. *Exp. Brain Res.* 166, 263–276.
- Williams, G. V, and Goldman-Rakic, P.S. (1995). Modulation of memory fields by dopamine D1 receptors in prefrontal cortex. *Nature* 376, 572–575.
- Zhong, P., and Yan, Z. (2016). Distinct Physiological Effects of Dopamine D4 Receptors on Prefrontal Cortical Pyramidal Neurons and Fast-Spiking Interneurons. *Cereb. Cortex* 26, 180–191.

## **Acknowledgments**

This work was supported by grants from the German Research Foundation (DFG) to A.N. (NI 618/5-1).

## **Author contributions**

T.O. designed and performed experiments, analyzed data and wrote the paper. A.M.S. performed experiments and analyzed data. A.N. designed experiments and wrote the paper.

## Figure legends

**Figure 1. Reward modulated working memory task and behavioral performance.** (A) Monkeys had to grab a lever and fixate a central fixation spot throughout the length of each trial. After a pure fixation period, a reward cue predicted the amount of liquid reward the monkeys received at the end of a trial for a correct choice. After the first delay period, a visual sample stimulus appeared on the screen, which had to be memorized during the second delay period. In the test period, monkeys had to release the lever if the same stimulus appeared (50 % of trials) and to keep holding the lever if a different stimulus appeared (50 % of trials) to receive a liquid reward. (B) Example sample stimuli. In each session, three new stimuli were used. (C) Two sets of cues indicated the reward size, a color set (red square for large reward, blue square for small reward) and a shape set (gray annulus for large reward, gray cross for small reward). (D) Behavioral performance for monkey L for all different conditions (left). Performance was lower on small reward trials (right). (E) Same conventions as in (D) for monkey T. (F) Percentage of aborted trials (i.e., trial in which the monkey broke eye fixation) for monkey L was higher for small reward trials. (G) Same conventions as in (F) for monkey T. (H) Reaction times of monkey L were longer for small reward trials. (I) Same conventions as in (H) for monkey T. \*\*\*  $p < 0.001$  (ANOVA).

**Figure 2. D1R and D2R modulation of reward expectancy selective neurons during the cue period.** (A) Example recorded during control conditions (left) and after stimulating D1Rs with SKF81297 (right) selective for large reward expectancy during the cue period (gray shaded area). (B) A different example neuron recorded during control conditions (left) and after stimulating D2Rs with quinpirole (right) selective for small reward expectancy. (C) Average normalized activity of all neurons selective for reward expectancy during the cue period (gray shaded area) recorded with SKF81297. Activity was pooled over reward cue sets. (D) Same conventions as in (C) for all neurons selective for reward expectancy recorded with quinpirole.

**Figure 3. D2Rs increase reward expectancy coding during the cue period.** (A) TIs quantifying the amount of reward expectancy selectivity during the cue period before and after stimulation D1Rs with SKF81297. Each dot corresponds to one reward expectancy selective neuron (left). Mean TIs were not changed by SKF81297 (right). (B) Conventions as in (A) for D2R stimulation with quinpirole, showing an increase in reward expectancy selectivity. (C) AUROCs quantifying the quality of reward expectancy coding during the cue period before and after stimulating D1Rs with SKF81297. Conventions as in (A). (D)

Conventions as in (C) showing that D2Rs increase reward expectancy coding.  
\*  $p < 0.05$ , n.s. not significant ( $p > 0.05$ ), signed rank test.

**Figure 4. D1R and D2R modulation of reward expectancy selective neurons during the delay period.** (A) Example recorded during control conditions (left) and after stimulating D1Rs with SKF81297 (right) selective for small reward expectancy during the delay period (gray shaded area). (B) A different example neuron recorded during control conditions (left) and after stimulating D2Rs with quinpirole (right) selective for small reward expectancy. (C) Average normalized activity of all neurons selective for reward expectancy during the cue period (gray shaded area) recorded with SKF81297. Activity was pooled over reward cue sets. (D) Same conventions as in (C) for all neurons selective for reward expectancy recorded with quinpirole.

**Figure 5. D1Rs and D2Rs oppositely modulate reward expectancy coding during the delay period.** (A) TIs quantifying the amount of reward expectancy selectivity during the delay period before and after stimulation D1Rs with SKF81297. Each dot corresponds to one reward expectancy selective neuron (left). Mean TIs were reduced by SKF81297 (right). (B) Conventions as in (A) for D2R stimulation with quinpirole, showing an increase in reward expectancy selectivity. (C) AUROCs quantifying the quality of reward expectancy coding during the delay period before and after stimulating D1Rs with SKF81297. Conventions as in (A). (D) Conventions as in (C) showing that D2Rs increase reward expectancy coding. \*\*  $p < 0.01$ , \*  $p < 0.05$ , signed rank test.

**Figure 6. Baseline modulation by D1Rs, but not D2Rs, predicts modulation of reward expectancy coding.** (A) Average baseline spike rate (pure fixation period) before and after application of SKF81297. (B) Correlation between the change of reward expectancy coding in the *cue* period and the change of log-baseline activity induced by D1R stimulation with SKF81297. Each dot corresponds to one neuron. (C) Same conventions as in (B) for D2R stimulation with quinpirole. (D) Same conventions as in (A) for quinpirole. (E) Correlation between the change of reward expectancy coding in the *delay* period and the change of log-baseline activity induced by D1R stimulation with SKF81297. Each dot corresponds to one neuron. (F) Same conventions as in (E) for D2R stimulation with quinpirole. \*\*\*  $p < 0.001$ , \*\*  $p < 0.01$ , \*  $p < 0.05$ , n.s. not significant ( $p > 0.05$ ), signed rank test, t-statistics for correlation analysis.

**Table 1. Number of reward expectancy selective neurons.**

	<b>Cue</b>	<b>Delay</b>	<b>All</b>
<b>SKF81297</b>	30	31	129
<b>Quinpirole</b>	28	43	127
<b>Σ</b>	58 (23 %)	74 (29 %)	256

**Table 2. Small and large reward preferring neurons (\*\*\*)  $p < 0.001$ , †  $p < 0.1$ ,  $\chi^2$  test).**

	<b>Cue</b>	<b>Delay</b>
<b>Large</b>	16	29
<b>Small</b>	42***	45†
<b>Σ</b>	58	74

**Figure 1**

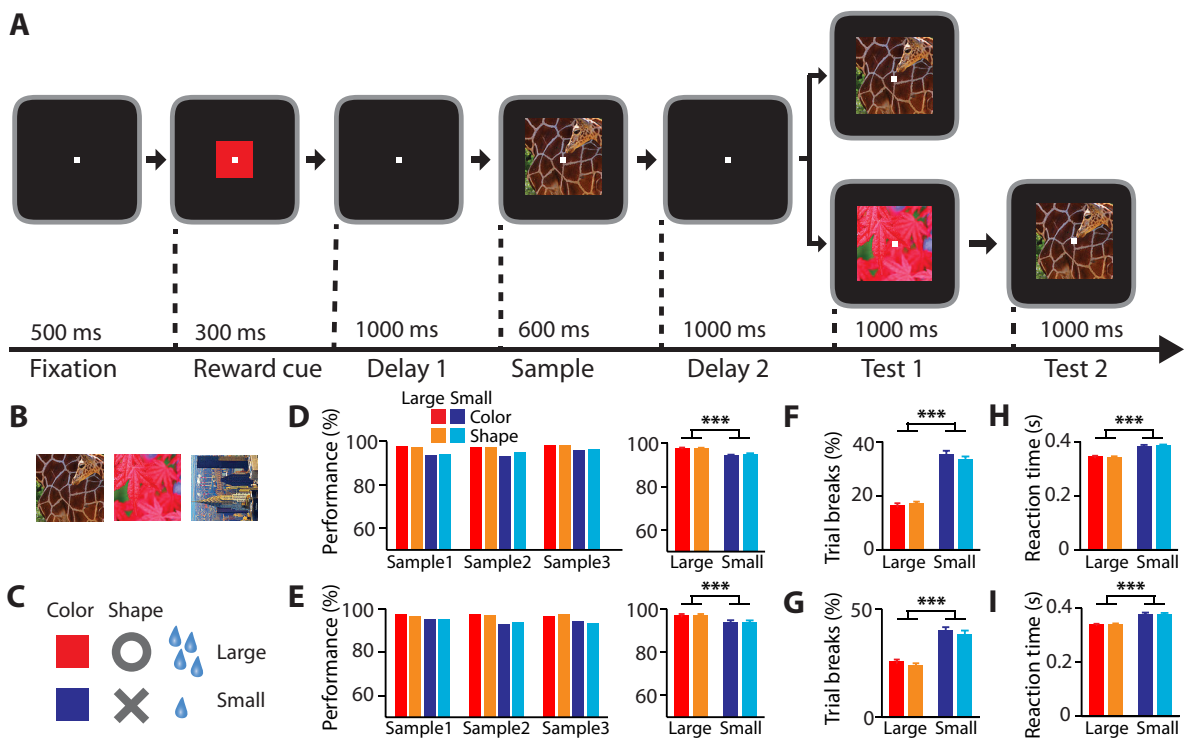


**Figure 2**

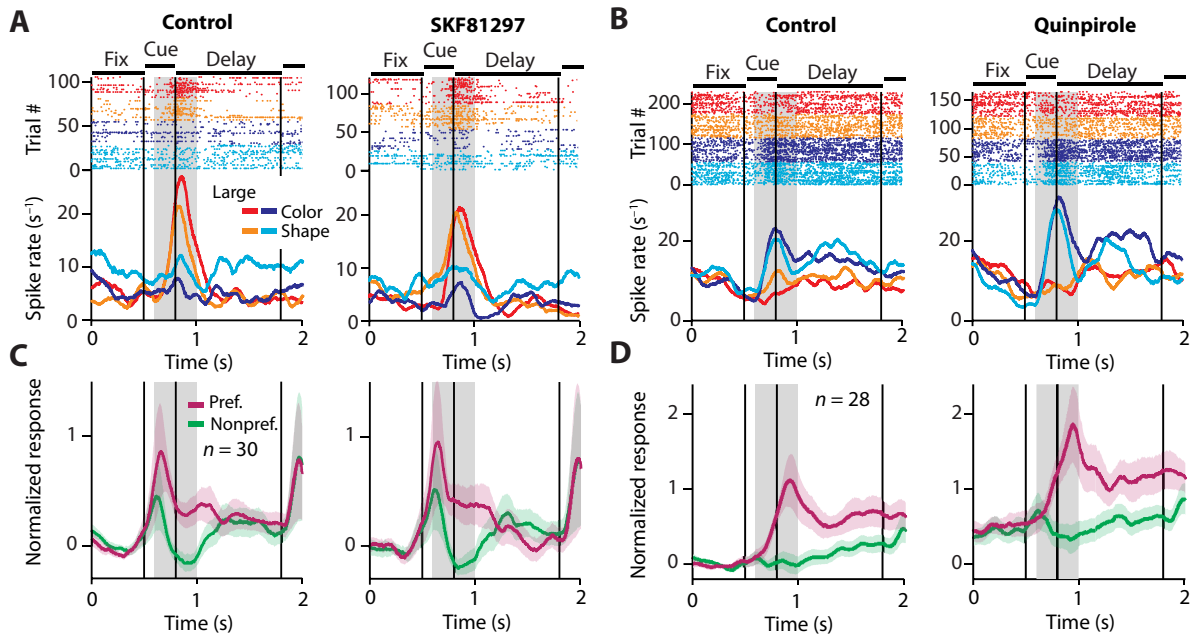


**Figure 3**

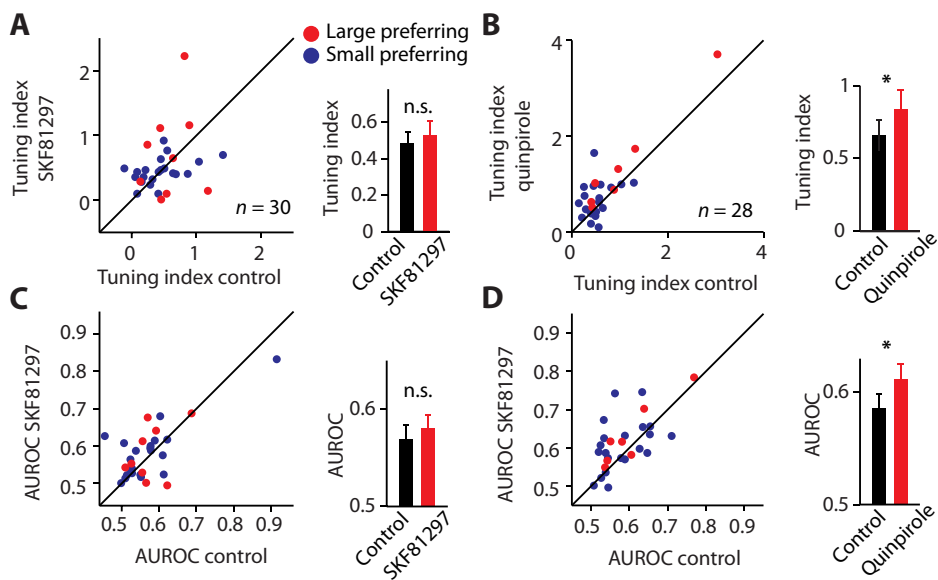


**Figure 4**

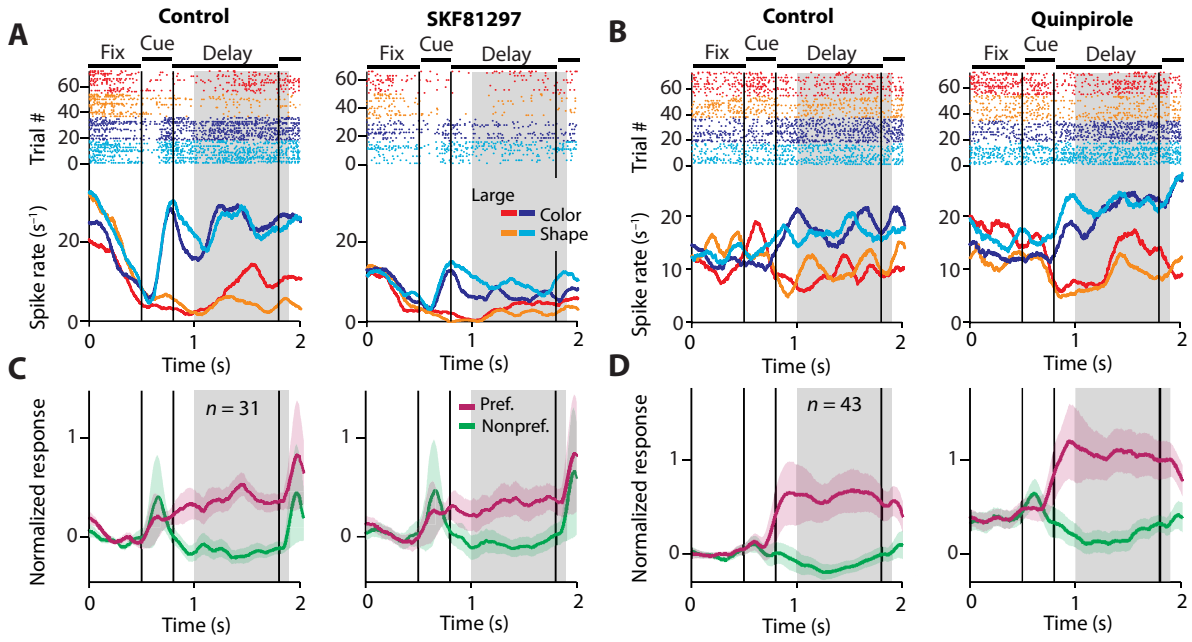


**Figure 5**

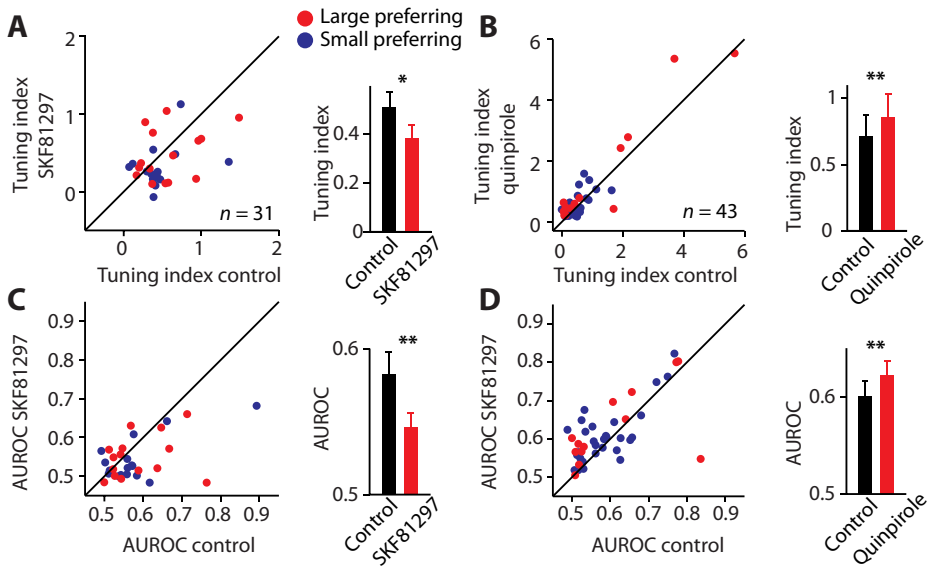
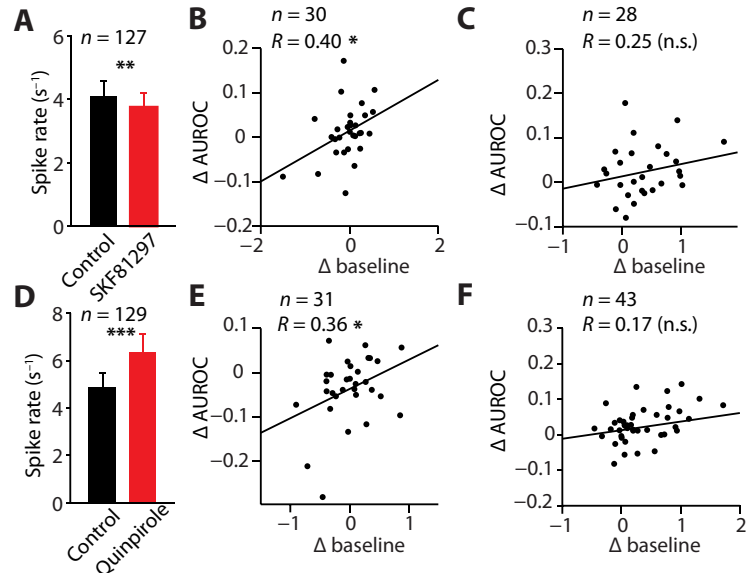


**Figure 6**







---

### **Study 5: Effects on prolonged training on behavioral well-being of rhesus monkeys**

Hage, S. R., **Ott, T.**, Eiselt, A.-K., Jacob, S. N., Nieder, A. (2014). Ethograms indicate stable well-being during prolonged training phases in rhesus monkeys used in neurophysiological research. *Laboratory Animals* **48**(1):82–7.



# Ethograms indicate stable well-being during prolonged training phases in rhesus monkeys used in neurophysiological research

Laboratory Animals  
 2014, Vol 48(1) 82–87  
 © The Author(s) 2013  
 Reprints and permissions:  
 sagepub.co.uk/  
 journalsPermissions.nav  
 DOI: 10.1177/0023677213514043  
 la.sagepub.com



Steffen R Hage, Torben Ott, Anne-Kathrin Eiselt, Simon N Jacob and Andreas Nieder

## Abstract

Awake, behaving rhesus monkeys are widely used in neurophysiological research. Neural signals are typically measured from monkeys trained with operant conditioning techniques to perform a variety of behavioral tasks in exchange for rewards. Over the past years, monkeys' psychological well-being during experimentation has become an increasingly important concern. We suggest objective criteria to explore whether training sessions during which the monkeys work under controlled water intake over many days might affect their behavior. With that aim, we analyzed a broad range of species-specific behaviors over several months ('ethogram') and used these ethograms as a proxy for the monkeys' well-being. Our results show that monkeys' behavior during training sessions is unaffected by the duration of training-free days in-between. Independently of the number of training-free days (two or nine days) with ad libitum food and water supply, the monkeys were equally active and alert in their home group cages during training phases. This indicates that the monkeys were well habituated to prolonged working schedules and that their well-being was stably ensured during the training sessions.

## Keywords

*Macaca mulatta*, non-human primate, neurophysiology, operant conditioning, species-specific behavior, water restriction

Non-human primates, and rhesus monkeys (*Macaca mulatta*) in particular, are widely used in neuroscience research.<sup>1,2</sup> Because of a variety of primate-specific features, ranging from behavioral capabilities (e.g. dexterity and advanced behavioral flexibility) to neuroanatomical homologies (e.g. a granular prefrontal cortex), monkeys are indispensable for studying the neuronal mechanisms of cognitive functions.<sup>3</sup> Macaques can be trained with operant conditioning techniques to perform a variety of behavioral tasks in exchange for positive rewards. While monkeys are engaged in such tasks, electrical activity of nerve cells as well as their behavior can be monitored.<sup>4,5</sup> Measuring neuronal activity simultaneously with behavioral performance presents a unique opportunity for experimental analyses of the neural foundation of behavioral utterances. Neuronal processing can be studied while the brain produces

perceptions and actions.<sup>6–8</sup> Because the brain lacks nociceptors ('pain sensors'), microelectrodes do not cause discomfort to the animals. In fact, electrodes are routinely implanted in humans for therapeutic access during illnesses such as Parkinson's disease, or epilepsy.<sup>9,10</sup>

Understanding the biology and behavior of primates bred and used for research is probably the single most important factor in the design and implementation of

---

Animal Physiology, Institute of Neurobiology, University of Tübingen, Tübingen, Germany

## Corresponding author:

Andreas Nieder, Animal Physiology, Institute of Neurobiology, University of Tübingen, Auf der Morgenstelle 28, 72076 Tübingen, Germany.

Email: andreas.nieder@uni-tuebingen.de

all types of refinement.<sup>11</sup> Given the relatively elaborate cognitive status of non-human primates, their psychological well-being, although poorly defined, has become an increasingly important concern over the past several years.<sup>12</sup> A frequent worry in neurophysiological research with monkeys is that the number of consecutive behavioral training days under controlled water intake might constitute accumulated discomfort to the animals.<sup>13</sup> We thus specifically explored whether prolonged training over many days might affect monkeys' behavior, putatively as a sign of discomfort. To that aim, we measured and analyzed a broad range of species-specific behaviors over several months (ethogram) and used these ethograms as a proxy for the monkeys' well-being.

## Material and methods

### Study animals

We compared monkeys' behavior during 12-day training periods following either short two-day training-free periods (including ad libitum water and food supply) or long nine-day training-free periods. We measured the behavior of seven male rhesus monkeys (*Macaca mulatta*) aged 4–11 years. All the monkeys were purchased from the German Primate Center, Göttingen, Germany. All procedures were approved by the local authority, the Regierungspräsidium Tübingen, Germany. All experiments were in accordance with the *European Convention for the Protection of Vertebrate Animals used for Experimental and Other Scientific Purposes*, and the *National Research Council Guide for the Care and Use of Laboratory Animals*.

### Housing and feeding routine

The animals were housed in several stable, small social groups in spacious group cages, each measuring 2.75 m(H) × 2.5 m(W) × 4.0 m(D) in a fully air-conditioned room (23 ± 1°C, 55 ± 10% relative humidity, maximum air change 15 times per hour) with daylight (10 to 16 h per day due to seasonal differences in Tübingen, Germany) and supplementary artificial light with 12 h day/12 h night cycle (07:00 to 19:00 h; 1500–2300 lux). Group cages were provided with hygienic animal bedding (Lignocel®, JRS, Rosenberg, Germany) and equipped with resting shelves, wooden branches, fire hoses, plastic tubs as well as cardboard tubes and boxes filled with nuts, seeds and raisins for environmental enrichment purposes. During behavioral investigation, the monkeys worked under a controlled water intake protocol. Water was provided as a reward to reinforce correct behavioral responses during

behavioral conditioning. Food (primate pellets, 10 mm, ssniff, Soest, Germany) was provided ad libitum at all times. Raisins, sunflower seeds, peanuts, walnuts and dried fruits were given after behavioral sessions on a daily basis. During training-free phases that interrupted the experimental sessions, monkeys had free access to water, fresh fruits (i.e. apples, bananas, pears and grapes) and vegetables (i.e. carrot, beetroot, salad and bell pepper) as well as primate pellets.

### Fluid control protocol

Determining a single standard by which all fluid control protocols can be evaluated or performed is difficult.<sup>12</sup> Baseline fluid intake varies depending on body size, age, housing, training protocol and physiological factors that are idiosyncratic to each animal.<sup>3</sup> Monkeys, like humans, appear to regulate hydration more or less efficiently, leading to substantial variation in the amount of fluid intake required each day. Such individual variations can only be appreciated if the history of the animal is known. We therefore determined the necessary fluid intake individually for each animal over a period of several days, when the monkey had a stable profile of behavior and physiology. The monkeys were required to obtain a substantial portion of their daily fluid requirement by earning it as a reward for performing a behavioral task once a day. In case a monkey was not able to earn its daily fluid requirement, a compensatory fluid supplement was provided; individual endpoints of the controlled water intake protocol were in place in order not to jeopardize the animal's health. Published figures comparable with ours are available<sup>14</sup> and strongly imply that the water access control procedures we employed allowed the monkeys to maintain a stable hydration state. Ad libitum access to fluid was provided on non-working days. With such a properly-managed fluid control, the animal could achieve all, or a substantial fraction, of its daily food/fluid requirement during training over many days and weeks. As an additional measure of physiological well-being, mean body weight did not differ between the two observation modes (i.e. two- or nine-day training-free periods) ( $P > 0.1$ , Wilcoxon sign rank test;  $n = 7$ ).

The veterinarian staff provided advice on all animal welfare issues and closely monitored the health of the monkeys (e.g. by regular inspections and frequently analyzing blood samples). The level of fluid control was approved by the regulatory authority and the institution's ethical review. Physiological data collected over many years indicated that the monkeys stayed in good health with the applied individualized fluid control protocols, while continuing to work proficiently in cognitively demanding tasks.

### Behavioral data collection

We used a combination of two sampling methods to assess the monkeys' behavior. During data collection, observers were in visual/olfactory/auditory proximity to the monkeys. However, the animals were very familiar with all observers whom they met on a daily basis. Thus, the monkeys were well habituated without noticeable reactions towards the observing person. All observers ran through an instruction phase, including test observations, in which they were introduced by SRH into the determination of each single behavioral category to assure uniform logging of the monkeys' behavior (inter-observer reliability). Data were collected over a five-month period (middle of May to end of October 2010).

First, we focally sampled the monkeys' behavior over 30 min in 1 min intervals ('30 min ethogram') immediately after the experimental animals were brought back to their home cage after training sessions (continuous sampling).<sup>15,16</sup> We recorded the monkeys' behavior on the first five days and last five days of the 12-day training session periods. Data of three sets for both 12-day training sessions following either short two-day training-free periods (3 × 10 days) or long nine-day training-free periods (3 × 10 days) were collected. In a few cases, we had to omit the focal sampling sessions due to unchangeable animal care routines (cage cleaning, etc.) resulting in a median number of 58 ± 2 focal sampling sessions for each monkey. Overall, we logged over 200 h of behavioral observations during focal continuous sampling.

In a second approach, we observed the behavior of all monkeys at one random minute for every single hour of the day during the first five and last five days of the 12-day training session periods (instantaneous scan sampling).<sup>16</sup> These so-called 'statistical days' provided a median behavioral performance of each monkey throughout the day. During both sampling methods, we logged several behaviors which had been established in earlier studies such as feed, forage, locomotion, comfort, curiosity, vocalization, groom/huddle, aggression, play, rest and abnormal behavior (see Table 1 for a detailed explanation of behavioral parameters).<sup>16–20</sup>

### Statistical analysis

Statistical analysis was performed with MATLAB (MathWorks, Statistics Toolbox, Cambridge, UK) by SRH. For the continuous sampling data-set, we performed a two-way analysis of variance (two-way ANOVA) to test for significant differences in the behavioral activity during observation periods preceded by two- or nine-day training-free periods. The Wilcoxon signed rank was used to test for significant differences

**Table 1.** Operational definitions for behaviors of rhesus monkeys.<sup>15,18–20</sup>

Behavior	Operational definition
Feed	Eating or manipulating monkey chow
Forage	Picking through the ground substrate with hands in search for food
Locomotion	Walking or running along the ground or over suspended surfaces (more than 1 m/min)
Comfort	Shaking; self-grooming; 'rest-yawning', i.e. yawns produced during transitions from rest to activity that are not followed by affiliative or agonistic inter-individual behavior <sup>21–23</sup>
Curiosity	Exploring alien items brought into the units
Vocalization	Utterance of species-specific calls <sup>24</sup>
Groom/Huddle	Sitting in physical or social contact with another animal and/or picking or manipulating another animal's fur or skin with hands or mouth
Aggression	Bared teeth display, lunge, stare, aggressive scream, slap, bite, push, hit, attack and chase
Play	Rough and tumble wrestling and chasing; play face displayed
Abnormal	Behavior with no obvious purpose or function such as pacing, head tossing, feces manipulation and licking of unit floor
Rest	Sitting alone, not in direct physical contact with other monkeys and not engaging in the other activity categories

in the mean activity of the monkey throughout the 'statistical day'. Differences in behavioral activity were considered significant at  $P < 0.05$ .

### Results

Figure 1a depicts the median occurrence of all observed behaviors during focal animal scanning ('30 min ethogram') shown by one representative example monkey on 30 days with a preceding two- and nine-day break, respectively. Several behaviors like feeding, foraging and locomotion occurred quite frequently within both observation periods, while others like curiosity, comfort and vocal behavior were shown only occasionally. Some behaviors like aggression or play were not shown. Comparing the behavioral activity during observation periods preceded by two- or nine-day training-free periods, respectively, revealed no significant differences ( $P > 0.5$ ,  $n = 540$ , two-way ANOVA). This indicates that this monkey showed similar behavior independent

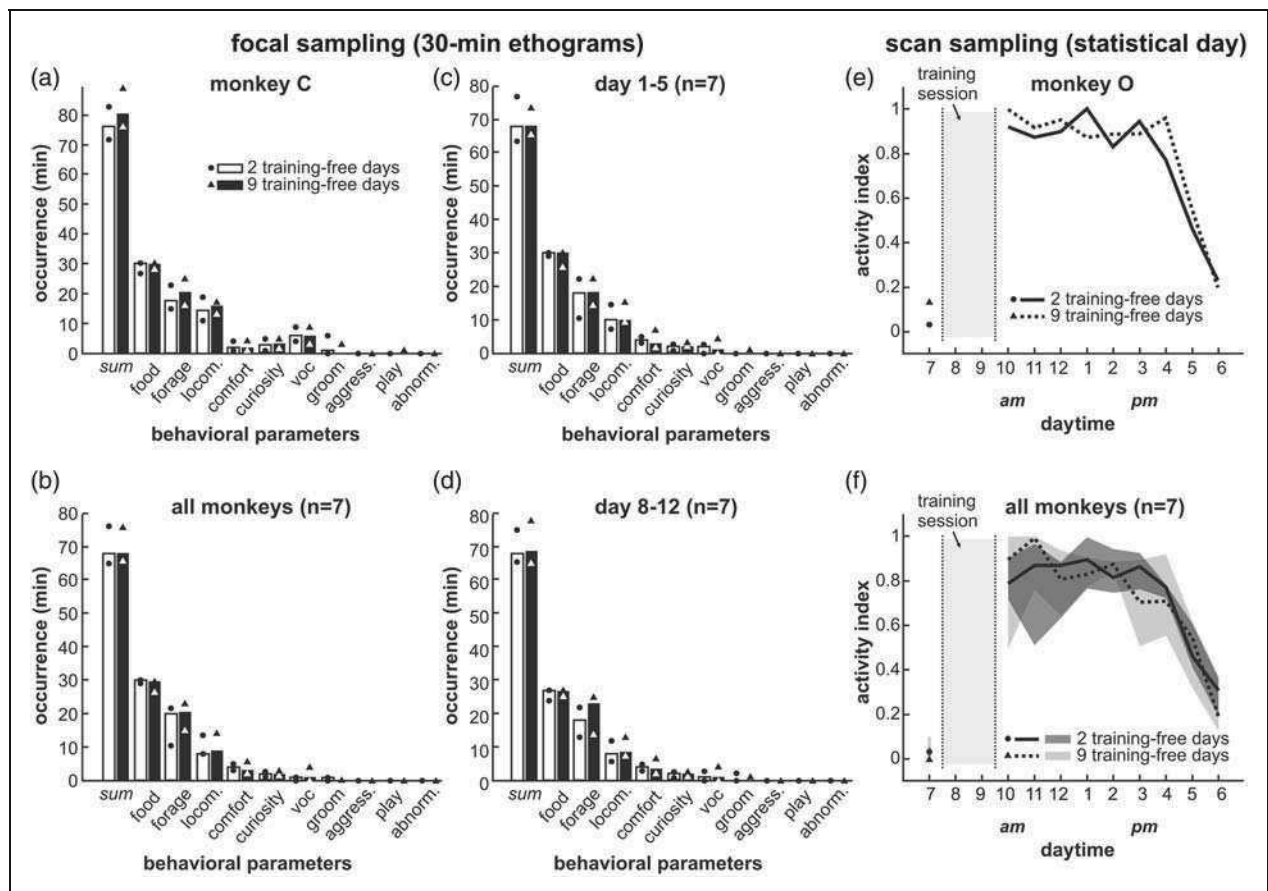


**Figure 1.** Comparison of monkey behavior observed with two types of focal animal analyses, focal animal sampling (a–d) and scan sampling (e, f), show no differences in relation to preceding training break modes. (a) Comparison of the median time a specific behavior was expressed by an individual monkey within 30 min observation intervals as a function of two or nine days of training-free phases, respectively ( $n = 30$  sessions). *Sum*: incidence of all observed behaviors during a session. Bars show medians, dots and triangles indicate the 1st and 3rd quartile. (b) Averaged behavior of seven monkeys within the two session types. Same layout as in (a). (c,d) Averaged behavior depicted in (b) divided into the first (c) and second week of the training session (d) revealed no behavioral differences. Same layout as in (a). (e) Activity indices of behaviors shown in (a–d) of a single monkey reveal no differences between observation periods associated with two- and nine-day training-free phases. After the first hour of the day (07:00 h), no behavioral data were collected for the time where the monkey performed its daily training session (usually between 07:30 and 10:00 h). (f) Averaged probability for behaviors occurring in seven monkeys confirms the results depicted in (e). Shaded areas indicate 1st and 3rd quartile. Same layout as in (e).

of the preceding training-free interval. Similar results revealing no differences between sessions with preceding two- or nine-day training-free phases, respectively, were obtained for the other monkeys ( $P > 0.1$  for all monkeys, two-way ANOVA). Figure 1b depicts the averaged occurrence of the logged behavior for all seven monkeys. Abnormal behavior was not observed in any monkey during the entire behavioral investigation.

To test whether the monkeys' behavior changed over time during training, we performed a more detailed analysis by splitting the data-set into the first five and the last five days of the 12-day training sessions. Again, we observed no differences in any of

the monkeys between the behavior shown during sessions with preceding two- or nine-day training-free phases, respectively, neither in the first five days, nor in the last five days of the training session ( $P > 0.1$  for all monkeys, two-way ANOVA). Moreover, we found no significant differences in the observed behavior of any monkey between the first five and the last five days of the 12-day training sessions, neither in combination with the two-day, nor with the nine-day training-free periods ( $P > 0.1$  for all monkeys, two-way ANOVA). Figures 1c and 1d show the averaged observed behaviors for all seven monkeys subdivided into the first five days and the last five days of the 12-day training session.

Instantaneous scan sampling revealed that the monkeys' behaviors were quite diverse throughout the day, resulting in the occurrence of most of the measured behaviors only occasionally. We defined an activity index that indicated a monkey's activity occurring within a single observation: An activity index of 1 revealed that a monkey showed at least one type of behavior during the observation; an activity index of 0 indicated that the monkey was resting. Figure 1e shows the mean activity indices for one example monkey during an average 'statistical day'<sup>16</sup> (30 days averaged for each of the two observation periods) for both observation periods tested. In both observation periods, the monkey was at rest in the morning and had its peak activity phase between 10:00 and 16:00 h, which declined towards the late afternoon/evening. (Between 08:00 and 10:00 h, no behavioral data were observed because the monkeys performed the daily training sessions during this period.) Statistical analysis revealed no significant difference in the mean activity of the monkey throughout the 'statistical day' ( $P > 0.2$ ,  $n = 10$ , Wilcoxon signed rank test). At a group level, statistical analysis of the mean activity indices throughout the 'statistical day' of all monkeys revealed no differences between the two observation modes ( $P > 0.1$ ,  $n = 10$ , Wilcoxon signed rank test). Figure 1f depicts the averaged distribution of the mean activity of all seven monkeys.

## Discussion

Our results obtained from both focal animal sampling and behavioral scans show that monkeys' behaviors during training sessions were not affected by the durations of training-free days. Independently of whether the monkeys obtained two or nine training-free days with ad libitum food and water supply, behavior in the home cages was equivalent. The monkeys were just as active and alert after a two-day training-free phase as after a nine-day training-free period. From this, we conclude that the monkeys' well-being was robustly guaranteed during the training sessions because if the training phase had caused accumulated discomfort to the animals, longer training-free phases (that might have been necessary for recovery from the training phase) would have resulted in modifications of behavioral utterances as measured by the ethograms. Based on these data, we also conclude that monkeys are well habituated to prolonged working schedules. Prolongation of the daily working routine under controlled water intake over at least 12 days does not act as a stressor. Our results may thus also help to settle the debate over how long a given individual animal should be used for experimentation. Our quantitative data suggest that the reuse of individual animals is favorable

over their replacement with new animals, thus allowing a reduction of the total number of animals used.

## Acknowledgements

We thank Annette Denzinger, Roland Hilgartner and Matthias H J Munk for critical comments on the manuscript. This work was supported by a start-up grant provided by the University of Tübingen to AN. This research received no specific grant from any funding agency in the public, commercial, or not-for-profit sectors.

## References

1. King FA, Yarbrough CJ, Anderson DC, Gordon TP and Gould KG. Primates. *Science* 1988; 240: 1475–1482.
2. Riederer BM. Do we need non-human primate research? *Lab Anim* 2012; 46: 177.
3. Newsome WT and Stein-Aviles JA. Nonhuman primate models of visually based cognition. *ILAR J* 1999; 40: 78–91.
4. Jasper H, Ricci GF and Doane B. Microelectrode analysis of cortical cell discharge during avoidance conditioning in the monkey. *Electroencephalogr Clin Neurophysiol* 1960; S13: 137–155.
5. Evarts EV. A technique for recording activity of subcortical neurons in moving animals. *Electroencephalogr Clin Neurophysiol* 1968; 24: 83–86.
6. McAdams CJ and Maunsell JH. Effects of attention on orientation-tuning functions of single neurons in macaque cortical area V4. *J Neurosci* 1999; 19: 431–441.
7. Velliste M, Perel S, Spalding MC, Whitford AS and Schwartz AB. Cortical control of a prosthetic arm for self-feeding. *Nature* 2008; 453: 1098–1101.
8. Nieder A. Supramodal numerosity selectivity of neurons in primate prefrontal and posterior parietal cortices. *Proc Natl Acad Sci USA* 2012; 109: 11860–11865.
9. Boon P, Vonck K, De Herdt V, et al. Deep brain stimulation in patients with refractory temporal lobe epilepsy. *Epilepsia* 2007; 48: 1551–1560.
10. Krack P, Hariz MI, Baunez C, Guridi J and Obeso JA. Deep brain stimulation: from neurology to psychiatry? *Trends Neurosci* 2010; 33: 474–484.
11. Jennings M, Prescott MJ (eds) and Members of the Joint Working Group on Refinement (Primates). Refinements in husbandry, care and common procedures for non-human primates: Ninth report of the BVAAWF/FRAME/RSPCA/UFAW Joint Working Group on Refinement. *Lab Anim* 2009; 43: 1–47.
12. Prescott MJ, Brown VJ, Flecknell PA, et al. Refinement of the use of food and fluid control as motivational tools for macaques used in behavioural neuroscience research: report of a Working Group of the NC3Rs. *J Neurosci Methods* 2010; 193: 167–188.
13. Desimone R, Olson C and Erickson R. The controlled water access paradigm. *ILAR J* 1992; 34: 27–29.
14. Yamada H, Louie K and Glimcher PW. Controlled water intake: a method for objectively evaluating thirst and hydration state in monkeys by the measurement of blood osmolality. *J Neurosci Methods* 2010; 191: 83–89.

15. Altmann J. Observational study of behavior: sampling methods. *Behaviour* 1974; 49: 227–267.
16. Martin P and Bateson P. *Measuring behaviour: an introductory guide*. Cambridge: University Press, 1993.
17. Altmann SA. A field study of the sociobiology of rhesus monkeys, *Macaca mulatta*. *Ann NY Acad Sci* 1962; 102: 338–435.
18. Beisner BA and Isbell LA. Ground substrate affects budgets and hair loss in outdoor captive groups of rhesus macaques (*Macaca mulatta*). *Am J Primatol* 2008; 70: 1160–1168.
19. Bauer SA, Pearl DL, Leslie KE, Fournier J and Turner PV. Causes of obesity in captive cynomolgus macaques: influence of body condition, social and management factors on behaviour around feeding. *Lab Anim* 2012; 46: 193–199.
20. Waitt C and Buchanan-Smith H. What time is feeding? How delays and anticipation of feeding schedules affect stump-tailed macaque behaviour. *Appl Anim Behav Sci* 2001; 75: 75–85.
21. Troisi A, Aureli F, Schino G, Rinaldi F and De Angelis N. The influence of age, sex, and rank on yawning behavior in two species of macaques (*Macaca fascicularis* and *M. fuscata*). *Ethology* 1990; 86: 303–310.
22. Deputte BL. Ethological study of yawning in primates. I. Quantitative analysis and study of causation in two species of old world monkeys (*Cercocebus albigena* and *Macaca fascicularis*). *Ethology* 1994; 98: 221–245.
23. Angst W. *Das Ausdrucksverhalten des Javaneraffen (Macaca fascicularis)*. Berlin: Paul Parey Verlag, 1974.
24. Hauser MD and Marler P. Food-associated calls in rhesus macaques (*Macaca mulatta*): I. Socioecological factors. *Behav Ecol* 1993; 4: 194–205.